Title
Effects of Early Life Environmental Tobacco Smoke Exposure on Pulmonary Immunity

Author
Haigh, Nathan Eugene

Publication Date
2021

Peer reviewed|Thesis/dissertation

Effects of Early Life Environmental Tobacco Smoke Exposure on Pulmonary Immunity

By

NATHAN EUGENE HAIGH
DISSERTATION

Submitted in partial satisfaction of the requirements for the degree of

DOCTOR OF PHILOSOPHY

in

Immunology

in the

OFFICE OF GRADUATE STUDIES

of the

UNIVERSITY OF CALIFORNIA

DAVIS

Approved:

Lisa A. Miller, Chair

Kent Pinkerton

Richart Harper

Committee in Charge

2022

Effects of Early Life Environmental Tobacco Smoke Exposure on Pulmonary Immunity

Table of Contents

Acknowledgements

I would like to start by acknowledging the funding sources that made this research possible. This project was supported by funding from the Tobacco Related Diseases Research Program 26IP-0045. I also received support from the department of Anatomy, Physiology, and Cell Biology at the University of California, Davis School of Veterinary Medicine; the UC Davis Graduate Group in Immunology; and especially the NIEHS T32 ES007059 Training Grant. I would like to acknowledge the assistance of the DNA Technologies and Expression Analysis Core, supported by NIH Shared Instrumentation Grant 1S10OD010786-01, for performing the transcriptomics in this disseration. The contents of this dissertation are solely the responsibility of the authors and do not necessarily represent the official views of the NIEHS, TRDRP, or UC Davis.

While my name is on the cover and the degree associated with this work is being awarded to me, the work that went into this dissertation is not mine alone. First, I want to thank my mentor Dr. Lisa Miller for her patience and guidance. Without her effort to secure funding and support during my rotation and ultimately her accepting me into her lab group, I would not have been able to complete this project. Dr. Miller gave me the opportunity to take on this project which included the challenge and rewards of identifying, mastering, and ultimately teaching other lab members the skills required to collect mouse lung samples. She also encouraged me to apply for the NIEHS T32 Training Grant to support my research and development as a scientist. Dr. Miller fosters a collaborative and welcoming lab environment that includes a number of fellow graduate students, undergraduates, post-doctoral fellows, and staff that were essential for completing sample collections. Specifically, I would like to thank our lab manager, Alexa Rindy, who provided significant support with mouse maintenance and sample collection from the beginning of the project. More recently, Diwash Shrestha, our junior specialist, has been essential in sample collection and processing, preparing and improving figures, and performing differential gene expression analysis of transcriptomic samples that were used in this dissertation. I would like to

thank all the other members of the lab past and present for assisting with sample collection and feedback on my writing and presentations. It truly has been the work of the entire lab group to get to this point. I would also like to thank the members of my dissertation committee, Drs. Kent Pinkerton and Richart Harper, for their feedback and support that made this dissertation possible.

Being part of the Graduate Group of Immunology has also been an incredibly rewarding experience from before I was even accepted. I want to thank Dr. Emanual Maverakis who took me on as a volunteer and CIRM trainee and who hired me to work in his lab while I completed my master's degree. Without the support and encouragement of Dr. Maverakis and his lab group I don't think I would have even found my way to GGI. I also want to thank the members of GGI that worked in nearby labs who provided a sense of comradery that assured me that GGI was the right program. Special acknowledgment goes Jessica Drushell for words of encouragement that she probably doesn't remember giving when I showed up to interview and for all the things she does behind the scenes to make GGI work; this program wouldn't be the same with her. I want to thank Dr. Grace Rosenquist for similar encouragement during recruitment, even though she thought I was Matt. I would like to thank our current and former chairs Drs. Charles Bevins, Huaijun Zhou, and Smita Iyer for their efforts to constantly improve GGI. The members of my qualifying exam committee, Drs. Renee Tsolis, Colin Reardon, and Paul Ashwood were extremely helpful in helping shape my research goals. A sincere thank you is due to Dr. Laura Van Winkle for her role on my QE committee, as a mentor in the NIEHS T32 Training Program, and for all her efforts with courses and the lung biology journal club, which were essential for my development in the field of lung toxicology.

Finally, I would like to thank my family and friends who have been a constant source of support and motivation. I'd like to thank the love of my live, my wife Thanh Tran, for being there every day when I needed someone to talk to and for organizing the best vacations ever. To Alex, Samantha, and Ophelia who are such an important reason I returned to school and finished my dissertation so your road will never be as difficult as mine was. I want to thank and encourage my

sister Marilyn, who is working on her terminal degree as a nurse practitioner, and her family for always supporting my goals and a good listener. My friend Diego who got me out of my shell and is a constant source of information and leads for work in biotech. My mother, Bonnie, father and stepmom, Clinton and Jill, for their support. And to the many other people who I've met along the way, personally and professionally. This dissertation is truly the culmination of all the experiences and trials, good and bad. It would not be possible without everyone who has been part of my life and the UC Davis family.

Effects of Early Life Environmental Tobacco Smoke Exposure on Pulmonary Immunity

Abstract

There is a long history detailing the health hazards of cigarette smoking and secondhand, or environmental tobacco smoke. More recently evidence has suggested that children that have reduced pulmonary function are more likely to grow into adults with reduced lung function. Severe respiratory infection and exposure to tobacco smoke are strongly associated with reduced lung function in early childhood, and exposure to environmental tobacco smoke is a contributing factor for increased number and frequency of respiratory infections. Despite declining tobacco usage in the United States, smoking globally continues to be a major public health issue, and novel inhalation exposures such as electronic cigarette usage and exposure to wildfire smoke from wildland-urban interfaces have become an increasing burden on human health. Tobacco smoke research is highly standardized and replicable, and tobacco smoke contains many classes of chemicals that may be concern from novel exposures. In this study, we examine the persistent impact of environmental tobacco smoke exposure on lung pathophysiology using a murine model of neonatal exposure. We found neonatal environmental tobacco smoke exposure resulted in sexually dimorphic responses with female but not male mice having increased lung damage and airways immune cells in adulthood, and using RNA-sequencing, we found neonatal environmental tobacco smoke exposure in female mice significantly altered Hallmark Pathways. We report a mechanism by which neonatal tobacco smoke exposure transiently induces an IL-22^{+} ILC3 population and that IL-22 modulates club cell secretory protein to alter lung function. Later in life, we found that neonatal environmental tobacco smoke exposure resulted in elevated macrophages in female but not male mice with novel alterations in gene expression in the lungs.

Early Life Immune Mechanisms of Environmental Tobacco Smoke

Nathan Eugene Haigh

1.1. Abstract

Tobacco smoke exposure is a known, preventable risk factor for several morbidities during childhood. Children exposed to secondhand or environmental tobacco smoke (ETS) are more likely to suffer from more frequent and severe respiratory infections, asthma exacerbations, wheezing, and other health issues. Many of the respiratory issues induced by ETS are associated with reductions in pulmonary function in children, and recent findings show that reduced lung function as early as the first two months of life is associated with reduced peak lung function in adulthood. Understanding how ETS elicits these effects is essential to remediating lung damage caused by exposure, but the complex composition of ETS changes over time depending on prevailing environmental factors, which can be a confounder in many models. Several mechanisms have been documented that illustrate the impact of ETS on childhood health. Understanding the mechanisms through which ETS alters immune and pulmonary functions is important for mitigating and correcting dysfunction induced by tobacco smoke. In addition, understanding molecular mechanisms of immune and pulmonary dysfunction can inform potential mechanisms of action from other inhalation toxicants including novel toxicant exposures. This can expedite the correct identification of novel toxicants and allow mitigation of the lasting effects on health earlier than has previously been possible.

1.2. Introduction

Cigarette smoking remains the leading preventable cause of death in the United States with approximately 14% of adults being cigarette smokers as of 2019 [1]. Tobacco was primarily used in pipes and cigars, chewed, or as snuff until the advent of commercial rolled cigarettes in the nineteenth century [2]. With the advent of the cigarette, tobacco use grew rapidly and was further increased during first half of the twentieth century in part due to the inclusion of cigarettes in soldiers' rations. While other tobacco products including chewing tobacco, snuff, cigars, pipes, hookahs, and loose smoking tobacco remain available, cigarettes are the most used tobacco product. Cigarette use peaked in the 1960s with as much as 67% of males born 1911-1930 and 44% of women born 1931-1940 being cigarette smokers [3]. Smoking rates declined as awareness improved of the danger posed by cigarette smoking for increased rates of many forms of cancer, heart disease, respiratory diseases including chronic obstructive pulmonary disease, and serious respiratory infections. This led to support for bans on smoking in public indoor spaces, advertising bans for tobacco products, increased smoking cessation programs and products, and education programs to reduce smoking uptake. However, reductions in smoking rates in the United States have decelerated in recent years while developing countries see more smokers than ever [4].

Of particular concern is the exposure of vulnerable populations to cigarette smoke. Maternal smoking in the United States has decreased from 9.2% in 2010 to 6.9% in 2017, which remains lower than the US average [5]. The reduced smoking rates from the first (7.1%) to the third trimester (5.7%) suggests that expectant mothers generally understand the risk of their smoking to the fetus [6]. Public health policies that increase awareness of the adverse impacts of tobacco use in women and children are likely reasons smoking rates particularly among pregnant women have decreased; however, this may also be resulting in discordance between self-reported tobacco use and physiological measurements which were previously reliable [7, 8]. Many smokers develop their habit between their teens to early twenties when their lungs are still

developing. Teen smoking in the United States has decreased dramatically since 2016, but use of electronic nicotine delivery systems has replaced cigarette smoking with potentially devastating future consequences [9]. Continued use of cigarettes presents a particular danger to vulnerable populations, including children, who are exposed to secondhand or environmental tobacco smoke (ETS), smoke both from the smoldering end of the cigarette and exhaled by smokers, at home or indoor public spaces.

1.3. Cigarette Smoke and Childhood Health

The adverse health effects of environmental tobacco smoke (ETS) were the focus of the 1986 Surgeon General's Report. Children are particularly vulnerable to ETS due to their respiratory system continuing to mature into early adulthood. In utero exposure is correlated with increased rates of miscarriage, preterm birth, reduced birth weight, and birth defects. Infants exposed to ETS or that were exposed in utero have odds ratios at least double that of unexposed infants for incidence of sudden infant death [10]. Children exposed to ETS experience increased rates and severity of respiratory tract infections, wheeze, asthma, cognitive and behavioral problems, and reduced pulmonary function [11]. In the United States in 2014-2015, 34.8% of expectant mothers in the Population Assessment of Tobacco and Health Study reported exposure to secondhand smoke [12]. Of those 38.8% reported being exposed to tobacco smoke at work, 54.4% reported being exposed at home, and the rest reported both work and home exposure. Exposure rates in other countries vary widely: 38.9%-75.1% between regions in China [13], 44.8% in Mongolia [14], 69.8% in India [15], and from 17.8% in Mexico to 72.3% in Vietnam in the home among 14 low and middle income countries [16]. The amount of exposure is even higher in public indoor spaces where the number of people sharing the space can generate upwards of 1 mg/m^3 of suspended ETS particles. Public smoking bans in many states have reduced the incidence of childhood exposure to ETS, yet exposure in the home environment remains a concern. Exposure to secondhand smoke remains a concern in the home and cars for those children who live with the

estimated 34 million smokers in the United States and millions more around the world [17]. As many as 77.8% of children in Europe are exposed to ETS in the home [18].

1.3.1. Preterm Birth/Low Birthweight

Tobacco usage was first shown to be associated with increased risk of pre-term birth in a dose-dependent manner independent of maternal age in a retrospective study [19]. A large prospective study showed 60% increase in very early preterm births among mothers that smoke after adjusting for confounding factors [20]. The influence of smoking on birth weight is dose-dependent [21-23]. Kleinman and Madans reported that the odds of low birth weight increases by 26% for every 5 cigarettes smoked per day for the duration of a pregnancy [22]. Additionally, in utero tobacco smoke exposure has been shown to result in reduced fetal growth independent of other factors including gestational age, maternal age, parity, or maternal weight [24]. Low birthweight is associated with a variety of short-term and long-term health complications of the pulmonary, gastrointestinal, cardiovascular, renal, and endocrine systems [25]. Pregnant women who smoke cigarettes are more likely to experience premature membrane ruptures as pregnancy complications, and when smoking women experience preeclamptic toxemia the rate of infant mortality is more than twice as high as for babies of non-smokers [26]. Importantly, studies have also shown adverse pregnancy related outcomes in women exposed to ETS [27-29]. Interestingly, at least one study of women in Mumbai, India found reduced birthweight and increased risk of preterm birth among smokeless tobacco users [30], but these results may be confounded by other environmental exposures that were not accounted for in the study. A study of 23,524 live births in Sweden found that the 789 expectant mothers who used snuff had increased rates of preeclampsia and preterm birth compared to non-tobacco users [31]. However, expectant mothers who smoked had larger reductions in birthweight compared to both snuff users and non-tobacco users and similar odds of preterm birth with reduced risk of preeclampsia compared to snuff users. This evidence suggests that combustion products from tobacco use may be important drivers of birth complications leading to low birthweight separate from smokeless tobacco.

1.3.2. Respiratory Tract Infections

A systemic review of the effects of parental smoking on childhood health showed increased odds ratios for lower respiratory infections, wheeze, asthma, middle ear disease, sudden infant death syndrome, and reduced pulmonary function based on parental smoking behaviors [32]. Another systemic review found ETS exposure resulted in increased odds ratios for hospitalization or emergency department visit due to laboratory confirmed respiratory syncytial virus (RSV) in 12 of the 14 studies included [33]. DiFranza et al also found ETS exposure resulted in increased odds ratios for hospitalization or outpatient treatment for clinically diagnosed RSV in 6 of 8 studies which may be due other pathogens with similar symptom profiles, and they found that ETS exposure increases hypoxemia among children hospitalized due to RSV in all 4 of the studies that assessed clinical severity of infection. While severe RSV infections are a factor for lifelong pulmonary function deficits, there are many other respiratory tract infections. ETS exposure is also associated with increased odds of recurrent otitis media or middle ear infections and need for tonsillectomy due to repeated tonsilitis as well as increased incidents, hospitalization, and severity for bronchiolitis and pneumonia (reviewed in [34]). A study of children admitted to a hospital in Rochester, New York with influenza found that patients with documented history of ETS exposure were more likely to have a bacterial infection, be admitted to the pediatric intensive care unit, require intubation, and have a longer hospital stay than unexposed children admitted with influenza [35]. While most children will contract several respiratory infections, severe respiratory infections are more common among children exposed to ETS and are associated with altered lung function through the lifespan.

1.3.3. Asthma and Wheeze

Numerous epidemiological studies have shown an association between in utero and postnatal exposure to smoke as a causative factor for childhood wheeze, a continuous high-pitched sound emanating from chest during expiration caused by narrowed airways (reviewed in [36]). Asthma is the reversible constriction of airways resulting in difficulty breathing and may be

the result of an allergic or hypersensitivity response. A study using data from the Southern California Children's Health Study found that children exposed to tobacco smoke in utero but not ETS only had higher asthma rates than unexposed children [37]. There were also associations between in utero exposure to tobacco smoke or current ETS exposure with all measures of wheezing assessed in the study. Both in utero and ETS exposure resulted in increased odds ratios of an emergency department visit within the past year. The literature has been mixed in whether ETS exposure is associated with asthma, but quantitative reviews of the literature by Cook and Strachan have demonstrated significant associations between ETS exposure and asthma incidence and wheezing [38, 39]. The discrepancies in findings between studies is likely due to the difficulty of conducting human studies with a broad range of histories and behaviors combined with relatively small numbers of subjects to assess risk for such a complex disease. Asthma exacerbations in children have also been linked to ETS exposure [39]. A retrospective study of 199 children age less than 1 to 13 found children with the highest ETS exposure had odds ratio of 1.8 for asthma exacerbation and decreased FEV_1/FVC ratio and FEF_{25-75} compared to children without ETS exposure [40]. More recently, a large survey of the Easy Breathing childhood asthma database found ETS exposure was associated with higher adjusted relative risk ratios for asthma exacerbation and mild and moderate persistent asthma [41]. When they accounted for public or private insurance, they found that only for children on private insurance was ETS exposure associated with persistent asthma, which suggests that other factors besides ETS exposure are influencing the natural history of asthma among lower income children. There are known genetic and environmental factors relevant to asthma development that will be discussed later. Childhood asthma may follow different courses with aging into adulthood. Atopic children often stop experiencing asthma symptoms as adults, but childhood asthma that alters pulmonary function may predispose those adults to lung disease later in life.

1.3.4. Altered Pulmonary Function

Exposure to ETS that results in severe or repeated respiratory tract infections or asthma present both acute risks to health and lifelong alterations in lung function as shown by Stern et al [42]. Their results Tucson Children's Respiratory Study followed 123 children from infancy to age 22 and showed that infants with pulmonary function in the bottom quartile had forced expiratory volume in one second to forced vital capacity (FEV_1/FVC) ratio reduced 5.2%, forced expiratory flow between 25% and 75% of the FVC ($FEF_{25–75}$) reduced 663 mL/s, and forced expiratory volume in one second (FEV_1) reduced 233 mL compared to all other subjects. As lung function peaks in early adulthood before declining with age, the factors that contribute to reduced pulmonary function in early life have been proposed to drive chronic lung disease including chronic obstructive pulmonary disease (COPD). COPD is diagnosed as having FEV_1/FVC of less than 70 percent of the predicted value based on age and sex [43]. The requirement of pulmonary function testing for diagnosis of COPD combines with peak lung function in early life to confound identification of COPD in young adults as evidenced by COPD rates over in those over 45 being more than four times that under 45 while the 35-49 demographic having a diagnosed COPD rate 40% of the 50-64 age group [44]. Exposure to ETS a is preventable cause of adverse health effects in children in much the same way smoking is the largest preventable cause of death in adults.

1.3.5. Obesity

Early research on the effect of tobacco smoke on children focused on in utero exposures of fetuses resulting in increases in low birthweight and early delivery [19], but the effect of tobacco smoke exposure on children does not end at birth. Numerous studies have looked at the impact of childhood ETS exposure on weight and found troubling trends of increased body mass and incidence of obesity among children exposed to ETS. The Southern California Children's Health Study showed combined impacts of traffic related air pollution (TRAP) with ETS exposure on body mass index (BMI) of children from age 10 to 18 that implicate both ETS and TRAP in increased BMI compared to children with low exposure [45]. Importantly, there was not accounting for the

family income as a confounding factor in the study; however, exposure to increased amounts of air pollution generally correlates with socioeconomic status within a geographical area. A study of school aged children in Korea showed associations between concentrations of 4-(methylnitrosamino)-1-(3-pyridyl)-1-butanol (NNAL) and cotinine in the children's urine and BMI particularly in the underweight and normal BMI groups. Only cotinine was significant in the overweight group, and the authors speculated that cotinine from food sources may be a confounding factor that needs further examination [46]. As school age children tend to spend more time with parents, the association between BMI and cotinine levels may also be due to the activity level of parents who smoke. A study that examined the results of the U.S. National Health and Nutrition Examination Survey 2003–2008 took into account family income, parental education, and the child's activity and caloric intake when examining the role of polycyclic aromatic hydrocarbons (PAHs) and ETS on BMI of children age 6-18 years [47]. Their findings showed that higher levels of PAHs, which are found in ETS and TRAP as well as many other sources, are associated with increased BMI and waist circumference even after accounting for confounding variables. ETS exposure was also associated strongly with increased BMI and waist circumference with combined high PAH and ETS exposure having the greatest effect on childhood obesity. The dangers of childhood obesity extend well beyond childhood as obesity is associated with increased risks for many other diseases including metabolic disorder, hypertension, and many cancers.

1.3.6. Cognitive and Behavioral Effects

Studies examining behavioral changes in children exposed to tobacco smoke in utero or postnatally are more recent. Nicotine acts on nicotinic cholinergic receptors in the central nervous system results in release of dopamine leading to the addictive property of tobacco products [48], so it is reasonable to expect behavioral modification in children exposed to nicotine through ETS. Children exposed to ETS tend to exhibit increased rates of cognitive impairment, attention deficit hyperactivity disorder, oppositional defiant disorder, and conduct disorder [49]. The effects of in

utero ETS has been reported in infancy with greater startle responses, tremors, hypertonicity, and fussiness compared to unexposed infants. It is important to account for confounding factors including socioeconomic status that is closely related to tobacco use and both in utero and postnatal exposure to ETS because socioeconomic status is also closely linked to antisocial behavior in children [50]. One study that conducted a regression analysis to account for confounding factors of maternal smoking and ETS exposure found that child behavioral was correlated to tobacco smoke exposure after accounting for the effects of income, parental behavioral tendencies, and poor parenting practices suggesting a direct association between tobacco smoke exposure and childhood behavior [51]. As with all human studies, there is considerable variation in subjects between studies, and not all methodologies are designed to account for confounding factors. This has left some debate over the effect size for cognitive and behavioral issues due to ETS exposures during childhood. A meta-analysis has also linked tobacco smoke with cognitive deficits in the elderly that puts smokers and those exposed to ETS at greater risk of cognitive decline, dementia, and Alzheimer's disease [52]. Given that similar effects have been observed in India [53], China [54], and the UK [55, 56], it is concerning that behavioral and cognitive issues begin during childhood as these may increase the risk for adverse effects later in life.

1.4. Tobacco Chemistry

Tobacco smoke is an aerosol of liquid and solids suspended in gasses consisting of more than 7000 chemical constituents including more than 250 toxicants and carcinogens [57]. Cigarettes are consumed primarily to deliver approximately 0.5 mg of the 1-2 mg of nicotine to the user. Cigarette smoke is mostly gasses with approximately 8% particulate matter and 5% vapor phase [57]. Along with nicotine, tobacco smoke also contains a variety of poisonous compounds, polycyclic aromatic hydrocarbons (PAHs), volatile organic compounds (VOC), metals, and particulate matter that pose a hazard to human health [58].

1.4.1. Mainstream Smoke

Mainstream tobacco smoke is the portion that cigarette smokers inhale directly through the unlit end of a cigarette. Nicotine acts on nicotinic cholinergic receptors in the peripheral and central nervous system, where it results in release of dopamine leading to the addictive property of tobacco products [48]. Cytochrome P450 Family 2 Subfamily A Member 6 (Cyp2A6) in the liver converts nicotine to its primary metabolite cotinine. The half-life of nicotine is relatively short 1-2 hours while cotinine has a half-life of 15 to 20 hours [59]. Nicotine functions as a vasoconstrictor, increases heart rate and blood pressure, and increased oxygen consumption. Nicotine is also acutely toxic with a lethal dose to 50% (LD50) of the population between 30 and 60 mg in adults and an LD 50 as low as 10 mg in children [60]. There are also reports of nicotine being a carcinogen including through *in vivo* generation of nicotine nitrosamines N-nitrosonornicotine (NNN) and 4-(methylnitrosamino)-1-(3-pyridyl)-1-butanone (NNK), which are known carcinogens typically created during tobacco combustion. In addition, nicotine and its metabolites can activate signal transduction pathways that signal through Bcl-2 and vascular epithelial growth factor receptor 2 that promote growth and survival of malignant cells. The role of nicotine in smooth muscle contraction in human airways was recently addressed in a report that examined expression of nicotinic acetylcholine receptors on human primary airway smooth muscle from lung biopsies of third to sixth generation bronchi from non-infectious patients [61]. Expression of nicotinic α7 acetylcholine receptor (α7nAChR) by qPCR and Western blot showed human airway smooth muscle cells express α7nAChR and that expression of α7nAChR is elevated in asthmatics and smokers. In vitro α7nAChR expression in human airway smooth muscle cells can be induced by as little as 1% cigarette smoke extract. As nicotinic acetylcholine receptors have roles in bronchoconstriction and mucus secretion, the presence of increased α7nAChR on airway smooth muscle cells of smokers suggests it is possible that nicotine directly reduces airflow contributing to altered lung function seen in smokers.

Other acutely poisonous compounds in tobacco smoke include carbon monoxide and cyanides. Carbon monoxide is generated from the incomplete combustion of organic matter,

including tobacco, and is of concern due to acute toxicity and lingering hypoxia due to the high-affinity binding to hemoglobin. Carbon monoxide forms carboxyhemoglobin when bound to hemoglobin and is eliminated in an activity-dependent manner with half-life of 1-8 hours [62]. Carbon monoxide has been investigated in relation to intrauterine and postnatal exposures under the premise that hypoxia may result in diminished fetal growth generally with reduced growth of fetuses. This includes reduced fetal growth, increased fetal mortality and resorption, and reduced growth prior to weaning [63]. Carbon monoxide poisoning can also cause memory lapse and cognitive issues that are slow to resolve [64]. Hydrogen cyanide has been identified in tobacco smoke at quantities as high as 30 to 200 ug per cigarette and is metabolized into thiocyanate in the liver [62]. Thiocyanate has a half-life of about 3 days and is significantly less toxic than cyanide; however, thiocyanate is still toxic particularly in inhibition of iodine transport. While carbon monoxide limits the carrying capacity of oxygen by red blood cells, cyanide acts at the other end of oxidative phosphorylation by the cytochrome complex where that oxygen could have been used to generate cellular energy with blood levels as low as 0.2 mg/mL in the blood [65].

At least 16 priority polycyclic aromatic hydrocarbons (PAHs) are found in tobacco smoke including anthracene, benzo[a]pyrene, naphthalene, and chrysene [66]. PAHs are generated by incomplete combustion of organic material including petrol products, wood, and tobacco. The primary impact of PAHs from tobacco smoke has been as a carcinogen based largely on the identification of benzo[a]pyrene from coal tar [67]. Different PAHs appear to have different functions with benzo[a]pyrene being highly carcinogenic alone, but several PAHs and PAH metabolites promote tumorigenesis in concert with other tobacco smoke constituents. The exact amount of various PAHs changes between cigarettes based on the tar level, the curing process for the tobacco, and the available nitrates during combustion [66]. While total PAH content from burning various cigarettes has been shown to have a narrow range, the composition of specific PAHs can vary. There is a correlation between tar level in a cigarette and benzo[a]pyrene in the smoke generated. However, air-cured tends to have more nitrates than flue- or sun-cured tobacco

resulting in a reduction in the concentration of some PAHs in the smoke. Nitrates have been shown to alter the combustion of organic compounds by forming free radical scavengers that reduce the PAH levels from tobacco combustion. It should be noted that the increase in nitrates is also correlated with increases in tobacco specific nitrosamines such as NNN and NNK discussed above, which are also carcinogens generated during tobacco combustion. PAHs can induce damage by binding purine bases in DNA to generate adducts [68]. Many PAHs are also exogenous ligands for the aryl hydrocarbon receptor (AhR) and alter gene expression following receptor binding [69]. There is substantial evidence that exogenous AhR agonists are detrimental to health through the induction of genes that increase reactive oxygen species, which has long been associated with exposure to tobacco smoke.

The gas phase of mainstream tobacco smoke contains hundreds of volatile organic compounds (VOCs) and represents the major source of VOC exposure in the United States [66]. These VOCs are recognized as aromatic hydrocarbons, carbonyls, aliphatic hydrocarbons, and nitriles based on their chemical structure. Aromatic hydrocarbons found in tobacco smoke are structurally similar to, and including, benzene. Exposure to aromatic hydrocarbons has been shown to have toxic effects that reduce immune function, disrupt development, and damage multiple organ systems and in addition to some being carcinogenic [70]. Carbonyls are highly reactive organic compounds consisting of aldehydes and ketones that are generated in abundance during tobacco combustion [66]. Compounds such as formaldehyde and acetone are well known acute respiratory irritants [71]. Chronic exposure to at least 60 parts per billion of formaldehyde has been linked to increased rates of asthma and bronchitis in children with linear correlation between level of formaldehyde exposure and reduction in peak expiratory flow rate [72]. Formaldehyde also exacerbates asthma in children exposed to levels below 50 parts per billion. Aliphatic hydrocarbons include saturated hydrocarbons, such methane and propane, as well as unsaturated hydrocarbons, notably 1,3-butadiene and isoprene [66]. While there is little evidence of adverse health effects from the short saturated hydrocarbons, 1,3-butadiene and

isoprene have been identified as carcinogens in animal models [73]. The final major group of VOCs common to tobacco smoke is nitriles**,** most prominent of which are hydrogen cyanide, acetonitrile, and acrylonitrile [66]. As discussed above, cyanide is acutely poisonous by inhibition of oxidative phosphorylation, and acetonitrile is metabolized into cyanide upon inhalation, absorption, or ingestion [74]. Acrylonitrile is known to be a carcinogen in rats through ingestion of inhalation [75].

Metals in tobacco smoke are generally due to presence of metals in the soil the tobacco is grown in being taken into the plant and moved into the leaves through irrigation and ground water [66]. As such, the quantity and species of metal in tobacco smoke will depend on the region the plants were grown in as well as conditions during the growing period. It was noted that lead levels in tobacco decreased as leaded gasoline was removed from the market, but cadmium, lead, and mercury can all be found in trace amounts in the particulate phase of tobacco smoke [66]. Cadmium accumulates throughout the lifespan due to reabsorption by the kidneys and causes bone density loss and kidney damage [76]. Cadmium exposure has also been correlated with lung cancer [77]. Lead is a toxic metal that damages the kidney and brain and causes anemia. Studies have shown that blood lead levels are correlated to smoke exposure as lead absorbs more readily through inhalation than through ingestion [78]. Exposure to metals through tobacco smoke may increase reactive oxygen species either directly or by depleting reactive oxygen species scavengers like glutathione. There are many more trace metals and compounds in tobacco smoke with some estimating that as many as 10,000 species will eventually be identified.

Particulate matter (PM) is a term that describes suspended liquids and solids from a wide range of natural and anthropogenic sources including tobacco smoke. Many constituents of tobacco smoke can move between vapor and liquid or solid phase, and many of the constituents already mentioned constitute a portion of the particulate matter from tobacco smoke. The composition of particulate matter is important for understanding the effect it will have on the body with carbonaceous and oily particulate generally having more adverse impacts than crustal

particulate in the form or sand and dust. The size of particulate matter is important to understand what region of the respiratory system may be affected by exposure [79]. Coarse particulate matter is any suspended particles between 2.5 mm and 10 mm aerodynamic diameter and will generally be deposited in the upper respiratory tract due to impaction, diffusion, and sedimentation. Fine particulate matter is less than 2.5 mm aerodynamic diameter and is capable of diffusing into the lower respiratory tract prior to deposition, and ultrafine particulate matter has an aerodynamic diameter less than 0.1 mm, which facilitate diffusion through the alveolar wall into the bloodstream [80]. The median particle size for tobacco smoke is 0.1 mm by count with a 2 mm geometric standard deviation that indicates the majority of tobacco smoke particles are in the ultrafine and fine particulate matter fraction [81]. These deposition patterns are important for understanding where tobacco smoke constituents deposit, which dictates what cells are affected.

1.4.2. SideStream or Secondhand Tobacco Smoke

Environmental tobacco smoke (ETS) or secondhand smoke tobacco smoke is a combination of firsthand tobacco smoke inhaled and subsequently exhaled by the smoker as well as the smoke generated by the smoldering cigarette when not being puffed. The Surgeon General's Report of 1986 focused on the health effects of ETS or passive smoking on nonsmokers. ETS contains unique compounds due to the reduced oxygen levels and lower burning temperature compared to mainstream smoke along with reactions between constituent compounds in the air as ETS ages. The concentration of many of the compounds are higher in ETS than in mainstream tobacco due to the longer time that ETS is generated [82]. Common tobacco smoke constituents like nicotine 2.7-fold, carbon monoxide 2.5-fold, benzo[a]pyrene 3.4-fold, 2-naphthylamine 39-fold, pyrene 3.6-fold, toluene 5.6-fold, phenol 2.6-fold, methylfuran 3.4-fold, and acetonitrile 3.9-fold more abundant in ETS than mainstream tobacco smoke. Significant research about the impact of secondhand smoke was carried out and hidden by cigarette manufacturers that showed ETS was more hazardous than mainstream tobacco smoke [83].

1.4.3. Thirdhand Tobacco Smoke

Thirdhand tobacco smoke refers to the components of tobacco smoke that settle on or are absorbed and adsorbed into surfaces following exposure to tobacco smoke. Unlike secondhand smoke that can be removed through ventilation, thirdhand persists long after visible smoke has been cleared. Since thirdhand smoke persists for an extended period, thirdhand smoke ages with exposure to heat, other chemical compounds, and light that generate compounds novel to thirdhand smoke or increased concentrations of compounds compared to secondhand smoke. Specifically, thirdhand smoke is shown to have increased levels of carcinogenic nitrosamines—N-nitrosonornicotine (NNN), 4-(methylnitrosamino)-1-(3-pyridyl)-1-butanone (NNK), and 4-(methylnitrosamino)-4-(3-pyridyl)-butanal (NNA)—compared to secondhand smoke. Due to the persistent nature of thirdhand smoke, smoke exposure can occur in buildings and cars that had been used by smokers recently even though current occupants were nonsmokers [52].

The first study of thirdhand smoke examined dust from 72 houses, 34 with at least one smoker and 38 with nonsmoker occupants and used gas chromatography to identify nicotine as a marker for tobacco particulate in the dust. From surveys of smoking habits, the authors were able to show a positive correlation between the mass of nicotine in the household dust and the amount the occupants smoked [53]. While the authors concluded nicotine exposure from household dust was small (<2%) compared to what a typical smoker experiences, nonsmokers would have exposures even without secondhand smoke. Importantly, they did not account for any other tobacco products. Subsequent studies have consistently found tobacco smoke constituents in household dust particularly of homes of smokers [54].

1.5. Mechanisms of Tobacco Effects on the Lung

Proposed mechanisms for the effects of ETS in include altered neuroendocrine and smooth muscle cell abundance and function, altered postnatal lung development in children, decreased mucociliary clearance, excess mucus production and goblet cell hyperplasia, adenoid hyperplasia, and altered club cell function. It is notable that several of these mechanisms are likely related.

Nicotine acts through nicotinic acetylcholine receptors on neurons as the primary cause of addiction to tobacco products including cigarettes. The role of nicotine in smooth muscle contraction in human airways was recently addressed in a report that examined expression of nicotinic acetylcholine receptors on human primary airway smooth muscle from lung biopsies of third to sixth generation bronchi from non-infectious patients [61]. Expression of nicotinic α7 acetylcholine receptor (α7nAChR) by qPCR and Western blot showed human airway smooth muscle cells express α7nAChR and that expression of α7nAChR is elevated in asthmatics and smokers. In vitro α7nAChR expression in human airway smooth muscle cells can be induced by as little as 1% cigarette smoke extract. As nicotinic acetylcholine receptors have roles in bronchoconstriction and mucus secretion, the presence of increased α7nAChR on airway smooth muscle cells of smokers suggests it is possible that nicotine directly reduces airflow contributing to altered lung function seen in smokers. Binding of nicotinic acetylcholine receptors in the brains of people exposed to ETS for an hour in a car with a smoker has been shown using positron emission tomography [84]. There are limits to studying increases in expression of nicotinic acetylcholine receptors in humans exposed to ETS.

Elevated leukocytes in the blood [85-87] and lavage [88-90] have been reported in smokers and people exposed to ETS. Wallace et al reported a survey of previous studies that have shown macrophages in bronchoalveolar lavage fluid from smokers increased 4.5-9.6 fold higher than that of nonsmokers [91]. Since smokers also have altered lung structure, the frequency of macrophages per alveolar wall area and per airspace volume was determined from lung biopsies for 12 smokers and 9 nonsmokers who were undergoing surgery. Consistent with findings of altered lung architecture, lungs of smokers had reduced alveolar wall area per airspace volume, similar to mean linear intercept. Even after correcting for alveolar wall area and airspace volume there were more alveolar macrophages in the lungs of smokers than nonsmokers, and smokers had more macrophages than nonsmokers with similar lung architecture. Since tobacco smoke is known to induce changes in lung structure, it is important that those changes do not

negate observations of elevated macrophages found in the BALF of smokers. There is an association between numbers of macrophages, neutrophils, and NK cells in the lungs of smokers with severity of disease and inverse correlations with FEV_1 [92]. There is also evidence of increased leukocytes in those exposed to ETS as seen by increased circulating neutrophils in nonsmokers following exposure to secondhand smoke [86]. The tobacco smoke induced increase in pulmonary macrophages is predictive of disease development, progression, and exacerbation.

The existence of a lung microbiome has only recently supported by evidence, and the connection between ETS exposure and the pulmonary microbiome has not been adequately addressed. One study recently examined the role of traffic related particulate matter under 2.5 mm in diameter on microbiota in both saliva and induced sputum in children age 14 [93]. There were 34 subject sputum samples and 36 saliva samples analyzed for bacterial sequencing using the V4 region of 16S. The induced sputum samples from subjects with higher exposure to traffic related air pollution exposures had significantly greater Shannon diversity, observed amplicon sequence variants, and Faith's phylogenetic diversity compared to those from the lower exposure group. These findings show that exposure to inhaled toxicants in children can alter the microbial community in the respiratory tract, which is consistent with reports that suggest inhaled particulate matter increases the ability of bacteria to stick to the epithelia. Given the increased frequency and severity of respiratory infections in children exposed to ETS, an understanding of how ETS alters the lung microbiome could provide crucial insights into reducing the harm caused by early life ETS exposure and other pulmonary insults.

Many previous mechanisms have been shown to be reversible through tobacco cessation, but some environmental exposures including tobacco smoke have been shown to alter gene expression though the lifespan. Alterations in the genetic code may occur when compounds covalently bind DNA or through intercalation between bases resulting in deformations of the helix that hinder transcription and repair mechanisms. These can result in single nucleotide polymorphisms, insertions, deletions, or large structural variations. Epigenetic modifications

include changes in covalent binding of molecules such as methyl groups to the DNA itself, alteration in covalent modification of histone tails, or by modifying transcription factors that are responsible for regulating gene networks. Exposure to tobacco smoke including ETS has been associated with changes to DNA methylation, histone 3 lysine 4 dimethylation, and 5-methylcytosine levels in zebrafish (reviewed in [94]). A report that examined 348 5–7-year-old children for global DNA methylation and another 272 children for targeted methylation based on prenatal tobacco smoke exposure in the Children's Health Study [95]. There was reduced methylation of the retrotransposon AluYb8 in children exposed to prenatal tobacco smoke compared to unexposed controls. Prenatally exposed children also had increased methylation in the promoter regions for the extracellular matrix-detecting tyrosine kinase AXL and the receptor tyrosine phosphatase PTPRO compared to the unexposed group. Children prenatally exposed to tobacco smoke that expressed glutathione-S transferase Mu-1 (GSTM1) also had increased methylation of LINE1 transposable elements compared to those without GSTM1. Of particular concern is changes induced by exposure to toxicants that can persist not just through the lifespan but can be passed to subsequent generations as well. Heritable changes occur through alteration of the genetic code or by altering the pattern of expression of genes through epigenetic modification. Genetic variability in humans and ethical questions about selected mating combine with the persistence of and ethical questions that are involved in continuing environmental exposures to make it difficult to assess transgenerational effects in humans.

Importantly tobacco smoke has been shown to alter expression of pulmonary surfactants and homeostatic proteins. Club cell secretory protein (CCSP), also known as club cell 10 kDa secretory protein, secretoglobin family 1A member 1, or uteroglobin, has been reported to be altered in smokers and in humans and animal models exposed to secondhand smoke. The first study to examine CCSP in prenatal tobacco exposure used timed-mated Sprague-Dawley rats and exposed them to aged and diluted sidestream cigarette smoke for 6 hours/day, 7 days/week from gestational day 5 until collection of samples at gestational day 14, 18, or 21 [96]. Control rats

were housed in filtered air. The exposure system used a Teague smoking machine to generate 1.00 ± 0.07 mg/m^3 total suspended particles from 1RF4 research cigarettes by a 2 second, 35 mL puff per minute per cigarette for 8 minutes per cigarette to fill a 0.44 m^3 exposure chamber. Rat fetuses exposed to tobacco smoke showed CCSP in the airways beginning at gestational day 18 with increased CCSP mRNA by in situ hybridization and protein by immunohistochemistry and increased abundance of CCSP positive cells in the bronchioles. Previous work by the same group on the effect of postnatal aged and diluted sidestream cigarette smoke showed no difference in CCSP protein levels by immunohistochemistry in Sprague-Dawley rats [97]. In that experiment, male rat pups were exposed to 1 mg/m^3 total suspended particles from the same exposure system with exposed dams rotated between filtered air and exposure groups. While no difference in CCSP was found, pups exposed to aged and diluted secondhand cigarette smoke did have reduced epithelial cell proliferation in the terminal bronchioles during the first 50 days of life and increased Cytochrome P450 Family 1 Subfamily A Member 1 (Cyp1a1) in the exposed pups' bronchiole epithelium.

One study divided mothers into nonsmokers, light smokers (<10 cigarettes/day), and heavy smokers (>10 cigarettes/day) and found increased systolic to diastolic ratio in the umbilical artery and fetal middle cerebral artery and presence of a diastolic notch, a sign of increased resistance, in the uterine arteries of both groups of smokers compared to nonsmoking expectant mothers [98]. Microscopic examination of the umbilical arteries of babies from smokers has shown vascular endothelial alterations including swelling, blebbing, contraction, expansion of the endoplasmic reticulum, and basement membrane widening compared to those born to non-smoking mothers [99].

A small controlled study of men from rural areas showed that heavy smokers have reduced inspiratory capacity, total lung capacity, and increased residual volume as a percentage of TLC compared to non-smokers [100]. Tobacco use is associated with increased rupture of alveolar septa and thickening of the pulmonary vasculature in an age and dose dependent manner that is

not seen in non-smokers [101]. There is abundant evidence that tobacco smoke affects lung function throughout the life with increased rates and severity of asthma and reduced lung function in children and chronic lung disease in late adulthood.

1.6. Mechanisms of Tobacco Effects on the Immune System

The number of circulating and airways leukocytes is elevated in smokers and those exposed to ETS with neutrophilia driving increased circulating leukocytes and macrophages being the largest portion in lavage while neutrophils and eosinophils were also significantly increased [85, 86, 89, 90]. The increased macrophage abundance may be restorative or an exacerbation of the disease state.

Most epidemiological studies incorporate data on chronic exposures in populations and are unable to assess acute effects of tobacco smoke exposure or provide for randomization of subjects. Acute tobacco smoke exposure is when an individual or animal is exposed to tobacco smoke for a defined amount of time when there has not typically been a history of exposure in their life. Exposure to ETS in a small study that exposed adults to acute levels of secondhand smoke in a controlled setting, circulating leukocytes, particularly neutrophils, were increased following exposure compared to preexposure levels [86]. The study used two groups of 8 nonsmokers paired with 6 smokers for 3 hours in a 65.1 m^3 room. To generate secondhand smoke, the smokers were encouraged to smoke as many cigarettes as they could, with 93 and 107 total cigarettes smoked during the 3-hour sessions. Average concentrations of CO were 17 ± 0.7 and 18 ± 2.2 ppm, and particulate matter with a diameter less than 10 mm was 2.579 and 2.326 mg/m^3. The neutrophils from smokers and nonsmokers exposed to secondhand smoke were also more responsive to chemotaxis in response to N-formylmethionyl-leucyl-phenylalanine and produced greater levels of reactive oxygen species when stimulated with phorbol myristate acetate. The post-exposure responses in nonsmokers exposed to ETS were greater than unexposed nonsmokers and generally similar to those of the smoker cohort. These data indicate that exposure to acute levels ETS alters circulating cell counts and activity. A similar designed

study evaluating sex and thyroid hormones found reduced testosterone and progesterone, increased T3 and T4, and increased IL-1B and systolic blood pressure in men after exposure to ETS for 1 hour compared to pre-exposure levels [102]. The study involved the exposure of 28 healthy young adults, half women, were exposed to 1 hour of ETS from various cigarette brands with CO concentrations maintained at 22-24 ppm and 1 hour of room air in an exposure chamber with blood drawn before and after each exposure. Women had reduced 17b-estradiol and progesterone following ETS exposure.

Neutrophils of smokers and those exposed to ETS have an activated phenotype that is not seen in healthy nonsmokers [86]. In healthy people exposed to secondhand smoke for 3 hours, neutrophil counts were elevated from baseline, and their neutrophils were more responsive to chemotactic factors and produced more reactive oxygen species when stimulated with PMA. In a smaller cohort, baseline blood draws were performed a week before exposure, after acute secondhand smoke exposure, and a week after exposure. The tobacco smoke-induced immune effects were transient with return to near baseline leukocytes, reactive oxygen species production, and chemotaxis a week following acute ETS exposure.

All circulating leukocytes develop from progenitor populations within the bone marrow, and at least a portion of tobacco smoke constituents reach the circulation. Consistent with changes in circulating blood cells in smokers and those exposed to ETS, changes in the leukocyte release from the bone marrow of smokers has been demonstrated. In a survey of 38 asymptomatic smokers who used at least 15 cigarettes per day for at least the past three years compared with 15 age-matched controls increased leukocytes, neutrophils, and immature neutrophils were noted [87]. There was also an increased mean fluorescence intensity for L-selectin on leukocytes of smokers versus controls, which the authors attributed to immature neutrophils. Neutrophils from smokers also had higher levels of myeloperoxidase compared to those from nonsmokers, and smokers with more reduced diffusing capacity for CO compared to predicted had higher myeloperoxidase levels than did smokers with less impaired diffusing

capacity for CO. The neutrophils with higher myeloperoxidase also had higher levels of L-selectin indicating a neutrophil phenotype that is both primed to release reactive oxygen species and more capable of attaching to vessel walls in capillary beds including the lung.

Macrophage phenotype and number have been seen to be altered in COPD and other chronic lung conditions. An examination of macrophages in 84 subjects—22 never smokers, 17 smokers with COPD, 25 former smokers with COPD, and 20 asymptomatic smokers—of whom 10-16 had bronchoalveolar lavage done found more cells and specifically more macrophages in the BALF of COPD patients and smokers compared to never smokers [89]. The macrophages from BALF of smokers and COPD patients also had reduced capacity to phagocytose dead cells compared to the never smokers. The reduced phagocytosis in smokers with COPD and asymptomatic smokers was explained by reduced expression of markers important for macrophage interaction with cells for their role as scavengers including CD91 (a collectin-binding receptor), CD31 (PECAM), and CD44 (a hyaluronic acid receptor). Macrophages in smokers with COPD and asymptomatic smokers have decreased levels of maturity marker CD71 as well as increased Ki-67 staining compared to the never smokers suggesting macrophages in the lungs of smokers are proliferating more rapidly than in nonsmokers. Expression of macrophage surface marks was inhibited in vitro by addition of 2.5 or 10% cigarette smoke extract to macrophages from never smokers showing a direct effect of tobacco smoke constituents on macrophages. The attenuation of macrophage phagocytic capacity due to tobacco smoke exposure may increase the instances of bacterial infection as well as reduce efferocytosis.

The human body hosts a collection of microbiomes consisting of bacteria and viruses that varies by body region and with age. While many organisms in the microbiome are beneficial, dysbiosis can involve the introduction in pathogenic microbes or opportunistic infections of otherwise symbiotic members of the microbiome. An indication of persistent infection is the formation of bacterial biofilms on mucosal surfaces as biofilms provide protection for resident microbes from host defenses and antibiotics. One study of children age 6-12 years who were

undergoing surgery to reduce blockages of the nasal airways looked at biofilm formation on the inferior nasal turbinate [103]. The authors collected biopsies during surgeries from 20 children who had been exposed to ETS for a prolonged time and another 20 children without a history of ETS exposure and validated tobacco exposure through urinary cotinine levels. Of the 20 biopsies from children with ETS exposure, 11 had biofilms primarily for Staphylococcus aureus compared to just one of the biopsies from the unexposed children. There were significant correlations between number of cigarettes smoked per day in the house, duration of ETS exposure, and urinary cotinine level and presence of biofilms from nasal biopsies. Many reports have shown correlations between exposure to ETS and increased frequency and severity of respiratory infections in children. This report shows a relationship between ETS exposure and formation of biofilms, which are indicators of established bacterial colonies that may progress into infections with higher risk of severe infection.

The role of lymphocytes in COPD has also been investigated. Hodge et al looked at peripheral blood and bronchoalveolar lavage from 30 smokers with COPD, 30 former-smokers with COPD, 20 asymptomatic smokers, and 30 never smokers [88]. Peripheral blood and bronchoalveolar lavage fluid were collected with leukocyte cell differentials, and lymphocyte phenotype was determined using flow cytometry. The authors found that current smokers and smokers with COPD had elevated leukocytes and both all smokers and former smokers with COPD had elevated $CD8^+$ lymphocytes in BALF. A greater percentage of peripheral blood and BALF cells from COPD patients were positive for granzyme b and perforin in both the $CD8^+$ and $CD3^+$ populations compared to never-smokers. The increased frequency of cytotoxic t-cells may represent either a mechanism by which lung epithelia is destroyed leading to disease or a response to increased damaged lung epithelial cells.

A recent study showed elevated BMP2 transcript was important for reducing beta-tubulin protein levels in coculture of THP-1 macrophages and BEAS-2B bronchial epithelial cells [104]. The number of macrophages was elevated in mice exposed to tobacco smoke for 4 or 16 weeks

which is consistent with findings in human smokers. The role of tobacco smoke in modulating the immune system is clearly shown in the literature. The immune system has roles in modulating many systems throughout the body, and dysfunction of the immune system is associated with many chronic conditions.

1.7. Conclusion

While the effects of smoking cigarettes in adults abates and some may be reversible if tobacco cessation is initiated before the onset of chronic disease, the impact of ETS exposure on children is less clearly reversible. During early childhood the size and complexity of the lung increases substantially in a short period of time, and the lungs continue to grow into early adulthood. Exposure to ETS causes changes to the lung at the cellular level that do not appear to be reversible and may be a factor in lung disease later in life. Many questions remain about the mechanisms by which the complex mixture of chemicals that comprises ETS initiate the damage caused during early life, and a greater understanding of these mechanisms may provide opportunities to halt damage only among children and possibly reverse damage in adults.

1.8. References

1. Cornelius, M.E., et al., *Tobacco Product Use Among Adults—United States, 2019.* Morbidity and Mortality Weekly Report, 2020. **69**(46): p. 1736.
2. U.S. Department of Health and Human Services, *Reducing Tobacco Use: A Report of the Surgeon General*, C.f.D.C.a.P. U.S. Department of Health and Human Services, National Center for Chronic Disease Prevention and Health Promotion, Office on Smoking and Health, Editor. 2000: Atlanta, Georgia.
3. US Department of Health Human Services, *Strategies to control tobacco use in the United States: A blueprint for public health action in the 1990's.* 1991.
4. Ng, M., et al., *Smoking prevalence and cigarette consumption in 187 countries, 1980-2012.* Jama, 2014. **311**(2): p. 183-192.
5. Azagba, S., et al., *Trends in smoking during pregnancy by socioeconomic characteristics in the United States, 2010–2017.* BMC pregnancy and childbirth, 2020. **20**(1): p. 1-7.
6. Kondracki, A.J., *Prevalence and patterns of cigarette smoking before and during early and late pregnancy according to maternal characteristics: the first national data based on the 2003 birth certificate revision, United States, 2016.* Reproductive health, 2019. **16**(1): p. 1-11.
7. Patrick, D.L., et al., *The validity of self-reported smoking: a review and meta-analysis.* American journal of public health, 1994. **84**(7): p. 1086-1093.
8. Shipton, D., et al., *Reliability of self reported smoking status by pregnant women for estimating smoking prevalence: a retrospective, cross sectional study.* Bmj, 2009. **339**.

9. Berry, K.M., et al., *Association of electronic cigarette use with subsequent initiation of tobacco cigarettes in US youths.* JAMA network open, 2019. **2**(2): p. e187794-e187794.

10. Anderson, H.R. and D.G. Cook, *Passive smoking and sudden infant death syndrome: review of the epidemiological evidence.* Thorax, 1997. **52**(11): p. 1003-1009.

11. Martinez, F.D., *Early-life origins of chronic obstructive pulmonary disease.* New England Journal of Medicine, 2016. **375**(9): p. 871-878.

12. Do, E.K., et al., *Social determinants of smoke exposure during pregnancy: Findings from waves 1 & 2 of the Population Assessment of Tobacco and Health (PATH) Study.* Preventive medicine reports, 2018. **12**: p. 312-320.

13. Zhang, L., et al., *Peer reviewed: Exposure to secondhand tobacco smoke and interventions among pregnant women in China: A systematic review.* Preventing chronic disease, 2015. **12**.

14. Hikita, N., et al., *Prevalence and risk factors of secondhand smoke (SHS) exposure among pregnant women in Mongolia.* Scientific reports, 2017. **7**(1): p. 1-8.

15. Singh, S., G.K. Mini, and K.R. Thankappan, *Tobacco use during pregnancy in rural Jharkhand, India.* International Journal of Gynecology & Obstetrics, 2015. **131**(2): p. 170-173.

16. Centers for Disease Control Prevention, *Current tobacco use and secondhand smoke exposure among women of reproductive age--14 countries, 2008-2010.* MMWR. Morbidity and mortality weekly report, 2012. **61**(43): p. 877-882.

17. Centers for Disease Control Prevention, *Current cigarette smoking among adults in the United States.* 2019.

18. Cheraghi, M. and S. Salvi, *Environmental tobacco smoke (ETS) and respiratory health in children.* European journal of pediatrics, 2009. **168**(8): p. 897-905.

19. Simpson, W.J., *A preliminary report on cigarette smoking and the incidence of prematurity.* American journal of obstetrics and gynecology, 1957. **73**(4): p. 808-815.

20. Shiono, P.H., M.A. Klebanoff, and G.G. Rhoads, *Smoking and drinking during pregnancy: their effects on preterm birth.* Jama, 1986. **255**(1): p. 82-84.

21. Dejmek, J., et al., *The exposure of nonsmoking and smoking mothers to environmental tobacco smoke during different gestational phases and fetal growth.* Environmental health perspectives, 2002. **110**(6): p. 601-606.

22. Kleinman, J.C. and J.H. Madans, *The effects of maternal smoking, physical stature, and educational attainment on the incidence of low birth weight.* American journal of epidemiology, 1985. **121**(6): p. 843-855.

23. Kline, J., Z. Stein, and M. Hutzler, *Cigarettes, alcohol and marijuana: varying associations with birthweight.* International Journal of Epidemiology, 1987. **16**(1): p. 44-51.

24. Lowe, C., *Effect of mothers' smoking habits on birth weight of their children*, in *Problems of Birth Defects*. 1959, Springer. p. 255-261.

25. Eichenwald, E.C. and A.R. Stark, *Management and outcomes of very low birth weight.* New England Journal of Medicine, 2008. **358**(16): p. 1700-1711.

26. Haworth, J., *Cigarette smoking during pregnancy and the effect upon the fetus.* Canadian Journal of Public Health/Revue Canadienne de Sante'e Publique, 1973: p. S20-S24.

27. Kharrazi, M., et al., *Environmental tobacco smoke and pregnancy outcome.* Epidemiology, 2004: p. 660-670.

28. Fantuzzi, G., et al., *Preterm delivery and exposure to active and passive smoking during pregnancy: a case–control study from Italy.* Paediatric and perinatal epidemiology, 2007. **21**(3): p. 194-200.

29. Salmasi, G., et al., *Environmental tobacco smoke exposure and perinatal outcomes: a systematic review and meta-analyses.* Acta obstetricia et gynecologica Scandinavica, 2010. **89**(4): p. 423-441.

30. Gupta, P.C. and S. Sreevidya, *Smokeless tobacco use, birth weight, and gestational age: population based, prospective cohort study of 1217 women in Mumbai, India.* Bmj, 2004. **328**(7455): p. 1538.

31. England, L.J., et al., *Adverse pregnancy outcomes in snuff users.* American journal of obstetrics and gynecology, 2003. **189**(4): p. 939-943.

32. Cook, D.G. and D.P. Strachan, *Summary of effects of parental smoking on the respiratory health of children and implications for research.* Thorax, 1999. **54**(4): p. 357-366.

33. DiFranza, J.R., et al., *Systematic literature review assessing tobacco smoke exposure as a risk factor for serious respiratory syncytial virus disease among infants and young children.* BMC pediatrics, 2012. **12**(1): p. 1-16.

34. Vanker, A., R. Gie, and H. Zar, *The association between environmental tobacco smoke exposure and childhood respiratory disease: a review.* Expert review of respiratory medicine, 2017. **11**(8): p. 661-673.

35. Wilson, K.M., et al., *Secondhand tobacco smoke exposure and severity of influenza in hospitalized children.* The Journal of pediatrics, 2013. **162**(1): p. 16-21.

36. Bonner, K., E. Scotney, and S. Saglani, *Factors and mechanisms contributing to the development of preschool wheezing disorders.* Expert Review of Respiratory Medicine, 2021. **15**(6): p. 745-760.

37. Gilliland, F.D., Y.-F. Li, and J.M. Peters, *Effects of maternal smoking during pregnancy and environmental tobacco smoke on asthma and wheezing in children.* American journal of respiratory and critical care medicine, 2001. **163**(2): p. 429-436.

38. Cook, D.G. and D.P. Strachan, *Health effects of passive smoking. 3. Parental smoking and prevalence of respiratory symptoms and asthma in school age children.* Thorax, 1997. **52**(12): p. 1081-1094.

39. Strachan, D.P. and D.G. Cook, *Parental smoking and childhood asthma: longitudinal and case-control studies.* Thorax, 1998. **53**(3): p. 204-212.

40. Chilmonczyk, B.A., et al., *Association between exposure to environmental tobacco smoke and exacerbations of asthma in children.* New England journal of medicine, 1993. **328**(23): p. 1665-1669.

41. Hollenbach, J.P., et al., *Exposure to secondhand smoke and asthma severity among children in Connecticut.* PloS one, 2017. **12**(3): p. e0174541.

42. Stern, D.A., et al., *Poor airway function in early infancy and lung function by age 22 years: a non-selective longitudinal cohort study.* The Lancet, 2007. **370**(9589): p. 758-764.

43. Soriano, J.B., F. Polverino, and B.G. Cosio, *What is early COPD and why is it important?* European Respiratory Journal, 2018. **52**(6).

44. National Center for Health Statistics, *Percentage of COPD, emphysema, or chronic bronchitis for adults aged 18 and over*, in *Nation Health Interview Survey*. 2019.

45. McConnell, R., et al., *A longitudinal cohort study of body mass index and childhood exposure to secondhand tobacco smoke and air pollution: the Southern California Children's Health Study.* Environmental health perspectives, 2015. **123**(4): p. 360-366.

46. Jeong, S.H., et al., *Association between parents' smoking status and tobacco exposure in school-age children: assessment using major urine biomarkers.* Scientific reports, 2021. **11**(1): p. 1-9.

47. Kim, H.-W., S. Kam, and D.-H. Lee, *Synergistic interaction between polycyclic aromatic hydrocarbons and environmental tobacco smoke on the risk of obesity in children and adolescents: the US National Health and Nutrition Examination Survey 2003–2008.* Environmental research, 2014. **135**: p. 354-360.

48. Benowitz, N.L., *Pharmacology of nicotine: addiction, smoking-induced disease, and therapeutics.* Annual review of pharmacology and toxicology, 2009. **49**: p. 57-71.

49. Zhou, S., et al., *Physical, behavioral, and cognitive effects of prenatal tobacco and postnatal secondhand smoke exposure.* Current problems in pediatric and adolescent health care, 2014. **44**(8): p. 219-241.

50. Piotrowska, P.J., et al., *Socioeconomic status and antisocial behaviour among children and adolescents: A systematic review and meta-analysis.* Clinical psychology review, 2015. **35**: p. 47-55.

51. Gatzke-Kopp, L.M. and T.P. Beauchaine, *Direct and passive prenatal nicotine exposure and the development of externalizing psychopathology.* Child psychiatry and human development, 2007. **38**(4): p. 255-269.

52. Anstey, K.J., et al., *Smoking as a risk factor for dementia and cognitive decline: a meta-analysis of prospective studies.* American journal of epidemiology, 2007. **166**(4): p. 367-378.

53. Muhammad, T., M. Govindu, and S. Srivastava, *Relationship between chewing tobacco, smoking, consuming alcohol and cognitive impairment among older adults in India: a cross-sectional study.* BMC geriatrics, 2021. **21**(1): p. 1-14.

54. Li, T., et al., *Non-linear dose-response relation between urinary levels of nicotine and its metabolites and cognitive impairment among an elderly population in China.* Ecotoxicology and Environmental Safety, 2021. **224**: p. 112706.

55. Cervilla, J., M. Prince, and A. Mann, *Smoking, drinking, and incident cognitive impairment: a cohort community based study included in the Gospel Oak project.* Journal of Neurology, Neurosurgery & Psychiatry, 2000. **68**(5): p. 622-626.

56. Llewellyn, D.J., et al., *Exposure to secondhand smoke and cognitive impairment in non-smokers: national cross sectional study with cotinine measurement.* Bmj, 2009. **338**.

57. US Department of Health and Human Services, *Public Health Services, National Toxicology Program 14th Report on Carcinogens*. 2016.

58. Stedman, R.L., *Chemical composition of tobacco and tobacco smoke.* Chemical reviews, 1968. **68**(2): p. 153-207.

59. Ion, R. and A.L. Bernal, *Smoking and preterm birth.* Reproductive Sciences, 2015. **22**(8): p. 918-926.

60. Mishra, A., et al., *Harmful effects of nicotine.* Indian journal of medical and paediatric oncology: official journal of Indian Society of Medical & Paediatric Oncology, 2015. **36**(1): p. 24.

61. Borkar, N.A., et al., *Nicotinic α7 acetylcholine receptor (α7nAChR) in human airway smooth muscle.* Archives of Biochemistry and Biophysics, 2021. **706**: p. 108897.

62. Benowitz, N.L., *Tobacco Smoke Consumption.* Measurement in the analysis and treatment of smoking behavior, 1983. **48**: p. 6.

63. Longo, L.D., *The biological effects of carbon monoxide on the pregnant woman, fetus, and newborn infant.* American journal of obstetrics and gynecology, 1977. **129**(1): p. 69-103.

64. Raub, J.A., et al., *Carbon monoxide poisoning—a public health perspective.* Toxicology, 2000. **145**(1): p. 1-14.

65. Vogel, S.N., T.R. Sultan, and R.P. Ten Eyck, *Cyanide poisoning.* Clinical toxicology, 1981. **18**(3): p. 367-383.

66. Office on Smoking Centers for Disease Control Prevention, *How tobacco smoke causes disease: The biology and behavioral basis for smoking-attributable disease: A report of the surgeon general.* 2010.

67. Rubin, H., *Synergistic mechanisms in carcinogenesis by polycyclic aromatic hydrocarbons and by tobacco smoke: a bio-historical perspective with updates.* Carcinogenesis, 2001. **22**(12): p. 1903-1930.

68. Pfeifer, G.P., et al., *Tobacco smoke carcinogens, DNA damage and p53 mutations in smoking-associated cancers.* Oncogene, 2002. **21**(48): p. 7435-7451.

69. Vogel, C.F., et al., *The aryl hydrocarbon receptor as a target of environmental stressors–Implications for pollution mediated stress and inflammatory responses.* Redox biology, 2020. **34**: p. 101530.

70. Bahadar, H., S. Mostafalou, and M. Abdollahi, *Current understandings and perspectives on non-cancer health effects of benzene: a global concern.* Toxicology and applied pharmacology, 2014. **276**(2): p. 83-94.

71. Main, D.M. and T.J. Hogan, *Health effects of low-level exposure to formaldehyde.* Journal of occupational medicine.: official publication of the Industrial Medical Association, 1983. **25**(12): p. 896-900.

72. Krzyzanowski, M., J.J. Quackenboss, and M.D. Lebowitz, *Chronic respiratory effects of indoor formaldehyde exposure.* Environmental research, 1990. **52**(2): p. 117-125.

73. Placke, M.E., et al., *Chronic inhalation oncogenicity study of isoprene in B6C3F1 mice.* Toxicology, 1996. **113**(1-3): p. 253-262.

74. Willhite, C.C., *Developmental toxicology of acetonitrile in the Syrian golden hamster.* Teratology, 1983. **27**(3): p. 313-325.

75. Woutersen, R.A., *Toxicologic profile of acrylonitrile.* Scandinavian journal of work, environment & health, 1998: p. 5-9.

76. Satarug, S. and M.R. Moore, *Adverse health effects of chronic exposure to low-level cadmium in foodstuffs and cigarette smoke.* Environmental health perspectives, 2004. **112**(10): p. 1099-1103.

77. Schoeters, G., et al., *Cadmium and children: exposure and health effects.* Acta Paediatrica, 2006. **95**: p. 50-54.

78. Apostolou, A., et al., *Secondhand tobacco smoke: a source of lead exposure in US children and adolescents.* American journal of public health, 2012. **102**(4): p. 714-722.

79. Sturm, R., *Modelling the deposition of fine particulate matter (PM2. 5) in the human respiratory tract.* AME Medical Journal, 2020. **5**(0).

80. Kwon, H.-S., M.H. Ryu, and C. Carlsten, *Ultrafine particles: unique physicochemical properties relevant to health and disease.* Experimental & molecular medicine, 2020. **52**(3): p. 318-328.

81. Anderson, P.J., J.D. Wilson, and F.C. Hiller, *Particle size distribution of mainstream tobacco and marijuana smoke.* Am Rev Respir Dis, 1989. **140**: p. 202-205.

82. Weiss, S.T., et al., *The health effects of involuntary smoking.* American Review of Respiratory Disease, 1983. **128**(5): p. 933-942.

83. Schick, S. and S. Glantz, *Philip Morris toxicological experiments with fresh sidestream smoke: more toxic than mainstream smoke.* Tobacco control, 2005. **14**(6): p. 396-404.

84. Brody, A.L., et al., *Effect of secondhand smoke on occupancy of nicotinic acetylcholine receptors in brain.* Archives of general psychiatry, 2011. **68**(9): p. 953-960.

85. Yarnell, J., et al., *Some long term effects of smoking on the haemostatic system: a report from the Caerphilly and Speedwell Collaborative Surveys.* Journal of clinical pathology, 1987. **40**(8): p. 909-913.

86. Anderson, R., et al., *Passive Smoking by Humans Sensitizes Circulating Neutrophils1-3.* Am Rev Respir Dis, 1991. **144**: p. 570-574.

87. Van Eeden, S. and J. Hogg, *The response of human bone marrow to chronic cigarette smoking.* European Respiratory Journal, 2000. **15**(5): p. 915-921.

88. Hodge, S., et al., *Increased airway granzyme b and perforin in current and ex-smoking COPD subjects.* COPD: Journal of Chronic Obstructive Pulmonary Disease, 2006. **3**(4): p. 179-187.

89. Hodge, S., et al., *Smoking alters alveolar macrophage recognition and phagocytic ability: implications in chronic obstructive pulmonary disease.* American journal of respiratory cell and molecular biology, 2007. **37**(6): p. 748-755.

90. Karimi, R., et al., *Cell recovery in bronchoalveolar lavage fluid in smokers is dependent on cumulative smoking history.* PloS one, 2012. **7**(3): p. e34232.

91. Wallace, W., M. Gillooly, and D. Lamb, *Intra-alveolar macrophage numbers in current smokers and non-smokers: a morphometric study of tissue sections.* Thorax, 1992. **47**(6): p. 437-440.

92. Di Stefano, A., et al., *Severity of airflow limitation is associated with severity of airway inflammation in smokers.* American journal of respiratory and critical care medicine, 1998. **158**(4): p. 1277-1285.

93. Niemeier-Walsh, C., et al., *Exposure to traffic-related air pollution and bacterial diversity in the lower respiratory tract of children.* Plos one, 2021. **16**(6): p. e0244341.

94. Breton, C.V., et al., *Exploring the evidence for epigenetic regulation of environmental influences on child health across generations.* Communications Biology, 2021. **4**(1): p. 1-15.

95. Breton, C.V., et al., *Prenatal tobacco smoke exposure affects global and gene-specific DNA methylation.* American journal of respiratory and critical care medicine, 2009. **180**(5): p. 462-467.

96. Ji, C.-M., et al., *Maternal exposure to environmental tobacco smoke alters Clara cell secretory protein expression in fetal rat lung.* American Journal of Physiology-Lung Cellular and Molecular Physiology, 1998. **275**(5): p. L870-L876.

97. Ji, C., et al., *Exposure to sidestream cigarette smoke alters bronchiolar epithelial cell differentiation in the postnatal rat lung.* American journal of respiratory cell and molecular biology, 1994. **11**(3): p. 312-320.

98. Albuquerque, C.A., et al., *Influence of maternal tobacco smoking during pregnancy on uterine, umbilical and fetal cerebral artery blood flows.* Early human development, 2004. **80**(1): p. 31-42.

99. Asmussen, I. and K. Kjeldsen, *Intimal ultrastructure of human umbilical arteries. Observations on arteries from newborn children of smoking and nonsmoking mothers.* Circulation research, 1975. **36**(5): p. 579-589.

100. Wilson, R.H., et al., *The pulmonary pathologic physiology of persons who smoke cigarettes.* New England Journal of Medicine, 1960. **262**(19): p. 956-961.

101. Auerbach, O., et al., *Smoking habits and age in relation to pulmonary changes: rupture of alveolar septums, fibrosis and thickening of walls of small arteries and arterioles.* New England Journal of Medicine, 1963. **269**(20): p. 1045-1054.

102. Flouris, A.D., et al., *Sexual dimorphism in the acute effects of secondhand smoke on thyroid hormone secretion, inflammatory markers and vascular function.* American Journal of Physiology-Endocrinology and Metabolism, 2008. **294**(2): p. E456-E462.

103. Elwany, S., M.A. Gamea, and I. Talaat, *Passive smoking induces nasal biofilms in children.* International Journal of Pediatric Otorhinolaryngology, 2021. **146**: p. 110755.

104. Wang, Z., et al., *Macrophages Inhibit Ciliary Protein Levels by Secreting BMP-2 Leading to Airway Epithelial Remodeling Under Cigarette Smoke Exposure.* Frontiers in Molecular Biosciences, 2021. **8**.

Chapter 2

Differential effects of environmental tobacco smoke exposure on lung injury and immune function due to age and sex

2.1. Abstract

Exposure to environmental tobacco smoke (ETS) is a known risk factor for increased rates and severity of respiratory infection and reduced pulmonary function. There are significant differences between the sexes regarding both immune response and sensitivity to ETS. There are many unknowns in how ETS effects males and females differently during early development. We hypothesize that neonatal ETS exposure induces persistent changes to the lung that correspond to altered gene expression in a sex-dependent manner. We used a murine model of neonatal ETS exposure to evaluate lung injury, immune cell recruitment following LPS challenge, and transcriptomic changes in adulthood. We evaluated gene ontology biological processes, KEGG pathways, and Hallmark Pathways. Female but not male mice showed elevated lavage protein an increased macrophages following neonatal ETS exposure. There were significant differences in gene expression in response to LPS challenge between the sexes. Male mice neonatally exposed to ETS had reduced resolution of inflammation compared to control males following LPS challenge. Female mice had significantly upregulated Hallmark Pathways based on neonatal ETS exposure with control mice having increased allograft rejection and oxidative phosphorylation pathways following sham and LPS challenge, respectively. These findings show mechanisms through which neonatal ETS exposure alters pulmonary gene expression and induces lung injury in a sex-dependent manner.

2.2. Introduction

Despite smoking continuing to decline in the United States for over 50 years, exposure to environmental tobacco smoke (ETS) remains a significant problem with millions of children exposed annually [1, 2]. Exposure to ETS is associated with increased rates of metabolic disorder, behavioral and cognitive issues, asthma, wheezing, and respiratory infections as well as asthma exacerbations and more severe respiratory infections [3]. Both exposure to ETS and severe respiratory infections are associated with reduced lung function during early life, which is then correlated with reduced lung function into adulthood and may contribute to increased rates of chronic lung disease [4]. There are several mechanisms through which tobacco smoke alters lung function: altering epithelial cell phenotype, inducing immune responses, and cytotoxicity. However, patterns of disease are not uniform across exposed populations. There are relevant sexual dimorphisms in some respiratory diseases. Asthma is more prevalent in boys than girls, but more common in women than men [5]. Men tend to have obstructive apnea than women in part due to morphological differences in the upper respiratory tract [6]. Essential to understanding the role of environmental exposures on pulmonary diseases is an understanding of pulmonary development.

The lungs begin development in utero as a lung bud off the foregut. As the fetus grows the lungs progress through organogenesis to the pseudoglandular, saccular, and finally alveolar stages of growth, which in humans begins during the third trimester. By contrast, rodents are born in the saccular stage and begin bulk alveolarization during the first postnatal week. The role of sex in lung development begins in utero where androgens and female sex hormones have been shown to have opposing effects on lung development with estrogens inducing the production of surfactants [6]. The expression of surfactant is one of the final stages of preterm lung development and is an indicator of reduced morbidity in late preterm births. The lungs continue to grow with increasing alveolarization and size into early adulthood. Boys then tend to have larger lungs with more total alveoli and alveolar surface area than girls throughout development, and males have

larger lung volumes and flows than women in all parameters except resistance as women have relatively larger airways [6]. Whether these differences confer an advantage to either sex is unclear. Chronic obstructive pulmonary disease is a leading cause of death with men traditionally having more diagnoses [7]; however, physician bias may be an important factor in underdiagnosing women with COPD particularly in the absence of spirometry [8]. The primary causative agent of COPD is smoking, and women who smoke are more likely than male smokers to develop COPD [9]. When normalized for confounding factors, women are more likely than men to develop COPD while other diseases such as pulmonary hypertension and pregnancy related asthma exacerbation occur primarily or exclusively in women [10]. How sex impacts disease progression during early life remains unknown.

Several reports have shown alterations in pulmonary cellular phenotype due to exposure to inhaled toxicants including ETS during the in utero and early postnatal periods. Ji et al showed that prenatal exposure to aged and diluted sidestream smoke increased expression of club cell secretory protein, a major homeostatic protein in the lung lining fluid and the principle marker for club cells, by gestational days 18 and 21 [11]. Similarly, tobacco smoke has been shown to induce goblet cell hyperplasia in rats [12] and induces expression of mucin 5ac, produced by pulmonary goblet cells during stress, in human bronchial epithelial cells in vitro by activating transcription factor Sp1 [13]. And several reports show induction of immune responses in the lung due to mainstream tobacco smoke and ETS [14-18]. Little work has assessed sexual disparities alongside the impact of ETS during development.

We hypothesized that neonatal ETS exposure produces persistent changes in pulmonary pathophysiology that is associated with an altered transcriptome. We sought to assess lung injury and immune recruitment in adult lungs using a neonatal murine model of ETS exposure. To assess immune responses and resolution, mice were challenged with lipopolysaccharide by oropharyngeal aspiration and assessed 24 hours later. Additional samples were collected for transcriptome sequencing and downstream analysis. To assess the impact of sex on early-life

ETS exposure, both male and female animals were included in all experiments and data segregated by sex in all analysis. These studies show important differences in pulmonary response to ETS between males and females even after exposure to inhaled toxicants ends.

2.3 Methods

2.3.1. Animals

All experiments were performed under the auspices of the Animal Care and Use Committee of the University of California at Davis (protocols 19980 and 21794). Gestational day 8 C57BL/6J dams were purchased from the Jackson Laboratory (Sacramento, CA) and allowed to acclimate at the California National Primate Research Center for 14 days until pups were 3 days old prior to treatments. Pups were maintained with their dams until weening at postnatal day 21. As controls, five-week-old male and female C57BL/6J (000664) mice were purchased and allowed to acclimate 1 week prior to treatment.

2.3.2. Environmental Tobacco Smoke Exposures

Starting at postnatal day 3, C57BL/6J mouse pups housed with dams or six-week-old adult controls co-housed up to 4 per cage were exposed to filtered air or whole-body tobacco smoke. Exposure was performed for 6 hours/day for 5 days at a concentration of 1-2 mg/m^3 total particulate matter. Tobacco smoke was generated using a TE10 cigarette smoking machine (Teague Enterprises, Woodland, CA) with a 35-mL puff volume, a 2-second puff duration, once per minute (Federal Trade Commission smoking standard) on two 3R4F reference cigarettes (Center for Tobacco Reference Products, University of Kentucky) at a time for 10 puffs per cigarette [19]. Total suspended particles were measured twice daily during the exposure by drawing air from the exposure chamber at a known rate and collecting particulate matter on a submicron filter for 1-hour and calculating the mass difference. Chamber carbon monoxide concentration was measured and recorded continuously during the week of exposure to assess consistency of exposure conditions. Following exposure, some mice were allowed to recover for 5 weeks in filtered air.

2.3.3. Oropharyngeal Aspiration of Lipopolysaccharide

Mice that were exposed to ETS or FA and allowed to recover were challenged by oropharyngeal aspiration of 0.25 μg LPS or sterile PBS and necropsied 24 hours later [20]. Briefly, mice were anesthetized by whole body exposure to 2% isoflurane in oxygen and then suspended by the cranial incisors by a silk suture tied to a slanted board. Anesthesia was maintained by continued administration of isoflurane through a nosecone. The tongue was pulled out and to the side to control the swallow reflex before 50 μL of LPS or PBS was injected into the pharynx with a micropipettor. The nose was held closed to force inhalation through the mouth. The fluid level and respiration were observed to ensure aspiration into the lungs which was accompanied with an audible crackling sound.

2.3.4. Bronchoalveolar Lavage Cell Count and Differential

Following exposure, mice were euthanized with an overdose of >100 mg/kg sodium pentobarbital diluted to 39 mg/mL in sterile PBS by intraperitoneal injection. The renal artery was severed, and lungs were perfused with 3 mL saline injected into the right ventricle. The trachea was cannulated, and 1 mL PBS was injected into the lungs and lavage was recovered immediately. Lavage was repeated with another 1 mL of PBS and both portions were pooled as bronchoalveolar lavage fluid (BALF).

BALF volume was measured with a serological pipet. BALF cellularity was determined by addition of 10 μL BALF to 10 μL trypan blue, and cells were counted on a Countess automated cell counter. Total BALF cells was calculated as the product of recovered volume and cell count. Cytospins were prepared by adding 100 μL BALF to a cytospin funnel and centrifuged onto slides for 5 minutes at 800 RPM in a Cytospin 4 (ThermoFisher, Waltham, MA). Slides were stained with Shandon Kwik-Diff (Thermo Shandon, Kalamazoo, MI) using manufacturer's protocol and differentials were counted by counting 300 cells per slide on an Olympus BH-2 polarizing trinocular microscope (Olympus Scientific Solutions Americas, Waltham, MA). Percent differential

is the quotient of number of each type of leukocyte and total leukocytes counted. Total leukocyte differential is the product of the percent and the total BALF cells.

2.3.5. Bronchoalveolar Lavage Protein Concentration

Collected bronchoalveolar lavage was centrifuged at 300 rcf for 5 minutes at 4° C to pellet lavage cells. BALF was removed to separate tubes and stored at -80° C. Protein concentration was determined using Pierce BCA protein assay (ThernoFisher) using manufacturer's protocol. Briefly, standards and samples were added to duplicate wells with working reagent and incubated for 30 minutes at 37° C before optical density was measured at 562 nm on a microplate reader. Protein concentration of samples was calculated by subtracting the optical density of the blank and multiplying the optical density by the slope of the standard curve.

2.3.6. Bulk RNA Sequencing and Analysis

At necropsy, lungs were perfused with 3 mL of saline injected into the right ventricle to remove circulating blood cells. The trachea was then canulated and 1 mL of RNALater was injected to permeate the lung tissue and preserve RNA integrity. The lungs were excised and stored with additional RNALater first at 4° C overnight and then at -80° C until RNA was isolated. RNA was isolated using a RNeasy Mini Plus kit and RNase-free DNase I (Qiagen, Germantown, MD) according to manufacturer's protocol. Purity of samples was determined using a Nanodrop ND-1000 (ThermoFisher). RNA was quantified using Qubit RNA broadrange kit and a Qubit 4 fluorometer (Invitrogen, Carlsbad, CA). RNA integrity was determined on a LabChip analyzer by the DNA Technologies and Expression Analysis Core at the UC Davis Genome Center. Libraries were prepared for Illumina NovaSeq 6000 S4 sequencing by the DNA Technologies and Expression Analysis Core. The sequencing was carried by the DNA Technologies and Expression

Analysis Core, supported by NIH Shared Instrumentation Grant 1S10OD010786-01. Initial QC was performed using the default Illumina chastity filter and data is exported as FASTQ files.

Once RNA counts were obtained, analysis was run by the UC Davis Bioinformatics core. Libraries were normalized in edgeR using the trimmed means of M-values, or TMM, method and genes with fewer than six counts per million reads in all samples were filtered out. Differential expression analysis was conducted using Limma-Voom to obtain differentially expressed genes between treatments and values for their logFC, average expression across all samples, and raw p-values. Adjusted p-values were calculated using the Benjamini-Hochberg method.

Further analysis was done by analyzing associated hallmark gene sets in the Molecular Signatures Database using the Gene Set Enrichment Analysis (GSEA) software (UC San Diego and the Broad Institute) [21-23]. Count data for each group and metadata were loaded into GSEA software and pairwise comparisons of relevant groups were carried out. Gene Ontology (GO) enrichment analysis of biological process pathways was done using GeneOntology with the PANTHER tool [24-26]. Kyoto Encyclopedia of Genes and Genomes (KEGG) pathway and reactome analysis were carried out using gProfiler [27]. Venn diagrams of differentially expressed genes were generated using GeneVenn [28].

2.3.7. Statistical Analysis

Statistical analysis was performed using Prism 9.0 software (Graphpad, San Diego, CA). Significance was determined with one-way ANOVA with Tukey post-hoc comparison of multiple means or student’s t-test.

2.4. Results

2.4.1. Neonatal environmental tobacco smoke exposure induces lung injury

Tobacco smoke exposure during early life is associated with increased rates and severity of respiratory infections [29]. To understand how neonatal environmental tobacco smoke (ETS) exposure effects the lungs in adulthood, postnatal day 3 mice were exposed to mixed mainstream and sidestream smoke (ETS) for 6 hours each day for 5 days along with 6-week-old adult controls and allowed to recover for 5 weeks in filtered air before immune challenge with 0.25 μg lipopolysaccharide in sterile PBS 24 hours prior to necropsy (Figure 1A). To administer a physiologically relevant LPS challenge, an LPS dose response was carried out prior to exposures (Supplemental Figure 1). A typical dose of LPS ranges from 1-10 μg based on our review of the literature, so single doses of 1, 5, and 10 μg were administered as well as titration down to 0.25 μg LPS. As the lowest dose showed induction of an inflammatory response as shown by increased neutrophils in the lavage fluid (Supplemental Figure 1G-H) that dose was used. Neonatal exposure to ETS resulted in increased protein concentration in the bronchoalveolar lavage fluid (BALF) in sham challenged (Figure 1B) and LPS challenged mice (Figure 1C) compared to age-matched and adult controls. We separated the mice by sex to determine if there was a difference between the response to neonatal ETS exposure between males and females. Female neonatally ETS exposed mice had significantly more BALF protein compared to age-matched and adult control in both sham (Figure 1D) and LPS challenge (Figure 1E). While male neonatally ETS exposed mice had more BALF protein than adult controls in sham challenge, there was no significant difference from age-matched controls (Figure 1F). There was no difference between BALF protein in LPS challenged males regardless of exposure or age. These findings suggest a sex-dependent effect of neonatal ETS exposure on lung injury.

2.4.2. Neonatal environmental tobacco smoke exposure results in elevated lavage cells

Lung injury involving increased BALF protein often also involves altered immune cells within the lung. We examined the abundance of BALF cells collected at necropsy. More BALF

cells per volume were recovered from the lungs of neonatally ETS exposed mice challenged with LPS compared to adult controls (Figure 2A). This difference was primarily attributable to neonatally ETS exposed female mice (Figure 2B) while male mice had no difference between treatments (Figure 2C). The abundance of BALF cells recovered was not significantly different between groups with sham challenge or by sex (Supplemental Figure 2C-E). The volume of lavage fluid recovered was not significantly different between groups (Supplemental Figure 2A-B). The total number of cells recovered from sham challenged, neonatally ETS exposed mice was higher than in age-matched controls and adult ETS exposed controls but not adult filtered air controls (Figure 2D). Neonatally ETS exposed female mice given sham challenge had more total cells than adult exposed ETS controls and a not significant trend over age-matched controls (Figure 2E). There was no difference between males on the total cells recovered based on exposure (Figure 2F). Neonatally ETS exposed mice challenged with LPS had more total cells than adult controls but not significantly more than age-matched controls (Figure 2G). When divided by sex, neonatally ETS exposed females had significantly higher total BALF cells than age-matched and adult controls (Figure 2H) while there was no difference in males between exposure groups following LPS challenge (Figure 2I). These results show a sex difference in total immune cells in the lung based on neonatal ETS exposure.

2.4.3. Neonatal environmental tobacco smoke exposure alters pulmonary immune composition

The typical composition of cells recovered from BALF in a resting state is predominantly macrophages with humans having 85% [30] and C57BL/6 mice having 94% macrophages [31]. To determine the effect of neonatal ETS exposure on BALF cell composition, cytospin slide were created with lavage fluid and fixed and stained for cell differential. With sham challenge, there was no difference between neonatally ETS exposed mice and age-matched or adult controls in the percent of lymphocytes (Figure 3A), macrophages (Supplemental Figure 3J-L), or neutrophils (Supplemental Figure 3P-R). When separated by sex, neonatally ETS exposed female mice had a reduced percentage of lymphocytes compared to adult ETS exposed mice with a trend toward

reduced lymphocytes compared to age-matched controls (Figure 3B) while there was no difference among males (Figure 3C). LPS challenge resulted in no differences in percent differential between neonatally ETS exposed and age-matched control in lymphocytes (Supplemental Figure 3G-I), macrophages (Supplemental Figure 3M-O), or neutrophils (Supplemental Figure 3S-U). Total lymphocytes (Supplemental Figure 3A-C) and neutrophils (Supplemental Figure 3D-F) were not different between exposures in sham challenged mice. Sham challenged neonatally ETS exposed mice had elevated macrophages compared to age matched and adult ETS exposed controls (Figure 3G) with females being significantly elevated over adult controls (Figure 3H) while there was no difference in males (Figure 3I). When challenged with LPS there was no difference in total lymphocytes (Figure 3D), but female neonatally ETS exposed mice had elevated lymphocytes compared to adult controls (Figure 3E) while males did not (Figure 3F). Neonatally ETS exposed mice challenged with LPS had elevated macrophages (Figure 3J) and neutrophils (Figure 3M) compared to adult controls. Only females had significantly higher total macrophages (Figure 3K) and neutrophils (Figure 3N) while no differences existed between males (Figures 3L, O). Collectively, this shows a sex-dependent dysregulation of the pulmonary immune profile in adulthood following neonatal ETS exposure.

2.4.4. Neonatal environmental tobacco smoke exposure alters pulmonary transcriptomics

Macrophages are known regulators of tissue function, so we performed paired-end transcriptomics on whole lung homogenate RNA using the Illumina NovaSeq platform to assess differences between the lungs of neonatally ETS exposed mice and age-matched filtered air controls in adulthood after either sham or LPS challenge. Differential gene expression was carried out using edgeR and Limma-Voom. Both males and females separated based on sham or LPS challenge (Figure 4A, D). Interestingly, neonatally ETS exposed female mice grouped more tightly than filtered air controls after sham challenge (Figure 4A). The sham challenge females from both exposures also grouped more closely together than the LPS challenge controls and ETS exposed females did (Figure 4A). By contrast the LPS challenged males did not cluster independently by

exposure (Figure 4D). The top 50 differentially expressed genes in sham challenged female (Figure 4B), LPS challenged female (Figure 4C), sham challenged male (Figure 4E), and LPS challenged male (Figure 4F) were generated using Gene Set Enrichment Analysis (GSEA). There was little overlap between the top 50 genes of males and females for each exposure and challenge (Figure 4G-J). Neonatally ETS exposed males and females given sham challenge have increased Hoxd4 (Figure 4H). LPS challenged filtered air control male and female mice have increased Cyp1a1, Cyp1b1, and Trdv2 (Figure 4I). Neonatally ETS exposed males and females have increased Proc (Figure 4J).

Differential gene expression using edgeR showed no significantly upregulated genes between control and neonatally ETS exposed mice following either sham or vehicle challenge. However, edgeR is relatively conservative in identifying differentially expressed genes relative to other commonly used software returning a moderate number of differentially expressed genes with a modest sensitivity due to a low false discovery rate [32]. In order to understand changes that result in the observed phenotype, we compared control sham and LPS challenged female mice to see the top differentially expressed genes in GSEA (Figure 5A) and compared those with neonatally ETS exposed sham and LPS challenged female mice (Figure 5B). There were 5931 differentially expressed genes between sham and LPS challenge in filtered air and 5161 differentially expressed genes between sham and LPS challenge in ETS with adjusted p-values below 0.05, and 3668 of those genes overlapped (Figure 5C). To further refine the comparison, a fold-change cut-off of 2 was used, which returned 893 differentially expressed genes in filtered air and 955 differentially expressed genes in neonatally ETS exposed female mice with 693 genes common between the exposures (Figure 5D). These results were further refined to show 713 differentially expressed genes up in filtered air and 781 differentially expressed genes up in neonatally exposed females with 603 overlapping due to LPS challenge (Figure 5E). Sham challenge resulted in 180 differentially expressed genes in control and 174 differentially expressed genes in neonatally exposed females with 90 overlapping (Figure 5F). Male filtered air control

(Figure 5G) and neonatally ETS exposed mice (Figure 5H) had more variation in their top differentially expressed genes. This carried over with 6654 differentially expressed genes in control and 1132 differentially expressed genes in neonatally ETS exposed male mice with 1066 common between the exposures (Figure 5I). There were 2341 differentially expressed genes in filtered air and 579 differentially expressed genes in neonatally ETS exposed males with 517 gene overlapping (Figure 5J). Of those, filter air control had 922 differentially expressed genes and neonatally ETS exposed male mice had 484 differentially expressed genes that were up due to LPS challenge (Figure 5K). By contrast, 1419 differentially expressed genes in filtered air control and only 95 differentially expressed genes in neonatally ETS exposed male mice were up due to sham challenge (Figure 5L). This shows a differential effect of neonatal ETS exposure on the lung transcriptome by sex.

2.4.5. Sexual dimorphism in Hallmark Pathways following neonatal ETS exposure

To further understand the changes in gene expression and how they may manifest as a phenotype, we ran Hallmark Pathway analysis within GSEA on the sequencing reads. Hallmark Pathway analysis uses defined sets of genes that are associated with specific phenotypes and relevant biological states [23]. We used the standard cutoff false discovery rate of 0.25 to identify Hallmark Pathways that are upregulated within each condition. In control females, LPS challenge resulted in 27 Hallmark Pathways being upregulated over sham challenge (Table 1) while there were no upregulated Hallmark Pathways due to sham challenge. Enrichment plots (Supplemental Figure 4) and core enrichment genes (Supplemental Figure 5) show LPS challenge increased gene expression of coherent gene sets in filtered air exposed female mice. Neonatal ETS exposed female mice challenged with LPS had 28 upregulated Hallmark Pathways compared to sham challenge (Table 2) while there were no upregulated pathways in sham challenged females. Enrichment plots (Supplemental Figure 6) and core enrichment gene sets (Supplemental Figure 7) show the pattern of genes upregulated by LPS challenge following neonatal ETS exposure in female mice. Between filtered air and neonatal ETS exposed females there were three unique

Hallmark Pathways. Filtered air females upregulate the oxidative phosphorylation pathway while neonatally ETS exposed females upregulate the estrogen response late and apical junction pathways.

In control males there were no Hallmark Pathways upregulated by either LPS and sham challenge. Neonatally ETS exposed males had 24 Hallmark Pathways upregulated by LPS challenge compared to sham (Table 3) while sham challenge upregulated no pathways. Enrichment plots (Supplemental Figure 8) and core enrichment gene sets (Supplemental Figure 9) show patterns of gene expression that define neonatally ETS exposed males in the response to LPS challenge. Interestingly, there are several unique Hallmark Pathways when comparing males and females. Beside the absence of Hallmark Pathways regulated by LPS challenge in control males compared to 27 pathways in control females, neonatally ETS exposed males surprisingly had upregulated spermatogenesis compared to sham challenge males. LPS challenge in neonatally ETS exposed females upregulated apical junctions, estrogen response late, glycolysis, epithelial mesenchymal transition, and angiogenesis while males did not.

When neonatally ETS exposed female mice were compared with filtered air controls with sham challenge, the allograft rejection Hallmark Pathway was upregulated in control female mice (Figure 6A-B). Following LPS challenge, filtered air control female mice had upregulated oxidative phosphorylation Hallmark Pathway compared to neonatally ETS exposed female mice (Figure 6C-D). No Hallmark Pathways were significantly enriched in male mice between the filtered air and neonatally ETS exposed chorts. These findings show biologically meaningful changes in groups of genes between males and females based on neonatal ETS exposure.

2.4.6 Differences in gene ontology, KEGG Pathways, and Reactome on the basis of sex

To further understand the changes in lung transcriptome due to neonatal ETS exposure, differentially expressed genes with at least 2-fold difference in expression were used to determine gene ontology biological processes. Gene ontology assigns genes to tiers of biological processes that range from broad to concise without determining dependency [24]. Differentially expressed

genes from filtered air control female mice challenged with LPS generated many gene ontology biological processes (GO:BP). The top 20 are in Table 4 and include regulation of MyD88 toll-like receptor signaling pathway and several other pathways expected to be upregulated following LPS challenge. The differentially expressed genes up in sham challenge control female mice only returned 18 GO:BP annotations (Table 5) including neuronal action potential, drug metabolic process, sodium ion transport, fatty acid metabolic process, and inorganic cation transmembrane transport. Differentially expressed genes from the lungs of neonatal ETS exposed female mice given LPS challenge returned many GO:BP. The top 20 GO:BP for ETS exposed females challenged with LPS is Table 6. Like control females challenged with LPS, many GO:BP are related to the immune response. The top differentially expressed genes from neonatally ETS exposed female mice given sham challenge returned only 10 GO:BP (Table 7).

in control males challenged with LPS, many GO:BP were returned (top-20 Table 8). However, the results for males is not predominantly immune responses as seen in females. Control males given sham challenged also generated many GO:BP with the top-20 in Table 9. Differentially expressed genes in neonatally ETS exposed males challenged with LPS generated many GO:BP with many immune responses represented (Table 10) similar to female mice under the same exposure and challenge (Table 6). Neonatally ETS exposed male mice given sham challenge also generated many GO:BP (top-20 Table 11) with response to oxygen deficit and toxicant metabolism seeming to be important. These shows a clear pattern of altered immune response following LPS challenge between males and females neonatally exposed to ETS.

We also examined the Kyoto Encyclopedia of Genes and Genomes (KEGG) Pathways using differentially expressed genes with at least 2-fold difference. Sham challenge of control female mice resulted in upregulation of only the drug metabolism – cytochrome P450 KEGG Pathway (Figure 7A). By contrast LPS challenge of control female mice resulted in upregulation of 52 mostly immune related KEGG Pathways (Figure 7B). Sham challenge in neonatally ETS exposed female mice resulted in upregulation of the valine, leucine, isoleucine degradation and

metabolic pathways as well as the drug metabolism – cytochrome P450 KEGG Pathway in control females (Figure 7C). And neonatal ETS exposed female mice challenged with LPS produced 56 mostly immune related KEGG Pathways (Figure 7D). In control males given sham challenge there were 43 KEGG Pathways representing a variety of cellular responses (Figure 7E). Control males given LPS challenge had 40 mostly immune related KEGG Pathways (Figure 7F). Neonatally ETS exposed males given sham challenge had only the drug metabolism – cytochrome P450 and metabolism of xenobiotics by cytochrome P450 KEGG Pathways (Figure 7G) while LPS challenge again resulted in 38 mostly immune KEGG Pathways (Figure 7H). This suggests an interesting counter regulation of cytochromes during immune response to LPS in addition to the differences between exposure-challenge cohorts on the basis of sex.

Finally, we looked at reactome pathways using the differentially expressed genes from each exposure challenge cohort. Reactome pathways are curated networks that represent our current understanding of the effect of an entity on the biological system it effects, such as a drug, vaccine or pathogen [33]. No reactome pathways were indicated in control females given a sham challenge. Control female mice challenged with LPS demonstrated 37 reactome pathways that include many immune responses (Figure 8A). Neonatally ETS exposed sham challenged female mice only upregulated the FMO oxidises nucleophiles and cysteine formation from homocysteine reactome pathways (Figure 8B) while LPS challenge resulted in 37 predominantly immune related reactomes (Figure 8C). Sham challenge of control male mice resulted in only 9 upregulated reactome pathways (Figure 8D) while LPS challenge resulted in 100 reactome pathways being upregulated (Figure 8E). Neonatally ETS exposed male mice given a sham challenge only upregulate the FMO oxidises nucleophiles reactome pathway (Figure 8F) while LPS challenge resulted in 30 mostly immune related reactome pathways to be increased (Figure 8G). This indicates additional differences between males and females based on early-life exposure and immune challenge.

2.5. Discussion

We demonstrate that neonatal ETS exposure in this murine model is sufficient to induce lung injury detectable by elevated BALF protein that coincides with altered immune cells profile and abundance in the lungs of females but not males in adulthood. Female mice exposed to ETS neonatally have elevated macrophages in their lungs and exacerbated immune responses to LPS with increased macrophages and neutrophils. Immune challenge with LPS also exacerbated lung injury with markedly increased BALF protein. This phenotype correlates to changes in the pulmonary transcriptome that are also sex dependent. Specifically neonatal ETS exposure results in reduction in genes in the allograft rejection Hallmark Pathway at rest and reduction in gene in the oxidative phosphorylation Hallmark Pathway following LPS challenge compared to age-matched controls. Males and females exhibit different clustering patterns based on neonatal ETS exposure following LPS challenge with males exposed to ETS clustering with males only exposed to filtered air. These differences also manifest in differences in Hallmark Pathways, KEGG Pathways, and reactome pathway between males and females depending on their ETS exposure. Interestingly we also note that immune challenge with LPS seems to be counter-regulated with cytochrome P450 responses that are important for xenobiotic metabolism and detoxification.

Lung injury is commonly associated with increased protein levels in the lung lining fluid due to disruption in the epithelium with increased abundance of serum protein which can be detected by lavage; however, protein level alone is insufficient to determine the relevance of lung injury as many homeostatic lung proteins are in found in high abundance in the lung lining fluid including surfactant proteins and club cell secretory protein [34]. Recent proteomic approaches have attempted to identify and quantify proteins in the lung lining to improve the diagnostic value of lavage samples. One study of BALF from 36 acute respiratory distress patients found 114 differentially abundant proteins between survivors and non-survivors that mapped to pathways such as coagulation/thrombosis, acute phase response signaling, and complement activation [35]. While we did not attempt to quantify any proteins in the lavage fluid from our subjects, we

did identify upregulation of complement and coagulation Hallmark Pathways following LPS challenge. A recent meta-analysis of protein abundances in lavage fluid found increased lavage fluid protein, albumin, phospholipase A2 activity, Serpine1, soluble receptor for advanced glycation end products, and platelet activating factor-acetyl choline to be predictive of acute respiratory distress syndrome [36]. The female neonatally exposed mice had elevated lavage protein and five not-significantly upregulated phospholipase A2 genes while serpine1 was not significantly downregulated compared to filtered air controls. As phospholipase A2 production of platelet activating factor is a common pathway in immune cells, which were elevating in the lungs of neonatally ETS exposed female mice, this may indicate a sex-dependent predisposition to future acute respiratory distress. Proteomic evaluation of lavage fluids from patients exposed to ETS in early childhood or in animal models may provide evidence of lasting pre-disposition to lung injury following neonatal ETS exposure.

Differences between male and female pediatric populations have been observed with regards to respiratory infections, asthma, wheezing, respiratory distress syndrome, and chronic lung diseases of prematurity [37]. Males have increased rates of most pediatric lung diseases including acute respiratory illness and interstitial lung disease during early life [37] while females have higher asthma rates and greater severity in adulthood [38]. Exposure to intrauterine tobacco smoke influences lung growth in females such as to increase airways resistance, which is normally much lower than males [39]. These sex differences that seem to favor females during early life may be largely attributable to the larger airways relative to lung volume in females relative to males [40]. This makes conditions such as common respiratory infections that can restrict airflow less pronounced in pediatric females relative to males despite males and females having equivalent rates of infection [37]. However, puberty is associated with the end of lung growth and the beginning of lung function decline in females at an earlier timepoint than males which may partially explain the increased asthma rates of women compared to men, whose lung continue growing for a lunger duration [40]. There is evidence that sex hormones also play an important

role in lung diseases. Immune cells express estrogen, androgen, and progesterone receptors and experiments have shown that estrogen signaling increases the number of macrophages as well as their expression of toll-like receptors and phagocytosis [41]. The increased number of macrophages found in neonatally ETS exposed mice may also contribute to sex hormone dependent effects due to their production of aromatase, which converts testosterone to estradiol [41]. As estrogen receptor signaling can recruit a variety of histone modifying enzymes including acetyl and methyl transferases [42], it is unclear if the altered immune response observed in neonatally ETS exposed females is caused by the presence of predominantly female sex hormones or if inflammation causes the generation of female sex hormones. Further research will need to be done to assess hormone levels and chromatin configurations in the lung through such exposures.

Studies have shown that ETS exposure alters pulmonary immune function in adults [43, 44] and children [45-48]. We found increased immune cells in the lavage fluid of neonatally ETS exposed females in adulthood that indicates lasting effects of such an exposure. By contrast no difference in lavage cells was seen in males. Increased immune cells, particularly neutrophils and polarized macrophages, in the lungs have been associated with a number of diseases including asthma [49, 50], chronic obstructive pulmonary disease [51, 52], and acute respiratory distress syndrome [53, 54]. Interestingly control males had no distinguishing Hallmark Pathways between sham and LPS challenge while neonatally ETS exposed males did. LPS challenge has been shown to induce gene transcription in waves with early response genes such as tumor necrosis factor alpha and interleukin 6 peaking within the first 4 hours post-challenge [55]. This study also found that interleukin 8 (IL-8) rose in the first wave and again in a second wave that peaked at the end of 24 hours. The cxcl8 gene that encodes IL-8 does not exist in the murine genome with other genes—cxcl1 and cxcl2—performing similar roles in immune cell recruitment. This confounds studying human lung diseases using a murine model. One study that examined expression of human Cxcl8 in murine bronchial epithelium found reduced mortality from

Pseudomonas aeruginosa with concurrent lung remodeling, elevated inflammation, and leaky tight junctions. They showed elevated neutrophils and TNF-a and reduced macrophages. While IL-8 was associated with increased TNF-a, there was no significant change in CXCL1, CXCL2, or IL-6. Importantly, they also found increased TGF-b1, Foxp3, Tbet, and IL-10 suggesting an induction of regulatory T helper cells [56]. A study in healthy human male adults age 18-40 years old found that gene expression largely returned to normal by 24 post LPS challenge using 2 or 3 ng/kg body mass of LPS intravenously [57]. It is difficult to associate human and mouse LPS dosing due to varying sensitivity to LPS between species with humans being at least a thousand times more sensitive to LPS than mice [58]. However, we intentionally used the lowest dose to produce a detectable immune response in the lungs in healthy adult mice for our study, and our dose is over 3000 fold less than the lethal dose for fifty percent (25.6 mg/kg) of similarly aged wild-type mice [59]. We assessed immune responses 24 hours post challenge when responses should be resolving, but female mice and neonatally ETS challenged males had increased expression of immune-related genes. The absence of Hallmark Pathways between sham and LPS challenged male mice is consistent with findings in healthy adult males. This failure to resolve immune responses following neonatal ETS exposure may represent a pathway in which ETS exposure exacerbates respiratory infections in males that are already more common than in females [60]. The induction of many of the same pathways seen in both control and neonatally ETS challenged females suggests both an important sex difference in response to immune challenge and a shift between the typical resolution of the immune response due to early life ETS in males. How this is controlled is an important question to answer given the higher mortality in infant males.

We found Hallmark Pathways upregulated in female but nor male mice in the control group compared to the neonatally ETS exposed cohorts. The increase in allograft rejection in the sham challenge group may indicate an impaired immune response following neonatal ETS challenge. The Hallmark Pathway for allograft rejection is itself composed from 200 genes from 190

collections generally associated with immune function [23]. Females of many species including mice and humans exhibit a different pattern of response to stimuli including immune responses that begin prior to sexual differentiation and is effected by sex hormones [61]. In general, females have more robust immune responses [62] and adaptive immune responses but also experience higher levels of autoimmune disease [63]. The downregulation of immune pathways following neonatal ETS exposure in females may predispose females to increased frequency or severity of respiratory infections [60]. In comparison of female mice challenged with LPS between control and neonatal ETS exposure, the control females had increased oxidative phosphorylation Hallmark Pathway. The oxidative phosphorylation hallmark pathway is 200 genes derived from 93 gene sets that are part of the oxidative phosphorylation pathway, which is the major source of cellular energy during respiration [23]. One study that examined human females found that increased oxidative phosphorylation Hallmark Pathway was associated with a longer reproductive age between menarche and menopause [64]. Maintenance of energy metabolism is important for brain health and cognitive function with several chronic neurological diseases being associated with disruptions to the cellular machinery essential for oxidative phosphorylation [64]. The oxidative phosphorylation Hallmark Pathway has also been shown to be decreased by estrogen receptor positive cancer cells lines treated with all-trans retinoic acid, the active metabolite of vitamin A [65]. In the context of cancer, all-trans retinoic acid is viewed as an effective disruptor of cellular processes that allow the cancer to grow [66]. There is evidence that ETS exposure does increase cancer rates [67] and particularly among women [68]. Recent studies have shown the oxidative phosphorylation Hallmark Pathway to be regulated in breast [69] and colon cancers [70]. Whether the increase in oxidative phosphorylation following neonatal ETS exposure is indicative of any predisposition to cancer would be entirely speculative at this point but may be of value as cancer remains the second leading cause of death.

Of interest is that we observed increased drug metabolism cytochrome P450 Kyoto Encyclopedia of Genes and Genomes (KEGG) pathways in sham challenged females compared

wot those challenged with LPS and sham challenged neonatally ETS exposed males compared to LPS challenge. Cytochrome P450 drug metabolism is an important pathway for metabolism of drugs as well es xenobiotics [71]. ETS contains several toxicants that require enzymes to detoxify and allow excretion from the body. The active addictive compound in tobacco smoke, nicotine, is metabolized by cytochrome family 2 subfamily A member 6 (CYP2A6) which is part of the drug metabolism cytochrome P450 KEGG pathway [72]. Another cytochrome P450, Cyp1A1 has been shown to be associated with sex differences in DNA alterations in smokers with females having more Cyp1A1 and more DNA adducts in non-tumor lung tissue [73]. Smokers are known to have increased Cyp1A1 expression compared to nonsmokers [74]. A study in rats showed that pulmonary Cyp1A1 can be induced by ETS as early as after one day of exposure in neonates [75]. One study showed that LPS reduced Cyp1A1 in bovine mammary epithelial cells [76] while another showed that LPS in conjunction with the plant oil constituent phenanthrene induced Cyp1A1 in Atlantic cod [77]. In the latter report, LPS was shown to induce expression of aryl hydrocarbon receptor, which then may be responsive to phenanthrene resulting in expression of Cyp1A1. This is supported by the finding that LPS-induced tumor necrosis factor alpha (TNFα) suppressed Cyp1A1 production in a mouse hepatoma cell line while LPS did not [78]. It has also been shown that LPS induction of aryl hydrocarbon receptor is dependent on nuclear factor kappa B in human dendritic cells with increased Cyp1A1 only following administration of 2,3,7,8-tetrachlorodibenzo-ρ-dioxin [79]. Other reports show that cytochrome family 2 subfamily C member11 and cytochrome family 2 subfamily B member 1 may also be suppressed by LPS in the liver [80]. In the lung, cytochrome family 2 subfamily C member 44, cytochrome family 2 subfamily J member 9, cytochrome family 4 subfamily A member 12a, cytochrome family 4 subfamily A member 12b, cytochrome family 4 subfamily F member 13, and cytochrome family 4 subfamily F member 16 were shown to be downregulated following intraperitoneal LPS challenge but the regulation of cytochromes differed by organ [81]. In our model, there was no administration of exogenous aryl hydrocarbon ligand and a reduction in the drug metabolism by cytochrome

P450 KEGG pathway. While Cyp1A1 is inducible by compounds in ETS while being immediately downregulated by LPS, other cytochromes may only be downregulated by inflammation. This introduces the possibility that exposure to ETS reduces immune responses that reduce gene expression of cytochromes that are required for clearance of inhaled toxicants creating a vicious cycle of toxicant and pathogen mediated lung damage.

Our study varied from a typical human exposure as we only exposed the neonatal mice to ETS for 5 days. Many children that are exposed to ETS are exposed in the home for the duration of their childhood for several hours each day [82, 83]. Our exposure model covered the period of rapid alveolarization that begins postnatally until postnatal day 7 in mice [84] but begins prenatally and lasts until age 3 in humans [85]. The mice were also moved out of ETS exposed cage immediately following exposure removing residual thirdhand tobacco smoke except what was on the pups and their dam. It is possible that increasing the duration of the exposure would alter the findings of the study. ETS is a known source of endotoxin (LPS) and studies have shown that sensitization with LPS reduces subsequent responses resulting in endotoxin tolerance [86]. We do not see evidence of endotoxin tolerance and used low endotoxin paper bedding to reduce exposure outside the experimental procedures [87]; however, we do not assess the activity of immune cells recruited to the lung directly. Sex differences in lung function may also contribute to differential responses to neonatal ETS, and this is an important question to answer by monitoring ETS dose during exposures which was outside the scope of this project.

The lungs continue to grow beyond the alveolar period. In mice the lungs continue to grow into adulthood with maximal size achieved at various ages depending on the strain [88]. One possible confounding factor in comparison of neonatally exposed versus adult controls is the smaller area of the lungs in younger mice making recovery of more cells per volume easier. Higashimoto et al found the number of lavage cells recovered from 26-month-old geriatric C57BL/6 mice to be not significantly higher than those in 6-week-old young adult mice [31]; however, 24-month-old C57BL/6 mice have reduced lung volume compared to 6-month-old mice

[89]. While the volume recovered did not change between exposure groups, we cannot be sure that the abundance of cells per surface area of lung did not influence the results. In humans, the lungs continue to grow into early adulthood when maximal lung function is achieved [3]. Measuring lung growth and density of lung immune cells *in situ* during or following neonatal ETS exposure could answer questions of whether there are changes to these parameters that impact the number of cells recovered by lavage.

Our study shows that neonatal ETS exposure produces lasting and sexually dimorphic effects on the immune system in a murine model. The findings suggest that exposure to ETS can affect immune resolution in males and strength of immune responses in females. In addition, we found evidence that immune responses and xenobiotic metabolism may be counter regulated, which may predispose ETS exposed children to a vicious circle of infection and reduced capacity to detoxify inhaled particulate from ETS. The result of such a cycle could be the significant decrease in pulmonary function seen in children exposed to ETS which is linked to reduced maximal lung function and reduced quality of life.

2.6. Figures and Tables

Figure 1:

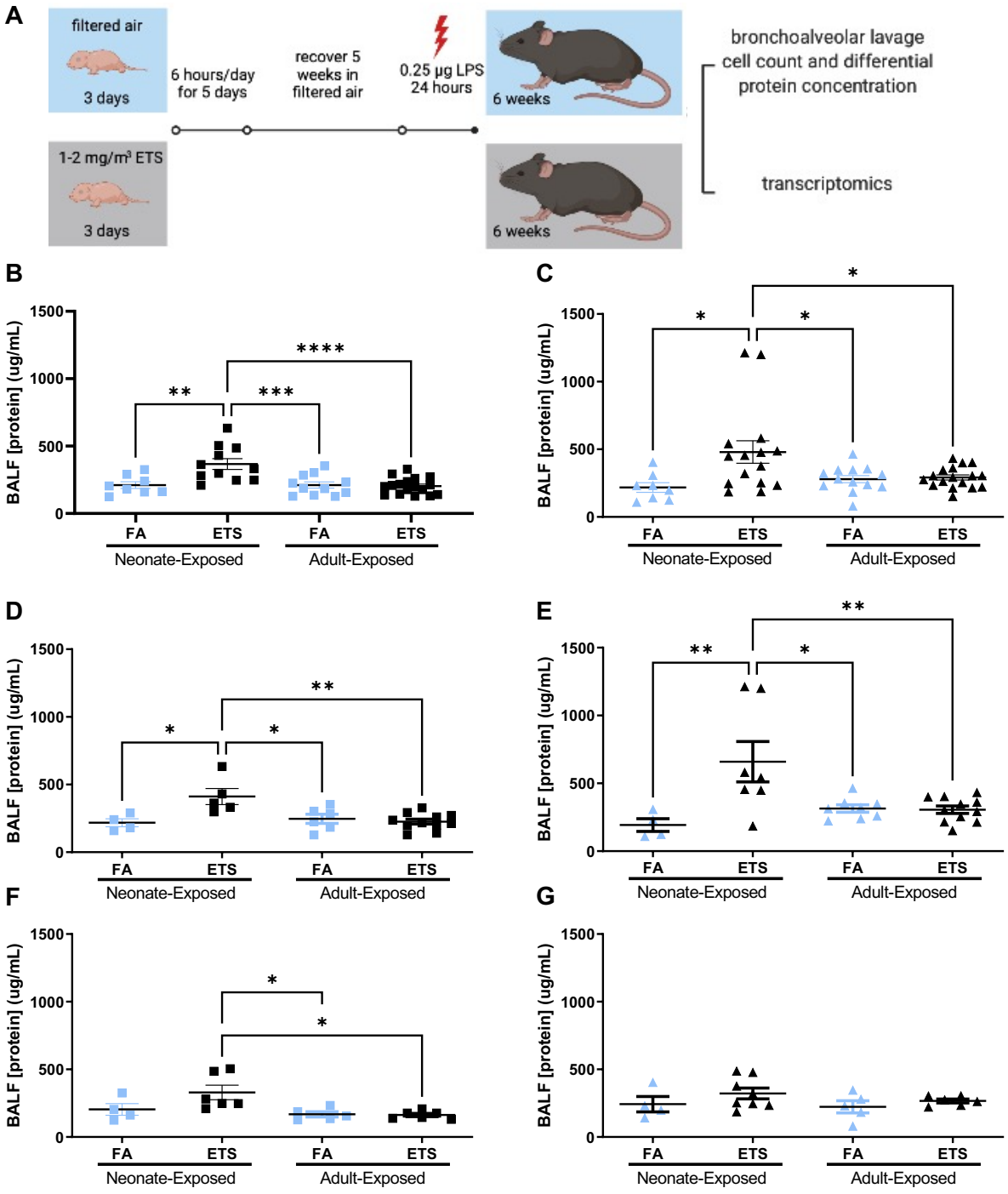

Figure 1: Early-life ETS Exposure Increases BALF Protein in Adult Mice After LPS and Vehicle Challenge Consistent with Lung Injury. Mouse pups at postnatal day 3 and 6-week-

old adult controls were exposed to ETS or filtered air for 6 hours per day for 5 days and then allowed to recover for 5 weeks in filtered air before oropharyngeal challenge 24 hours prior to bronchoalveolar lavage fluid being collected at necropsy **(A)**. Protein concentration was determined by BCA assay. Neonatally exposed mice had elevated lung proteins in BALF compared to age-matched and adult control mice when challenged with vehicle (PBS) **(B)** or 0.25 μg LPS **(C)**. The increase in BALF proteins was more pronounced in female mice challenged with vehicle **(D)** or LPS **(E)** than in males challenged with vehicle **(F)** or LPS **(G)**. * $p<0.05$, ** $p<0.01$, *** $p<0.001$, **** $p<0.0001$ by ANOVA with Tukey post-hoc correction for multiple comparisons.

Figure 2:

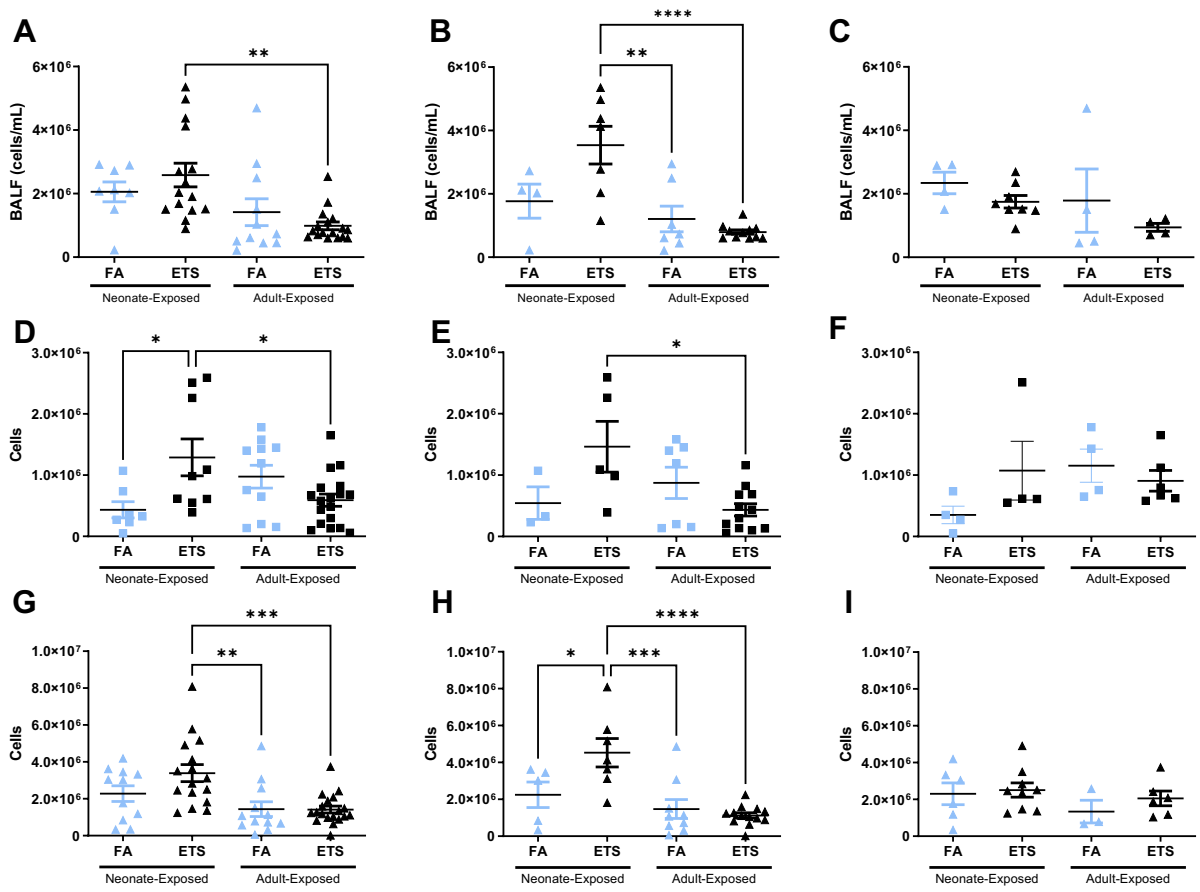

Figure 2: Abundance of Immune Cells in the BALF of Adult Mice Exposed to ETS During the Early Postnatal Period is Altered Compared to Age-Matched and Adult Controls. BALF cells were counted, and total BALF volume measured. Total cells were the product of cell concentration and BALF volume for samples with 50% recovery or greater. Following LPS challenge, neonatally ETS exposed mice had more cells/mL than adult controls **(A)**, which was drive by female neonatally ETS exposed adult mice **(B)** not males **(C)**. Neonatally ETS exposed mice had more total cells in their BALF when challenged with vehicle than age-matched or adult controls **(D)** which was driven by increased numbers of cells in females **(E)** not males **(F)**. Following LPS challenge, more BALF cells were recovered from neonatally ETS exposed mice than adult controls **(G)** and females had more BALF cells than age-matched or adult controls **(H)**

while males did not **(I)**. * $p<0.05$, ** $p<0.01$, *** $p<0.001$, **** $p<0.0001$ by ANOVA with Tukey post-hoc correction for multiple comparisons.

Figure 3:

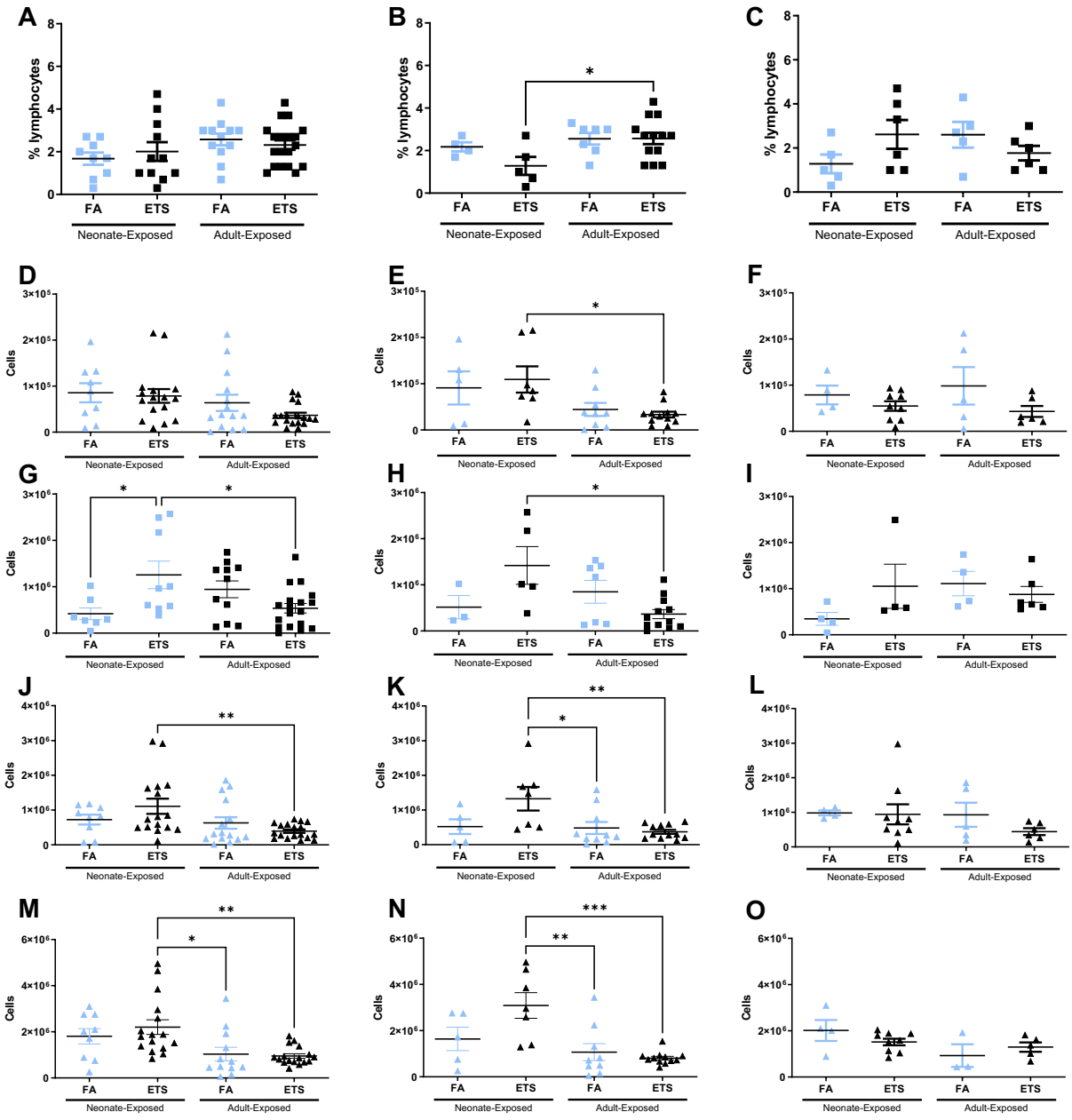

Figure 3: BALF Cell Differentials are Altered by Early-life ETS Exposure in Adult Mice. BALF cells were fixed to cytospin slides and stained using KwikDiff. Cell differentials were determined by counting 300 cells per slide and calculating percentage of each cell type. Total cell differentials were the product of the percent differential and total cells for samples with 50% or greater recovery. Vehicle challenged neonatally exposed adult mice trended toward reduced lymphocytes

as a percent of BALF cells compared to adult controls **(A)**, and female neonatally ETS exposed **(B)** but not male **(C)** adult mice had reduced lymphocytes as a percent of BALF cells compared to adult controls. Total lymphocytes were not different between groups when challenged with LPS **(D)**; however, female neonatally ETS exposed adult mice had more lymphocytes in their BALF than female adult control mice **(E)** while males did not **(F)**. Neonatally ETS exposed adult mice had more macrophages when challenged with vehicle than age-matched and adult controls **(G)**, which was more pronounced in females **(H)** than males **(I)**. Neonatally ETS exposed adult mice had more macrophages when challenged with LPS than adult controls **(J)** which was more pronounced in females **(K)** than males **(L)**. Neonatally ETS exposed adult mice had more neutrophils when challenged with LPS than adult controls **(M)** which was more pronounced in females **(N)** than males **(O)**. * $p<0.05$, ** $p<0.01$, *** $p<0.001$, **** $p<0.0001$ by ANOVA with Tukey post-hoc correction for multiple comparisons.

Figure 4:

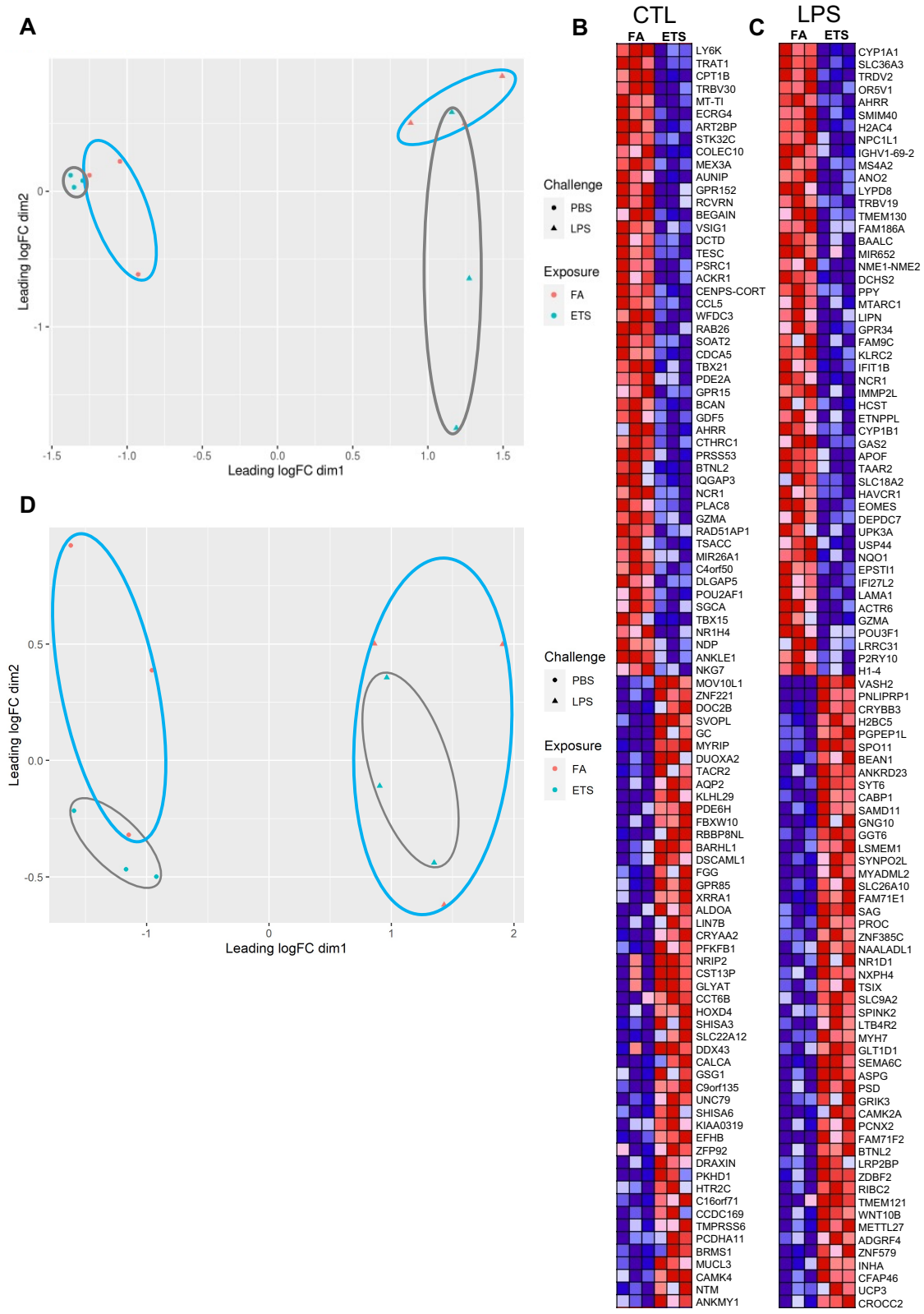
A
Leading logFC dim2
Leading logFC dim1
Challenge
PBS
LPS
Exposure
FA
ETS
B
CTL
FA
ETS
C
LPS
FA
ETS
D
Leading logFC dim2
Leading logFC dim1
Challenge
PBS
LPS
Exposure
FA
ETS

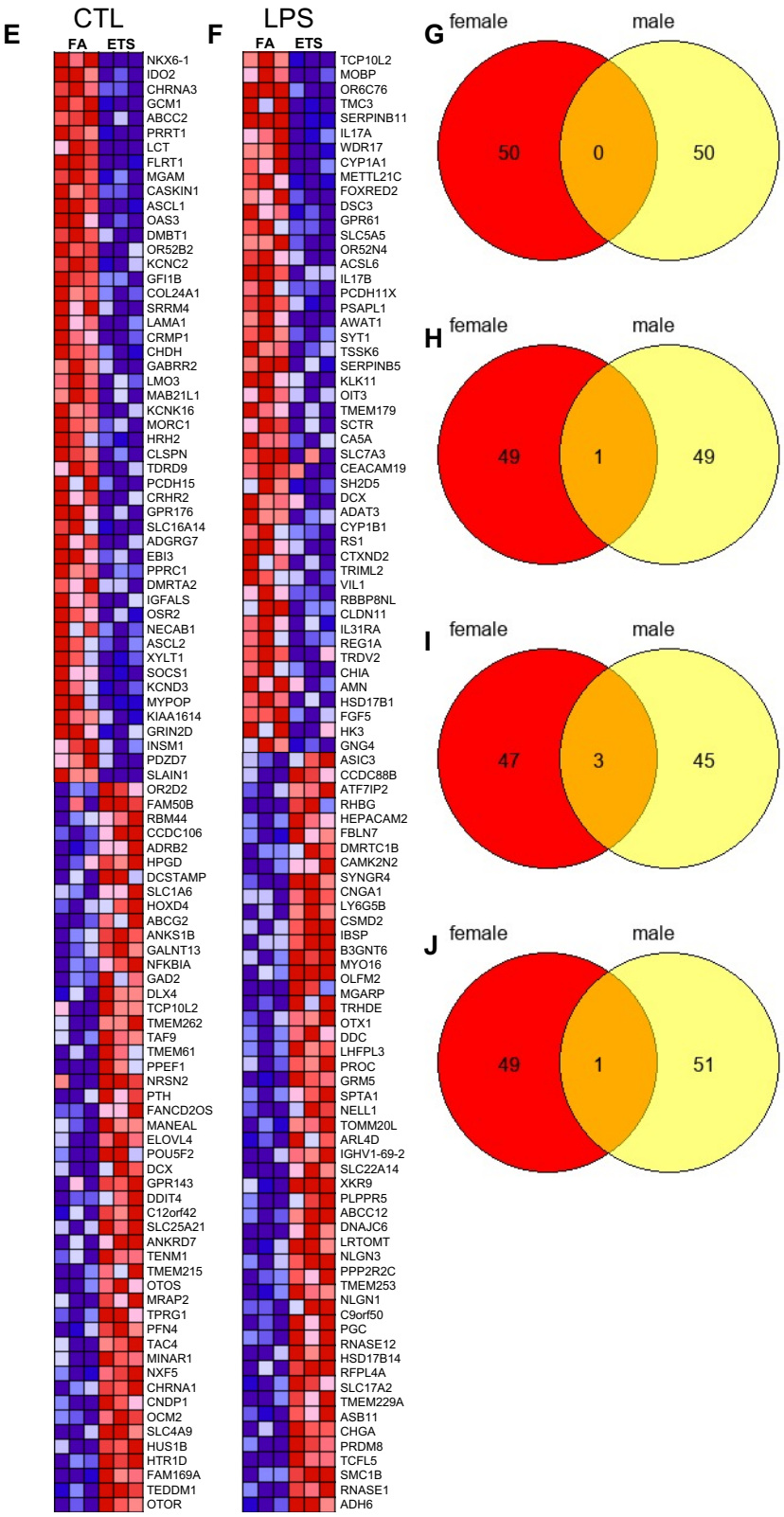
E
CTL
FA
ETS
NKX6-1
IDO2
CHRNA3
GCM1
ABCC2
PRRT1
LCT
FLRT1
MGAM
CASKIN1
ASCL1
OAS3
DMBT1
OR52B2
KCNC2
GFI1B
COL24A1
SRRM4
LAMA1
CRMP1
CHDH
GABRR2
LMO3
MAB21L1
KCNK16
MORC1
HRH2
CLSPN
TDRD9
PCDH15
CRHR2
GPR176
SLC16A14
ADGRG7
EBI3
PPRC1
DMRTA2
IGFALS
OSR2
NECAB1
ASCL2
XYLT1
SOCS1
KCND3
MYPOP
KIAA1614
GRIN2D
INSM1
PDZD7
SLAIN1
OR2D2
FAM50B
RBM44
CCDC106
ADRB2
HPGD
DCSTAMP
SLC1A6
HOXD4
ABCG2
ANKS1B
GALNT13
NFKBIA
GAD2
DLX4
TCP10L2
TMEM262
TAF9
TMEM61
PPEF1
NRSN2
PTH
FANCD2OS
MANEAL
ELOVL4
POU5F2
DCX
GPR143
DDIT4
C12orf42
SLC25A21
ANKRD7
TENM1
TMEM215
OTOS
MRAP2
TPRG1
PFN4
TAC4
MINAR1
NXF5
CHRNA1
CNDP1
OCM2
SLC4A9
HUS1B
HTR1D
FAM169A
TEDDM1
OTOR
F
LPS
FA
ETS
TCP10L2
MOBP
OR6C76
TMC3
SERPINB11
IL17A
WDR17
CYP1A1
METTL21C
FOXRED2
DSC3
GPR61
SLC5A5
OR52N4
ACSL6
IL17B
PCDH11X
PSAPL1
AWAT1
SYT1
TSSK6
SERPINB5
KLK11
OIT3
TMEM179
SCTR
CA5A
SLC7A3
CEACAM19
SH2D5
DCX
ADAT3
CYP1B1
RS1
CTXND2
TRIML2
VIL1
RBBP8NL
CLDN11
IL31RA
REG1A
TRDV2
CHIA
AMN
HSD17B1
FGF5
HK3
GNG4
ASIC3
CCDC88B
ATF7IP2
RHBG
HEPACAM2
FBLN7
DMRTC1B
CAMK2N2
SYNGR4
CNGA1
LY6G5B
CSMD2
IBSP
B3GNT6
MYO16
OLFM2
MGARP
TRHDE
OTX1
DDC
LHFPL3
PROC
GRM5
SPTA1
NELL1
TOMM20L
ARL4D
IGHV1-69-2
SLC22A14
XKR9
PLPPR5
ABCC12
DNAJC6
LRTOMT
NLGN3
PPP2R2C
TMEM253
NLGN1
C9orf50
PGC
RNASE12
HSD17B14
RFPL4A
SLC17A2
TMEM229A
ASB11
CHGA
PRDM8
TCFL5
SMC1B
RNASE1
ADH6
G
female
male
50
0
50
H
female
male
49
1
49
I
female
male
47
3
45
J
female
male
49
1
51

Figure 4: Early-life ETS Exposure Alters Gene Expression Profiles in the Lungs of Adult Mice Compared to Control. Total RNA from lung plucks of 6-week-old mice exposed to ETS or filtered air from for 5 days starting at postnatal day 3 and allowed to recover in filtered air for 5 weeks was isolated and used for transcriptomic analysis. Differentially expressed genes (DEGs) were determined from count data using edgeR and Limma-Voom. Multidimensional scaling plot shows that ETS-exposed female mice cluster more closely with filtered air controls when challenged with vehicle than when challenged with LPS **(A)**. Top 50 DEGs for filtered air control and ETS exposed female mice challenged with vehicle **(B)** and LPS **(C)**. Multidimensional scaling plot shows neonatally ETS exposed mice are virtually indistinguishable from filtered air mice 24 hours after LPS challenge **(D)**. Top 50 DEGs for filtered air control and ETS exposed male mice challenged with vehicle **(E)** and LPS **(F)**. Common genes between female and male filtered air sham challenged **(G)**, ETS exposed sham challenged **(H)**, filtered air LPS challenged **(I)**, and ETS exposed LPS challenged mice **(J)**.

Figure 5:

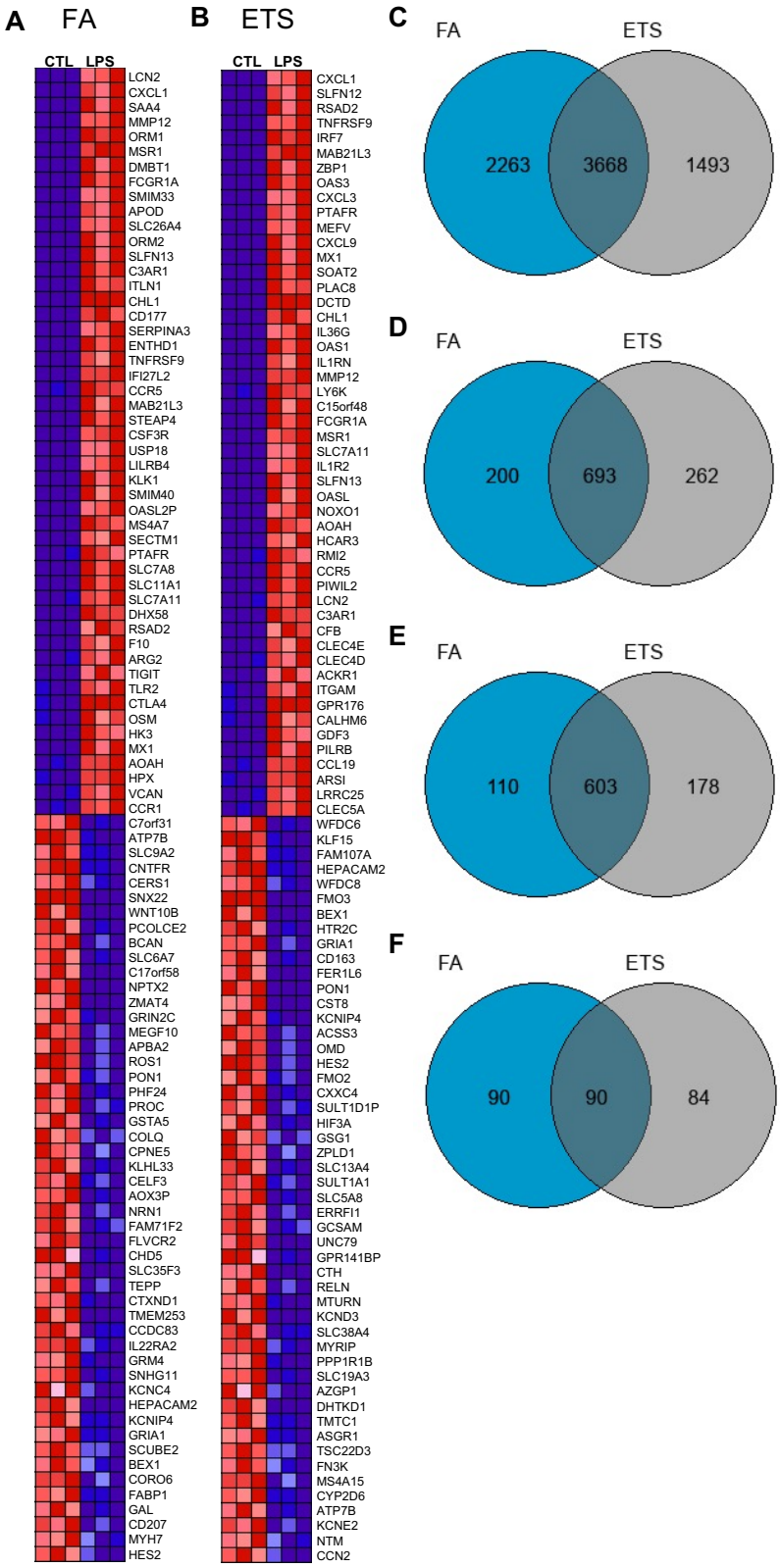
A
FA
CTL LPS
LCN2
CXCL1
SAA4
MMP12
ORM1
MSR1
DMBT1
FCGR1A
SMIM33
APOD
SLC26A4
ORM2
SLFN13
C3AR1
ITLN1
CHL1
CD177
SERPINA3
ENTHD1
TNFRSF9
IFI27L2
CCR5
MAB21L3
STEAP4
CSF3R
USP18
LILRB4
KLK1
SMIM40
OASL2P
MS4A7
SECTM1
PTAFR
SLC7A8
SLC11A1
SLC7A11
DHX58
RSAD2
F10
ARG2
TIGIT
TLR2
CTLA4
OSM
HK3
MX1
AOAH
HPX
VCAN
CCR1
C7orf31
ATP7B
SLC9A2
CNTFR
CERS1
SNX22
WNT10B
PCOLCE2
BCAN
SLC6A7
C17orf58
NPTX2
ZMAT4
GRIN2C
MEGF10
APBA2
ROS1
PON1
PHF24
PROC
GSTA5
COLQ
CPNE5
KLHL33
CELF3
AOX3P
NRN1
FAM71F2
FLVCR2
CHD5
SLC35F3
TEPP
CTXND1
TMEM253
CCDC83
IL22RA2
GRM4
SNHG11
KCNC4
HEPACAM2
KCNIP4
GRIA1
SCUBE2
BEX1
CORO6
FABP1
GAL
CD207
MYH7
HES2
B
ETS
CTL LPS
CXCL1
SLFN12
RSAD2
TNFRSF9
IRF7
MAB21L3
ZBP1
OAS3
CXCL3
PTAFR
MEFV
CXCL9
MX1
SOAT2
PLAC8
DCTD
CHL1
IL36G
OAS1
IL1RN
MMP12
LY6K
C15orf48
FCGR1A
MSR1
SLC7A11
IL1R2
SLFN13
OASL
NOXO1
AOAH
HCAR3
RMI2
CCR5
PIWIL2
LCN2
C3AR1
CFB
CLEC4E
CLEC4D
ACKR1
ITGAM
GPR176
CALHM6
GDF3
PILRB
CCL19
ARSI
LRRC25
CLEC5A
WFDC6
KLF15
FAM107A
HEPACAM2
WFDC8
FMO3
BEX1
HTR2C
GRIA1
CD163
FER1L6
PON1
CST8
KCNIP4
ACSS3
OMD
HES2
FMO2
CXXC4
SULT1D1P
HIF3A
GSG1
ZPLD1
SLC13A4
SULT1A1
SLC5A8
ERRFI1
GCSAM
UNC79
GPR141BP
CTH
RELN
MTURN
KCND3
SLC38A4
MYRIP
PPP1R1B
SLC19A3
AZGP1
DHTKD1
TMTC1
ASGR1
TSC22D3
FN3K
MS4A15
CYP2D6
ATP7B
KCNE2
NTM
CCN2
C
FA
ETS
2263
3668
1493
D
FA
ETS
200
693
262
E
FA
ETS
110
603
178
F
FA
ETS
90
90
84

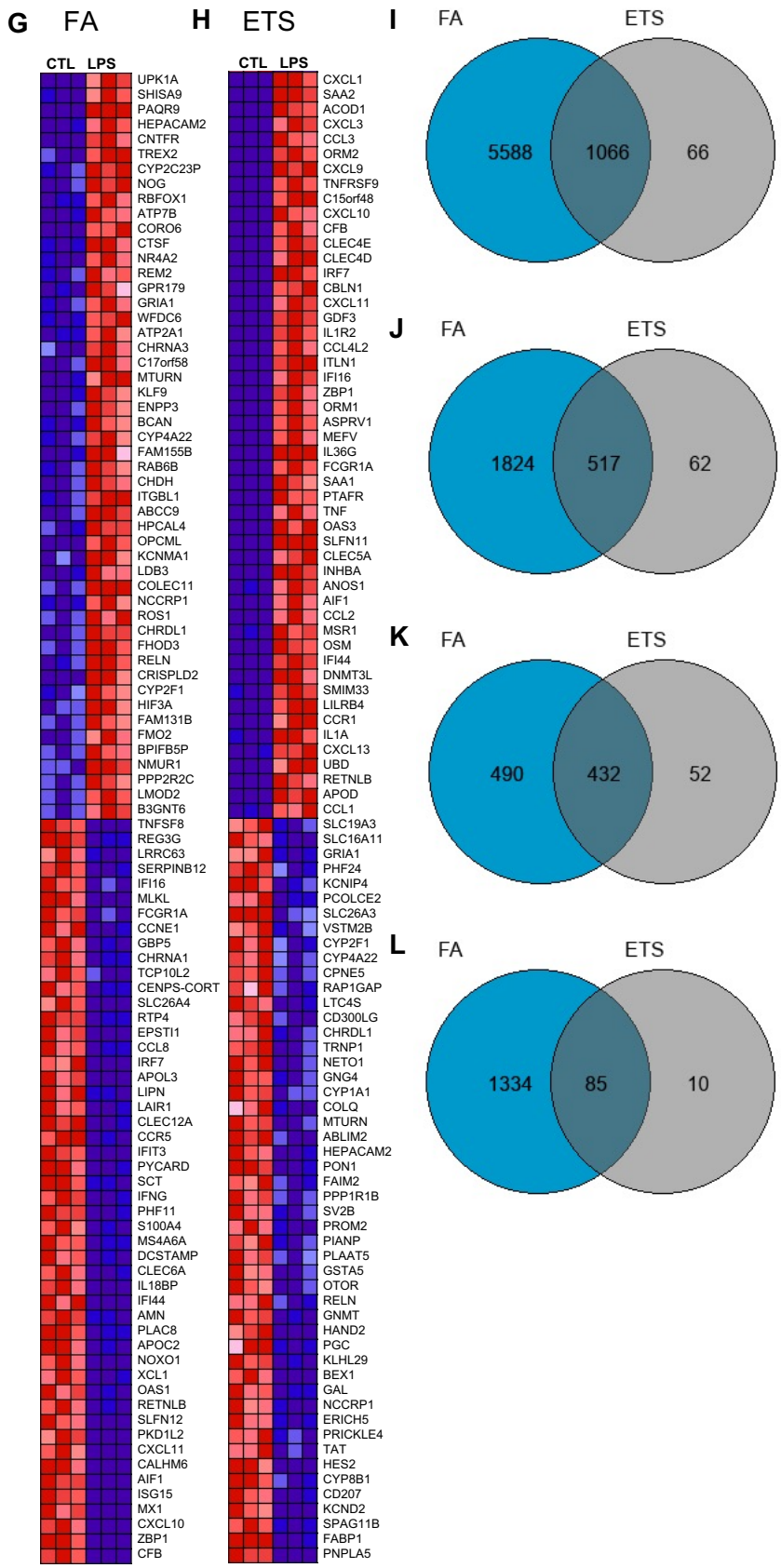
G
FA
CTL LPS
UPK1A
SHISA9
PAQR9
HEPACAM2
CNTFR
TREX2
CYP2C23P
NOG
RBFOX1
ATP7B
CORO6
CTSF
NR4A2
REM2
GPR179
GRIA1
WFDC6
ATP2A1
CHRNA3
C17orf58
MTURN
KLF9
ENPP3
BCAN
CYP4A22
FAM155B
RAB6B
CHDH
ITGBL1
ABCC9
HPCAL4
OPCML
KCNMA1
LDB3
COLEC11
NCCRP1
ROS1
CHRDL1
FHOD3
RELN
CRISPLD2
CYP2F1
HIF3A
FAM131B
FMO2
BPIFB5P
NMUR1
PPP2R2C
LMOD2
B3GNT6
TNFSF8
REG3G
LRRC63
SERPINB12
IFI16
MLKL
FCGR1A
CCNE1
GBP5
CHRNA1
TCP10L2
CENPS-CORT
SLC26A4
RTP4
EPSTI1
CCL8
IRF7
APOL3
LIPN
LAIR1
CLEC12A
CCR5
IFIT3
PYCARD
SCT
IFNG
PHF11
S100A4
MS4A6A
DCSTAMP
CLEC6A
IL18BP
IFI44
AMN
PLAC8
APOC2
NOXO1
XCL1
OAS1
RETNLB
SLFN12
PKD1L2
CXCL11
CALHM6
AIF1
ISG15
MX1
CXCL10
ZBP1
CFB
H
ETS
CTL LPS
CXCL1
SAA2
ACOD1
CXCL3
CCL3
ORM2
CXCL9
TNFRSF9
C15orf48
CXCL10
CFB
CLEC4E
CLEC4D
IRF7
CBLN1
CXCL11
GDF3
IL1R2
CCL4L2
ITLN1
IFI16
ZBP1
ORM1
ASPRV1
MEFV
IL36G
FCGR1A
SAA1
PTAFR
TNF
OAS3
SLFN11
CLEC5A
INHBA
ANOS1
AIF1
CCL2
MSR1
OSM
IFI44
DNMT3L
SMIM33
LILRB4
CCR1
IL1A
CXCL13
UBD
RETNLB
APOD
CCL1
SLC19A3
SLC16A11
GRIA1
PHF24
KCNIP4
PCOLCE2
SLC26A3
VSTM2B
CYP2F1
CYP4A22
CPNE5
RAP1GAP
LTC4S
CD300LG
CHRDL1
TRNP1
NETO1
GNG4
CYP1A1
COLQ
MTURN
ABLIM2
HEPACAM2
PON1
FAIM2
PPP1R1B
SV2B
PROM2
PIANP
PLAAT5
GSTA5
OTOR
RELN
GNMT
HAND2
PGC
KLHL29
BEX1
GAL
NCCRP1
ERICH5
PRICKLE4
TAT
HES2
CYP8B1
CD207
KCND2
SPAG11B
FABP1
PNPLA5
I
FA
ETS
5588
1066
66
J
FA
ETS
1824
517
62
K
FA
ETS
490
432
52
L
FA
ETS
1334
85
10

Figure 5: Indirect comparison of transcriptomes from early-life ETS exposed lungs to controls shows additional differences. DEGs from female mouse lungs from vehicle-LPS FA **(A)** and ETS **(B)** were compared to determine differences between the regulated genes. There were 5,161 DEGs in ETS exposed mice and 5,931 DGEs in FA exposed female mice when comparing vehicle and LPS challenges **(C)**. A cut-off of 2-fold expression was used to focus on the highest differentially expressed transcripts induced by LPS challenge **(D)**. There were many more DEGs upregulated by LPS and a greater percentage of shared DEGs between control and ETS exposed female mice **(E)** than in PBS between control and ETS **(F)**. DEGs from male mouse lungs from vehicle-LPS FA **(G)** and ETS **(H)**. There were 1,132 DEGs in ETS exposed mice and 5,654 DGEs in FA exposed male mice when comparing vehicle and LPS challenges **(I)**. A cut-off of 2-fold expression was used to focus on the highest differentially expressed transcripts induced by LPS challenge **(J)**. LPS challenge resulted in upregulation of more genes in neonatally ETS exposed males **(K)** than PBS, which resulted in significant upregulation of genes in control males **(L)**.

Figure 6:

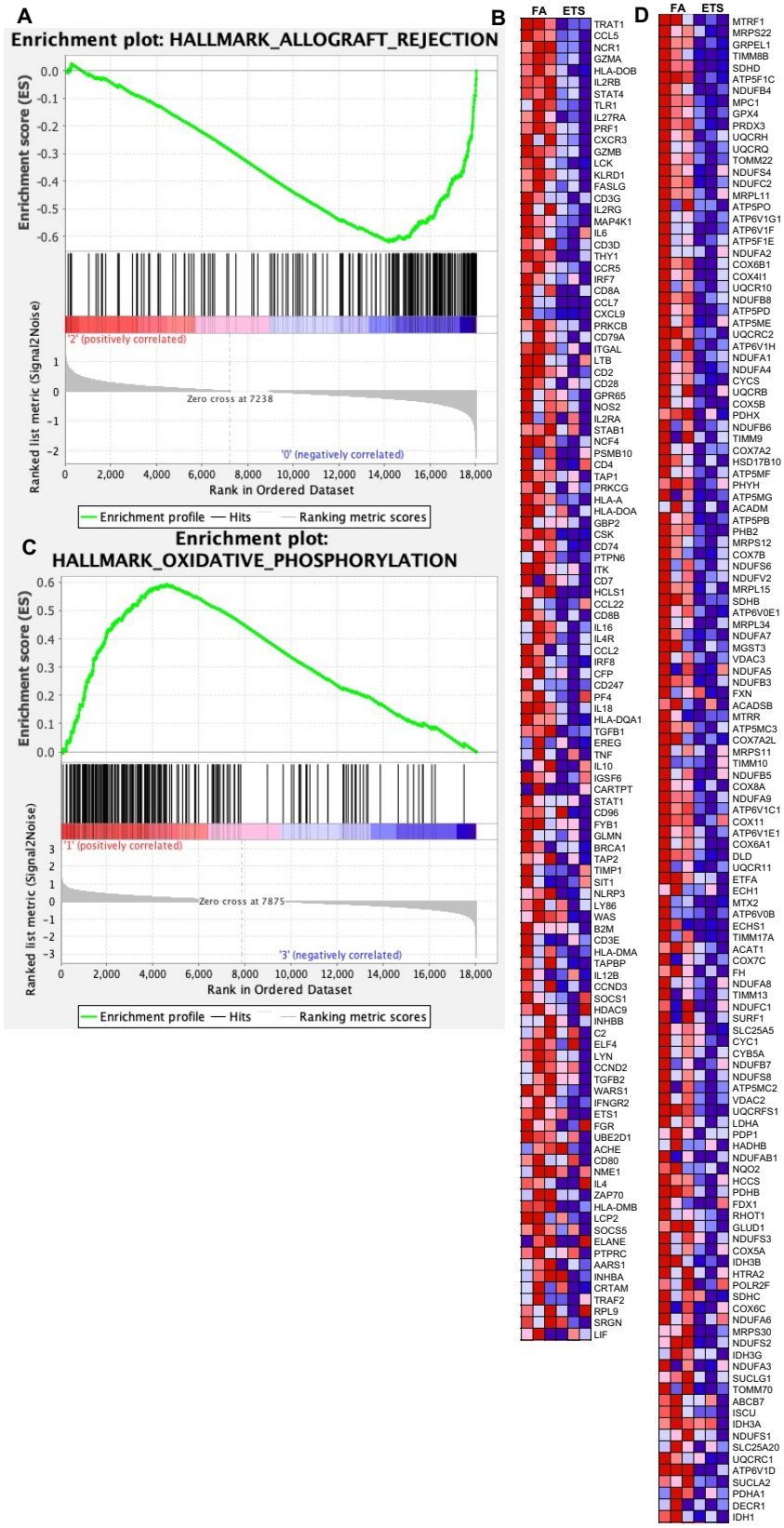
A
Enrichment plot: HALLMARK_ALLOGRAFT_REJECTION
Enrichment score (ES)
Ranked list metric (Signal2Noise)
'2' (positively correlated)
'0' (negatively correlated)
Zero cross at 7238
Rank in Ordered Dataset
Enrichment profile
Hits
Ranking metric scores
B
FA
ETS
TRAT1
CCL5
NCR1
GZMA
HLA-DOB
IL2RB
STAT4
TLR1
IL27RA
PRF1
CXCR3
GZMB
LCK
KLRD1
FASLG
CD3G
IL2RG
MAP4K1
IL6
CD3D
THY1
CCR5
IRF7
CD8A
CCL7
CXCL9
PRKCB
CD79A
ITGAL
LTB
CD2
CD28
GPR65
NOS2
IL2RA
STAB1
NCF4
PSMB10
CD4
TAP1
PRKCG
HLA-A
HLA-DOA
GBP2
CSK
CD74
PTPN6
ITK
CD7
HCLS1
CCL22
CD8B
IL16
IL4R
CCL2
IRF8
CFP
CD247
PF4
IL18
HLA-DQA1
TGFB1
EREG
TNF
IL10
IGSF6
CARTPT
STAT1
CD96
FYB1
GLMN
BRCA1
TAP2
TIMP1
SIT1
NLRP3
LY86
WAS
B2M
CD3E
HLA-DMA
TAPBP
IL12B
CCND3
SOCS1
HDAC9
INHBB
C2
ELF4
LYN
CCND2
TGFB2
WARS1
IFNGR2
ETS1
FGR
UBE2D1
ACHE
CD80
NME1
IL4
ZAP70
HLA-DMB
LCP2
SOCS5
ELANE
PTPRC
AARS1
INHBA
CRTAM
TRAF2
RPL9
SRGN
LIF
C
Enrichment plot:
HALLMARK_OXIDATIVE_PHOSPHORYLATION
Enrichment score (ES)
Ranked list metric (Signal2Noise)
'1' (positively correlated)
'3' (negatively correlated)
Zero cross at 7875
Rank in Ordered Dataset
Enrichment profile
Hits
Ranking metric scores
D
FA
ETS
MTRF1
MRPS22
GRPEL1
TIMM8B
SDHD
ATP5F1C
NDUFB4
MPC1
GPX4
PRDX3
UQCRH
UQCRQ
TOMM22
NDUFS4
NDUFC2
MRPL11
ATP5PO
ATP6V1G1
ATP6V1F
ATP5F1E
NDUFA2
COX6B1
COX4I1
UQCR10
NDUFB8
ATP5PD
ATP5ME
UQCRC2
ATP6V1H
NDUFA1
NDUFA4
CYCS
UQCRB
COX5B
PDHX
NDUFB6
TIMM9
COX7A2
HSD17B10
ATP5MF
PHYH
ATP5MG
ACADM
ATP5PB
PHB2
MRPS12
COX7B
NDUFS6
NDUFV2
MRPL15
SDHB
ATP6V0E1
MRPL34
NDUFA7
MGST3
VDAC3
NDUFA5
NDUFB3
FXN
ACADSB
MTRR
ATP5MC3
COX7A2L
MRPS11
TIMM10
NDUFB5
COX8A
NDUFA9
ATP6V1C1
COX11
ATP6V1E1
COX6A1
DLD
UQCR11
ETFA
ECH1
MTX2
ATP6V0B
ECHS1
TIMM17A
ACAT1
COX7C
FH
NDUFA8
TIMM13
NDUFC1
SURF1
SLC25A5
CYC1
CYB5A
NDUFB7
NDUFS8
ATP5MC2
VDAC2
UQCRFS1
LDHA
PDP1
HADHB
NDUFAB1
NQO2
HCCS
PDHB
FDX1
RHOT1
GLUD1
NDUFS3
COX5A
IDH3B
HTRA2
POLR2F
SDHC
COX6C
NDUFA6
MRPS30
NDUFS2
IDH3G
NDUFA3
SUCLG1
TOMM70
ABCB7
ISCU
IDH3A
NDUFS1
SLC25A20
UQCRC1
ATP6V1D
SUCLA2
PDHA1
DECR1
IDH1

Figure 6: Gene Set Enrichment Analysis Reveals Significant Differences in Hallmark Pathways Between Adult Mice Neonatally Exposed to ETS compared to Controls. Trimmed counts and sample metadata were used to determine differential Hallmark Pathways using Gene Set Enrichment Analysis (GSEA). Hallmark Allograft Rejection pathway is upregulated in female mice exposed to FA compared to ETS with vehicle challenge illustrated by the enrichment score **(A)** and core enrichment genes **(B)**. Hallmark Oxidative Phosphorylation pathway is upregulated in female mice exposed to FA compared to ETS with LPS challenge **(C)** with core enrichment genes **(D)**.

Figure 7:

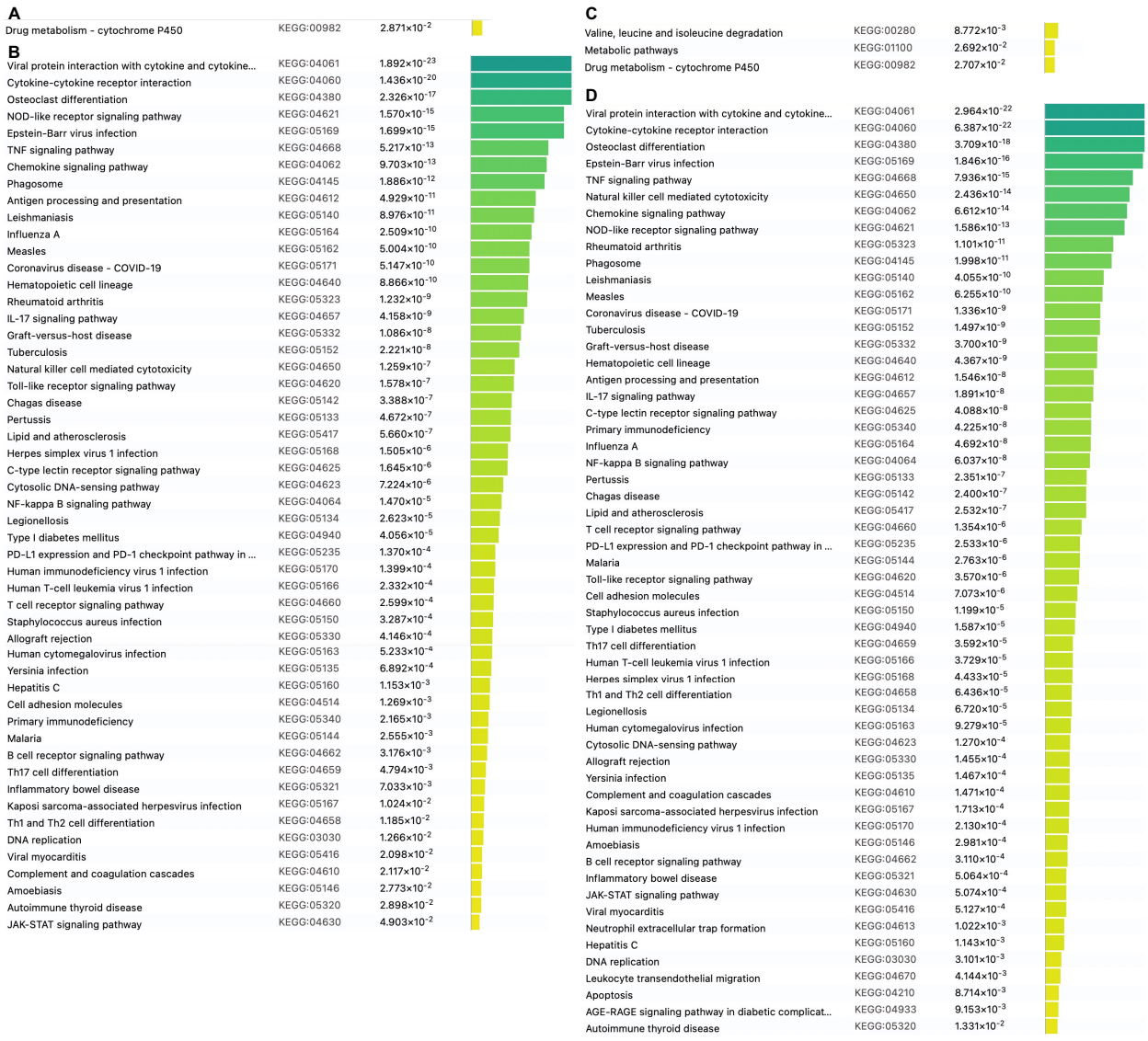
A
Drug metabolism - cytochrome P450 KEGG:00982 2.871×10-2
B
Viral protein interaction with cytokine and cytokine... KEGG:04061 1.892×10-23
Cytokine-cytokine receptor interaction KEGG:04060 1.436×10-20
Osteoclast differentiation KEGG:04380 2.326×10-17
NOD-like receptor signaling pathway KEGG:04621 1.570×10-15
Epstein-Barr virus infection KEGG:05169 1.699×10-15
TNF signaling pathway KEGG:04668 5.217×10-13
Chemokine signaling pathway KEGG:04062 9.703×10-13
Phagosome KEGG:04145 1.886×10-12
Antigen processing and presentation KEGG:04612 4.929×10-11
Leishmaniasis KEGG:05140 8.976×10-11
Influenza A KEGG:05164 2.509×10-10
Measles KEGG:05162 5.004×10-10
Coronavirus disease - COVID-19 KEGG:05171 5.147×10-10
Hematopoietic cell lineage KEGG:04640 8.866×10-10
Rheumatoid arthritis KEGG:05323 1.232×10-9
IL-17 signaling pathway KEGG:04657 4.158×10-9
Graft-versus-host disease KEGG:05332 1.086×10-8
Tuberculosis KEGG:05152 2.221×10-8
Natural killer cell mediated cytotoxicity KEGG:04650 1.259×10-7
Toll-like receptor signaling pathway KEGG:04620 1.578×10-7
Chagas disease KEGG:05142 3.388×10-7
Pertussis KEGG:05133 4.672×10-7
Lipid and atherosclerosis KEGG:05417 5.660×10-7
Herpes simplex virus 1 infection KEGG:05168 1.505×10-6
C-type lectin receptor signaling pathway KEGG:04625 1.645×10-6
Cytosolic DNA-sensing pathway KEGG:04623 7.224×10-6
NF-kappa B signaling pathway KEGG:04064 1.470×10-5
Legionellosis KEGG:05134 2.623×10-5
Type I diabetes mellitus KEGG:04940 4.056×10-5
PD-L1 expression and PD-1 checkpoint pathway in ... KEGG:05235 1.370×10-4
Human immunodeficiency virus 1 infection KEGG:05170 1.399×10-4
Human T-cell leukemia virus 1 infection KEGG:05166 2.332×10-4
T cell receptor signaling pathway KEGG:04660 2.599×10-4
Staphylococcus aureus infection KEGG:05150 3.287×10-4
Allograft rejection KEGG:05330 4.146×10-4
Human cytomegalovirus infection KEGG:05163 5.233×10-4
Yersinia infection KEGG:05135 6.892×10-4
Hepatitis C KEGG:05160 1.153×10-3
Cell adhesion molecules KEGG:04514 1.269×10-3
Primary immunodeficiency KEGG:05340 2.165×10-3
Malaria KEGG:05144 2.555×10-3
B cell receptor signaling pathway KEGG:04662 3.176×10-3
Th17 cell differentiation KEGG:04659 4.794×10-3
Inflammatory bowel disease KEGG:05321 7.033×10-3
Kaposi sarcoma-associated herpesvirus infection KEGG:05167 1.024×10-2
Th1 and Th2 cell differentiation KEGG:04658 1.185×10-2
DNA replication KEGG:03030 1.266×10-2
Viral myocarditis KEGG:05416 2.098×10-2
Complement and coagulation cascades KEGG:04610 2.117×10-2
Amoebiasis KEGG:05146 2.773×10-2
Autoimmune thyroid disease KEGG:05320 2.898×10-2
JAK-STAT signaling pathway KEGG:04630 4.903×10-2
C
Valine, leucine and isoleucine degradation KEGG:00280 8.772×10-3
Metabolic pathways KEGG:01100 2.692×10-2
Drug metabolism - cytochrome P450 KEGG:00982 2.707×10-2
D
Viral protein interaction with cytokine and cytokine... KEGG:04061 2.964×10-22
Cytokine-cytokine receptor interaction KEGG:04060 6.387×10-22
Osteoclast differentiation KEGG:04380 3.709×10-18
Epstein-Barr virus infection KEGG:05169 1.846×10-16
TNF signaling pathway KEGG:04668 7.936×10-15
Natural killer cell mediated cytotoxicity KEGG:04650 2.436×10-14
Chemokine signaling pathway KEGG:04062 6.612×10-14
NOD-like receptor signaling pathway KEGG:04621 1.586×10-13
Rheumatoid arthritis KEGG:05323 1.101×10-11
Phagosome KEGG:04145 1.998×10-11
Leishmaniasis KEGG:05140 4.055×10-10
Measles KEGG:05162 6.255×10-10
Coronavirus disease - COVID-19 KEGG:05171 1.336×10-9
Tuberculosis KEGG:05152 1.497×10-9
Graft-versus-host disease KEGG:05332 3.700×10-9
Hematopoietic cell lineage KEGG:04640 4.367×10-9
Antigen processing and presentation KEGG:04612 1.546×10-8
IL-17 signaling pathway KEGG:04657 1.891×10-8
C-type lectin receptor signaling pathway KEGG:04625 4.088×10-8
Primary immunodeficiency KEGG:05340 4.225×10-8
Influenza A KEGG:05164 4.692×10-8
NF-kappa B signaling pathway KEGG:04064 6.037×10-8
Pertussis KEGG:05133 2.351×10-7
Chagas disease KEGG:05142 2.400×10-7
Lipid and atherosclerosis KEGG:05417 2.532×10-7
T cell receptor signaling pathway KEGG:04660 1.354×10-6
PD-L1 expression and PD-1 checkpoint pathway in ... KEGG:05235 2.533×10-6
Malaria KEGG:05144 2.763×10-6
Toll-like receptor signaling pathway KEGG:04620 3.570×10-6
Cell adhesion molecules KEGG:04514 7.073×10-6
Staphylococcus aureus infection KEGG:05150 1.199×10-5
Type I diabetes mellitus KEGG:04940 1.587×10-5
Th17 cell differentiation KEGG:04659 3.592×10-5
Human T-cell leukemia virus 1 infection KEGG:05166 3.729×10-5
Herpes simplex virus 1 infection KEGG:05168 4.433×10-5
Th1 and Th2 cell differentiation KEGG:04658 6.436×10-5
Legionellosis KEGG:05134 6.720×10-5
Human cytomegalovirus infection KEGG:05163 9.279×10-5
Cytosolic DNA-sensing pathway KEGG:04623 1.270×10-4
Allograft rejection KEGG:05330 1.455×10-4
Yersinia infection KEGG:05135 1.467×10-4
Complement and coagulation cascades KEGG:04610 1.471×10-4
Kaposi sarcoma-associated herpesvirus infection KEGG:05167 1.713×10-4
Human immunodeficiency virus 1 infection KEGG:05170 2.130×10-4
Amoebiasis KEGG:05146 2.981×10-4
B cell receptor signaling pathway KEGG:04662 3.110×10-4
Inflammatory bowel disease KEGG:05321 5.064×10-4
JAK-STAT signaling pathway KEGG:04630 5.074×10-4
Viral myocarditis KEGG:05416 5.127×10-4
Neutrophil extracellular trap formation KEGG:04613 1.022×10-3
Hepatitis C KEGG:05160 1.143×10-3
DNA replication KEGG:03030 3.101×10-3
Leukocyte transendothelial migration KEGG:04670 4.144×10-3
Apoptosis KEGG:04210 8.714×10-3
AGE-RAGE signaling pathway in diabetic complicat... KEGG:04933 9.153×10-3
Autoimmune thyroid disease KEGG:05320 1.331×10-2

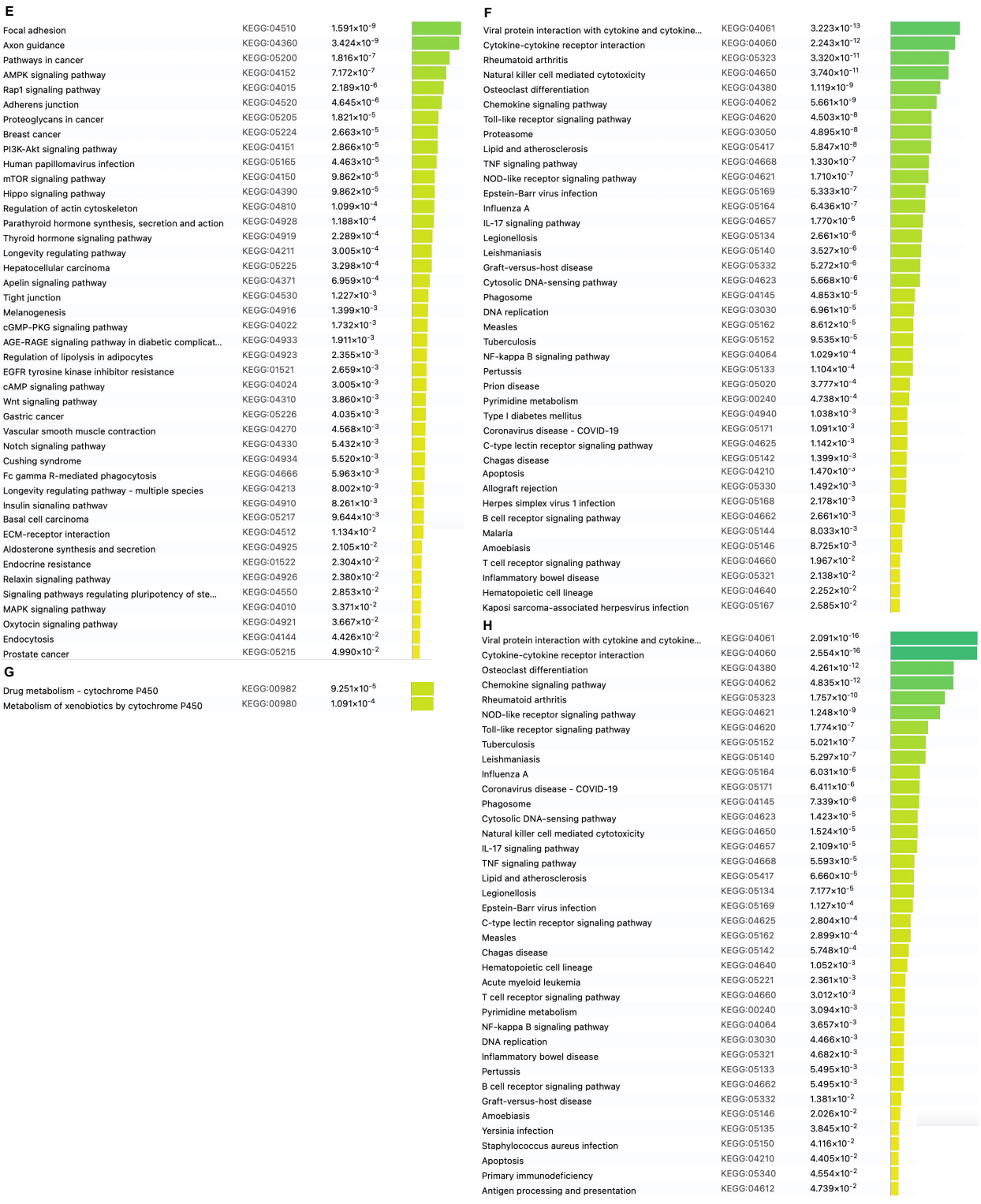

Figure 7: KEGG Pathway Analysis Reveals Altered Metabolic Pathways in ETS Exposed Lungs Compared to Control. DEGs with adjusted p-values < 0.05 and at least 2-fold expression difference were entered into gProfiler to determine KEGG pathways that are distinct between

treatments. Only one pathway was upregulated by vehicle challenge versus LPS challenge in control female mouse lungs **(A)**. By Contrast 52 KEGG pathways were upregulated by LPS challenge versus vehicle challenge in control female mouse lungs **(B)**. Early postnatal ETS exposure resulted in 3 KEGG pathways being significantly upregulated in female mice following vehicle challenge **(C)** and 56 KEGG pathways due to LPS challenge following early postnatal ETS exposure **(D)**. Male control mice had 43 KEGG pathways upregulated by sham challenge **(E)** compared to LPS challenge with 40 KEGG pathways upregulated **(F)**. Neonatally ETS exposed males had only 2 upregulated KEGG pathways with sham challenge **(G)** compared to 38 with LPS challenge **(H)**.

Figure 8:


A
Immune System REAC:R-MMU-... 2.346×10-46
Innate Immune System REAC:R-MMU-... 2.180×10-37
Neutrophil degranulation REAC:R-MMU-... 7.444×10-23
Chemokine receptors bind chemokines REAC:R-MMU-... 1.325×10-15
DAP12 interactions REAC:R-MMU-... 3.979×10-11
DAP12 signaling REAC:R-MMU-... 3.280×10-9
Antigen processing-Cross presentation REAC:R-MMU-... 3.446×10-9
Immunoregulatory interactions between a Lymphoi... REAC:R-MMU-... 1.956×10-8
PD-1 signaling REAC:R-MMU-... 2.836×10-8
Cytokine Signaling in Immune system REAC:R-MMU-... 4.293×10-8
Generation of second messenger molecules REAC:R-MMU-... 6.939×10-8
Adaptive Immune System REAC:R-MMU-... 2.142×10-7
Peptide ligand-binding receptors REAC:R-MMU-... 8.001×10-7
Class A/1 (Rhodopsin-like receptors) REAC:R-MMU-... 8.682×10-7
Translocation of ZAP-70 to Immunological synapse REAC:R-MMU-... 1.061×10-6
Phosphorylation of CD3 and TCR zeta chains REAC:R-MMU-... 4.754×10-6
ER-Phagosome pathway REAC:R-MMU-... 1.064×10-5
Activation of the pre-replicative complex REAC:R-MMU-... 1.099×10-4
RHO GTPases Activate NADPH Oxidases REAC:R-MMU-... 1.255×10-4
Antigen Presentation: Folding, assembly and pepti... REAC:R-MMU-... 1.292×10-4
GPCR ligand binding REAC:R-MMU-... 1.831×10-4
Signal regulatory protein family interactions REAC:R-MMU-... 1.879×10-4
Costimulation by the CD28 family REAC:R-MMU-... 2.139×10-4
Signaling by Interleukins REAC:R-MMU-... 2.978×10-4
TCR signaling REAC:R-MMU-... 3.778×10-4
DNA Replication REAC:R-MMU-... 5.004×10-4
Endosomal/Vacuolar pathway REAC:R-MMU-... 8.680×10-4
DNA Replication Pre-Initiation REAC:R-MMU-... 9.982×10-4
G1/S Transition REAC:R-MMU-... 1.140×10-3
Cross-presentation of particulate exogenous antig... REAC:R-MMU-... 1.373×10-3
Synthesis of DNA REAC:R-MMU-... 3.248×10-3
Interferon Signaling REAC:R-MMU-... 3.719×10-3
Downstream TCR signaling REAC:R-MMU-... 3.875×10-3
Mitotic G1 phase and G1/S transition REAC:R-MMU-... 1.597×10-2
S Phase REAC:R-MMU-... 1.854×10-2
Activation of ATR in response to replication stress REAC:R-MMU-... 3.958×10-2
GPVI-mediated activation cascade REAC:R-MMU-... 4.933×10-2
B
FMO oxidises nucleophiles REAC:R-MMU-... 3.207×10-4
Cysteine formation from homocysteine REAC:R-MMU-... 3.144×10-2
C
Immune System REAC:R-MMU-... 4.779×10-47
Innate Immune System REAC:R-MMU-... 1.819×10-32
Neutrophil degranulation REAC:R-MMU-... 3.482×10-21
Chemokine receptors bind chemokines REAC:R-MMU-... 1.232×10-14
DAP12 interactions REAC:R-MMU-... 2.835×10-10
Immunoregulatory interactions between a Lymphoi... REAC:R-MMU-... 6.899×10-10
Cytokine Signaling in Immune system REAC:R-MMU-... 3.143×10-9
DAP12 signaling REAC:R-MMU-... 1.758×10-8
Adaptive Immune System REAC:R-MMU-... 3.929×10-8
PD-1 signaling REAC:R-MMU-... 8.497×10-8
Class A/1 (Rhodopsin-like receptors) REAC:R-MMU-... 1.091×10-7
Generation of second messenger molecules REAC:R-MMU-... 2.249×10-7
Antigen processing-Cross presentation REAC:R-MMU-... 1.103×10-6
Peptide ligand-binding receptors REAC:R-MMU-... 1.933×10-6
Translocation of ZAP-70 to Immunological synapse REAC:R-MMU-... 2.625×10-6
Phosphorylation of CD3 and TCR zeta chains REAC:R-MMU-... 1.166×10-5
RHO GTPases Activate NADPH Oxidases REAC:R-MMU-... 2.124×10-5
Activation of the pre-replicative complex REAC:R-MMU-... 2.475×10-5
ER-Phagosome pathway REAC:R-MMU-... 3.284×10-5
GPCR ligand binding REAC:R-MMU-... 4.732×10-5
Costimulation by the CD28 family REAC:R-MMU-... 1.179×10-4
Signaling by Interleukins REAC:R-MMU-... 2.716×10-4
Antigen Presentation: Folding, assembly and pepti... REAC:R-MMU-... 3.851×10-4
Activation of ATR in response to replication stress REAC:R-MMU-... 1.487×10-3
GPVI-mediated activation cascade REAC:R-MMU-... 1.990×10-3
Cross-presentation of particulate exogenous antig... REAC:R-MMU-... 2.322×10-3
DNA Replication Pre-Initiation REAC:R-MMU-... 3.453×10-3
Dectin-2 family REAC:R-MMU-... 5.939×10-3
DNA Replication REAC:R-MMU-... 8.431×10-3
Interferon Signaling REAC:R-MMU-... 1.038×10-2
G1/S Transition REAC:R-MMU-... 1.734×10-2
Antiviral mechanism by IFN-stimulated genes REAC:R-MMU-... 1.813×10-2
Endosomal/Vacuolar pathway REAC:R-MMU-... 1.813×10-2
ROS and RNS production in phagocytes REAC:R-MMU-... 1.942×10-2
TCR signaling REAC:R-MMU-... 2.483×10-2
Interleukin-2 family signaling REAC:R-MMU-... 4.035×10-2
ISG15 antiviral mechanism REAC:R-MMU-... 4.770×10-2
D
Nervous system development REAC:R-MMU-... 7.576×10-9
Axon guidance REAC:R-MMU-... 2.175×10-8
Signaling by Receptor Tyrosine Kinases REAC:R-MMU-... 6.503×10-7
Developmental Biology REAC:R-MMU-... 1.273×10-5
Signal Transduction REAC:R-MMU-... 5.364×10-4
Carnitine metabolism REAC:R-MMU-... 1.137×10-2
RET signaling REAC:R-MMU-... 2.262×10-2
Negative regulation of the PI3K/AKT network REAC:R-MMU-... 4.281×10-2
Muscle contraction REAC:R-MMU-... 4.689×10-2
E
Immune System REAC:R-MMU-... 1.893×10-23
Innate Immune System REAC:R-MMU-... 4.613×10-21
Neutrophil degranulation REAC:R-MMU-... 7.497×10-13
DNA Replication REAC:R-MMU-... 2.793×10-12
Chemokine receptors bind chemokines REAC:R-MMU-... 1.030×10-11
Synthesis of DNA REAC:R-MMU-... 1.720×10-11
S Phase REAC:R-MMU-... 5.223×10-11
G1/S Transition REAC:R-MMU-... 1.054×10-10
DNA Replication Pre-Initiation REAC:R-MMU-... 5.492×10-9
Downstream TCR signaling REAC:R-MMU-... 8.607×10-9
Antigen processing-Cross presentation REAC:R-MMU-... 1.432×10-8
Mitotic G1 phase and G1/S transition REAC:R-MMU-... 1.733×10-8
SCF(Skp2)-mediated degradation of p27/p21 REAC:R-MMU-... 5.691×10-8
TCR signaling REAC:R-MMU-... 5.976×10-8
Cell Cycle, Mitotic REAC:R-MMU-... 6.229×10-8
Cyclin E associated events during G1/S transition REAC:R-MMU-... 1.407×10-7
Cyclin A:Cdk2-associated events at S phase entry REAC:R-MMU-... 2.429×10-7
Cytokine Signaling in Immune system REAC:R-MMU-... 3.546×10-7
Cell Cycle Checkpoints REAC:R-MMU-... 4.705×10-7
Cell Cycle REAC:R-MMU-... 4.847×10-7
C-type lectin receptors (CLRs) REAC:R-MMU-... 5.154×10-7
Cross-presentation of soluble exogenous antigens ... REAC:R-MMU-... 5.319×10-7
Mitotic Anaphase REAC:R-MMU-... 5.927×10-7
Activation of NF-kappaB in B cells REAC:R-MMU-... 6.295×10-7
Mitotic Metaphase and Anaphase REAC:R-MMU-... 6.743×10-7
Transcriptional regulation by RUNX2 REAC:R-MMU-... 8.387×10-7
Separation of Sister Chromatids REAC:R-MMU-... 1.082×10-6
Regulation of RUNX2 expression and activity REAC:R-MMU-... 1.459×10-6
Ubiquitin Mediated Degradation of Phosphorylated... REAC:R-MMU-... 2.007×10-6
p53-Independent DNA Damage Response REAC:R-MMU-... 2.007×10-6
p53-Independent G1/S DNA damage checkpoint REAC:R-MMU-... 2.007×10-6
G1/S DNA Damage Checkpoints REAC:R-MMU-... 2.489×10-6
The role of GTSE1 in G2/M progression after G2 ch... REAC:R-MMU-... 2.747×10-6
Interleukin-1 signaling REAC:R-MMU-... 3.365×10-6
APC/C-mediated degradation of cell cycle proteins REAC:R-MMU-... 3.517×10-6
Regulation of mitotic cell cycle REAC:R-MMU-... 3.517×10-6
TNFR2 non-canonical NF-kB pathway REAC:R-MMU-... 4.136×10-6
FBXL7 down-regulates AURKA during mitotic entry... REAC:R-MMU-... 4.968×10-6
Interleukin-1 family signaling REAC:R-MMU-... 6.655×10-6
Regulation of ornithine decarboxylase (ODC) REAC:R-MMU-... 8.940×10-6
p53-Dependent G1 DNA Damage Response REAC:R-MMU-... 1.022×10-5
p53-Dependent G1/S DNA damage checkpoint REAC:R-MMU-... 1.022×10-5
Metabolism of polyamines REAC:R-MMU-... 1.152×10-5
CDT1 association with the CDC6:ORC:origin compl... REAC:R-MMU-... 1.152×10-5
Ubiquitin-dependent degradation of Cyclin D REAC:R-MMU-... 1.206×10-5
CLEC7A (Dectin-1) signaling REAC:R-MMU-... 1.240×10-5
Downstream signaling events of B Cell Receptor (B... REAC:R-MMU-... 1.366×10-5
Autodegradation of the E3 ubiquitin ligase COP1 REAC:R-MMU-... 1.613×10-5
Assembly of the pre-replicative complex REAC:R-MMU-... 1.672×10-5
APC/C:Cdc20 mediated degradation of mitotic pro... REAC:R-MMU-... 1.711×10-5
Activation of APC/C and APC/C:Cdc20 mediated d... REAC:R-MMU-... 2.134×10-5
Regulation of RUNX3 expression and activity REAC:R-MMU-... 2.823×10-5
Degradation of AXIN REAC:R-MMU-... 2.823×10-5
Orc1 removal from chromatin REAC:R-MMU-... 3.368×10-5
Signaling by Interleukins REAC:R-MMU-... 4.073×10-5
Degradation of GLI1 by the proteasome REAC:R-MMU-... 4.806×10-5
Stabilization of p53 REAC:R-MMU-... 4.806×10-5
AUF1 (hnRNP D0) binds and destabilizes mRNA REAC:R-MMU-... 4.806×10-5
Cdc20:Phospho-APC/C mediated degradation of C... REAC:R-MMU-... 5.253×10-5
CDK-mediated phosphorylation and removal of Cdc6 REAC:R-MMU-... 5.253×10-5
Switching of origins to a post-replicative state REAC:R-MMU-... 5.424×10-5
NIK-->noncanonical NF-kB signaling REAC:R-MMU-... 6.209×10-5
Dectin-1 mediated noncanonical NF-kB signaling REAC:R-MMU-... 6.209×10-5
Degradation of DVL REAC:R-MMU-... 6.209×10-5
APC/C:Cdh1 mediated degradation of Cdc20 and o... REAC:R-MMU-... 6.518×10-5
APC:Cdc20 mediated degradation of cell cycle pro... REAC:R-MMU-... 6.518×10-5
PD-1 signaling REAC:R-MMU-... 6.608×10-5
DNA strand elongation REAC:R-MMU-... 6.608×10-5
Oxygen-dependent proline hydroxylation of Hypoxi... REAC:R-MMU-... 6.610×10-5
GLI3 is processed to GLI3R by the proteasome REAC:R-MMU-... 7.973×10-5
RUNX1 regulates transcription of genes involved in... REAC:R-MMU-... 8.306×10-5
Adaptive Immune System REAC:R-MMU-... 1.171×10-4
Cellular response to hypoxia REAC:R-MMU-... 1.603×10-4
Asymmetric localization of PCP proteins REAC:R-MMU-... 2.049×10-4
DAP12 interactions REAC:R-MMU-... 2.049×10-4
Autodegradation of Cdh1 by Cdh1:APC/C REAC:R-MMU-... 2.560×10-4
Hedgehog ligand biogenesis REAC:R-MMU-... 2.560×10-4
MAPK6/MAPK4 signaling REAC:R-MMU-... 2.975×10-4
Termination of translesion DNA synthesis REAC:R-MMU-... 3.311×10-4
G2/M Checkpoints REAC:R-MMU-... 4.080×10-4
Regulation of RAS by GAPs REAC:R-MMU-... 4.855×10-4
Signal regulatory protein family interactions REAC:R-MMU-... 5.486×10-4
APC/C:Cdc20 mediated degradation of Securin REAC:R-MMU-... 5.956×10-4
DNA Damage Bypass REAC:R-MMU-... 7.177×10-4
Regulation of PTEN stability and activity REAC:R-MMU-... 8.851×10-4
DAP12 signaling REAC:R-MMU-... 1.249×10-3
Peptide ligand-binding receptors REAC:R-MMU-... 1.250×10-3
Regulation of mRNA stability by proteins that bind ... REAC:R-MMU-... 1.844×10-3
PCNA-Dependent Long Patch Base Excision Repair REAC:R-MMU-... 1.874×10-3
Lagging Strand Synthesis REAC:R-MMU-... 1.874×10-3
Recognition of DNA damage by PCNA-containing r... REAC:R-MMU-... 2.288×10-3
Translesion synthesis by Y family DNA polymerase... REAC:R-MMU-... 3.309×10-3
Transcriptional regulation by RUNX3 REAC:R-MMU-... 3.721×10-3
Degradation of beta-catenin by the destruction co... REAC:R-MMU-... 3.721×10-3
ABC-family proteins mediated transport REAC:R-MMU-... 4.269×10-3
M Phase REAC:R-MMU-... 5.014×10-3
G2/M Transition REAC:R-MMU-... 5.474×10-3
Leading Strand Synthesis REAC:R-MMU-... 5.667×10-3
Polymerase switching REAC:R-MMU-... 5.667×10-3
Immunoregulatory interactions between a Lymphoi... REAC:R-MMU-... 6.478×10-3

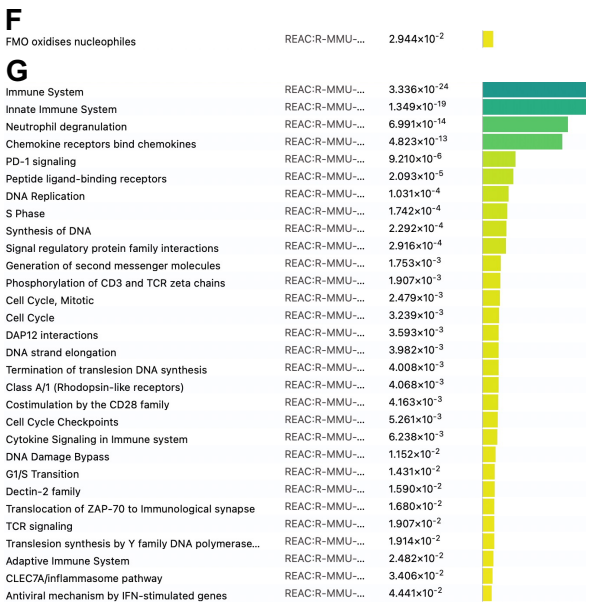

Figure 8: Reactome Analysis Reveals Altered Metabolic Pathways in ETS Exposed Lungs Compared to Control. DEGs with adjusted p-values < 0.05 and at least 2-fold expression difference were entered into gProfiler to determine Reactomes that are distinct between treatments. LPS challenge in control female mouse lungs resulted in 37 reactomes being upregulated compared to vehicle challenge **(A)**. In early-life ETS exposed female mice, only 2 reactomes were upregulated by vehicle challenge compared to LPS **(B)** LPS challenge resulted in upregulation of 37 reactomes compared to vehicle challenge **(C)**. Sham challenge in male control mice resulted in 9 reactomes being upregulated **(D)** compared to LPS challenge, which had 100 upregulated reactomes **(E)**. Neonatally ETS exposed males with sham challenge only had one upregulated reactome **(F)** while LPS challenge resulted in 30 upregulated reactomes **(G)**.

Table 1: Distinct Hallmark Pathways Signature is Generated Following LPS Challenge in Control Female Mice

NAME	SIZE	ES	NES	NOM p-val	FDR q-val
HALLMARK_COMPLEMENT	193	0.5877	1.5379	0.0000	0.0998
HALLMARK_KRAS_SIGNALING_UP	199	0.4720	1.6524	0.0000	0.1104
HALLMARK_INFLAMMATORY_RESPONSE	198	0.7036	1.4943	0.0000	0.1202
HALLMARK_IL2_STAT5_SIGNALING	199	0.5159	1.5777	0.0000	0.1257
HALLMARK_APOPTOSIS	161	0.4528	1.4518	0.0000	0.1442
HALLMARK_MTORC1_SIGNALING	199	0.6142	1.3816	0.0000	0.1542
HALLMARK_MYC_TARGETS_V1	200	0.7002	1.2778	0.0000	0.1568
HALLMARK_MYC_TARGETS_V2	57	0.6784	1.3283	0.0990	0.1600
HALLMARK_REACTIVE_OXYGEN_SPECIES_PATHWAY	49	0.5722	1.2787	0.0978	0.1613
HALLMARK_PI3K_AKT_MTOR_SIGNALING	105	0.4493	1.3874	0.0000	0.1629
HALLMARK_TNFA_SIGNALING_VIA_NFKB	198	0.6490	1.4577	0.0000	0.1634
HALLMARK_GLYCOLYSIS	200	0.3766	1.2960	0.0000	0.1638
HALLMARK_IL6_JAK_STAT3_SIGNALING	87	0.7577	1.3937	0.0000	0.1644
HALLMARK_ANGIOGENESIS	36	0.3963	1.3842	0.0000	0.1648
HALLMARK_P53_PATHWAY	200	0.3742	1.2869	0.0000	0.1663
HALLMARK_INTERFERON_ALPHA_RESPONSE	95	0.8286	1.2541	0.0000	0.1665
HALLMARK_UNFOLDED_PROTEIN_RESPONSE	112	0.5374	1.3304	0.2169	0.1666
HALLMARK_HYPOXIA	198	0.3239	1.2975	0.0000	0.1694
HALLMARK_DNA_REPAIR	149	0.5444	1.3349	0.0000	0.1712
HALLMARK_COAGULATION	138	0.4494	1.4043	0.0000	0.1721
HALLMARK_OXIDATIVE_PHOSPHORYLATION	198	0.5642	1.2510	0.1118	0.1746
HALLMARK_UV_RESPONSE_UP	156	0.3856	1.3002	0.0000	0.1754
HALLMARK_E2F_TARGETS	200	0.6666	1.3078	0.0858	0.1778
HALLMARK_EPITHELIAL_MESENCHYMAL_TRANSITION	196	0.3473	1.3351	0.0996	0.1794
HALLMARK_G2M_CHECKPOINT	196	0.5553	1.3624	0.1824	0.1869
HALLMARK_ALLOGRAFT_REJECTION	196	0.7596	1.3354	0.0000	0.1888
HALLMARK_INTERFERON_GAMMA_RESPONSE	195	0.8208	1.3390	0.0000	0.1955

Table 2: Distinct Hallmark Pathway Signature is Generated Following LPS Challenge in Neonatally ETS Exposed Female Mice

NAME	SIZE	ES	NES	NOM p-val	FDR q-val
HALLMARK_P53_PATHWAY	200	0.4379	1.5549	0.0000	0.0822
HALLMARK_INFLAMMATORY_RESPONSE	198	0.7413	1.5669	0.0000	0.0881
HALLMARK_IL2_STAT5_SIGNALING	199	0.5470	1.6105	0.0000	0.0892
HALLMARK_KRAS_SIGNALING_UP	199	0.4760	1.6019	0.0000	0.0960
HALLMARK_APOPTOSIS	161	0.4449	1.6128	0.0000	0.1013
HALLMARK_UNFOLDED_PROTEIN_RESPONSE	112	0.5237	1.4757	0.0000	0.1208
HALLMARK_COAGULATION	138	0.4802	1.6157	0.0000	0.1214
HALLMARK_TNFA_SIGNALING_VIA_NFKB	198	0.6859	1.7060	0.0000	0.1287
HALLMARK_PI3K_AKT_MTOR_SIGNALING	105	0.4353	1.4802	0.0000	0.1288
HALLMARK_DNA_REPAIR	149	0.5328	1.4583	0.0875	0.1318
HALLMARK_IL6_JAK_STAT3_SIGNALING	87	0.7772	1.4867	0.0000	0.1386
HALLMARK_INTERFERON_GAMMA_RESPONSE	195	0.7953	1.3486	0.0000	0.1500
HALLMARK_E2F_TARGETS	200	0.6922	1.3695	0.0000	0.1542
HALLMARK_G2M_CHECKPOINT	196	0.6045	1.3915	0.0000	0.1544
HALLMARK_REACTIVE_OXYGEN_SPECIES_PATHWAY	49	0.5313	1.3488	0.2179	0.1558
HALLMARK_UV_RESPONSE_UP	156	0.4131	1.3830	0.0000	0.1586
HALLMARK_MTORC1_SIGNALING	199	0.5128	1.3509	0.0000	0.1595
HALLMARK_APICAL_JUNCTION	198	0.3754	1.3569	0.0000	0.1599
HALLMARK_COMPLEMENT	193	0.5881	1.6726	0.0000	0.1616
HALLMARK_ALLOGRAFT_REJECTION	196	0.7901	1.3942	0.0000	0.1631
HALLMARK_ESTROGEN_RESPONSE_LATE	197	0.3810	1.3215	0.0000	0.1644
HALLMARK_MYC_TARGETS_V1	200	0.6263	1.2972	0.0000	0.1704
HALLMARK_INTERFERON_ALPHA_RESPONSE	95	0.8235	1.2987	0.0000	0.1763
HALLMARK_MYC_TARGETS_V2	57	0.6236	1.2902	0.1030	0.1771
HALLMARK_GLYCOLYSIS	200	0.3571	1.2329	0.2317	0.2182
HALLMARK_EPITHELIAL_MESENCHYMAL_TRANSITION	196	0.4761	1.2351	0.2398	0.2234
HALLMARK_HYPOXIA	198	0.3092	1.2143	0.0000	0.2314
HALLMARK_ANGIOGENESIS	36	0.5000	1.2045	0.0922	0.2444

Table 3: Distinct Hallmark Pathway Signature is Generated Following LPS Challenge in Neonatally ETS Exposed Male Mice

NAME	SIZE	ES	NES	NOM p-val	FDR q-val
HALLMARK_INFLAMMATORY_RESPONSE	198	-0.6711	-1.6619	0.0000	0.1247
HALLMARK_TNFA_SIGNALING_VIA_NFKB	198	-0.5768	-1.6581	0.0000	0.0894
HALLMARK_COMPLEMENT	191	-0.5074	-1.5842	0.0000	0.0894
HALLMARK_G2M_CHECKPOINT	196	-0.6134	-1.5594	0.0000	0.0805
HALLMARK_E2F_TARGETS	200	-0.7120	-1.5274	0.0000	0.0894
HALLMARK_APOPTOSIS	161	-0.3832	-1.5077	0.0000	0.0894
HALLMARK_IL6_JAK_STAT3_SIGNALING	87	-0.6893	-1.5052	0.0000	0.0843
HALLMARK_IL2_STAT5_SIGNALING	199	-0.4338	-1.4915	0.0000	0.1132
HALLMARK_INTERFERON_GAMMA_RESPONSE	195	-0.7737	-1.4706	0.0000	0.1309
HALLMARK_DNA_REPAIR	147	-0.4840	-1.4524	0.0000	0.1344
HALLMARK_ALLOGRAFT_REJECTION	196	-0.7368	-1.4402	0.0000	0.1329
HALLMARK_MTORC1_SIGNALING	199	-0.4894	-1.4391	0.0000	0.1263
HALLMARK_INTERFERON_ALPHA_RESPONSE	95	-0.8207	-1.4263	0.0000	0.1266
HALLMARK_UNFOLDED_PROTEIN_RESPONSE	112	-0.4084	-1.4103	0.1751	0.1280
HALLMARK_KRAS_SIGNALING_UP	199	-0.4038	-1.4010	0.0000	0.1290
HALLMARK_MYC_TARGETS_V1	200	-0.6491	-1.3464	0.0000	0.1723
HALLMARK_MYC_TARGETS_V2	57	-0.5502	-1.3440	0.0876	0.1701
HALLMARK_OXIDATIVE_PHOSPHORYLATION	197	-0.4338	-1.3119	0.0994	0.1792
HALLMARK_PI3K_AKT_MTOR_SIGNALING	105	-0.3431	-1.3028	0.0876	0.1792
HALLMARK_SPERMATOGENESIS	134	-0.3443	-1.3025	0.0905	0.1729
HALLMARK_REACTIVE_OXYGEN_SPECIES_PATHWAY	49	-0.4257	-1.2976	0.2154	0.1689
HALLMARK_COAGULATION	138	-0.3763	-1.2682	0.0856	0.1870
HALLMARK_UV_RESPONSE_UP	156	-0.3061	-1.2604	0.1751	0.1883
HALLMARK_P53_PATHWAY	199	-0.3042	-1.2283	0.0866	0.2017

Table 4: Top 20 Gene Ontology Biological Processes Upregulated in Control Female Mouse Lungs by LPS Challenge Versus Vehicle.

GO biological process complete	FDR
regulation of MyD88-dependent toll-like receptor signaling pathway (GO:0034124)	1.35E-03
cellular response to triacyl bacterial lipopeptide (GO:0071727)	1.01E-02
response to triacyl bacterial lipopeptide (GO:0071725)	1.01E-02
stimulatory C-type lectin receptor signaling pathway (GO:0002223)	1.35E-03
cellular response to lectin (GO:1990858)	1.34E-03
response to lectin (GO:1990840)	1.34E-03
regulation of interleukin-4-mediated signaling pathway (GO:1902214)	1.01E-02
detection of bacterial lipopeptide (GO:0070340)	1.00E-02
vertebrate eye-specific patterning (GO:0150064)	1.00E-02
complement-mediated synapse pruning (GO:0150062)	1.34E-03
positive regulation of interferon-gamma-mediated signaling pathway (GO:0060335)	3.83E-05
positive regulation of response to interferon-gamma (GO:0060332)	3.82E-05
innate immune response activating cell surface receptor signaling pathway (GO:0002220)	3.81E-05
regulation of natural killer cell chemotaxis (GO:2000501)	2.26E-03
positive regulation of T-helper 17 cell differentiation (GO:2000321)	2.25E-03
interleukin-27-mediated signaling pathway (GO:0070106)	2.25E-03
regulation of microglial cell mediated cytotoxicity (GO:1904149)	2.25E-03
antigen processing and presentation of exogenous peptide antigen via MHC class I (GO:0042590)	8.40E-06
cellular response to diacyl bacterial lipopeptide (GO:0071726)	1.61E-02
response to diacyl bacterial lipopeptide (GO:0071724)	1.60E-02

Table 5: Gene Ontology Biological Processes Upregulated in Control Female Mouse Lungs by Vehicle Challenge Versus LPS.

GO biological process complete	#	#	expected	Fold Enrichment	+/-	raw P value	FDR
neuronal action potential	35	6	.26	22.84	+	5.65E-07	4.45E-03
↳action potential	92	7	.69	10.14	+	9.38E-06	1.85E-02
↳transmission of nerve impulse	67	6	.50	11.93	+	1.76E-05	2.52E-02
↳multicellular organismal signaling	116	7	.87	8.04	+	3.85E-05	3.57E-02
↳cellular process	15109	140	113.38	1.23	+	2.77E-06	1.09E-02
drug metabolic process	68	7	.51	13.72	+	1.45E-06	7.63E-03
sodium ion transport	163	9	1.22	7.36	+	5.90E-06	1.55E-02
↳cation transport	730	17	5.48	3.10	+	4.47E-05	3.92E-02
↳ion transport	1073	23	8.05	2.86	+	6.99E-06	1.57E-02
fatty acid metabolic process	338	12	2.54	4.73	+	1.30E-05	2.05E-02
↳cellular lipid metabolic process	857	19	6.43	2.95	+	3.01E-05	3.16E-02
↳lipid metabolic process	1108	24	8.31	2.89	+	3.63E-06	1.14E-02
↳carboxylic acid metabolic process	754	18	5.66	3.18	+	1.92E-05	2.52E-02
↳oxoacid metabolic process	770	18	5.78	3.12	+	2.51E-05	3.05E-02
↳organic acid metabolic process	804	19	6.03	3.15	+	1.27E-05	2.23E-02
inorganic cation transmembrane transport	435	13	3.26	3.98	+	3.27E-05	3.22E-02
↳transmembrane transport	928	24	6.96	3.45	+	1.69E-07	2.67E-03
↳inorganic ion transmembrane transport	489	14	3.67	3.82	+	2.55E-05	2.88E-02

Table 6: Top 20 Gene Ontology Biological Processes Upregulated in Neonatally ETS Exposed Female Mouse Lungs by LPS Challenge Versus Vehicle.

GO biological process complete	FDR
positive regulation of antigen processing and presentation of peptide antigen (GO:0002585)	1.21E-02
cellular response to triacyl bacterial lipopeptide (GO:0071727)	1.21E-02
response to triacyl bacterial lipopeptide (GO:0071725)	1.21E-02
inflammasome complex assembly (GO:0140632)	1.21E-02
detection of bacterial lipopeptide (GO:0070340)	1.21E-02
vertebrate eye-specific patterning (GO:0150064)	1.20E-02
stimulatory C-type lectin receptor signaling pathway (GO:0002223)	1.68E-03
cellular response to lectin (GO:1990858)	1.68E-03
response to lectin (GO:1990840)	1.68E-03
complement-mediated synapse pruning (GO:0150062)	1.68E-03
positive regulation of interferon-gamma-mediated signaling pathway (GO:0060335)	6.12E-05
positive regulation of response to interferon-gamma (GO:0060332)	6.10E-05
innate immune response activating cell surface receptor signaling pathway (GO:0002220)	6.09E-05
Fc-gamma receptor signaling pathway (GO:0038094)	4.05E-04
positive regulation of apoptotic cell clearance (GO:2000427)	4.04E-04
regulation of natural killer cell chemotaxis (GO:2000501)	2.83E-03
positive regulation of T-helper 17 cell differentiation (GO:2000321)	2.82E-03
interleukin-27-mediated signaling pathway (GO:0070106)	2.82E-03
detection of bacterial lipoprotein (GO:0042494)	2.82E-03
regulation of microglial cell mediated cytotoxicity (GO:1904149)	2.81E-03

Table 7: Gene Ontology Biological Processes Upregulated in Neonatally ETS Exposed Female Mouse Lungs by Vehicle Challenge Versus LPS.

GO biological process complete	#	#	expected	Fold Enrichment	+/-	raw P value	FDR
homocysteine metabolic process	13	4	.10	41.00	+	6.55E-06	1.72E-02
↳sulfur amino acid metabolic process	29	5	.22	22.98	+	5.04E-06	1.59E-02
↳sulfur compound metabolic process	295	12	2.21	5.42	+	3.46E-06	2.73E-02
↳organic acid metabolic process	804	20	6.03	3.31	+	3.52E-06	1.85E-02
positive regulation of steroid metabolic process	37	5	.28	18.01	+	1.47E-05	2.89E-02
drug metabolic process	68	7	.51	13.72	+	1.45E-06	2.29E-02
cell-substrate adhesion	177	9	1.33	6.78	+	1.11E-05	2.50E-02
steroid metabolic process	245	10	1.84	5.44	+	2.24E-05	3.54E-02
regulation of hormone levels	549	15	4.12	3.64	+	2.21E-05	3.87E-02
response to chemical	3492	50	26.20	1.91	+	5.04E-06	1.98E-02

Table 8: Top 20 Gene Ontology Biological Processes Upregulated in Control Male Mouse Lungs by LPS Challenge Versus Vehicle.

GO biological process complete	FDR
p38MAPK cascade (GO:0038066)	1.06E-03
glomerular basement membrane development (GO:0032836)	1.99E-02
positive regulation of cell migration by vascular endothelial growth factor signaling pathway (GO:0038089)	3.87E-02
adherens junction assembly (GO:0034333)	1.47E-02
regulation of nuclear-transcribed mRNA poly(A) tail shortening (GO:0060211)	5.46E-03
lung saccule development (GO:0060430)	2.82E-02
glomerulus morphogenesis (GO:0072102)	2.82E-02
stress fiber assembly (GO:0043149)	2.03E-03
contractile actin filament bundle assembly (GO:0030038)	2.02E-03
negative regulation of sprouting angiogenesis (GO:1903671)	1.05E-02
positive regulation of nuclear-transcribed mRNA poly(A) tail shortening (GO:0060213)	2.05E-02
astral microtubule organization (GO:0030953)	2.05E-02
cardiac vascular smooth muscle cell differentiation (GO:0060947)	2.05E-02
lymphangiogenesis (GO:0001946)	7.62E-03
hippo signaling (GO:0035329)	2.87E-03
kidney vasculature development (GO:0061440)	2.87E-03
renal system vasculature development (GO:0061437)	2.87E-03
glomerulus vasculature development (GO:0072012)	5.52E-03
vascular endothelial growth factor signaling pathway (GO:0038084)	2.05E-03
positive regulation of vacuole organization (GO:0044090)	3.89E-02

Table 9: Gene Ontology Biological Processes Upregulated in Control Male Mouse Lungs by Vehicle Challenge Versus LPS.

GO biological process complete	FDR
regulation of basement membrane organization (GO:0110011)	3.45E-03
positive regulation of basement membrane assembly involved in embryonic body morphogenesis (GO:1904261)	3.45E-03
regulation of basement membrane assembly involved in embryonic body morphogenesis (GO:1904259)	3.44E-03
cellular response to water stimulus (GO:0071462)	2.17E-02
response to hydrostatic pressure (GO:0051599)	2.17E-02
intramembranous ossification (GO:0001957)	3.16E-02
regulation of Rho-dependent protein serine/threonine kinase activity (GO:2000298)	3.16E-02
direct ossification (GO:0036072)	3.16E-02
ureteric bud elongation (GO:0060677)	3.16E-02
glomerular basement membrane development (GO:0032836)	4.78E-03
regulation of keratinocyte apoptotic process (GO:1902172)	4.42E-02
angiogenesis involved in coronary vascular morphogenesis (GO:0060978)	4.42E-02
positive regulation of extracellular matrix assembly (GO:1901203)	1.75E-02
lung saccule development (GO:0060430)	6.65E-03
p38MAPK cascade (GO:0038066)	6.64E-03
response to water (GO:0009415)	6.64E-03
axonogenesis involved in innervation (GO:0060385)	2.36E-02
positive regulation of cholesterol biosynthetic process (GO:0045542)	2.36E-02
transferrin transport (GO:0033572)	2.35E-02
glycogen catabolic process (GO:0005980)	2.35E-02

Table 10: Top 20 Gene Ontology Biological Processes Upregulated in Neonatally ETS Exposed Male Mouse Lungs by LPS Challenge Versus Vehicle.

GO biological process complete	FDR
complement-mediated synapse pruning (GO:0150062)	2.59E-03
cellular response to triacyl bacterial lipopeptide (GO:0071727)	1.66E-02
response to triacyl bacterial lipopeptide (GO:0071725)	1.66E-02
positive regulation of type III hypersensitivity (GO:0001805)	1.65E-02
regulation of type III hypersensitivity (GO:0001803)	1.65E-02
regulation of interleukin-4-mediated signaling pathway (GO:1902214)	1.65E-02
detection of bacterial lipopeptide (GO:0070340)	1.65E-02
vertebrate eye-specific patterning (GO:0150064)	1.65E-02
regulation of natural killer cell chemotaxis (GO:2000501)	6.25E-04
microglial cell activation involved in immune response (GO:0002282)	4.27E-03
pyrimidine deoxyribonucleoside triphosphate metabolic process (GO:0009211)	4.26E-03
regulation of microglial cell mediated cytotoxicity (GO:1904149)	4.25E-03
regulation of MyD88-dependent toll-like receptor signaling pathway (GO:0034124)	2.62E-02
cellular response to diacyl bacterial lipopeptide (GO:0071726)	2.62E-02
response to diacyl bacterial lipopeptide (GO:0071724)	2.62E-02
positive regulation of natural killer cell chemotaxis (GO:2000503)	2.61E-02
positive regulation of microglial cell mediated cytotoxicity (GO:1904151)	2.61E-02
opsonization (GO:0008228)	2.61E-02
positive regulation of interferon-gamma-mediated signaling pathway (GO:0060335)	9.92E-04
positive regulation of response to interferon-gamma (GO:0060332)	9.90E-04

Table 11: Gene Ontology Biological Processes Upregulated in Neonatally ETS Exposed Male Mouse Lungs by Vehicle Challenge Versus LPS.

GO biological process complete	FDR
N-acylethanolamine metabolic process (GO:0070291)	3.58E-02
NADPH oxidation (GO:0070995)	1.14E-02
regulation of type B pancreatic cell proliferation (GO:0061469)	2.23E-02
renal system process involved in regulation of systemic arterial blood pressure (GO:0003071)	1.91E-02
positive regulation of cholesterol efflux (GO:0010875)	3.15E-02
positive regulation of steroid metabolic process (GO:0045940)	2.22E-02
positive regulation of glucose import (GO:0046326)	2.19E-02
negative regulation of BMP signaling pathway (GO:0030514)	1.34E-02
positive regulation of glucose transmembrane transport (GO:0010828)	3.62E-02
xenobiotic metabolic process (GO:0006805)	9.68E-04
regulation of glucose import (GO:0046324)	2.87E-02
cellular response to hypoxia (GO:0071456)	2.09E-02
actomyosin structure organization (GO:0031032)	8.23E-03
regulation of BMP signaling pathway (GO:0030510)	1.43E-02
cellular response to decreased oxygen levels (GO:0036294)	2.51E-02
cellular response to xenobiotic stimulus (GO:0071466)	5.14E-04
cellular response to oxygen levels (GO:0071453)	1.79E-02
cholesterol homeostasis (GO:0042632)	2.96E-02
sterol homeostasis (GO:0055092)	3.13E-02
positive regulation of endothelial cell migration (GO:0010595)	1.93E-02

2.7. Supplementary Figures

Supplementary Figure 1:

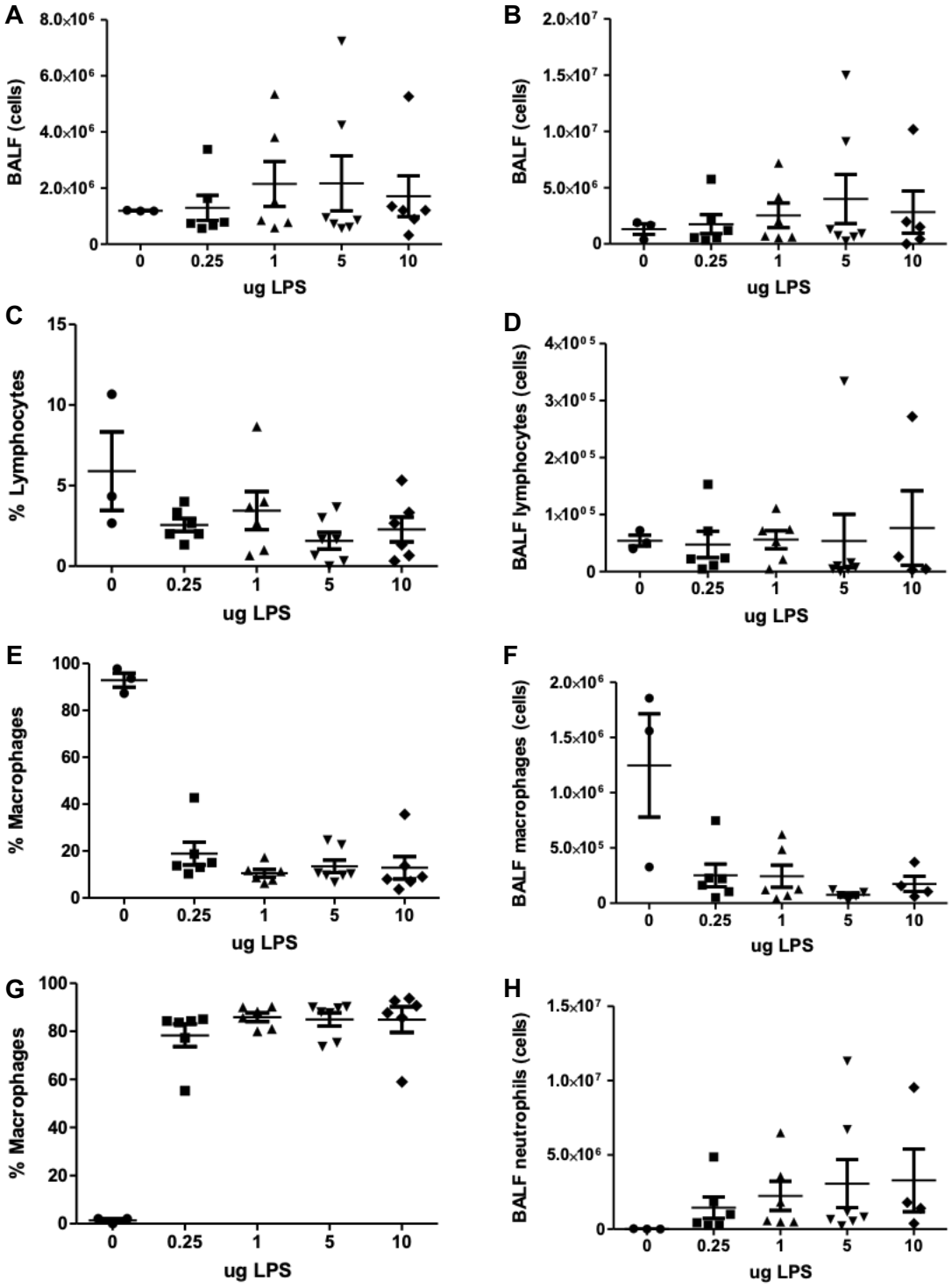

Supplementary Figure 1: LPS Dose Response for Oropharyngeal Aspiration in Control Mice. 5-week-old mice were purchased from the Jackson Labs and allowed to acclimate to the vivarium for one week prior to oropharyngeal aspiration of LPS at 0 μg, 0.25 μg, 1 μg, 5μg, or 10 μg in PBS. BALF was collected 24-hours later at necropsy. Cells were counted **(A)** and total cells were calculated as the product of BALF volume and cells **(B)**. Cytospin slides were fixed and stained, and 300 cells were counted to determine the % lymphocytes **(C)**, % macrophages **(E)**, and %neutrophils **(G)**. The product of total cells and percent differentials was used to determine total lymphocytes **(D)**, total macrophages **(F)**, and total neutrophils **(H)**.

Supplementary Figure 2:

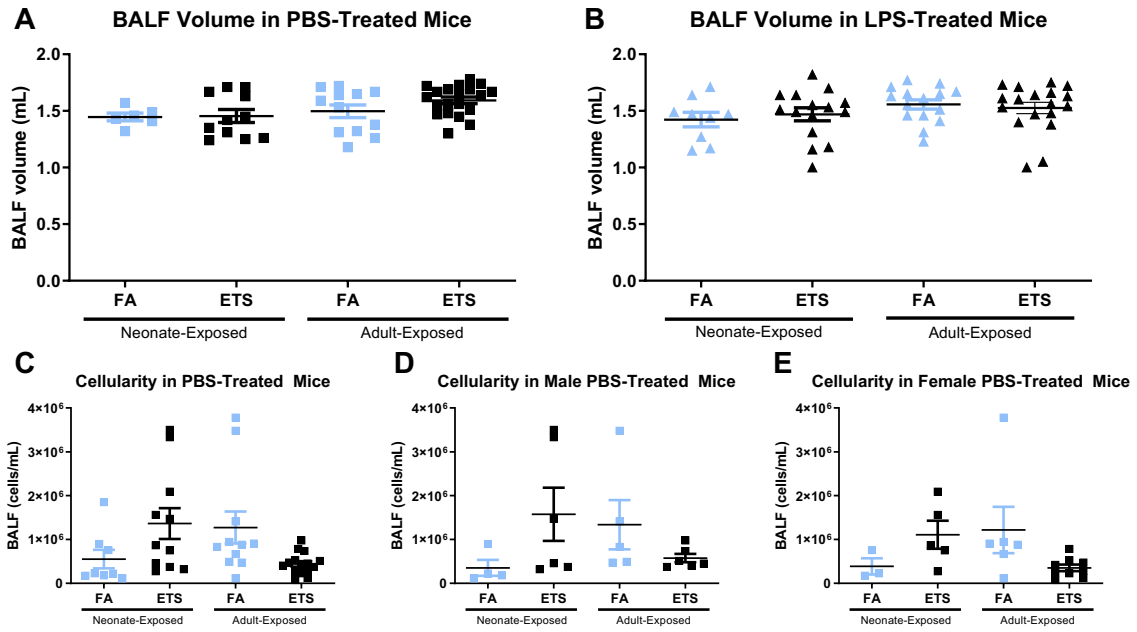

Supplementary Figure 2: No differences were observed in BALF volumes or cellularity in vehicle challenged mice. BALF was collected and the volume was measured following vehicle **(A)** and LPS challenge **(B)**. Cellular concentration of the BALF was not different between groups when comparing all mice **(C)** or males **(D)** or females **(E)** alone.

Supplemental Figure 3:

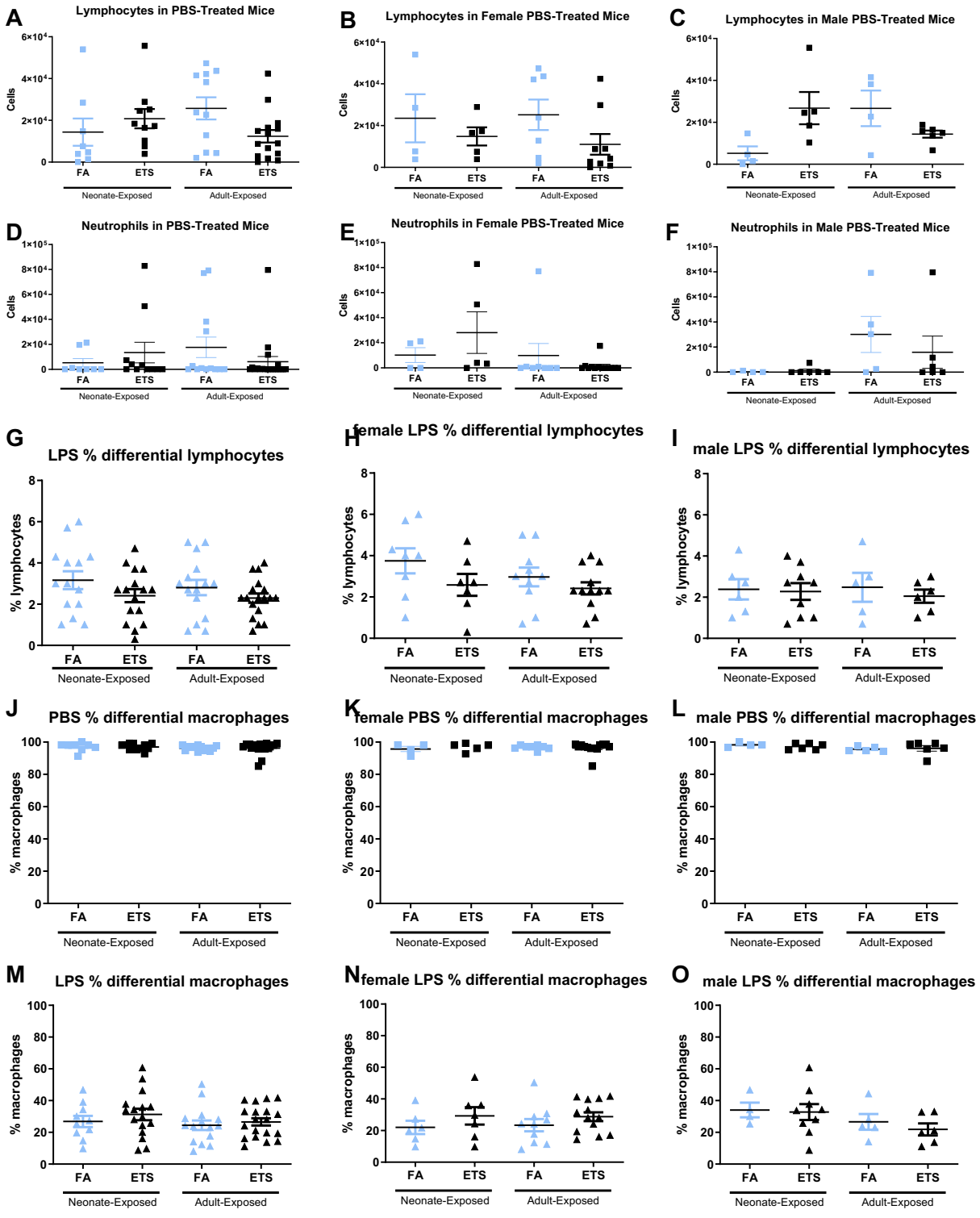

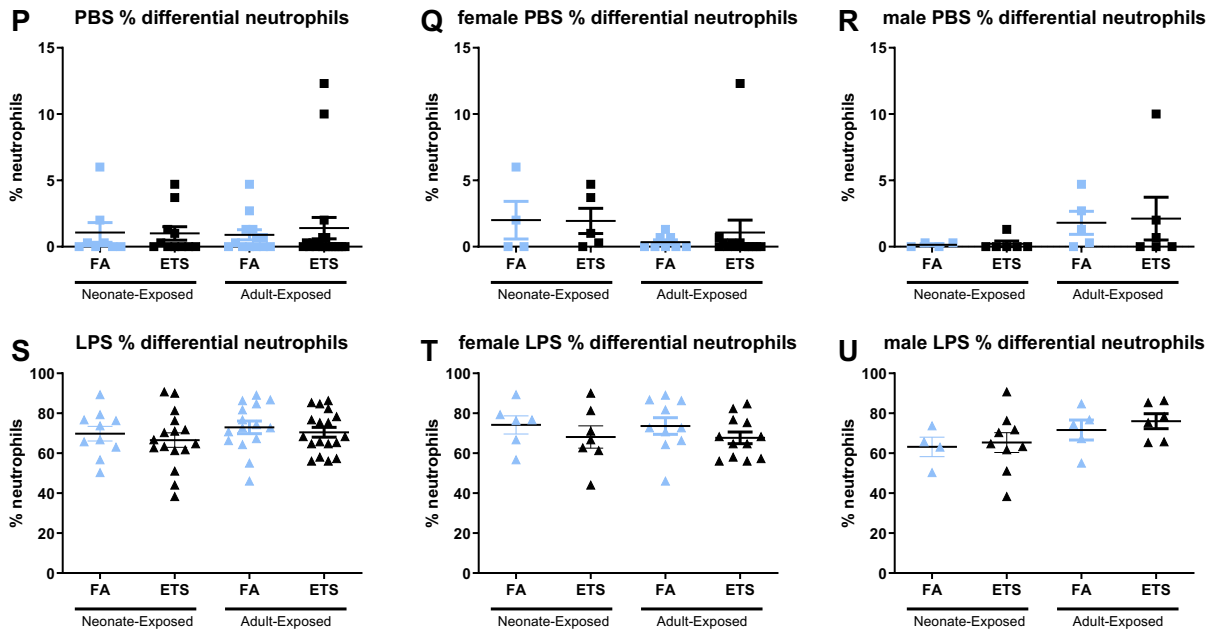

Supplemental Figure 3: BALF Cell Differential Data for Vehicle and LPS Challenged Mice. 6-week-old mice exposed to ETS or filtered air during the early postnatal period showed no differences in lymphocytes compared to adult controls when challenged with vehicle **(A)**, and no difference was seen in females **(B)** or males alone **(C)**. No difference in total BALF neutrophils between treatment groups was seen in vehicle challenged mice **(D)**, which was true in females alone **(E)** and males alone **(F)**. Lymphocytes did not comprise a significantly different percentage of BALF cells in LPS challenged mice **(G)**, and no difference was seen in females **(H)** or males **(I)**. Macrophages as a percent of BALF cells in vehicle challenged animals was not different between groups **(J)**, which remained true when females **(K)** and males **(L)** were examined. Macrophages as a percent of BALF cells in LPS challenged animals was not different between groups **(M)**, which remained true when females **(N)** and males **(O)** were examined. Neutrophils as a percent of BALF cells in vehicle challenged animals was not different between groups **(P)**, which remained true when females **(Q)** and males **(R)** were examined. Neutrophils as a percent of BALF cells in LPS challenged animals was not different between groups **(S)**, which remained true when females **(T)** and males **(U)** were examined.

Supplemental Figure 4:

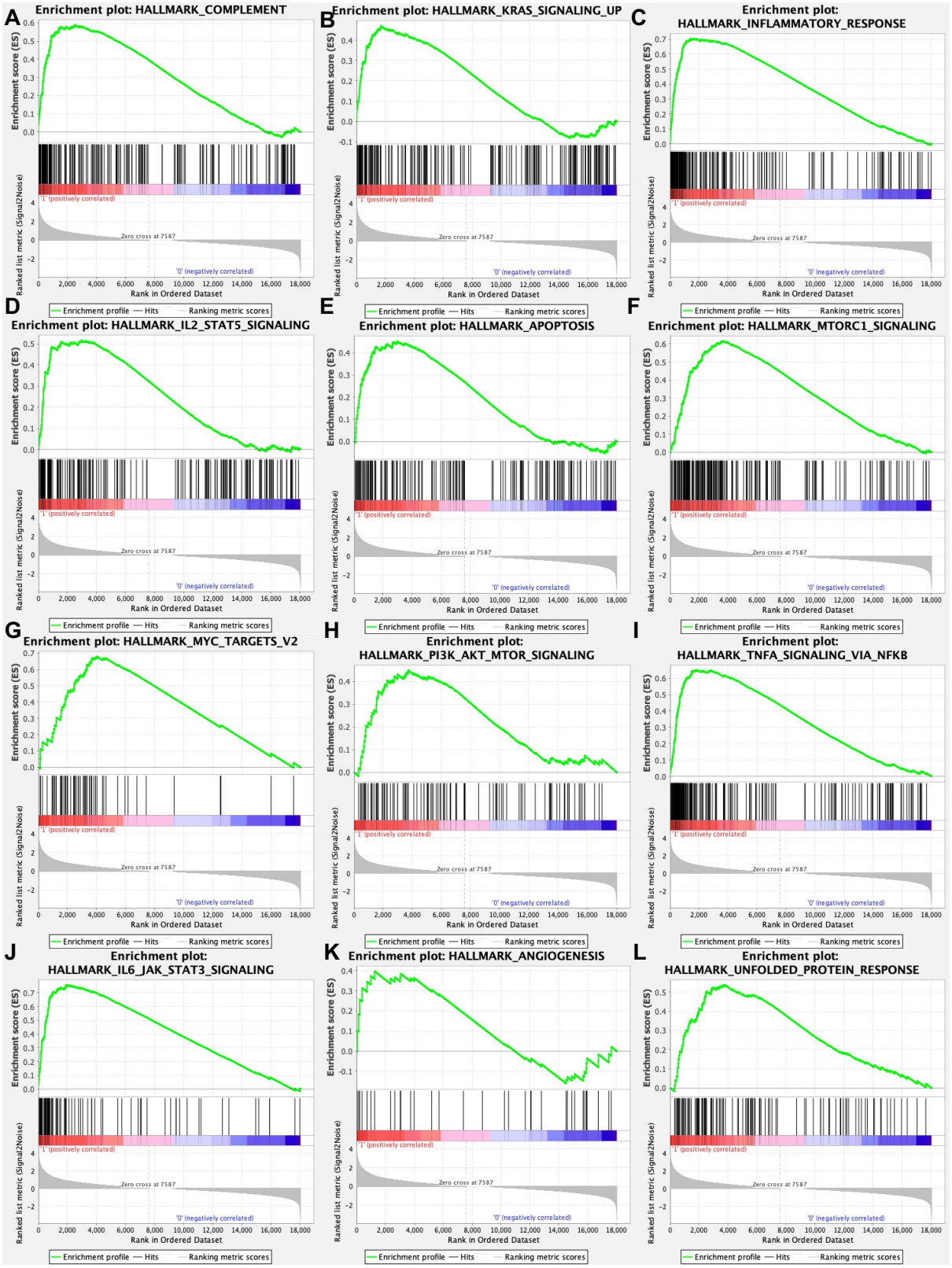

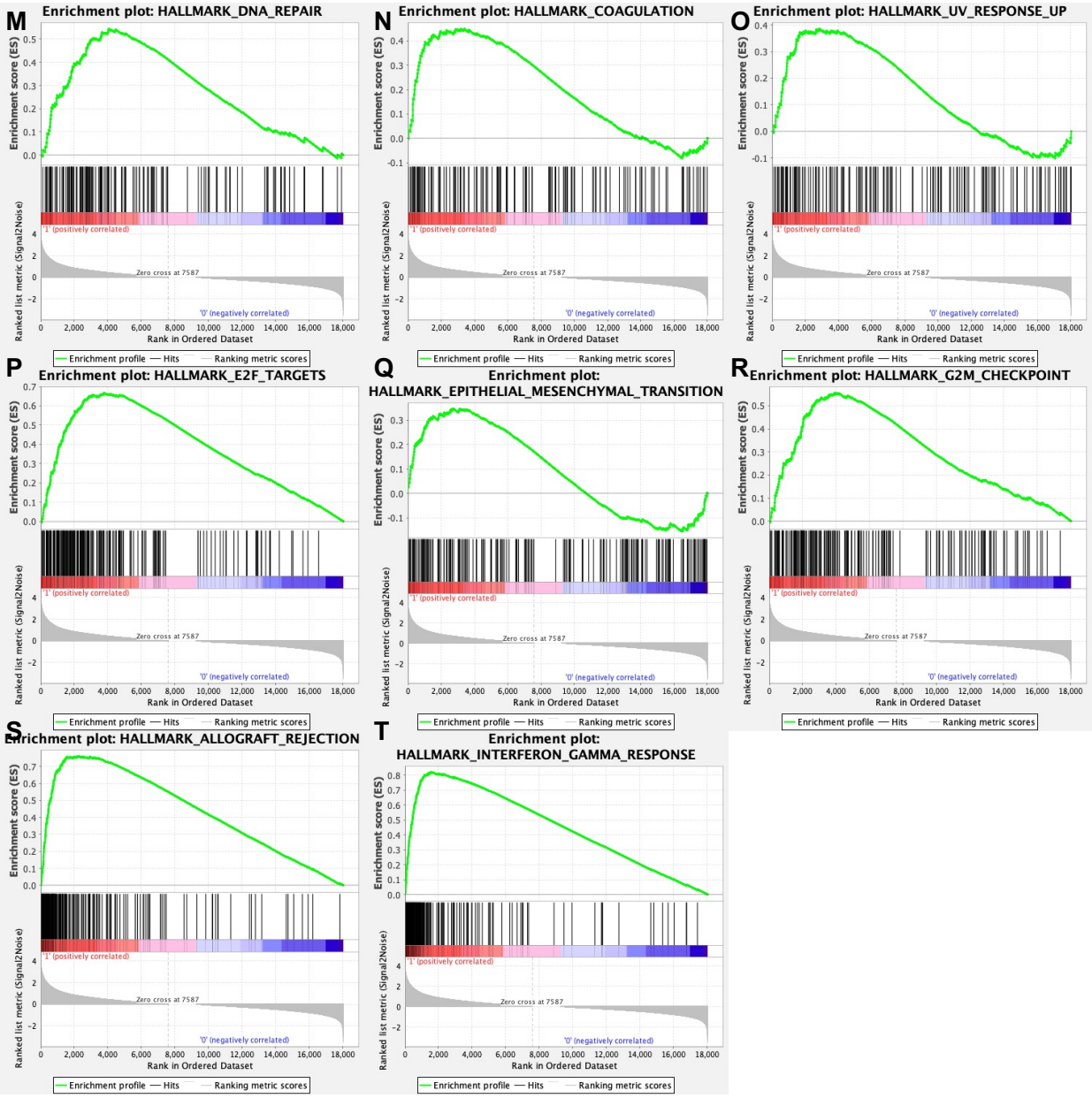

Supplemental Figure 4: Enrichment plots for hallmark pathways enriched following LPS Challenge in control female mouse lungs. GSEA hallmark pathway analysis was used to find differences between transcriptomes of control mouse lung challenged with LPS versus control. A FDR cutoff of 0.25 was used.

Supplemental Figure 5:

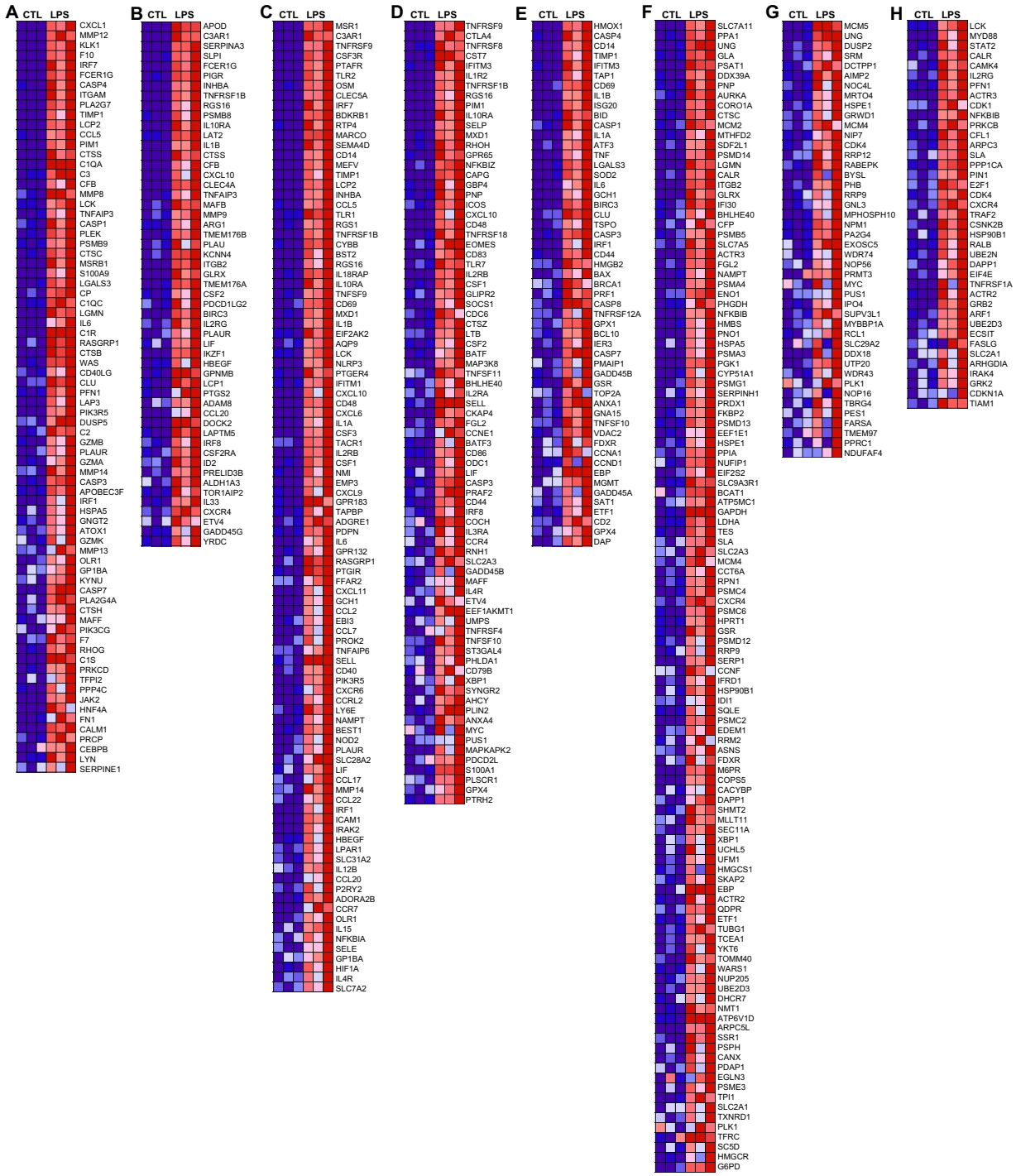

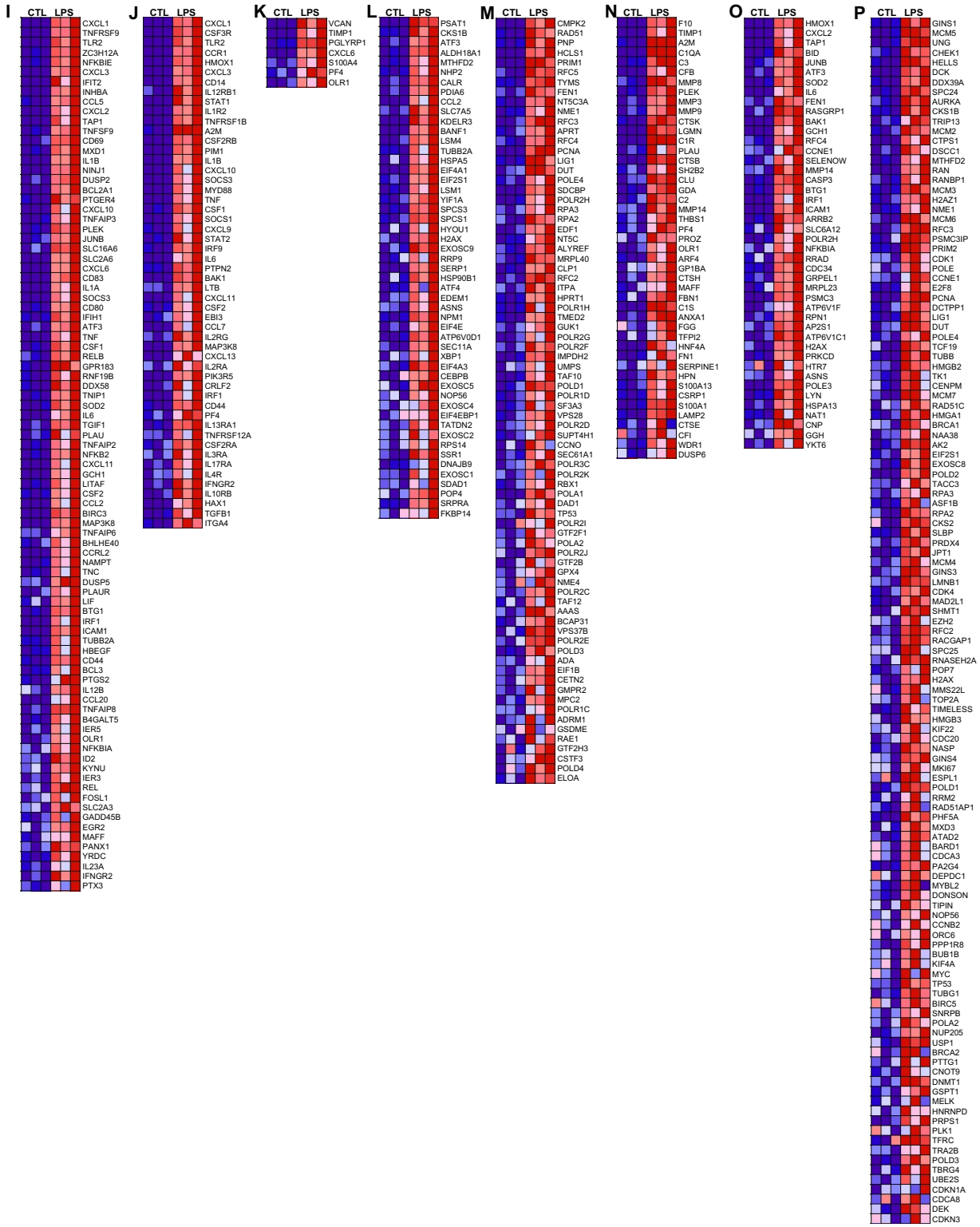
I
CTL LPS
CXCL1
TNFRSF9
TLR2
ZC3H12A
NFKBIE
CXCL3
IFIT2
INHBA
CCL5
CXCL2
TAP1
TNFSF9
CD69
MXD1
IL1B
NINJ1
DUSP2
BCL2A1
PTGER4
CXCL10
TNFAIP3
PLEK
JUNB
SLC16A6
SLC2A6
CXCL6
CD83
IL1A
SOCS3
CD80
IFIH1
ATF3
TNF
CSF1
RELB
GPR183
RNF19B
DDX58
TNIP1
SOD2
IL6
TGIF1
PLAU
TNFAIP2
NFKB2
CXCL11
GCH1
LITAF
CSF2
CCL2
BIRC3
MAP3K8
TNFAIP6
BHLHE40
CCRL2
NAMPT
TNC
DUSP5
PLAUR
LIF
BTG1
IRF1
ICAM1
TUBB2A
HBEGF
CD44
BCL3
PTGS2
IL12B
CCL20
TNFAIP8
B4GALT5
IER5
OLR1
NFKBIA
ID2
KYNU
IER3
REL
FOSL1
SLC2A3
GADD45B
EGR2
MAFF
PANX1
YRDC
IL23A
IFNGR2
PTX3
J
CTL LPS
CXCL1
CSF3R
TLR2
CCR1
HMOX1
CXCL3
CD14
IL12RB1
STAT1
IL1R2
TNFRSF1B
A2M
CSF2RB
PIM1
IL1B
CXCL10
SOCS3
MYD88
TNF
CSF1
SOCS1
CXCL9
STAT2
IRF9
IL6
PTPN2
BAK1
LTB
CXCL11
CSF2
EBI3
CCL7
IL2RG
MAP3K8
CXCL13
IL2RA
PIK3R5
CRLF2
IRF1
CD44
PF4
IL13RA1
TNFRSF12A
CSF2RA
IL3RA
IL17RA
IL4R
IFNGR2
IL10RB
HAX1
TGFB1
ITGA4
K
CTL LPS
VCAN
TIMP1
PGLYRP1
CXCL6
S100A4
PF4
OLR1
L
CTL LPS
PSAT1
CKS1B
ATF3
ALDH18A1
MTHFD2
NHP2
CALR
PDIA6
CCL2
SLC7A5
KDELR3
BANF1
LSM4
TUBB2A
HSPA5
EIF4A1
EIF2S1
LSM1
YIF1A
SPCS3
SPCS1
HYOU1
H2AX
EXOSC9
RRP9
SERP1
HSP90B1
ATF4
EDEM1
ASNS
NPM1
EIF4E
ATP6V0D1
SEC11A
XBP1
EIF4A3
CEBPB
EXOSC5
NOP56
EXOSC4
EIF4EBP1
TATDN2
EXOSC2
RPS14
SSR1
DNAJB9
EXOSC1
SDAD1
POP4
SRPRA
FKBP14
M
CTL LPS
CMPK2
RAD51
PNP
HCLS1
PRIM1
RFC5
TYMS
FEN1
NT5C3A
NME1
RFC3
APRT
RFC4
PCNA
LIG1
DUT
POLE4
SDCBP
POLR2H
RPA3
RPA2
EDF1
NT5C
ALYREF
MRPL40
CLP1
RFC2
ITPA
HPRT1
POLR1H
TMED2
GUK1
POLR2G
POLR2F
IMPDH2
UMPS
TAF10
POLD1
POLR1D
SF3A3
VPS28
POLR2D
SUPT4H1
CCNO
SEC61A1
POLR3C
POLR2K
RBX1
POLA1
DAD1
TP53
POLR2I
GTF2F1
POLA2
POLR2J
GTF2B
GPX4
NME4
POLR2C
TAF12
AAAS
BCAP31
VPS37B
POLR2E
POLD3
ADA
EIF1B
CETN2
GMPR2
MPC2
POLR1C
ADRM1
GSDME
RAE1
GTF2H3
CSTF3
POLD4
ELOA
N
CTL LPS
F10
TIMP1
A2M
C1QA
C3
CFB
MMP8
PLEK
MMP3
MMP9
CTSK
LGMN
C1R
PLAU
CTSB
SH2B2
CLU
GDA
C2
MMP14
THBS1
PF4
PROZ
OLR1
ARF4
GP1BA
CTSH
MAFF
FBN1
C1S
ANXA1
FGG
TFPI2
HNF4A
FN1
SERPINE1
HPN
S100A13
CSRP1
S100A1
LAMP2
CTSE
CFI
WDR1
DUSP6
O
CTL LPS
HMOX1
CXCL2
TAP1
BID
JUNB
ATF3
SOD2
IL6
FEN1
RASGRP1
BAK1
GCH1
RFC4
CCNE1
SELENOW
MMP14
CASP3
BTG1
IRF1
ICAM1
ARRB2
SLC6A12
POLR2H
NFKBIA
RRAD
CDC34
GRPEL1
MRPL23
PSMC3
ATP6V1F
RPN1
AP2S1
ATP6V1C1
H2AX
PRKCD
HTR7
ASNS
POLE3
LYN
HSPA13
NAT1
CNP
GGH
YKT6
P
CTL LPS
GINS1
MCM5
UNG
CHEK1
HELLS
DCK
DDX39A
SPC24
AURKA
CKS1B
TRIP13
MCM2
CTPS1
DSCC1
MTHFD2
RAN
RANBP1
MCM3
H2AZ1
NME1
MCM6
RFC3
PSMC3IP
PRIM2
CDK1
POLE
CCNE1
E2F8
PCNA
DCTPP1
LIG1
DUT
POLE4
TCF19
TUBB
HMGB2
TK1
CENPM
MCM7
RAD51C
HMGA1
BRCA1
NAA38
AK2
EIF2S1
EXOSC8
POLD2
TACC3
RPA3
ASF1B
RPA2
CKS2
SLBP
PRDX4
JPT1
MCM4
GINS3
LMNB1
CDK4
MAD2L1
SHMT1
EZH2
RFC2
RACGAP1
SPC25
RNASEH2A
POP7
H2AX
MMS22L
TOP2A
TIMELESS
HMGB3
KIF22
CDC20
NASP
GINS4
MKI67
ESPL1
POLD1
RRM2
RAD51AP1
PHF5A
MXD3
ATAD2
BARD1
CDCA3
PA2G4
DEPDC1
MYBL2
DONSON
TIPIN
NOP56
CCNB2
ORC6
PPP1R8
BUB1B
KIF4A
MYC
TP53
TUBG1
BIRC5
SNRPB
POLA2
NUP205
USP1
BRCA2
PTTG1
CNOT9
DNMT1
GSPT1
MELK
HNRNPD
PRPS1
PLK1
TFRC
TRA2B
POLD3
TBRG4
UBE2S
CDKN1A
CDCA8
DEK
CDKN3

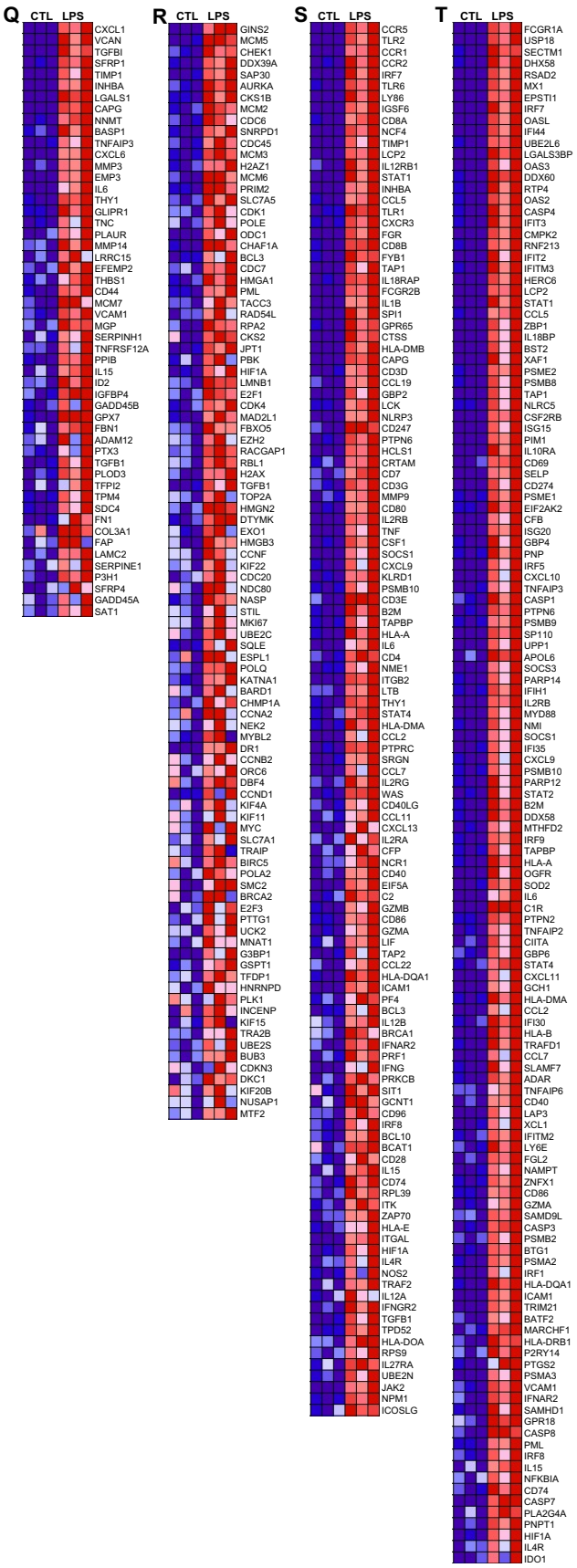
Q
CTL LPS
CXCL1
VCAN
TGFBI
SFRP1
TIMP1
INHBA
LGALS1
CAPG
NNMT
BASP1
TNFAIP3
CXCL6
MMP3
EMP3
IL6
THY1
GLIPR1
TNC
PLAUR
MMP14
LRRC15
EFEMP2
THBS1
CD44
MCM7
VCAM1
MGP
SERPINH1
TNFRSF12A
PPIB
IL15
ID2
IGFBP4
GADD45B
GPX7
FBN1
ADAM12
PTX3
TGFB1
PLOD3
TFPI2
TPM4
SDC4
FN1
COL3A1
FAP
LAMC2
SERPINE1
P3H1
SFRP4
GADD45A
SAT1
R
CTL LPS
GINS2
MCM5
CHEK1
DDX39A
SAP30
AURKA
CKS1B
MCM2
CDC6
SNRPD1
CDC45
MCM3
H2AZ1
MCM6
PRIM2
SLC7A5
CDK1
POLE
ODC1
CHAF1A
BCL3
CDC7
HMGA1
PML
TACC3
RAD54L
RPA2
CKS2
JPT1
PBK
HIF1A
LMNB1
E2F1
CDK4
MAD2L1
FBXO5
EZH2
RACGAP1
RBL1
H2AX
TGFB1
TOP2A
HMGN2
DTYMK
EXO1
HMGB3
CCNF
KIF22
CDC20
NDC80
NASP
STIL
MKI67
UBE2C
SQLE
ESPL1
POLQ
KATNA1
BARD1
CHMP1A
CCNA2
NEK2
MYBL2
DR1
CCNB2
ORC6
DBF4
CCND1
KIF4A
KIF11
MYC
SLC7A1
TRAIP
BIRC5
POLA2
SMC2
BRCA2
E2F3
PTTG1
UCK2
MNAT1
G3BP1
GSPT1
TFDP1
HNRNPD
PLK1
INCENP
KIF15
TRA2B
UBE2S
BUB3
CDKN3
DKC1
KIF20B
NUSAP1
MTF2
S
CTL LPS
CCR5
TLR2
CCR1
CCR2
IRF7
TLR6
LY86
IGSF6
CD8A
NCF4
TIMP1
LCP2
IL12RB1
STAT1
INHBA
CCL5
TLR1
CXCR3
FGR
CD8B
FYB1
TAP1
IL18RAP
FCGR2B
IL1B
SPI1
GPR65
CTSS
HLA-DMB
CAPG
CD3D
CCL19
GBP2
LCK
NLRP3
CD247
PTPN6
HCLS1
CRTAM
CD7
CD3G
MMP9
CD80
IL2RB
TNF
CSF1
SOCS1
CXCL9
KLRD1
PSMB10
CD3E
B2M
TAPBP
HLA-A
IL6
CD4
NME1
ITGB2
LTB
THY1
STAT4
HLA-DMA
CCL2
PTPRC
SRGN
CCL7
IL2RG
WAS
CD40LG
CCL11
CXCL13
IL2RA
CFP
NCR1
CD40
EIF5A
C2
GZMB
CD86
GZMA
LIF
TAP2
CCL22
HLA-DQA1
ICAM1
PF4
BCL3
IL12B
BRCA1
IFNAR2
PRF1
IFNG
PRKCB
SIT1
GCNT1
CD96
IRF8
BCL10
BCAT1
CD28
IL15
CD74
RPL39
ITK
ZAP70
HLA-E
ITGAL
HIF1A
IL4R
NOS2
TRAF2
IL12A
IFNGR2
TGFB1
TPD52
HLA-DOA
RPS9
IL27RA
UBE2N
JAK2
NPM1
ICOSLG
T
CTL LPS
FCGR1A
USP18
SECTM1
DHX58
RSAD2
MX1
EPSTI1
IRF7
OASL
IFI44
UBE2L6
LGALS3BP
OAS3
DDX60
RTP4
OAS2
CASP4
IFIT3
CMPK2
RNF213
IFIT2
IFITM3
HERC6
LCP2
STAT1
CCL5
ZBP1
IL18BP
BST2
XAF1
PSME2
PSMB8
TAP1
NLRC5
CSF2RB
ISG15
PIM1
IL10RA
CD69
SELP
CD274
PSME1
EIF2AK2
CFB
ISG20
GBP4
PNP
IRF5
CXCL10
TNFAIP3
CASP1
PTPN6
PSMB9
SP110
UPP1
APOL6
SOCS3
PARP14
IFIH1
IL2RB
MYD88
NMI
SOCS1
IFI35
CXCL9
PSMB10
PARP12
STAT2
B2M
DDX58
MTHFD2
IRF9
TAPBP
HLA-A
OGFR
SOD2
IL6
C1R
PTPN2
TNFAIP2
CIITA
GBP6
STAT4
CXCL11
GCH1
HLA-DMA
CCL2
IFI30
HLA-B
TRAFD1
CCL7
SLAMF7
ADAR
TNFAIP6
CD40
LAP3
XCL1
IFITM2
LY6E
FGL2
NAMPT
ZNFX1
CD86
GZMA
SAMD9L
CASP3
PSMB2
BTG1
PSMA2
IRF1
HLA-DQA1
ICAM1
TRIM21
BATF2
MARCHF1
HLA-DRB1
P2RY14
PTGS2
PSMA3
VCAM1
IFNAR2
SAMHD1
GPR18
CASP8
PML
IRF8
IL15
NFKBIA
CD74
CASP7
PLA2G4A
PNPT1
HIF1A
IL4R
IDO1

Supplemental Figure 5: Core enrichment genes for Hallmark Pathways in control female mouse lungs challenged with vehicle and LPS. Core enrichment genes for **(A)** Complement, **(B)** KRAS signaling, **(C)** Inflammatory response, **(D)** IL2 STAT5 signaling, **(E)** Apoptosis, **(F)** MTORC1 signaling, **(G)** Myc targets V2, **(H)** PI3K AKT MTOR signaling pathway, **(I)** TNFα signaling via NFκB, **(J)** IL6 JAK STAT signaling, **(K)** Angiogenesis, **(L)** Unfolded Protein Response, **(M)** DNA Repair, **(N)** Coagulation, **(O)** UV Response Up, **(P)** E2F Targets, **(Q)** Epithelial Mesenchymal Transition, **(R)** G2M Checkpoint, **(S)** Allograft Rejection, and **(T)** Gamma Interferon Response Hallmark Pathways.

Supplemental Figure 6:

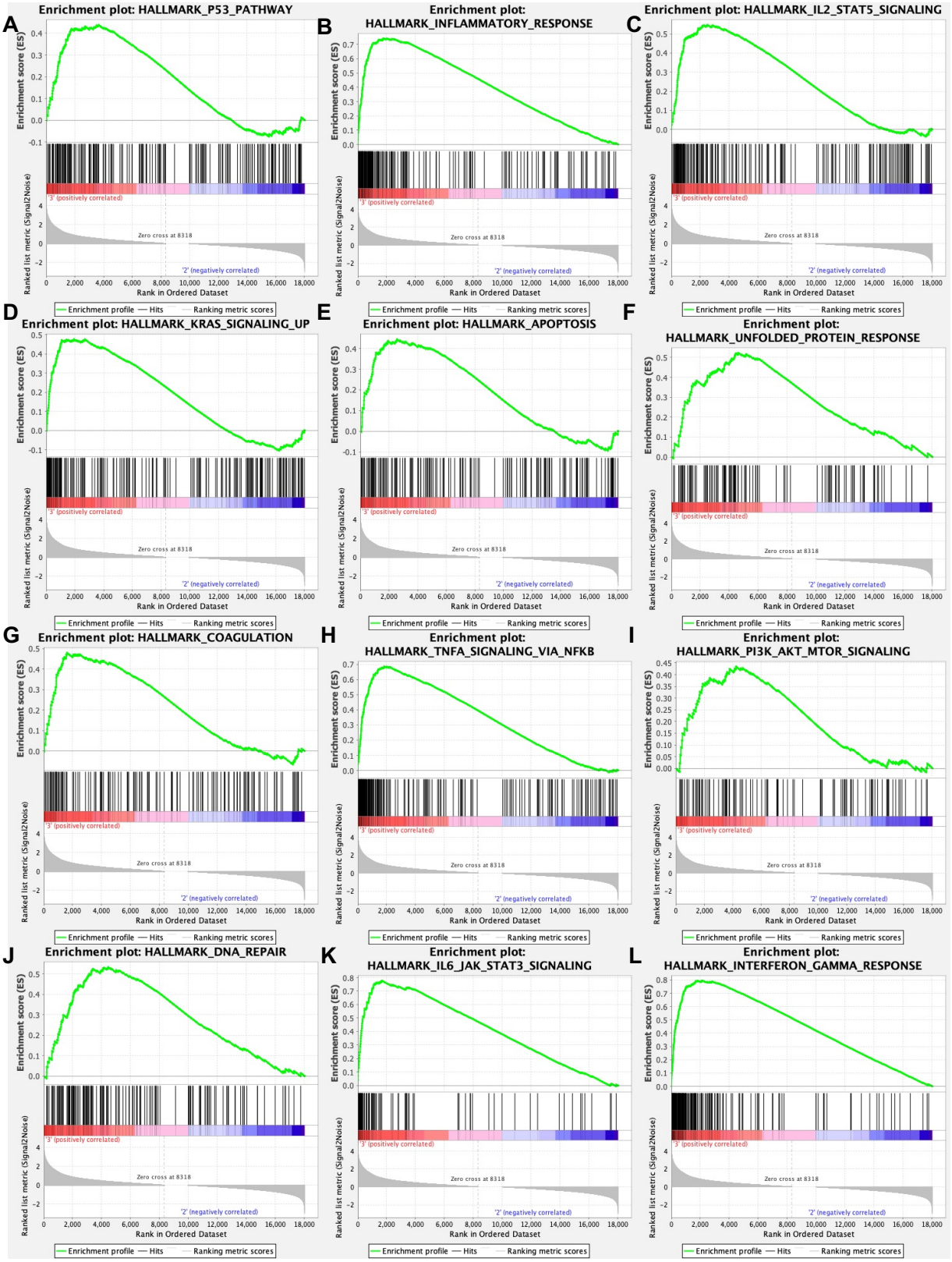

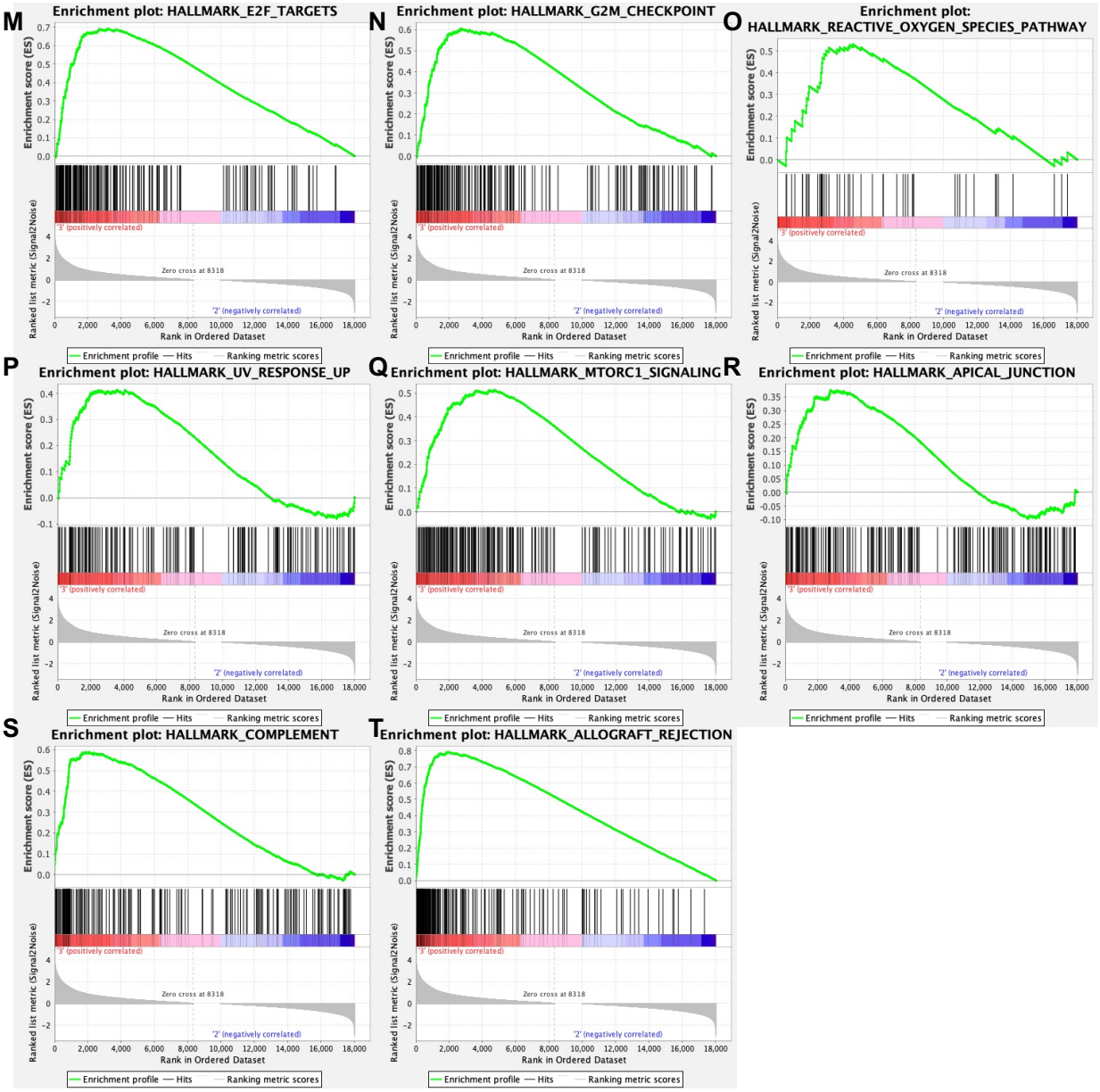

Supplemental Figure 6: Enrichment plots for hallmark pathways enriched following LPS challenge in neonatally ETS exposed female mouse lungs. GSEA hallmark pathway analysis was used to find differences between transcriptomes of control mouse lung challenged with LPS versus control. A FDR cutoff of 0.25 was used.

Supplemental Figure 7:

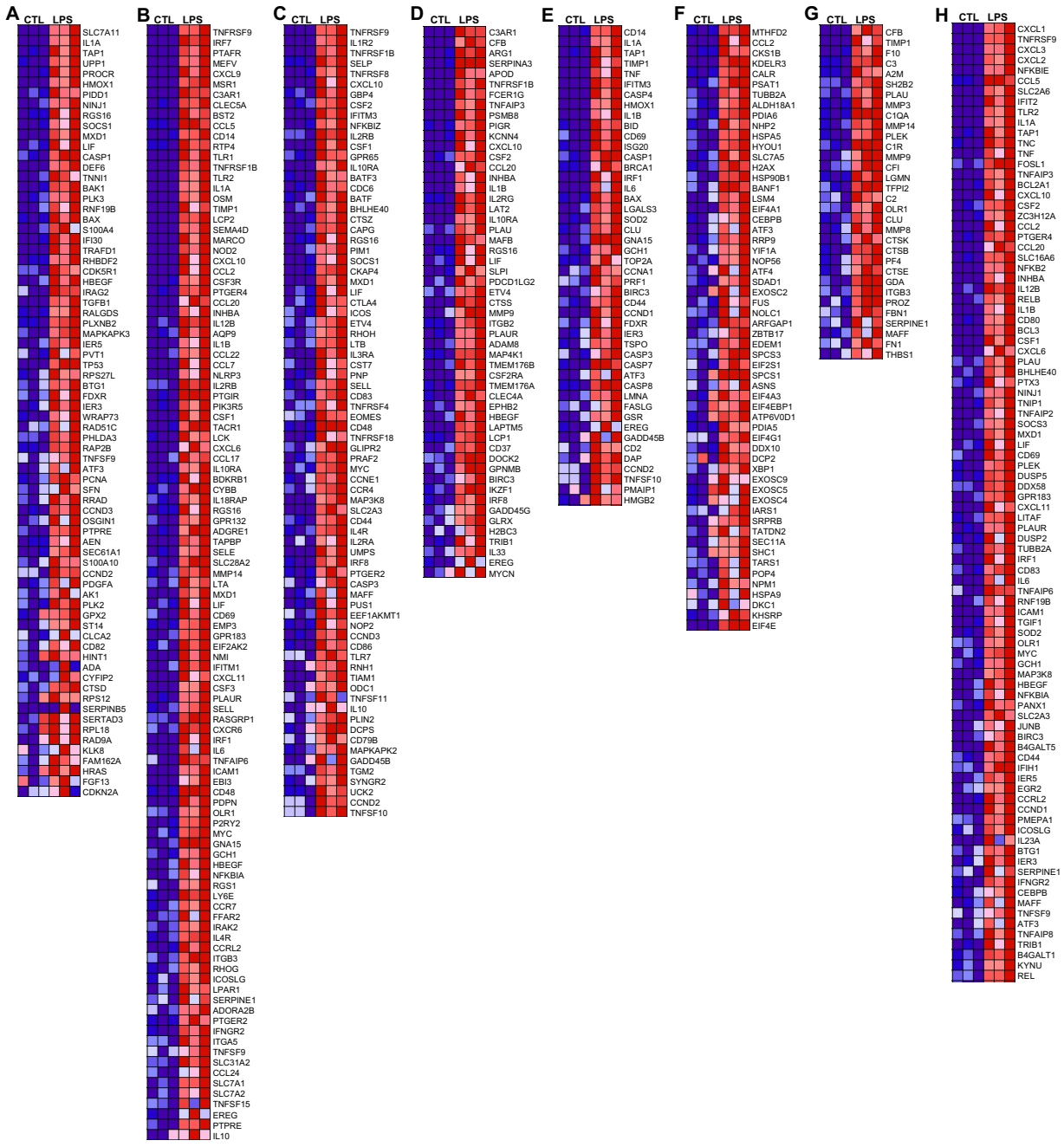

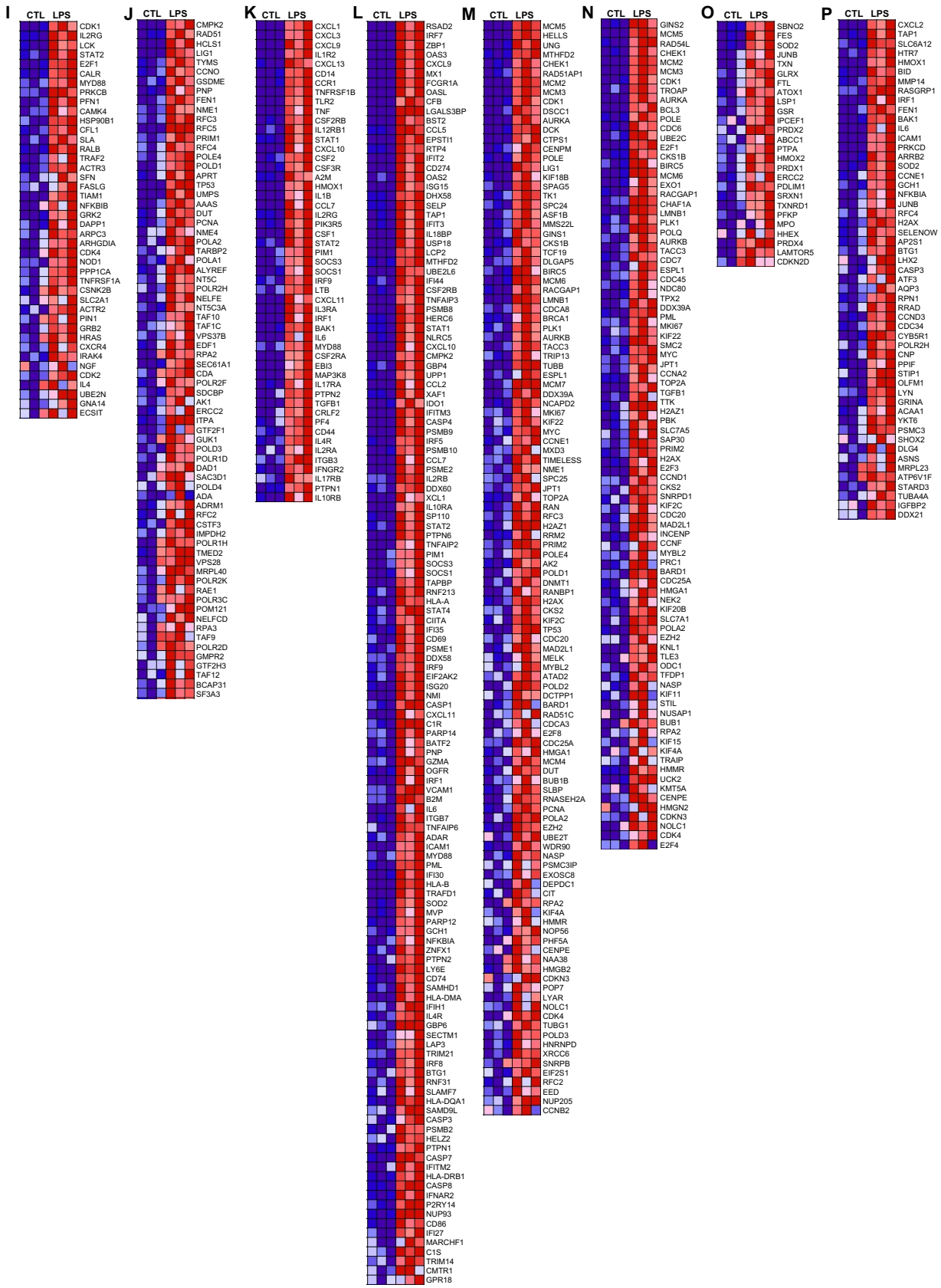
I
CTL LPS
CDK1
IL2RG
LCK
STAT2
E2F1
CALR
MYD88
PRKCB
PFN1
CAMK4
HSP90B1
CFL1
SLA
RALB
TRAF2
ACTR3
SFN
FASLG
TIAM1
NFKBIB
GRK2
DAPP1
ARPC3
ARHGDIA
CDK4
NOD1
PPP1CA
TNFRSF1A
CSNK2B
SLC2A1
ACTR2
PIN1
GRB2
HRAS
CXCR4
IRAK4
NGF
CDK2
IL4
UBE2N
GNA14
ECSIT
J
CTL LPS
CMPK2
RAD51
HCLS1
LIG1
TYMS
CCNO
GSDME
PNP
FEN1
NME1
RFC3
RFC5
PRIM1
RFC4
POLE4
POLD1
APRT
TP53
UMPS
AAAS
DUT
PCNA
NME4
POLA2
TARBP2
POLA1
ALYREF
NT5C
POLR2H
NELFE
NT5C3A
TAF10
TAF1C
VPS37B
EDF1
RPA2
SEC61A1
CDA
POLR2F
SDCBP
AK1
ERCC2
ITPA
GTF2F1
GUK1
POLD3
POLR1D
DAD1
SAC3D1
POLD4
ADA
ADRM1
RFC2
CSTF3
IMPDH2
POLR1H
TMED2
VPS28
MRPL40
POLR2K
RAE1
POLR3C
POM121
NELFCD
RPA3
TAF9
POLR2D
GMPR2
GTF2H3
TAF12
BCAP31
SF3A3
K
CTL LPS
CXCL1
CXCL3
CXCL9
IL1R2
CXCL13
CD14
CCR1
TNFRSF1B
TLR2
TNF
CSF2RB
IL12RB1
STAT1
CXCL10
CSF2
CSF3R
A2M
HMOX1
IL1B
CCL7
IL2RG
PIK3R5
CSF1
STAT2
PIM1
SOCS3
SOCS1
IRF9
LTB
CXCL11
IL3RA
IRF1
BAK1
IL6
MYD88
CSF2RA
EBI3
MAP3K8
IL17RA
PTPN2
TGFB1
CRLF2
PF4
CD44
IL4R
IL2RA
ITGB3
IFNGR2
IL17RB
PTPN1
IL10RB
L
CTL LPS
RSAD2
IRF7
ZBP1
OAS3
CXCL9
MX1
FCGR1A
OASL
CFB
LGALS3BP
BST2
CCL5
EPSTI1
RTP4
IFIT2
CD274
OAS2
ISG15
DHX58
SELP
TAP1
IFIT3
IL19BP
USP18
LCP2
MTHFD2
UBE2L6
IFI44
CSF2RB
TNFAIP3
PSMB8
HERC6
STAT1
NLRC5
CXCL10
CMPK2
GBP4
UPP1
CCL2
XAF1
IDO1
IFITM3
CASP4
PSMB9
IRF5
PSMB10
CCL7
PSME2
IL2RB
DDX60
XCL1
IL10RA
SP110
STAT2
PTPN6
TNFAIP2
PIM1
SOCS3
SOCS1
TAPBP
RNF213
HLA-A
STAT4
CIITA
IFI35
CD69
PSME1
DDX58
IRF9
EIF2AK2
ISG20
NMI
CASP1
CXCL11
C1R
PARP14
BATF2
PNP
GZMA
OGFR
IRF1
VCAM1
B2M
IL6
ITGB7
TNFAIP6
ADAR
ICAM1
MYD88
PML
IFI30
HLA-B
TRAFD1
SOD2
MVP
PARP12
GCH1
NFKBIA
ZNFX1
PTPN2
LY6E
CD74
SAMHD1
HLA-DMA
IFIH1
IL4R
GBP6
SECTM1
LAP3
TRIM21
IRF8
BTG1
RNF31
SLAMF7
HLA-DQA1
SAMD9L
CASP3
PSMB2
HELZ2
PTPN1
CASP7
IFITM2
HLA-DRB1
CASP8
IFNAR2
P2RY14
NUP93
CD86
IFI27
MARCHF1
C1S
TRIM14
CMTR1
GPR18
M
CTL LPS
MCM5
HELLS
UNG
MTHFD2
CHEK1
RAD51AP1
MCM2
MCM3
CDK1
DSCC1
AURKA
DCK
CTPS1
CENPM
POLE
LIG1
KIF18B
SPAG5
TK1
SPC24
ASF1B
MMS22L
GINS1
CKS1B
TCF19
DLGAP5
BIRC5
MCM6
RACGAP1
LMNB1
CDCA8
BRCA1
PLK1
AURKB
TACC3
TUBB
ESPL1
MCM7
DDX39A
NCAPD2
MKI67
KIF22
MYC
CCNE1
MXD3
TIMELESS
NME1
SPC25
JPT1
TOP2A
RAN
RFC3
H2AZ1
RRM2
PRIM2
POLE4
AK2
POLD1
DNMT1
RANBP1
H2AX
CKS2
KIF2C
TP53
CDC20
MAD2L1
MELK
MYBL2
ATAD2
POLD2
DCTPP1
BARD1
RAD51C
CDCA3
E2F8
CDC25A
HMGA1
MCM4
DUT
BUB1B
SLBP
RNASEH2A
PCNA
POLA2
EZH2
UBE2T
WDR90
NASP
PSMC3IP
EXOSC8
DEPDC1
CIT
RPA2
KIF4A
HMMR
NOP56
PHF5A
CENPE
NAA38
HMGB2
CDKN3
POP7
LYAR
NOLC1
CDK4
TUBG1
POLD3
HNRNPD
XRCC6
SNRPB
EIF2S1
RFC2
EED
NUP205
CCNB2
N
CTL LPS
GINS2
MCM5
RAD54L
CHEK1
MCM2
MCM3
CDK1
TROAP
AURKA
BCL3
POLE
CDC6
UBE2C
E2F1
CKS1B
BIRC5
MCM6
EXO1
RACGAP1
CHAF1A
LMNB1
PLK1
POLQ
AURKB
TACC3
CDC7
ESPL1
CDC45
NDC80
TPX2
DDX39A
PML
MKI67
KIF22
SMC2
MYC
JPT1
CCNA2
TOP2A
TGFB1
TTK
H2AZ1
PBK
SLC7A5
SAP30
PRIM2
H2AX
E2F3
CCND1
CKS2
SNRPD1
KIF2C
CDC20
MAD2L1
INCENP
CCNF
MYBL2
PRC1
BARD1
CDC25A
HMGA1
NEK2
KIF20B
SLC7A1
POLA2
EZH2
KNL1
TLE3
ODC1
TFDP1
NASP
KIF11
STIL
NUSAP1
BUB1
RPA2
KIF15
KIF4A
TRAIP
HMMR
UCK2
KMT5A
CENPE
HMGN2
CDKN3
NOLC1
CDK4
E2F4
O
CTL LPS
SBNO2
FES
SOD2
JUNB
TXN
GLRX
FTL
ATOX1
LSP1
GSR
IPCEF1
PRDX2
ABCC1
PTPA
HMOX2
PRDX1
ERCC2
PDLIM1
SRXN1
TXNRD1
PFKP
MPO
HHEX
PRDX4
LAMTOR5
CDKN2D
P
CTL LPS
CXCL2
TAP1
SLC6A12
HTR7
HMOX1
BID
MMP14
RASGRP1
IRF1
FEN1
BAK1
IL6
ICAM1
PRKCD
ARRB2
SOD2
CCNE1
GCH1
NFKBIA
JUNB
RFC4
H2AX
SELENOW
AP2S1
BTG1
LHX2
CASP3
ATF3
AQP3
RPN1
RRAD
CCND3
CDC34
CYB5R1
POLR2H
CNP
PPIF
STIP1
OLFM1
LYN
GRINA
ACAA1
YKT6
PSMC3
SHOX2
DLG4
ASNS
MRPL23
ATP6V1F
STARD3
TUBA4A
IGFBP2
DDX21

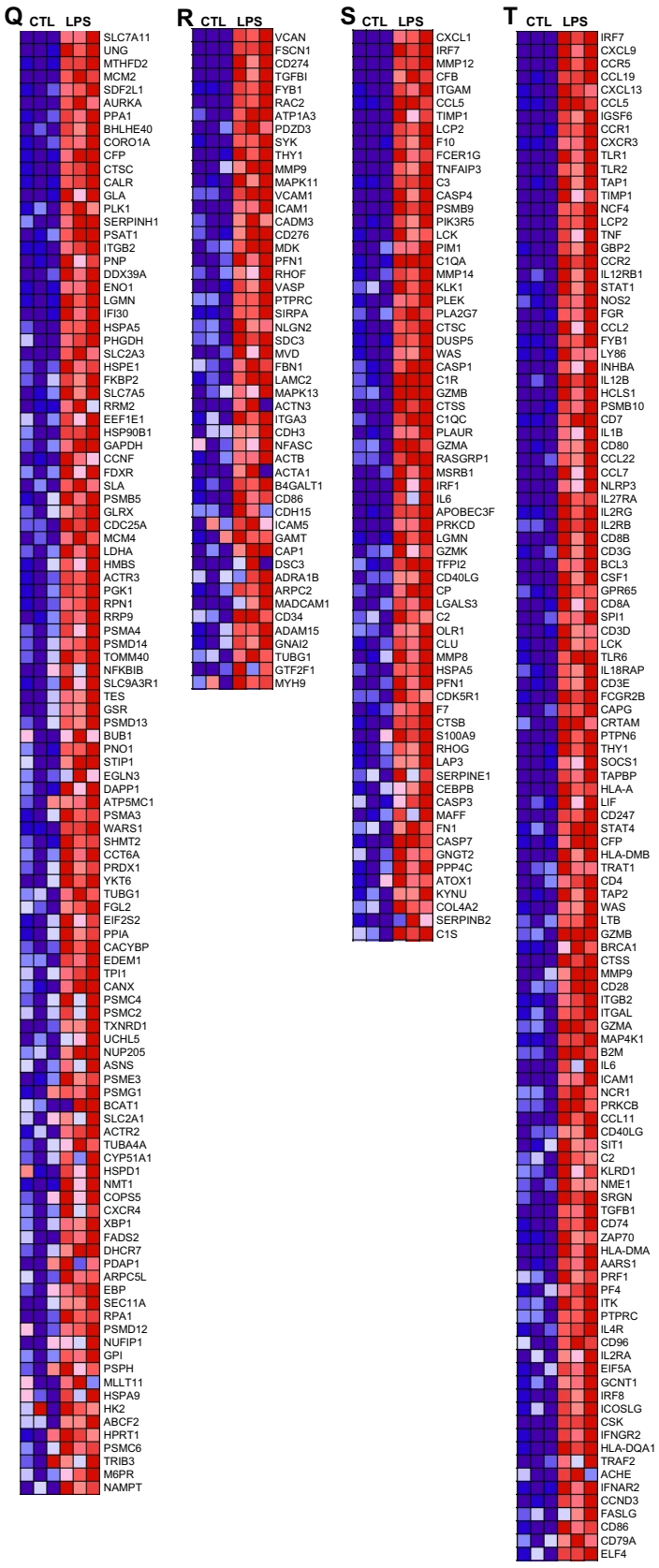
Q
CTL
LPS
SLC7A11
UNG
MTHFD2
MCM2
SDF2L1
AURKA
PPA1
BHLHE40
CORO1A
CFP
CTSC
CALR
GLA
PLK1
SERPINH1
PSAT1
ITGB2
PNP
DDX39A
ENO1
LGMN
IFI30
HSPA5
PHGDH
SLC2A3
HSPE1
FKBP2
SLC7A5
RRM2
EEF1E1
HSP90B1
GAPDH
CCNF
FDXR
SLA
PSMB5
GLRX
CDC25A
MCM4
LDHA
HMBS
ACTR3
PGK1
RPN1
RRP9
PSMA4
PSMD14
TOMM40
NFKBIB
SLC9A3R1
TES
GSR
PSMD13
BUB1
PNO1
STIP1
EGLN3
DAPP1
ATP5MC1
PSMA3
WARS1
SHMT2
CCT6A
PRDX1
YKT6
TUBG1
FGL2
EIF2S2
PPIA
CACYBP
EDEM1
TPI1
CANX
PSMC4
PSMC2
TXNRD1
UCHL5
NUP205
ASNS
PSME3
PSMG1
BCAT1
SLC2A1
ACTR2
TUBA4A
CYP51A1
HSPD1
NMT1
COPS5
CXCR4
XBP1
FADS2
DHCR7
PDAP1
ARPC5L
EBP
SEC11A
RPA1
PSMD12
NUFIP1
GPI
PSPH
MLLT11
HSPA9
HK2
ABCF2
HPRT1
PSMC6
TRIB3
M6PR
NAMPT
R
CTL
LPS
VCAN
FSCN1
CD274
TGFBI
FYB1
RAC2
ATP1A3
PDZD3
SYK
THY1
MMP9
MAPK11
VCAM1
ICAM1
CADM3
CD276
MDK
PFN1
RHOF
VASP
PTPRC
SIRPA
NLGN2
SDC3
MVD
FBN1
LAMC2
MAPK13
ACTN3
ITGA3
CDH3
NFASC
ACTB
ACTA1
B4GALT1
CD86
CDH15
ICAM5
GAMT
CAP1
DSC3
ADRA1B
ARPC2
MADCAM1
CD34
ADAM15
GNAI2
TUBG1
GTF2F1
MYH9
S
CTL
LPS
CXCL1
IRF7
MMP12
CFB
ITGAM
CCL5
TIMP1
LCP2
F10
FCER1G
TNFAIP3
C3
CASP4
PSMB9
PIK3R5
LCK
PIM1
C1QA
MMP14
KLK1
PLEK
PLA2G7
CTSC
DUSP5
WAS
CASP1
C1R
GZMB
CTSS
C1QC
PLAUR
GZMA
RASGRP1
MSRB1
IRF1
IL6
APOBEC3F
PRKCD
LGMN
GZMK
TFPI2
CD40LG
CP
LGALS3
C2
OLR1
CLU
MMP8
HSPA5
PFN1
CDK5R1
F7
CTSB
S100A9
RHOG
LAP3
SERPINE1
CEBPB
CASP3
MAFF
FN1
CASP7
GNGT2
PPP4C
ATOX1
KYNU
COL4A2
SERPINB2
C1S
T
CTL
LPS
IRF7
CXCL9
CCR5
CCL19
CXCL13
CCL5
IGSF6
CCR1
CXCR3
TLR1
TLR2
TAP1
TIMP1
NCF4
LCP2
TNF
GBP2
CCR2
IL12RB1
STAT1
NOS2
FGR
CCL2
FYB1
LY86
INHBA
IL12B
HCLS1
PSMB10
CD7
IL1B
CD80
CCL22
CCL7
NLRP3
IL27RA
IL2RG
IL2RB
CD8B
CD3G
BCL3
CSF1
GPR65
CD8A
SPI1
CD3D
LCK
TLR6
IL18RAP
CD3E
FCGR2B
CAPG
CRTAM
PTPN6
THY1
SOCS1
TAPBP
HLA-A
LIF
CD247
STAT4
CFP
HLA-DMB
TRAT1
CD4
TAP2
WAS
LTB
GZMB
BRCA1
CTSS
MMP9
CD28
ITGB2
ITGAL
GZMA
MAP4K1
B2M
IL6
ICAM1
NCR1
PRKCB
CCL11
CD40LG
SIT1
C2
KLRD1
NME1
SRGN
TGFB1
CD74
ZAP70
HLA-DMA
AARS1
PRF1
PF4
ITK
PTPRC
IL4R
CD96
IL2RA
EIF5A
GCNT1
IRF8
ICOSLG
CSK
IFNGR2
HLA-DQA1
TRAF2
ACHE
IFNAR2
CCND3
FASLG
CD86
CD79A
ELF4

Supplemental Figure 7: Core enrichment genes for Hallmark Pathways in neonatally ETS exposed female mouse lungs challenged with vehicle and LPS. Core enrichment genes for **(A)** p53, **(B)** Inflammatory response, **(C)** IL-2 STAT5 signaling, **(D)** Kras signaling, **(E)** Apoptosis, **(F)** Unfolded Protein Response, **(G)** Coagulation, **(H)** TNFα signaling via NFκB, **(I)** PI3K AKT MTOR signaling, **(J)** DNA Repair, **(K)** Interferon gamma response, **(L)** IL6 Jak STAT3 signaling, **(M)** E2F targets, **(N)** G2M checkpoint, **(O)** Reactive Oxygen Species, **(P)** UV Response pathway, **(Q)** MTORC1 signaling, **(R)** Apical Junction, **(S)** Complement pathway, and **(T)** Allograft Rejection Hallmark Pathways.

Supplemental Figure 8:

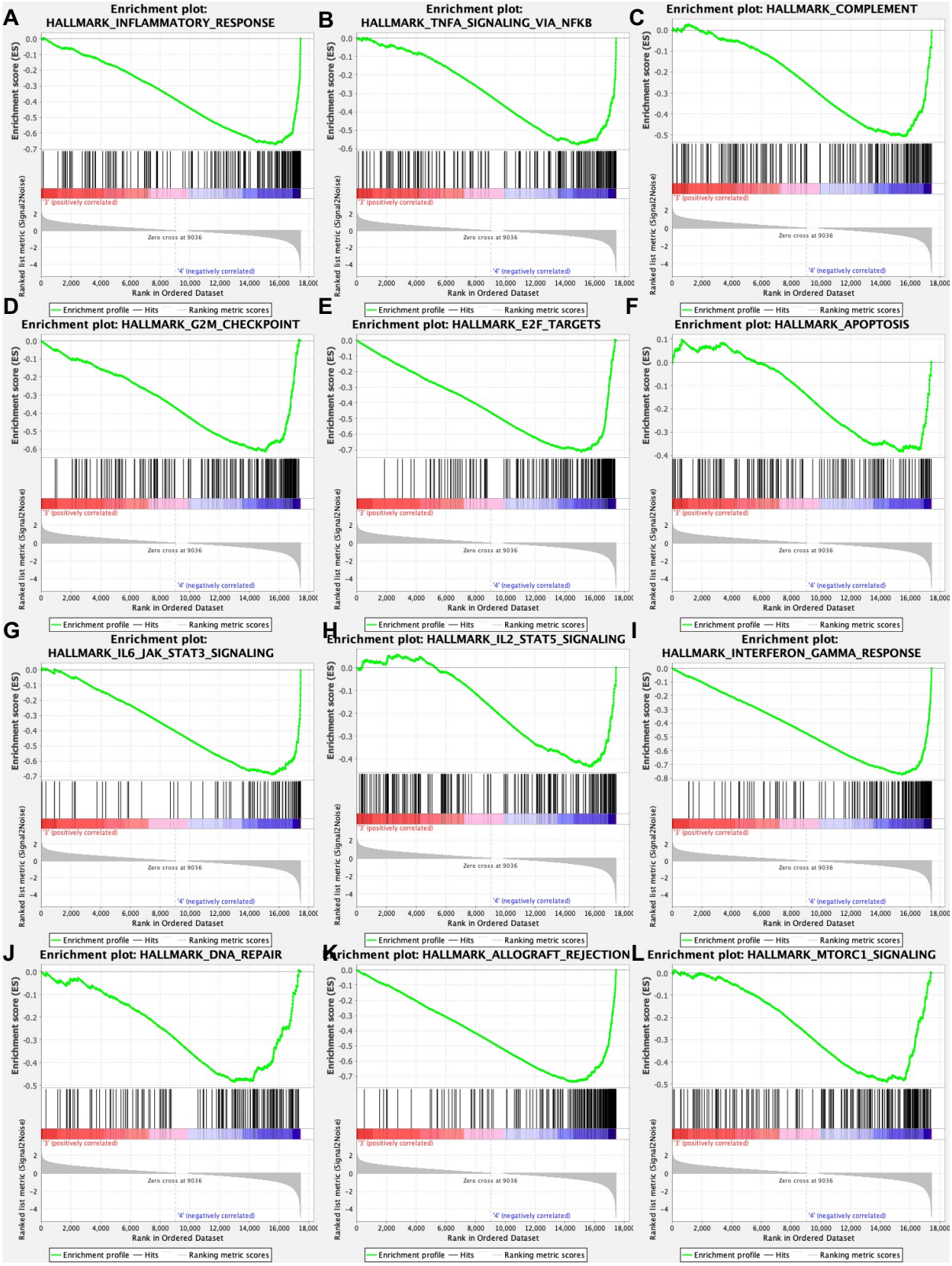

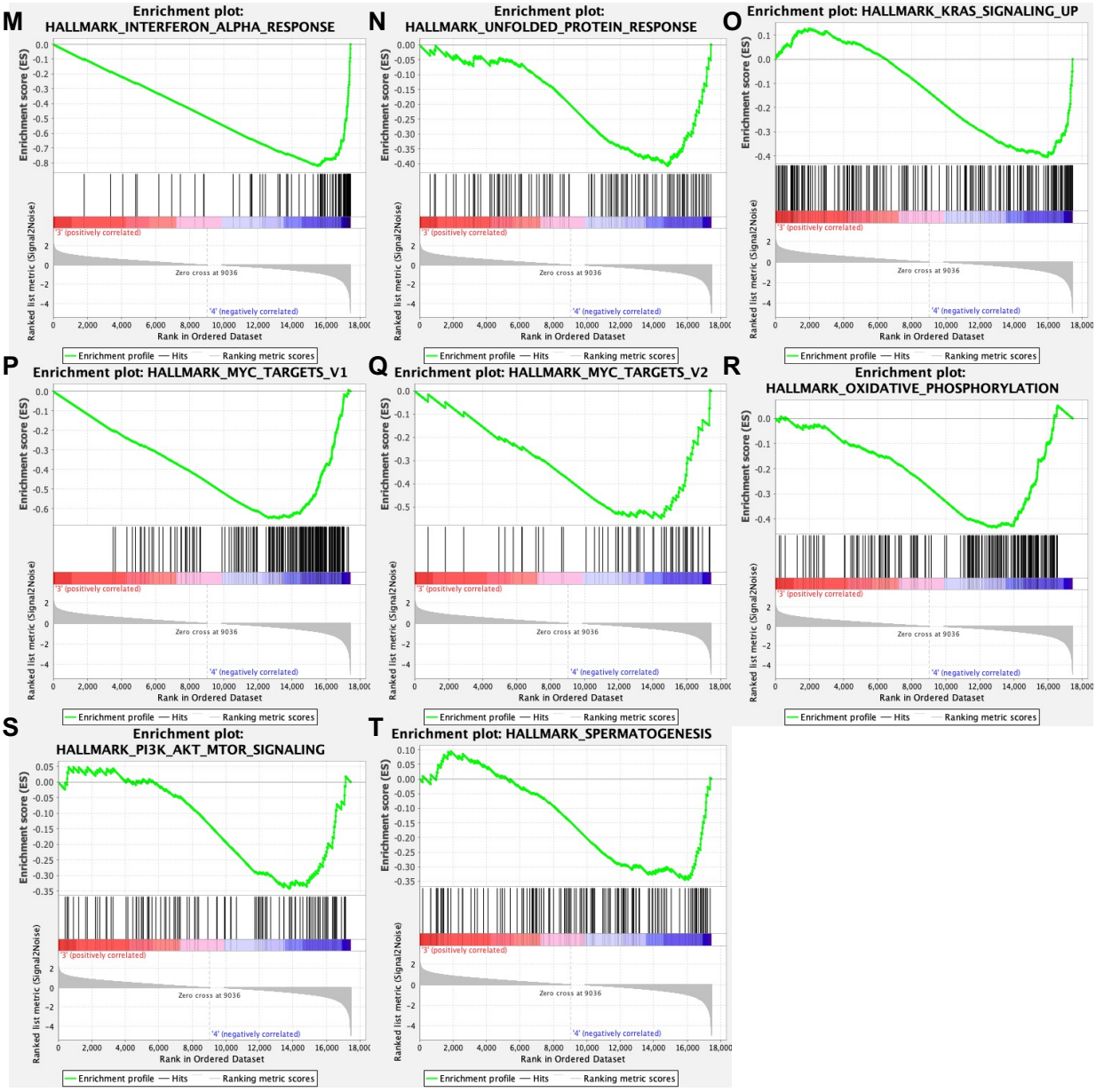

Supplemental Figure 8: Enrichment plots for hallmark pathways enriched following LPS challenge in neonatally ETS exposed male mouse lungs. GSEA Hallmark Pathway analysis was used to find differences between transcriptomes of control mouse lung challenged with LPS versus control. A FDR cutoff of 0.25 was used.

Supplemental Figure 9:

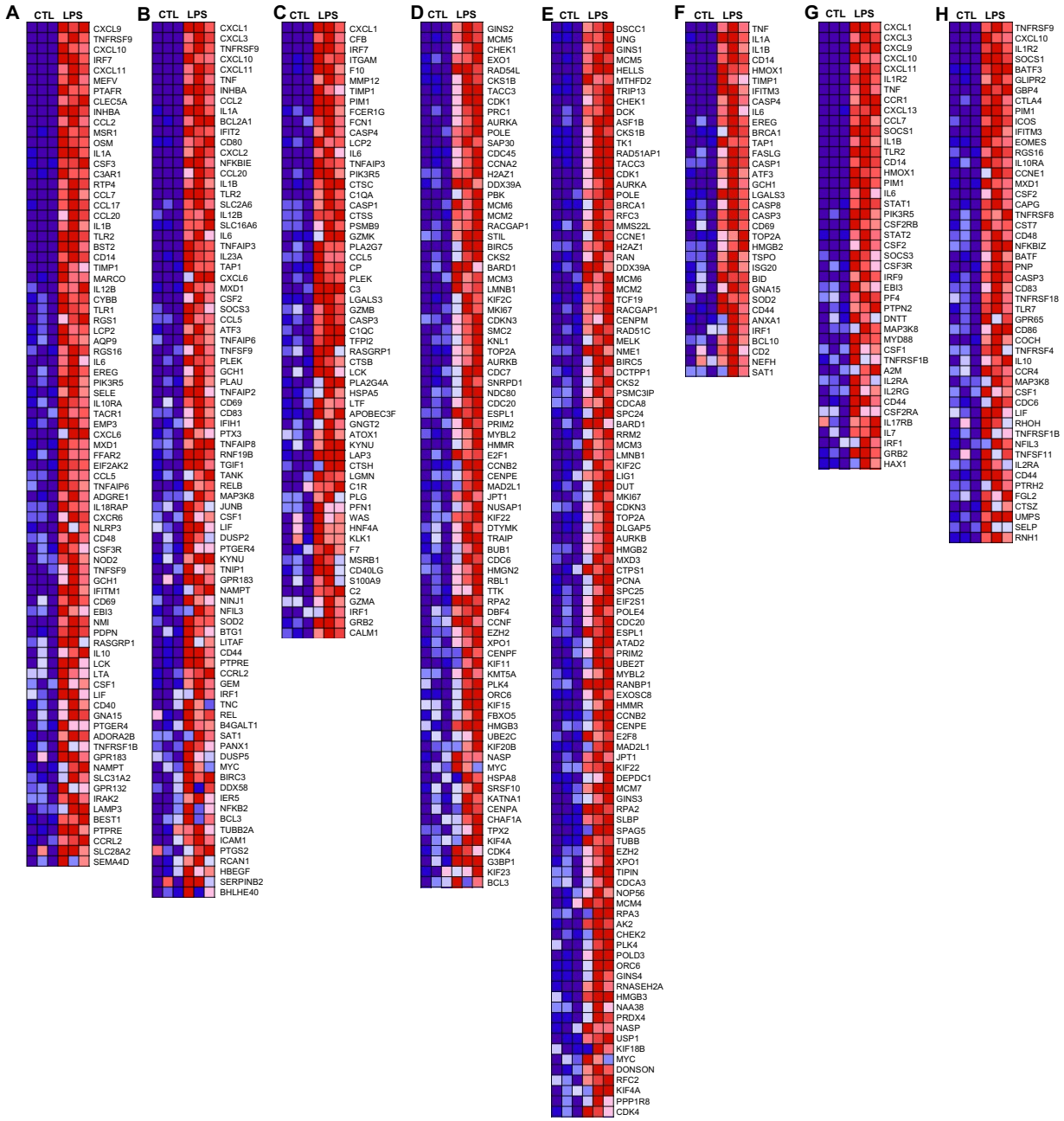

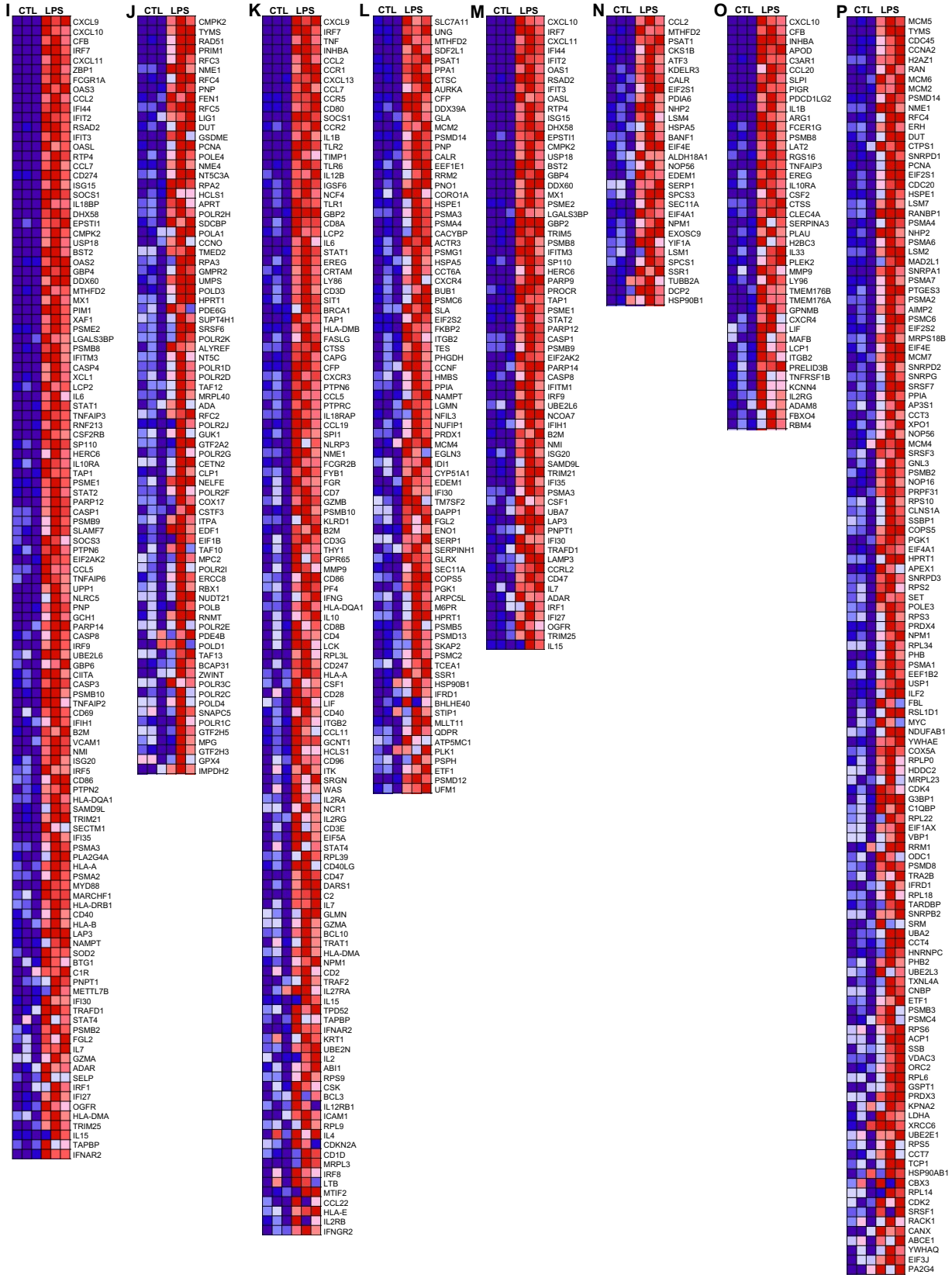
I CTL LPS
CXCL9
CXCL10
CFB
IRF7
CXCL11
ZBP1
FCGR1A
OAS3
CCL2
IFI44
IFIT2
RSAD2
IFIT3
OASL
RTP4
CCL7
CD274
ISG15
SOCS1
IL18BP
DHX58
EPSTI1
CMPK2
USP18
BST2
OAS2
GBP4
DDX60
MTHFD2
MX1
PIM1
XAF1
PSME2
LGALS3BP
PSMB8
IFITM3
CASP4
XCL1
LCP2
IL6
STAT1
TNFAIP3
RNF213
CSF2RB
SP110
HERC6
IL10RA
TAP1
PSME1
STAT2
PARP12
CASP1
PSMB9
SLAMF7
SOCS3
PTPN6
EIF2AK2
CCL5
TNFAIP6
UPP1
NLRC5
PNP
GCH1
PARP14
CASP8
IRF9
UBE2L6
GBP6
CIITA
CASP3
PSMB10
TNFAIP2
CD69
IFIH1
B2M
VCAM1
NMI
ISG20
IRF5
CD86
PTPN2
HLA-DQA1
SAMD9L
TRIM21
SECTM1
IFI35
PSMA3
PLA2G4A
HLA-A
PSMA2
MYD88
MARCHF1
HLA-DRB1
CD40
HLA-B
LAP3
NAMPT
SOD2
BTG1
C1R
PNPT1
METTL7B
IFI30
TRAFD1
STAT4
PSMB2
FGL2
IL7
GZMA
ADAR
SELP
IRF1
IFI27
OGFR
HLA-DMA
TRIM25
IL15
TAPBP
IFNAR2
J CTL LPS
CMPK2
TYMS
RAD51
PRIM1
RFC3
NME1
RFC4
PNP
FEN1
RFC5
LIG1
DUT
GSDME
PCNA
POLE4
NME4
NT5C3A
RPA2
HCLS1
APRT
POLR2H
SDCBP
POLA1
CCNO
TMED2
RPA3
GMPR2
UMPS
POLD3
HPRT1
PDE6G
SUPT4H1
SRSF6
POLR2K
ALYREF
NT5C
POLR1D
POLR2D
TAF12
MRPL40
ADA
RFC2
POLR2J
GUK1
GTF2A2
POLR2G
CETN2
CLP1
NELFE
POLR2F
COX17
CSTF3
ITPA
EDF1
EIF1B
TAF10
MPC2
POLR2I
ERCC8
RBX1
NUDT21
POLB
RNMT
POLR2E
PDE4B
POLD1
TAF13
BCAP31
ZWINT
POLR3C
POLR2C
POLD4
SNAPC5
POLR1C
GTF2H5
MPG
GTF2H3
GPX4
IMPDH2
K CTL LPS
CXCL9
IRF7
TNF
INHBA
CCL2
CCR1
CXCL13
CCL7
CCR5
CD80
SOCS1
CCR2
IL1B
TLR2
TIMP1
TLR6
IL12B
IGSF6
NCF4
TLR1
GBP2
CD8A
LCP2
IL6
STAT1
EREG
CRTAM
LY86
CD3D
SIT1
BRCA1
TAP1
HLA-DMB
FASLG
CTSS
CAPG
CFP
CXCR3
PTPN6
CCL5
PTPRC
IL18RAP
CCL19
SPI1
NLRP3
NME1
FCGR2B
FYB1
FGR
CD7
GZMB
PSMB10
KLRD1
B2M
CD3G
THY1
GPR65
MMP9
CD86
PF4
IFNG
HLA-DQA1
IL10
CD8B
CD4
LCK
RPL3L
CD247
HLA-A
CSF1
CD28
LIF
CD40
ITGB2
CCL11
GCNT1
HCLS1
CD96
ITK
SRGN
WAS
IL2RA
NCR1
IL2RG
CD3E
EIF5A
STAT4
RPL39
CD40LG
CD47
DARS1
C2
IL7
GLMN
GZMA
BCL10
TRAT1
HLA-DMA
NPM1
CD2
TRAF2
IL27RA
IL15
TPD52
TAPBP
IFNAR2
KRT1
UBE2N
IL2
ABI1
RPS9
CSK
BCL3
IL12RB1
ICAM1
RPL9
IL4
CDKN2A
CD1D
MRPL3
IRF8
LTB
MTIF2
CCL22
HLA-E
IL2RB
IFNGR2
L CTL LPS
SLC7A11
UNG
MTHFD2
SDF2L1
PSAT1
PPA1
CTSC
AURKA
CFP
DDX39A
GLA
MCM2
PSMD14
PNP
CALR
EEF1E1
RRM2
PNO1
CORO1A
HSPE1
PSMA3
PSMA4
CACYBP
ACTR3
PSMG1
HSPA5
CCT6A
CXCR4
BUB1
PSMC6
SLA
EIF2S2
FKBP2
ITGB2
TES
PHGDH
CCNF
HMBS
PPIA
NAMPT
LGMN
NFIL3
NUFIP1
PRDX1
MCM4
EGLN3
IDI1
CYP51A1
EDEM1
IFI30
TM7SF2
DAPP1
FGL2
ENO1
SERP1
SERPINH1
GLRX
SEC11A
COPS5
PGK1
ARPC5L
M6PR
HPRT1
PSMB5
PSMD13
SKAP2
PSMC2
TCEA1
SSR1
HSP90B1
IFRD1
BHLHE40
STIP1
MLLT11
QDPR
ATP5MC1
PLK1
PSPH
ETF1
PSMD12
UFM1
M CTL LPS
CXCL10
IRF7
CXCL11
IFI44
IFIT2
OAS1
RSAD2
IFIT3
OASL
RTP4
ISG15
DHX58
EPSTI1
CMPK2
USP18
BST2
GBP4
DDX60
MX1
PSME2
LGALS3BP
GBP2
TRIM5
PSMB8
IFITM3
SP110
HERC6
PARP9
PROCR
TAP1
PSME1
STAT2
PARP12
CASP1
PSMB9
EIF2AK2
PARP14
CASP8
IFITM1
IRF9
UBE2L6
NCOA7
IFIH1
B2M
NMI
ISG20
SAMD9L
TRIM21
IFI35
PSMA3
CSF1
UBA7
LAP3
PNPT1
IFI30
TRAFD1
LAMP3
CCRL2
CD47
IL7
ADAR
IRF1
IFI27
OGFR
TRIM25
IL15
N CTL LPS
CCL2
MTHFD2
PSAT1
CKS1B
ATF3
KDELR3
CALR
EIF2S1
PDIA6
NHP2
LSM4
HSPA5
BANF1
EIF4E
ALDH18A1
NOP56
EDEM1
SERP1
SPCS3
SEC11A
EIF4A1
NPM1
EXOSC9
YIF1A
LSM1
SPCS1
SSR1
TUBB2A
DCP2
HSP90B1
O CTL LPS
CXCL10
CFB
INHBA
APOD
C3AR1
CCL20
SLPI
PIGR
PDCD1LG2
IL1B
ARG1
FCER1G
PSMB8
LAT2
RGS16
TNFAIP3
EREG
IL10RA
CSF2
CTSS
CLEC4A
SERPINA3
PLAU
H2BC3
IL33
PLEK2
MMP9
LY96
TMEM176B
TMEM176A
GPNMB
CXCR4
LIF
MAFB
LCP1
ITGB2
PRELID3B
TNFRSF1B
KCNN4
IL2RG
ADAM8
FBXO4
RBM4
P CTL LPS
MCM5
TYMS
CDC45
CCNA2
H2AZ1
RAN
MCM6
MCM2
PSMD14
NME1
RFC4
ERH
DUT
CTPS1
SNRPD1
PCNA
EIF2S1
CDC20
HSPE1
LSM7
RANBP1
PSMA4
NHP2
PSMA6
LSM2
MAD2L1
SNRPA1
PSMA7
PTGES3
PSMA2
AIMP2
PSMC6
EIF2S2
MRPS18B
EIF4E
MCM7
SNRPD2
SNRPG
SRSF7
PPIA
AP3S1
CCT3
XPO1
NOP56
MCM4
SRSF3
GNL3
PSMB2
NOP16
PRPF31
RPS10
CLNS1A
SSBP1
COPS5
PGK1
EIF4A1
HPRT1
APEX1
SNRPD3
RPS2
SET
POLE3
RPS3
PRDX4
NPM1
RPL34
PHB
PSMA1
EEF1B2
USP1
ILF2
FBL
RSL1D1
MYC
NDUFAB1
YWHAE
COX5A
RPLP0
HDDC2
MRPL23
CDK4
G3BP1
C1QBP
RPL22
EIF1AX
VBP1
RRM1
ODC1
PSMD8
TRA2B
IFRD1
RPL18
TARDBP
SNRPB2
SRM
UBA2
CCT4
HNRNPC
PHB2
UBE2L3
TXNL4A
CNBP
ETF1
PSMB3
PSMC4
RPS6
ACP1
SSB
VDAC3
ORC2
RPL6
GSPT1
PRDX3
KPNA2
LDHA
XRCC6
UBE2E1
RPS5
CCT7
TCP1
HSP90AB1
CBX3
RPL14
CDK2
SRSF1
RACK1
CANX
ABCE1
YWHAQ
EIF3J
PA2G4

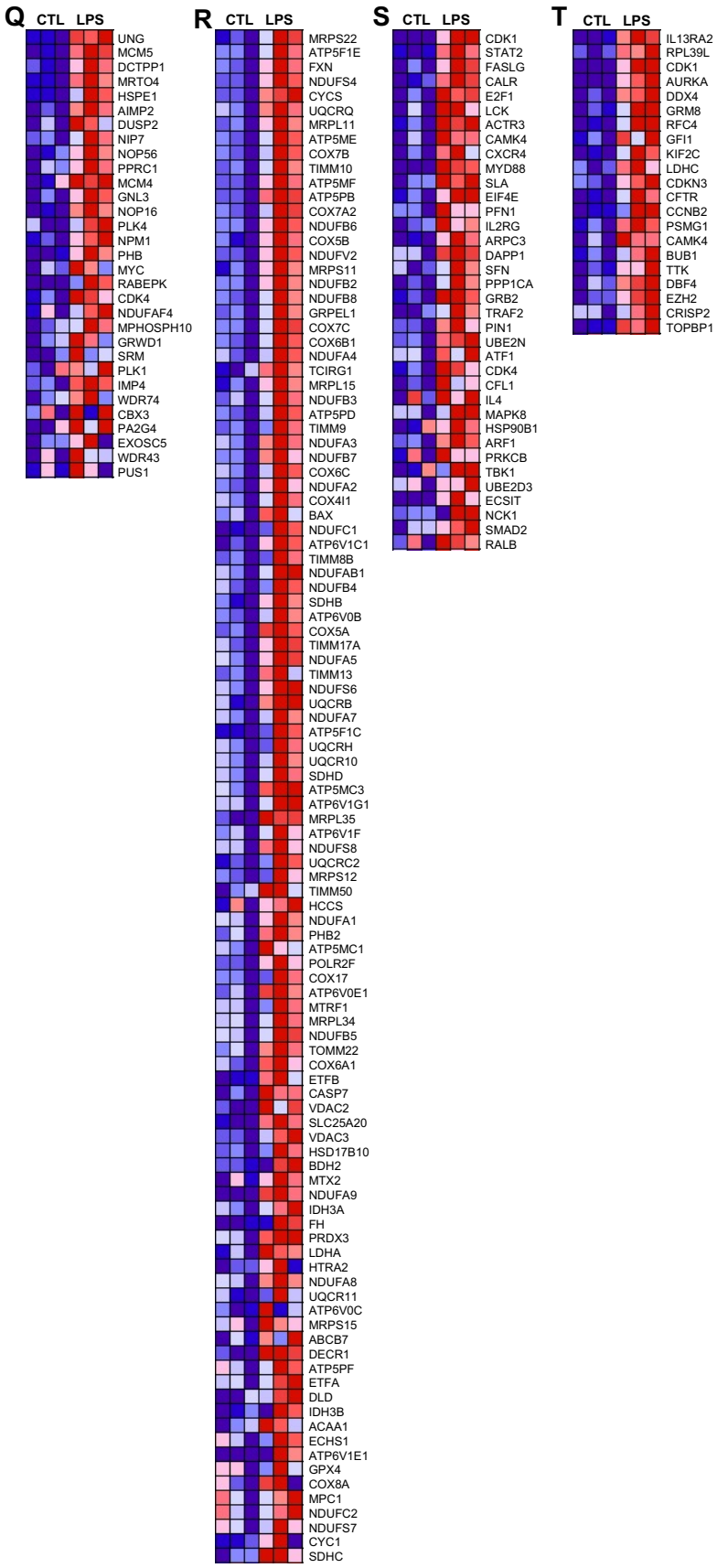
Q
CTL LPS
UNG
MCM5
DCTPP1
MRTO4
HSPE1
AIMP2
DUSP2
NIP7
NOP56
PPRC1
MCM4
GNL3
NOP16
PLK4
NPM1
PHB
MYC
RABEPK
CDK4
NDUFAF4
MPHOSPH10
GRWD1
SRM
PLK1
IMP4
WDR74
CBX3
PA2G4
EXOSC5
WDR43
PUS1
R
CTL LPS
MRPS22
ATP5F1E
FXN
NDUFS4
CYCS
UQCRQ
MRPL11
ATP5ME
COX7B
TIMM10
ATP5MF
ATP5PB
COX7A2
NDUFB6
COX5B
NDUFV2
MRPS11
NDUFB2
NDUFB8
GRPEL1
COX7C
COX6B1
NDUFA4
TCIRG1
MRPL15
NDUFB3
ATP5PD
TIMM9
NDUFA3
NDUFB7
COX6C
NDUFA2
COX4I1
BAX
NDUFC1
ATP6V1C1
TIMM8B
NDUFAB1
NDUFB4
SDHB
ATP6V0B
COX5A
TIMM17A
NDUFA5
TIMM13
NDUFS6
UQCRB
NDUFA7
ATP5F1C
UQCRH
UQCR10
SDHD
ATP5MC3
ATP6V1G1
MRPL35
ATP6V1F
NDUFS8
UQCRC2
MRPS12
TIMM50
HCCS
NDUFA1
PHB2
ATP5MC1
POLR2F
COX17
ATP6V0E1
MTRF1
MRPL34
NDUFB5
TOMM22
COX6A1
ETFB
CASP7
VDAC2
SLC25A20
VDAC3
HSD17B10
BDH2
MTX2
NDUFA9
IDH3A
FH
PRDX3
LDHA
HTRA2
NDUFA8
UQCR11
ATP6V0C
MRPS15
ABCB7
DECR1
ATP5PF
ETFA
DLD
IDH3B
ACAA1
ECHS1
ATP6V1E1
GPX4
COX8A
MPC1
NDUFC2
NDUFS7
CYC1
SDHC
S
CTL LPS
CDK1
STAT2
FASLG
CALR
E2F1
LCK
ACTR3
CAMK4
CXCR4
MYD88
SLA
EIF4E
PFN1
IL2RG
ARPC3
DAPP1
SFN
PPP1CA
GRB2
TRAF2
PIN1
UBE2N
ATF1
CDK4
CFL1
IL4
MAPK8
HSP90B1
ARF1
PRKCB
TBK1
UBE2D3
ECSIT
NCK1
SMAD2
RALB
T
CTL LPS
IL13RA2
RPL39L
CDK1
AURKA
DDX4
GRM8
RFC4
GFI1
KIF2C
LDHC
CDKN3
CFTR
CCNB2
PSMG1
CAMK4
BUB1
TTK
DBF4
EZH2
CRISP2
TOPBP1

Supplemental Figure 9: Core enrichment genes for Hallmark Pathways in neonatally ETS exposed male mouse lungs challenged with vehicle and LPS. Core enrichment genes for **(A)** inflammatory response, **(B)** TNFα signaling via NFκB, **(C)** complement, **(D)** G2M checkpoint, **(E)** E2F targets, **(F)** apoptosis, **(G)** IL6 JAK STAT3 signaling, **(H)** IL-2 STAT5 signaling, **(I)** interferon gamma response, **(J)** DNA repair, **(K)** allograft rejection, **(L)** MTORC1 signaling, **(M)** interferon alpha response, **(N)** unfolded protein response, **(O)** Kras signaling, **(P)** Myc targets V1, **(Q)** Myc targets V2, **(R)** oxidative phosphorylation, **(S)** PI3K AKT MTOR signaling, and **(T)** spermatogenesis Hallmark Pathways.

2.8. References

1. Centers for Disease Control Prevention, *Current cigarette smoking among adults in the United States.* 2019.
2. Do, E.K., et al., *Social determinants of smoke exposure during pregnancy: Findings from waves 1 & 2 of the Population Assessment of Tobacco and Health (PATH) Study.* Preventive medicine reports, 2018. **12**: p. 312-320.
3. Martinez, F.D., *Early-life origins of chronic obstructive pulmonary disease.* New England Journal of Medicine, 2016. **375**(9): p. 871-878.
4. Stern, D.A., et al., *Poor airway function in early infancy and lung function by age 22 years: a non-selective longitudinal cohort study.* The Lancet, 2007. **370**(9589): p. 758-764.
5. Bonner, K., E. Scotney, and S. Saglani, *Factors and mechanisms contributing to the development of preschool wheezing disorders.* Expert Review of Respiratory Medicine, 2021. **15**(6): p. 745-760.
6. LoMauro, A. and A. Aliverti, *Sex differences in respiratory function.* Breathe, 2018. **14**(2): p. 131-140.
7. Ntritsos, G., et al., *Gender-specific estimates of COPD prevalence: a systematic review and meta-analysis.* International journal of chronic obstructive pulmonary disease, 2018. **13**: p. 1507-1514.
8. Han, M.K., et al., *Gender and chronic obstructive pulmonary disease: why it matters.* American journal of respiratory and critical care medicine, 2007. **176**(12): p. 1179-1184.
9. Barnes, P.J., *Sex differences in chronic obstructive pulmonary disease mechanisms*. 2016, American Thoracic Society.
10. Pinkerton, K.E., et al., *Women and lung disease. Sex differences and global health disparities.* American journal of respiratory and critical care medicine, 2015. **192**(1): p. 11-16.

11. Ji, C.-M., et al., *Maternal exposure to environmental tobacco smoke alters Clara cell secretory protein expression in fetal rat lung.* American Journal of Physiology-Lung Cellular and Molecular Physiology, 1998. **275**(5): p. L870-L876.

12. Lamb, D. and L. Reid, *Goblet cell increase in rat bronchial epithelium after exposure to cigarette and cigar tobacco smoke.* Br Med J, 1969. **1**(5635): p. 33-35.

13. Di, Y.P., J. Zhao, and R. Harper, *Cigarette smoke induces MUC5AC protein expression through the activation of Sp1.* Journal of Biological Chemistry, 2012. **287**(33): p. 27948-27958.

14. Hodge, S., et al., *Increased airway granzyme b and perforin in current and ex-smoking COPD subjects.* COPD: Journal of Chronic Obstructive Pulmonary Disease, 2006. **3**(4): p. 179-187.

15. Hodge, S., et al., *Smoking alters alveolar macrophage recognition and phagocytic ability: implications in chronic obstructive pulmonary disease.* American journal of respiratory cell and molecular biology, 2007. **37**(6): p. 748-755.

16. Karimi, R., et al., *Cell recovery in bronchoalveolar lavage fluid in smokers is dependent on cumulative smoking history.* PloS one, 2012. **7**(3): p. e34232.

17. Wallace, W., M. Gillooly, and D. Lamb, *Intra-alveolar macrophage numbers in current smokers and non-smokers: a morphometric study of tissue sections.* Thorax, 1992. **47**(6): p. 437-440.

18. Di Stefano, A., et al., *Severity of airflow limitation is associated with severity of airway inflammation in smokers.* American journal of respiratory and critical care medicine, 1998. **158**(4): p. 1277-1285.

19. Teague, S.V., et al., *Sidestream cigarette smoke generation and exposure system for environmental tobacco smoke studies.* Inhalation toxicology, 1994. **6**(1): p. 79-93.

20. Lakatos, H.F., et al., *Oropharyngeal aspiration of a silica suspension produces a superior model of silicosis in the mouse when compared to intratracheal instillation.* Exp Lung Res, 2006. **32**(5): p. 181-99.

21. Mootha, V.K., et al., *PGC-1α-responsive genes involved in oxidative phosphorylation are coordinately downregulated in human diabetes.* Nature Genetics, 2003. **34**(3): p. 267-273.

22. Subramanian, A., et al., *Gene set enrichment analysis: A knowledge-based approach for interpreting genome-wide expression profiles.* Proceedings of the National Academy of Sciences, 2005. **102**(43): p. 15545-15550.

23. Liberzon, A., et al., *The Molecular Signatures Database (MSigDB) hallmark gene set collection.* Cell systems, 2015. **1**(6): p. 417-425.

24. Ashburner, M., et al., *Gene ontology: tool for the unification of biology.* Nature genetics, 2000. **25**(1): p. 25-29.

25. *The Gene Ontology resource: enriching a GOld mine.* Nucleic Acids Research, 2021. **49**(D1): p. D325-D334.

26. Mi, H., et al., *PANTHER version 14: more genomes, a new PANTHER GO-slim and improvements in enrichment analysis tools.* Nucleic acids research, 2019. **47**(D1): p. D419-D426.

27. Raudvere, U., et al., *g: Profiler: a web server for functional enrichment analysis and conversions of gene lists (2019 update).* Nucleic acids research, 2019. **47**(W1): p. W191-W198.

28. Pirooznia, M., V. Nagarajan, and Y. Deng, *GeneVenn-A web application for comparing gene lists using Venn diagrams.* Bioinformation, 2007. **1**(10): p. 420.

29. Bhat, T.A., et al., *Secondhand smoke induces inflammation and impairs immunity to respiratory infections.* The Journal of Immunology, 2018. **200**(8): p. 2927-2940.

30. *Bronchoalveolar lavage constituents in healthy individuals, idiopathic pulmonary fibrosis, and selected comparison groups. The BAL Cooperative Group Steering Committee.* Am Rev Respir Dis, 1990. **141**(5 Pt 2): p. S169-202.

31. Higashimoto, Y., et al., *The effects of aging on the function of alveolar macrophages in mice.* Mechanisms of ageing and development, 1993. **69**(3): p. 207-217.

32. Wang, T., et al., *Comparative analysis of differential gene expression analysis tools for single-cell RNA sequencing data.* BMC bioinformatics, 2019. **20**(1): p. 1-16.

33. Croft, D., et al., *Reactome: a database of reactions, pathways and biological processes.* Nucleic acids research, 2011. **39**(Database issue): p. D691-D697.

34. Noël-Georis, I., et al., *Database of bronchoalveolar lavage fluid proteins.* Journal of Chromatography B, 2002. **771**(1-2): p. 221-236.

35. Bhargava, M., et al., *Bronchoalveolar lavage fluid protein expression in acute respiratory distress syndrome provides insights into pathways activated in subjects with different outcomes.* Scientific reports, 2017. **7**(1): p. 1-11.

36. Wang, Y., et al., *Lung fluid biomarkers for acute respiratory distress syndrome: a systematic review and meta-analysis.* Critical Care, 2019. **23**(1): p. 1-15.

37. Liptzin, D.R., L.I. Landau, and L.M. Taussig, *Sex and the lung: observations, hypotheses, and future directions.* Pediatric pulmonology, 2015. **50**(12): p. 1159-1169.

38. Zein, J.G. and S.C. Erzurum, *Asthma is different in women.* Current allergy and asthma reports, 2015. **15**(6): p. 1-10.

39. Gilliland, F.D., Y.-F. Li, and J.M. Peters, *Effects of maternal smoking during pregnancy and environmental tobacco smoke on asthma and wheezing in children.* American journal of respiratory and critical care medicine, 2001. **163**(2): p. 429-436.

40. Townsend, E.A., V.M. Miller, and Y. Prakash, *Sex differences and sex steroids in lung health and disease.* Endocrine reviews, 2012. **33**(1): p. 1-47.

41. Kadel, S. and S. Kovats, *Sex hormones regulate innate immune cells and promote sex differences in respiratory virus infection.* Frontiers in Immunology, 2018. **9**: p. 1653.

42. Mann, M., V. Cortez, and R.K. Vadlamudi, *Epigenetics of estrogen receptor signaling: role in hormonal cancer progression and therapy.* Cancers, 2011. **3**(2): p. 1691-1707.

43. Anderson, R., et al., *Passive Smoking by Humans Sensitizes Circulating Neutrophils1-3.* Am Rev Respir Dis, 1991. **144**: p. 570-574.

44. Flouris, A.D., et al., *Sexual dimorphism in the acute effects of secondhand smoke on thyroid hormone secretion, inflammatory markers and vascular function.* American Journal of Physiology-Endocrinology and Metabolism, 2008. **294**(2): p. E456-E462.

45. Cook, D.G. and D.P. Strachan, *Summary of effects of parental smoking on the respiratory health of children and implications for research.* Thorax, 1999. **54**(4): p. 357-366.

46. DiFranza, J.R., et al., *Systematic literature review assessing tobacco smoke exposure as a risk factor for serious respiratory syncytial virus disease among infants and young children.* BMC pediatrics, 2012. **12**(1): p. 1-16.

47. Vanker, A., R. Gie, and H. Zar, *The association between environmental tobacco smoke exposure and childhood respiratory disease: a review.* Expert review of respiratory medicine, 2017. **11**(8): p. 661-673.

48. Wilson, K.M., et al., *Secondhand tobacco smoke exposure and severity of influenza in hospitalized children.* The Journal of pediatrics, 2013. **162**(1): p. 16-21.

49. Wood, L.G., et al., *The neutrophilic inflammatory phenotype is associated with systemic inflammation in asthma.* Chest, 2012. **142**(1): p. 86-93.

50. Saradna, A., et al., *Macrophage polarization and allergic asthma.* Translational Research, 2018. **191**: p. 1-14.

51. Jasper, A.E., et al., *Understanding the role of neutrophils in chronic inflammatory airway disease.* F1000Research, 2019. **8**.

52. Hey, J., et al., *Epigenetic reprogramming of airway macrophages promotes polarization and inflammation in muco-obstructive lung disease.* Nature communications, 2021. **12**(1): p. 1-18.

53. Garnier, M., et al., *Macrophage polarization favors epithelial repair during acute respiratory distress syndrome.* Critical care medicine, 2018. **46**(7): p. e692-e701.

54. Rebetz, J., J.W. Semple, and R. Kapur, *The pathogenic involvement of neutrophils in acute respiratory distress syndrome and transfusion-related acute lung injury.* Transfusion Medicine and Hemotherapy, 2018. **45**(5): p. 290-298.

55. DeForge, L. and D.G. Remick, *Kinetics of TNF, IL-6, and IL-8 gene expression in LPS-stimulated human whole blood.* Biochemical and biophysical research communications, 1991. **174**(1): p. 18-24.

56. Reynolds, C.J., et al., *Lung defense through IL-8 carries a cost of chronic lung remodeling and impaired function.* American journal of respiratory cell and molecular biology, 2018. **59**(5): p. 557-571.

57. Prabhakar, U., et al., *Correlation of protein and gene expression profiles of inflammatory proteins after endotoxin challenge in human subjects.* DNA and cell biology, 2005. **24**(7): p. 410-431.

58. Warren, H.S., et al., *Resilience to bacterial infection: difference between species could be due to proteins in serum.* The Journal of infectious diseases, 2010. **201**(2): p. 223-232.

59. Tateda, K., et al., *Lipopolysaccharide-induced lethality and cytokine production in aged mice.* Infection and immunity, 1996. **64**(3): p. 769-774.

60. Falagas, M.E., E.G. Mourtzoukou, and K.Z. Vardakas, *Sex differences in the incidence and severity of respiratory tract infections.* Respiratory medicine, 2007. **101**(9): p. 1845-1863.

61. Penaloza, C., et al., *Sex of the cell dictates its response: differential gene expression and sensitivity to cell death inducing stress in male and female cells.* The FASEB Journal, 2009. **23**(6): p. 1869-1879.

62. McClelland, E.E. and J.M. Smith, *Gender specific differences in the immune response to infection.* Archivum immunologiae et therapiae experimentalis, 2011. **59**(3): p. 203-213.

63. Beagley, K.W. and C.M. Gockel, *Regulation of innate and adaptive immunity by the female sex hormones oestradiol and progesterone.* FEMS Immunology & Medical Microbiology, 2003. **38**(1): p. 13-22.

64. Bove, R.M., et al., *Reproductive period and epigenetic modifications of the oxidative phosphorylation pathway in the human prefrontal cortex.* PloS one, 2018. **13**(7): p. e0199073.

65. Terao, M., et al., *Role of mitochondria and cardiolipins in growth inhibition of breast cancer cells by retinoic acid.* Journal of Experimental & Clinical Cancer Research, 2019. **38**(1): p. 1-20.

66. Siddikuzzaman, C. Guruvayoorappan, and V.M. Berlin Grace, *All trans retinoic acid and cancer.* Immunopharmacol Immunotoxicol, 2011. **33**(2): p. 241-9.

67. Besaratinia, A. and G.P. Pfeifer, *Second-hand smoke and human lung cancer.* The lancet oncology, 2008. **9**(7): p. 657-666.

68. Kim, A., et al., *Exposure to secondhand smoke and risk of cancer in never smokers: a meta-analysis of epidemiologic studies.* International journal of environmental research and public health, 2018. **15**(9): p. 1981.

69. Gale, M., et al., *Acquired resistance to HER2-targeted therapies creates vulnerability to ATP synthase inhibition.* Cancer research, 2020. **80**(3): p. 524-535.

70. Sakai, K., et al., *Transcriptome profiling and metagenomic analysis help to elucidate interactions in an inflammation-associated cancer mouse model.* Cancers, 2021. **13**(15): p. 3683.

71. Kanehisa, M., et al., *KEGG as a reference resource for gene and protein annotation.* Nucleic acids research, 2016. **44**(D1): p. D457-D462.

72. Messina, E., R. Tyndale, and E. Sellers, *A major role for CYP2A6 in nicotine C-oxidation by human liver microsomes.* Journal of Pharmacology and Experimental Therapeutics, 1997. **282**(3): p. 1608-1614.

73. Mollerup, S., et al., *Sex differences in lung CYP1A1 expression and DNA adduct levels among lung cancer patients.* Cancer research, 1999. **59**(14): p. 3317-3320.

74. Anttila, S., et al., *CYP1A1 levels in lung tissue of tobacco smokers and polymorphisms of CYP1A1 and aromatic hydrocarbon receptor.* Pharmacogenetics and Genomics, 2001. **11**(6): p. 501-509.

75. Lee, C.Z., et al., *Effect of in utero and postnatal exposure to environmental tobacco smoke on the developmental expression of pulmonary cytochrome P450 monooxygenases.* Journal of biochemical and molecular toxicology, 2000. **14**(3): p. 121-130.

76. Zhang, W.-Y., et al., *CYP1A1 relieves lipopolysaccharide-induced inflammatory responses in bovine mammary epithelial cells.* Mediators of inflammation, 2018. **2018**.

77. Holen, E. and P.A. Olsvik, *Aryl hydrocarbon receptor protein and Cyp1A1 gene induction by LPS and phenanthrene in Atlantic cod (Gadus morhua) head kidney cells.* Fish & shellfish immunology, 2014. **40**(2): p. 384-391.

78. Paton, T.E. and K.W. Renton, *Cytokine-mediated down-regulation of CYP1A1 in Hepa1 cells.* Biochemical pharmacology, 1998. **55**(11): p. 1791-1796.

79. Vogel, C.F., et al., *Cross-talk between aryl hydrocarbon receptor and the inflammatory response: a role for nuclear factor-κB.* Journal of Biological Chemistry, 2014. **289**(3): p. 1866-1875.

80. Morgan, E.T., T. Li-Masters, and P.-Y. Cheng, *Mechanisms of cytochrome P450 regulation by inflammatory mediators.* Toxicology, 2002. **181**: p. 207-210.

81. Theken, K.N., et al., *Activation of the acute inflammatory response alters cytochrome P450 expression and eicosanoid metabolism.* Drug metabolism and disposition, 2011. **39**(1): p. 22-29.

82. Mannino, D.M., et al., *Health effects related to environmental tobacco smoke exposure in children in the United States: data from the Third National Health and Nutrition Examination Survey.* Archives of pediatrics & adolescent medicine, 2001. **155**(1): p. 36-41.

83. Scherer, G., et al., *Assessment of the exposure of children to environmental tobacco smoke (ETS) by different methods.* Human & experimental toxicology, 1999. **18**(4): p. 297-301.

84. Mund, S.I., M. Stampanoni, and J.C. Schittny, *Developmental alveolarization of the mouse lung.* Developmental dynamics: an official publication of the American Association of Anatomists, 2008. **237**(8): p. 2108-2116.

85. Herring, M.J., et al., *Growth of alveoli during postnatal development in humans based on stereological estimation.* American Journal of Physiology-Lung Cellular and Molecular Physiology, 2014. **307**(4): p. L338-L344.

86. Biswas, S.K. and E. Lopez-Collazo, *Endotoxin tolerance: new mechanisms, molecules and clinical significance.* Trends in immunology, 2009. **30**(10): p. 475-487.

87. Whiteside, T.E., et al., *Endotoxin, coliform, and dust levels in various types of rodent bedding.* Journal of the American association for laboratory animal science, 2010. **49**(2): p. 184-189.

88. Pinkerton, K. and R. Harding, *The lung: development, aging and the environment*. 2014: Elsevier.

89. Glassberg, M.K., et al., *17β-estradiol replacement reverses age-related lung disease in estrogen-deficient C57BL/6J mice.* Endocrinology, 2014. **155**(2): p. 441-448.

Chapter 3

Neonatal environmental tobacco smoke exposure induces IL-22 through aryl hydrocarbon receptor activation and modulates pulmonary club cell secretory protein expression

3.1. Abstract

The finding that children with pulmonary function deficits have reduced maximal lung function in adulthood makes the need to understand mechanisms of early life pulmonary function deficits more crucial. Exposure to environmental tobacco smoke (ETS) during childhood is associated with a wide range of health conditions from obesity and behavioral problems to asthma exacerbation and increased rate and severity of respiratory infection. ETS is also a major contributor to reduced pulmonary function during early life. ETS is a complex mixture that includes numerous polycyclic aromatic hydrocarbons that serve as exogenous ligand for the aryl hydrocarbon receptor (AhR). We hypothesized that AhR ligands from tobacco smoke mediate pulmonary dysfunction that persist into adulthood. We used a neonatal murine model of early life ETS exposure, assessing both acute and persistent responses using gene expression by Taqman; protein by ELISA, Western blot, and immunofluorescence; immunophenotype by flow cytometry; and pulmonary function by flexiVent. Mice exposed to ETS during the first week of life had transiently elevated IL-22^{+} ILCs following exposure and reduced CCSP and increased tissue damping in adulthood. AhR ligand was able to recapitulate while AhR antagonist was able to mitigate induction of IL-22^{+} cells. Additionally, anti-IL-22 neutralizing antibodies reduced CCSP in adulthood, and ILC3 lung homing chemokines were reduced in neonatally ETS exposed mice. Together these findings suggest that aberrant induction of IL-22 during neonatal ETS exposure is linked to modulation of CCSP expression. This study presents a novel IL-22-mediated mechanism for pulmonary pathogenesis following neonatal ETS exposure.

3.2. Introduction

Exposure to environmental tobacco smoke (ETS) has been recognized as a major contributor to morbidity for almost four decades; however, millions of children are exposed in utero and during early life [1, 2]. ETS exposure during early life is associated with increased rates of respiratory infection, asthma, and wheezing in childhood and reduced lung function during early adulthood when pulmonary function is highest [3]. ETS has been shown to be more hazardous than mainstream smoke due to higher concentrations of many constituents from longer duration and lower combustion temperatures during generation and changes that occur from exposure to air along with secondary reactions in the air [4]. The challenge with understanding molecular mechanisms behind the adverse impact of ETS stems in part from the complexity of tobacco smoke particularly as the concentration and composition changes with time and depending on environmental conditions

Tobacco smoke is a complex mixture of at least 7000 different chemicals including several polycyclic aromatic hydrocarbons (PAHs) [5, 6]. PAHs are organic compounds containing at least two rings primarily composed of carbon atoms and may have halogenated functional groups [7]. PAHs are created from incomplete combustion of organic matter, including tobacco, but the amount of PAHs formed depends on the strain of tobacco, the curing process, and the combustion temperature [8]. Many PAHs in tobacco smoke serve as exogenous ligands for the aryl hydrocarbon receptor (AhR) and alter gene expression acutely following exposure [9].

AhR is a cytosolic receptor that translocates into the nucleus upon endogenous or exogenous ligand binding with the assistance of the aryl hydrocarbon nuclear translocator (ARNT) where it binds xenobiotic response elements and modifies gene transcription [10]. Endogenous ligands include products of bacterial fermentation products and tryptophan metabolism, which makes AhR an important conduit between the body and the microbiome. Exogenous ligands include some classes of drugs as well as a variety of toxicants including dioxins from wood pulp processing and PAHs from tobacco combustion. In the lung, AhR signaling has been reported to

alter expression of mucin 5ac (MUC5AC) and pulmonary club cell 10 kDa protein or club cell secretory protein (CCSP), an important homeostatic and immunomodulatory protein secreted by non-ciliated cells of the airways [11]. AhR signaling is also important in the development of antimicrobial immune responses. Specifically AhR signaling has been reported to be essential to maintenance of retinoic-acid-related orphan receptor gamma t (RORγt) in helper T cells and innate lymphoid cells [12, 13]. IL-22 has been implicated in psoriasis [14], ulcerative colitis [15, 16], and pancreatic fibrosis [17], but only one recent study links IL-22 and its receptor to lung disease [18].

IL-22 is a member of the interleukin 10 (IL-10) family of cytokines. Among cytokines, IL-22 is unique in that it is expressed exclusively by lymphoid cells and signals to epithelial cells [19]. The IL-22 receptor is a heterodimer consisting of the ubiquitously expressed interleukin 10 receptor beta (IL-10β) and the epithelial-cell-restricted interleukin 22 receptor alpha 1 (IL-22Ra1) that results in phosphorylation of signal transducer and activator of transcription 3 (STAT3) [20, 21]. IL-22Ra1 is responsible for IL-22 binding and has expression limited to epithelial cells in health [19]. Expression of IL-22Ra1 in the lung is restricted to airways epithelium in the absence of infection in mice; although, expression can be induced in the parenchyma via signal transducer and activator of transcription 1 (STAT1) [22, 23]. Our lab has previously shown that in the rhesus monkey lungs, IL-22Ra1 is spatiotemporally regulated with expression increasing in the airways epithelium during the first year of life [24]. Most studies examining AhR or IL-22 signaling have been in animal models of adult disease leaving the question of their roles in early life origins of disease largely unaddressed.

We hypothesize that exposure to AhR ligands from ETS during a key developmental window alters pulmonary gene expression, including expression of CCSP and IL-22. We further hypothesize that IL-22 signaling regulates CCSP expression during early life. To test this, we use a murine model of ETS exposure beginning in early life and ending at the end of the bulk

alveolarization stage of lung development. The equivalent developmental timepoint in humans begins at gestational week 36 and ends at approximately 3 years old [25]. Exposure of adult mice to short duration ETS has been reported with no discernable impact on pulmonary pathophysiology [18]. However, there is no report on the impact of early-life ETS exposure on IL-22 in the lungs or whether IL-22 signaling modifies pulmonary CCSP.

3.3. Methods

3.3.1. Animals

All experiments were performed under the auspices of the Animal Care and Use Committee of the University of California at Davis (protocols 19980 and 21794). Gestational day 8 C57BL/6J dams were purchased from the Jackson Laboratory (Sacramento, CA) and allowed to acclimate at the California National Primate Research Center for 14 days until pups were 3 days old prior to treatments. Pups were maintained with their dams until weening at postnatal day 21. As controls, five-week-old male and female C57BL/6J (000664) mice were purchased and allowed to acclimate 1 week prior to treatment.

3.3.2. Environmental Tobacco Smoke Exposures

Starting at postnatal day 3, C57BL/6J mouse pups housed with dams or six-week-old adult controls co-housed up to 4 per cage were exposed to filtered air or whole-body tobacco smoke. Exposure was performed for 6 hours/day for 5 days at a concentration of 1-2 mg/m^3 total particulate matter. Tobacco smoke was generated using a TE10 cigarette smoking machine (Teague Enterprises, Woodland, CA) with a 35-mL puff volume, a 2-second puff duration, once per minute (Federal Trade Commission smoking standard) on two 3R4F reference cigarettes (Center for Tobacco Reference Products, University of Kentucky) at a time for 10 puffs per cigarette [26]. Total suspended particles were measured twice daily during the exposure by drawing air from the exposure chamber at a known rate and collecting particulate matter on a submicron filter for 1-hour. Chamber carbon monoxide concentration was measured and recorded continuously during the week of exposure to assess consistency of exposure conditions. Ambient temperature and humidity were monitored daily. Following exposure, some mice were allowed to recover for 5 weeks in filtered air.

3.3.3. Treatment of Neonatal Mice with Aryl Hydrocarbon Receptor Modulating Compounds

C57BL/6J mice age postnatal day 3 or six-weeks-old were administered intraperitoneal injections of 2,3,7,8-tetrachlor-dibenzo-p-dioxin (TCDD) (Agilent, Santa Clara, CA) at 15 μg/kg, 0.6 μg/kg, 5 ng/kg, or corn oil (Sigma-Aldrich, St. Louis, MO) and housed in filtered air [11, 27-29]. Neonatal mice were given up to 50 μL injections while six-week-old mice were given up to 100 μL injections. Additional mice were administered intraperitoneal injections of 10 mg/kg 2-methyl-2H-pyrazole-3-carboxylic acid (2-methyl-4-o-tolylazo-phenyl)-amide (CH223191) (ApexBio Technology, Houston, TX) or corn oil immediately prior to the start of tobacco smoke exposure [30]. Following injections, animals were housed in cages along with animals undergoing environmental tobacco smoke exposure or in filtered air.

3.3.4. Treatment of Neonatal Mice with Interleukin-22 Neutralizing Antibody

C57BL/6J mice age postnatal day 3 or six-weeks-old were administered intraperitoneal injections of interleukin-22 neutralizing antibody (monoclonal IL22JOP) or rat IgG2a kappa functional grade isotype control (eBioscience, San Diego, CA) at 5 g/kg body weight immediately prior to the start of tobacco smoke exposure [31]. Neonatal mice were given up to 50 μL injections while six-week-old mice were given up to 100 μL injections. Following injections, animals were housed in cages along with animals undergoing environmental tobacco smoke exposure.

3.3.5. Immune Challenge with Lipopolysaccharide

C57BL/6J mice exposed to ETS or filtered air starting at postnatal day 3 and allowed to recover for 5 weeks along with adult controls were challenged by oropharyngeal aspiration of 0.25 μg LPS or sterile PBS and necropsied 24 hours later [32]. Briefly, mice were anesthetized by whole body exposure to 2% isoflurane in oxygen and then suspended by the cranial incisors by a silk suture tied to a slanted board. Anesthesia was maintained by continued administration of isoflurane through a nosecone. The tongue was pulled out and to the side to control the swallow

reflex before 50 μL of LPS solution or PBS was injected into the pharynx with a micropipettor. The nose was held closed to force inhalation through the mouth. The fluid level and respiration were observed to ensure aspiration into the lungs which was accompanied with an audible crackling sound.

3.3.6. Bronchoalveolar Lavage Cell Collection and Protein Concentration

Following exposure, mice were euthanized with an overdose of >100 mg/kg sodium pentobarbital diluted to 39 mg/mL in sterile PBS by intraperitoneal injection. The renal artery was severed, and lungs were perfused with 3 mL saline injected into the right ventricle. The trachea was cannulated, and 1 mL PBS was injected into the lungs and lavage was recovered immediately. Lavage was repeated with another 1 mL of PBS and both portions were pooled as bronchoalveolar lavage fluid (BALF).

Collected bronchoalveolar lavage was centrifuged at 300 rcf for 5 minutes at 4° C to pellet lavage cells. BALF was removed to separate tubes and stored at -80° C. Protein concentration was determined using Pierce BCA protein assay (ThernoFisher) using manufacturer's protocol. Briefly, standards and samples were added to duplicate wells with working reagent and incubated for 30 minutes at 37° C before optical density was measured at 562 nm on a microplate reader. Protein concentration of samples was calculated by subtracting the optical density of the blank and multiplying the optical density by the slope of the standard curve.

3.3.7. Pulmonary Function Testing

Some animals had pulmonary function testing completed at 5 weeks post exposure using a flexiVent forced oscillation system with FX Module 2 (SciReq, Montreal, QC, Canada). Mice were anesthetized with 50 mg/kg sodium pentobarbital in sterile PBS to achieve a surgical plane of anesthesia before being massed. Mice were tracheotomized and cannulated with an 18- or 19-

gauge cannula which was secured with a suture. Anesthetized mice were subjected to deep inflation, quick prime, snapshot, and pressure-volume loop maneuvers three times. Only mice independently respirating that complied with oscillation maneuvers were included. Adult exposed and neonatally exposed mice were compared separately due to significant differences in mass between the two groups.

3.3.8. mRNA Isolation, cDNA Synthesis, and Gene Expression qPCR

Following perfusion, lungs were collected and homogenized in Trizol reagent (Invitrogen, Carlsbad, CA) using a tissue homogenizer. Extraction of mRNA was carried out according to the manufacturer's protocol. Concentration and purity of mRNA was measured on a Nanodrop ND-1000 (ThermoFisher). Reverse transcription and synthesis of 500 ng cDNA was performed using High-Capacity cDNA Reverse Transcription Kit (Applied Biosystems, Waltham, MA) in a Mastercycler Gradient thermocycler (Eppendorf, Enfield, CT). Gene expression was carried out using TaqMan Gene Expression Master Mix (Applied Biosystems) and FAM TaqMan Gene Expression Assays in Table 1 (Applied Biosystems) on a QuantStudio 12 (Applied Biosystems) in the Primate Assay Laboratory at the California National Primate Research Center.

3.3.9. Determination of Concentration of Club Cell Secretory Protein and Interleukin 22 in BALF by ELISA

The concentration of Club Cell Secretory Protein (CCSP or SCGB1A1) in bronchoalveolar lavage fluid (BALF) was determined by enzyme linked immunosorbent assay (ELISA) using a Mouse Uteroglobin/SCGB1A1 ELISA Kit (Novus Biologicals, Littleton, CO) according to manufacturer's directions. Briefly BALF was diluted two-fold with Reference Standard & Sample Diluent added to wells in duplicate. CCSP was immobilized by capture antibodies bound to the well bottom during a 90-minute incubation at 37° C. Biotinylated detection antibody was bound to captured CCSP during a 60-minute incubation at 37° C after which excess detection antibody was

removed by three washes. Detection antibody was then bound by streptavidin conjugated horseradish peroxidase (HRP) during a 30-minute incubation at 37° C after which excess HRP Conjugate was removed by five washes. Finally, Substrate reagent was added and incubated for 15-minutes at 37° C before Stop Solution was added, and optical density measured at 450 nm on a microplate reader.

The concentration of interleukin 22 (IL-22) in the BALF was determined by ELISA using a Mouse IL-22 DuoSet ELISA kit (R & D Systems, Minneapolis, MN) according to manufacturer's protocol. Briefly, capture antibody was reconstituted with PBS and incubated overnight at room temperature in a 96-well plate. Excess capture antibody was removed with three washes of wash buffer before blocking with reagent diluent for 1 hour at room temperature. Excess blocking solution was removed by three washes with wash buffer before standards and samples were incubated in duplicate for 2 hours at room temperature. Wells were washed three times with wash buffer before detection antibody incubation in reagent diluent for 2 hours at room temperature. Excess detection antibody was removed with three washes of wash buffer before binding with streptavidin-HRP for 20 minutes in the dark at room temperature. Excess streptavidin-HRP was removed with three washes of wash buffer and substrate solution was added to each well for 20 minutes in the dark at room temperature. Stop solution was added to each well and the plate was tapped gently to mix and read at 450 nm and 540 nm on a microplate reader. Optical density is the difference between the 450 nm reading and the 540 nm background.

3.3.10. Determination of Club Cell Secretory Protein by Western Blot

Protein from snap frozen whole lungs was isolated by homogenization on ice in ice cold Pierce RIPA buffer (ThermoFisher, Waltham, MA) with Halt protease inhibitor (ThermoFisher). Lung homogenate was then incubated on ice over 30 minutes and vortexed occasionally before being sonicated for 3 minutes at 180 watts in 10 second intervals. Lung protein was then

centrifuged for 2 minutes at 10,000 rcf at 4° C to pellet cellular debris. Protein concentration was determined using Pierce BCA protein assay (ThernoFisher) using manufacturer's protocol.

20 ug protein was mixed with Laemmli buffer (BioRad, Hercules, CA) and 50 mM dithiothreitol to disrupt disulfide bonds and heated to denature proteins. Samples were loaded onto Mini Protean TGX gels (BioRad) with biotinylated ladder (Cell Signaling Technology, Danvers, MA) in one lane. Samples were run at 40 V for 30 minutes to stack the samples and 70 V until the dye approached the edge of the gel. Proteins were transferred to a Trans-Blot Turbo Transfer Pack (BioRad) membrane in a Trans-Blot Turbo (BioRad). The membrane was blocked with 5% BSA in TBST for 1 hour at room temperature. Primary antibodies listed in Table 2 in 5% BSA in TBST were added to the membrane and incubated overnight at 4° C with rocking. After washing excess primary antibody away, the membrane was incubated with secondary antibody listed in Table 2 in 5% BSA in TBST for 30 minutes with rocking at room temperature. Excess secondary antibody was washed away before incubation with SuperSignal West Dura Extended Duration Substrate (ThermoFisher) and images collected on FluorChem E system (ProteinSimple, San Jose, CA). Images were quantified using ImageJ (NIH).

3.3.11. Identification and Quantification of IL-22$^+$ Cells in the Lung by Flow Cytometry

Whole lungs were excised and kept on ice in complete RPMI (10% fetal bovine serum, 1% penicillin-streptomycin, and 1% L-glutamine) until digestion. Immediately prior to digestion, 300 units type IV collagenase and 10 μg DNase were added to each set of lungs [31]. Lungs were incubated in a shaking water bath at 37° C for 30 minutes at 150 rpm. The cell suspension was filtered through a 100 μm nylon filter and rinsed with DPBS. Cell suspension was centrifuged for 5 minutes at 500 rcf a 4° C in a Eppendorf 5810R tabletop centrifuge (Eppendorf, Enfield, CT). The supernatant was discarded, and red blood cells were lysed by incubation with 100 uL AKC

buffer for 3 minutes. AKC lysis was stopped by the addition of excess PBS and centrifuged for 5 minutes at 500 rcf a 4° C in a tabletop centrifuge. The supernatant was discarded.

Cells were counted by addition of 10 μL trypan blue to 10 μL cell suspension on a Countess automated cell counter, and pellet resuspended to 10^6 cells/mL in RPMI. Cells were stimulated for 6 hours with the addition of 500x Cell Activation Cocktail (phorbol-12-myristate 13-acetate (40.5 μM) (PMA) and ionomycin (669.3 μM) in DMSO), 1000x Brefeldin A, and 1000x Monensin (Biolegend, San Diego, CA).

Cells were counted by addition of 10 μL trypan blue to 10 μL cell suspension on a Countess automated cell counter. Cell suspension was brought to 10^7 cells/mL in staining buffer, and 100 μL per well was added to round bottom 96-well culture dish. To each well, 50 μL antibody cocktail composed of antibodies in Table 2 and Zombie UV Fixable Viability dye (Biolegend) was added and incubated for 30 minutes at 4° C. Excess antibody was removed by washing twice with FACS buffer (5% fetal bovine serum and 0.09% sodium azide) centrifugation at 1000 rcf for 1 minute at 4° C and three washes with 200 μL FACS buffer (10% fetal calf serum and 0.4% sodium azide in PBS). Extracellular antibodies were fixed with BD Cytofix/Cytoperm (BD Biosciences, San Jose, CA). Cells were permeabilized with Perm/Wash Buffer (BD Biosciences), and intracellular proteins were stained using antibodies in Table 2 in a 50 μL volume of Perm/Wash Buffer for 60 minutes at room temperature. Excess antibody was removed by washing twice with Perm/Wash Buffer centrifugation at 1000 rcf for 1 minute at 4° C. Cells were resuspended in 200 uL FACS buffer and filtered into filter top polystyrene FACS tubes to remove clumps. Cell suspensions were counted on a BD Symphony running FACSDiva (BD Biosciences) with 500,000 events collected per sample. Results were analyzed on FlowJo v8 (BD Biosciences).

3.3.12. Localization of IL-22Ra1 by Immunofluorescence

Lungs from freshly euthanized mice were cannulated via the trachea and removed. Lungs were inflation fixed with 4% formalin with constant pressure for 30 minutes before being tied with #4 suture and stored overnight in 4% formalin at 4° C. Formalin was then replaced with 70% ethanol in water until embedding. Lungs were placed in cassettes and embedded in paraffin and 5 μm slices were affixed to slides. Sections were deparaffinized with three successive 5-minute incubations in 100% xylene followed by rehydration by two 10-minute washes in 100% ethanol and two 10-minute washes in 95% ethanol. Antigen retrieval was performed by incubating slides for 1 hour in Dako Target Retrieval Solution (Agilent, Santa Clara, CA).

Slides were blocked with 5% bovine serum albumin (BSA) and 5% goat serum in PBS with 0.3% triton X (Sigma-Aldrich, St Louis, MO). Slides were stained with primary antibodies in PBS with 5% BSA and 5% goat serum overnight at 4° C using antibodies listed in Table 2. Excess antibody was removed by 3 successive washed in PBS. Secondary antibodies in PBS listed in Table 2 were added and incubated for 1 hour at room temperature. Excess antibody was removed by three washes in PBS. Nuclei were stained with 100 μL 300 nM DAPI (4',6-Diamidino-2-Phenylindole, Dilactate) (Life Technologies, Carlsbad, CA) for 5 minutes. Excess DAPI was removed by three washes with PBS. Autofluorescence was quenched using Vector trueView Autofluorescence Quenching kit (Vector Labs, Burlingame, CA) according to manufacturer's protocol. Slides were covered using VECTASHIELD Vibrance Antifade Mounting Medium (Vector Labs). Slides were visualized in the Advanced Imaging Core at the California National Primate Research Center.

3.3.13. Statistical Analysis

Statistical analysis was performed using Prism 7.0 software (Graphpad, San Diego, CA). Significance was determined with one-way or two-way ANOVA with Tukey's post-hoc test for multiple comparisons or student's t-test.

3.4. Results

3.4.1. Neonatal environmental tobacco smoke exposure alters growth and pulmonary function in adulthood

To understand the impact of exposure to environmental tobacco smoke (ETS) during the key early-life developmental window, neonatal pups were exposed to 1-2 mg/m^3 mixed mainstream and sidestream tobacco smoke for 6 hours per day for 5 days from postnatal day 3 until postnatal day 7 along with 6-week-old adult controls (Figure 1A). Exposure levels were monitored by twice-daily particulate matter collections with a mean total suspended particulate of 1.533±0.359 mg/m^3 (mean ± standard deviation) (supplemental Figure 1A) and continuous monitoring of carbon monoxide levels of 8.263±1.359 PPM (mean ± standard deviation) (Supplemental Figure 1B). Tobacco smoke exposure has been correlated with reduced growth in human epidemiological studies [33-35]. Following a 5-week recovery in filtered air, the mass of animals was determined. Neonatally ETS exposed mice had lower body mass than age-matched controls while there was no difference between adult control groups (Figure 1B, C). Neonatally ETS exposed mice had increased tissue damping (G), a measure of tissue resistance reflecting the energy dissipation of the alveoli, compared to age-matched controls (Figure 1D) while adult ETS exposed controls had an opposite effect in tissue damping (Figure 1E). Most measures of pulmonary function were not significantly different between ETS exposed and age-matched filtered air controls following recovery (Table 3, Supplemental Figure 2). Altered pulmonary function including has been reported in children with reduced serum CCSP and increased tissue damping has been reported in CCSP$^{-/-}$ mice [36]. Since club cell secretory protein (CCSP) has a homeostatic role in lung function, we looked at gene expression of CCSP in whole lung homogenates. Neonatally ETS exposed mice had decreased expression of CCSP in adulthood compared to age-matched or adult controls (Figure 1F). Protein levels of CCSP were assessed by Western blot of protein from whole lung homogenate from neonatally ETS exposed mice and age-matched controls in adulthood to confirm the gene expression results (Figure 1I, J). CCSP

has anti-inflammatory properties and pulmonary CCSP protein levels have been shown to be altered during infection [37], so the levels of CCSP in mouse lungs following sham or LPS challenge were assessed. As CCSP is a major constituent of lung lining fluid, CCSP levels in the bronchoalveolar lavage fluid (BALF) of neonatally ETS exposed and age-matched controls were assessed by ELISA in sham (Figure 1G) and LPS challenged mice (Figure 1H).

3.4.2. Aryl hydrocarbon receptor agonist TCDD also reduces pulmonary CCSP

CCSP has been reported to be regulated through the aryl hydrocarbon receptor (AhR) in response to xenobiotic metabolites including dioxins such as 2,3,7,8-tetrachlor-dibenzo-p-dioxin (TCDD) [11]. Tobacco smoke is known to be a source of AhR ligands including anthracene, benzo-a-pyrene, naphthalene, and chrysene [8], and CCSP has been shown to be reduced in smokers [38]. To understand if AhR signaling could be involved in down regulation of CCSP following early-life ETS exposure, postnatal day 3 mice and six-week-old adult controls were given intraperitoneal injections of TCDD and allowed to recover for one or six weeks (Figure 2A). Neonatally treated mice at the acute one-week timepoint demonstrated dose-response CCSP gene expression curve with TCDD treatment (Figure 2B). The results in neonatally treated mice at six weeks after treatment were mixed with only the lowest dose of TCDD showing a statistically significant decrease compared to vehicle treated age-matched controls (Figure 2C). Adult mice had significantly reduced CCSP gene expression at both acute (Figure 2D) and persistent (Figure 2E) timepoints in both doses with no difference in expression between amount of TCDD.

3.4.3. Aryl hydrocarbon receptor antagonist CH223191 abrogates the reduction of CCSP in neonatally ETS exposed mice

The finding that an AhR ligand TCDD has a differential effect in neonates that is distinct from that seen in adult mice suggests that if AhR signalling is important for the reduced CCSP gene expression in neonatally ETS exposed mice, it may be more subtle than the signal generated by TCDD. The strength and concentration of AhR agonists has been reported to effect downstream gene expression following exposure [39]. Neonate mice and humans are deficient in

several phase 1 and phase 2 detoxification gene expression [40, 41], which could make dosing of an AhR agonist technically challenging as individual gene expression changes during development. To further assess if AhR signaling was necessary for ETS-induced CCSP deficiency in neonatally exposed mice in adulthood, we used the AhR antagonist 2-methyl-2H-pyrazole-3-carboxylic acid (2-methyl-4-o-tolylazo-phenyl)-amide (CH223191). Postnatal day 3 mice and six-week-old adult controls were administered CH223191 or vehicle immediately prior to ETS exposure and assessed acutely following exposure or following a five-week recovery period in filtered air (Figure 3A). Neonatal CH223191 administration significantly increased CCSP gene expression in ETS exposed mice compared to vehicle age-matched controls both acutely (Figure 3B) and persistently (Figure 3C). Adult control mice administered AhR antagonist prior to ETS exposure did not have a change in CCSP gene expression compared to vehicle controls at either the acute (Figure 3D) or persistent timepoint (Figure 3E). These results suggest that AhR signaling is necessary for reduced CCSP gene expression during early life due to ETS exposure.

3.4.4. IL-22^{+} natural-killer cell receptor^{-} type 3 innate lymphoid cells are increased by neonatal ETS exposure in an AhR-dependent manner

AhR signaling regulated numerous genes in a variety of cells. AhR has been reported to be an important transcription factor for IL-22 production in helper T cell lineages and innate lymphoid cells (ILCs) [13, 39, 42]. Type 3 cytokines IL-17 and IL-22 have been shown to be increased in the serum and sputum of smokers and patient with COPD [43]. Additionally, interleukin 6 (IL-6) is important for initiating type 3 immune responses along with transforming growth factor beta (TGFβ) and has been shown to be essential for environmental air pollution induced CCSP reductions in an experimental rat model [44]. To examine whether IL-22 is implicated in the effects of early-life ETS exposure, we homogenized whole lungs to single cells suspensions from mice following exposure to ETS or filtered air starting at postnatal day 3 or six-week-old and stained for flow cytometry with antibodies for IL-22 and lineage markers for helper T cells, B cells, natural killer cells, ILCs, invariant natural killer T cells, and gamma-delta T cells.

Neonatally ETS exposed mice had an increased percentage and number of IL-22$^+$ cells compared to age-matched and adult controls acutely following exposure at postnatal day 9 (Figures 4A, B). The neonatally ETS exposed mice expressed RORγt, a master regulator of IL-22, in a greater percentage of IL-22$^+$ cells and more cells than age-matched and adult controls (Figures 4C, D). Percentages and counts of IL-22$^+$ natural killer cells (Figures 4E, F), lymphoid tissue inducer-like (LTi) ILC3s (Figures 4G, H), and natural killer cell receptor positive (NCR+) ILC3s (Figures 4I, J) were lower or not different in neonatally ETS exposed mice than controls. Importantly, none of the counts of these cell types were a significant portion of the IL-22$^+$ RORγt$^+$ cell fraction in neonatally ETS exposed mice (Figure 4D). The largest portion of IL-22$^+$ RORγt$^+$ cells in neonatally ETS exposed mice by percent and count were natural killer cell receptor negative (NCR-) ILC3s (Figures 4K, L). ETS exposed adults had a similar percentage of NCR- ILC3s compared to neonatally exposed mice (Figure 4K); however, the total number of NCR- ILC3s was significantly lower in adults than neonates (Figure 4L).

Following 5-week recovery in filtered air, additional mice were assessed for pulmonary IL-22$^+$ cells. In contrast to the acute increase in IL-22$^+$ cells, there were no differences in the percentage or number of IL-22$^+$ cells in the lungs between treatment group (Supplemental Figure 3). Consistent with the essential role of RORγt in maintaining IL-22, all treatment groups had RORγt mean frequencies below 60% (Supplemental Figure 3C) compared to 97% for neonatally ETS exposed mice in the acute group (Figure 4C). These results suggest that the AhR ligands in ETS are not capable of maintaining RORγt following neonatal exposure for extended periods of time after exposure to ETS.

To determine if a similar induction of IL-22$^+$ cells was responsible for reduced CCSP following treatment with AhR modulating compounds, single cell lung homogenate from mice treated with TCDD and kept in filtered air and mice treated with CH223191 and exposed to ETS were stained for flow cytometry. Postnatal day 3 TCDD treated mice had a small but significant

dose response in IL-22$^+$ NCR- ILC3s acutely (Figure 4M). Unlike neonatally ETS exposed mice, neonatally TCDD treated mice had a more profound dose response at six weeks post treatment (Figure 4N). Adult mice treated with TCDD had no induction of IL-22$^+$ NCR- ILC3s acutely or persistently (Supplemental Figure 4A, B). Postnatal day 3 AhR antagonist CH223191 treated mice exposed to ETS had a significant reduction in IL-22$^+$ NCR- ILC3s acutely compared to vehicle (Figure 4O), and there was no difference between CH223191 and vehicle at the persistent timepoint (Supplemental Figure 4C). Treatment with CH223191 did not change numbers of IL-22$^+$ NCR- ILC3s in filtered air control neonates either acutely or persistently compared to vehicle (Supplemental Figure 4D, E). CH223191 treated adults also did not have any differences in IL-22$^+$ NCR- ILC3s between CH223191 and vehicle either acutely or persistently (Supplemental Figure 4F, G).

IL-22 is induced by bacterial products lipopolysaccharide and flagellin through toll-like receptors (TLR) 4 and 5, respectively [45]. LPS is a constituent of tobacco smoke and could contribute to the observation that IL-22 is elevated in smokers [43]. Since IL-22$^+$ cells were transiently increased in neonatally ETS exposed murine lungs, we examined IL-22 in BALF from LPS challenged mice by ELISA. Following LPS challenge, IL-22 was lowest in the BALF of neonatally ETS exposed mice at six weeks (Figure 4P). This suggests that following early-life ETS exposure IL-22 induction in response to LPS is impaired.

3.4.5. IL-22 neutralizing antibodies partially mitigate the loss of pulmonary CCSP following early-life ETS exposure

Since IL-22$^+$ cells were transiently increased in the lungs following postnatal ETS exposure and pulmonary CCSP was subsequently reduced, we interrogated the IL-22/IL-22Ra1 signaling axis. Postnatal day 3 mice and adult controls were given 5 g/kg body weight neutralizing anti-IL-22 antibodies or isotype control and exposed to ETS for five days (Figure 5A). At postnatal day 9, CCSP gene expression was elevated in anti-IL-22 treated mice compared to isotype control

(Figure 5B); however, by six weeks the increase in pulmonary CCSP in antibody treated mice was no longer significant compared to isotype control (Figure 5C).

When lungs from neonatally exposed anti-IL-22 treated mice were homogenized and stained for flow cytometry, there was a trend toward reduced IL-22^{+} NCR- ILC3s at the acute (Figure 5D) but not the persistent timepoint (Figure 5E). Neonatal treatment with anti-IL-22 neutralizing antibodies did not change the number of IL-22^{+} NCR- ILC3s in filtered air exposed controls at either timepoint (Supplemental Figures 5A, B). Similarly, adult controls treated with anti-IL-22 neutralizing antibody or isotype control and exposed to ETS had no differences in the number of IL-22^{+} NCR- ILC3s at the acute timepoint (Supplemental Figure 5C). Pulmonary CCSP protein detected by ELISA showed a small and not significant increase in neonatally ETS exposed, anti-IL-22 antibody treated mice (Figure 5F).

IL-22 is produced by immune cell populations and signals to epithelial cells via IL-22Ra1 with the co-receptor IL-10Rβ [21, 46]. IL-22Ra1 has been previously reported by our lab to be spatiotemporally regulated within the lung of rhesus monkeys with restriction to airways epithelial cells [24] and in mice to airways of uninfected animals [22]. Lungs of neonatally ETS-exposed and age-matched controls mice were inflation fixed with paraformaldehyde at six-weeks-old and immunohistochemistry was performed to determine localization and abundance of IL-22Ra1. Control mice expressed low levels of IL-22Ra1 (Figures 5G-H) compared to neonatally ETS exposed mice (Figures 5I-K). Co-localization of IL-22Ra1 with CCSP showed that club cells were the predominant cells in the airways of neonatally ETS exposed mice that express IL-22Ra1 (Figures 5H, J). Despite the reduced levels of CCSP protein in the lungs of neonatally ETS exposed murine lungs (Figures 1I, J), there was no noticeable difference in CCSP fluorescence intensity between control and ETS lungs (Figures 5J-K). This indicates a persistent change in IL-22Ra1, the receptor on epithelial cells responsible for binding IL-22.

CCSP deficiency is associated with altered pulmonary function in human children and mice [36], and we found altered CCSP and tissue damping in neonatally ETS exposed mice in

adulthood that was partially abrogated by pre-treatment with anti-IL-22 neutralizing antibodies. To determine if blocking IL-22 could restore normal pulmonary function, postnatal day 3 mice were administered anti-IL-22 neutralizing antibodies or isotype control and exposed to ETS followed by recovery in filtered air. At six-weeks-old, pulmonary function was assessed by flexiVent forced oscillation maneuvers as before. No measure of pulmonary function was significantly altered by pre-treatment with anti-IL-22 neutralizing antibodies compared to isotype control treated mice (Supplemental Figure 6).

Since IL-22 antibody blockade induced a trend toward reduced CCSP in adulthood among neonates exposed to filtered air (Figure 5F), we examined expression of cytokines that induce IL-22. IL-23 and IL-1β have been shown to have roles in inducing IL-22 in lymphocytes [47]. Expression of IL-1β was lower during acute exposure at postnatal day 9 than at six weeks, and neonatally ETS exposed mice had reduced IL-1β in adulthood (Figure 6A). In contrast, IL-23 expression was higher during the neonatal period in the lung but not significantly different based on ETS exposure (Figure 6B).

ILC homing to the lung is governed by C-C motif chemokine receptor 4 (CCR4) ligands [48, 49]. To assess the role of CCR4 ligands, C-C motif chemokine ligand 17 (CCL17) and CCL22 gene expression was determined acutely at postnatal day 9 (Figure 6C) and following recovery at six weeks of age (Figure 6D). Lung expressed CCL17 trended lower at postnatal day 9 (Figure 6C) and was lower at six weeks of age (Figure 6D) while CCL22 was not significantly different at either timepoint (Figure 6C, D).

3.5. Discussion

We show that exposure to ETS during neonatal development reduces pulmonary CCSP in our murine model of early life ETS exposure. We also show that exposure to AhR agonist TCDD replicates the decrease in CCSP in neonatally treated mice while also generating profound decreases in adult controls, and AhR antagonist CH223191 restored CCSP gene expression in neonatally ETS exposed mice. Reduction in CCSP gene expression *in vitro* in NCI-H441 human lung epithelial cells and *in vivo* in adult male C57BL/6J mice following injection with TCDD has been reported [11]. Our results in adult mice are consistent with this previous report. AhR-mediated stimulation of cytochrome P450 family 1 subfamily A member 1 (CYP1A1) by ETS exposure has previously been reported by comparing exposure of C57BL/6N and AhR deficient DBA2/N mice [50]. The dose of TCDD used in Wong et al [11] and the highest dose used in our study, 15 ug/kg, is in excess of the lifetime dose required to induce cancer in mice and rats, reduced thymus size in newborn rats, and reproductive harm in female rats [51]. Differential effects of AhR ligands that depends on the strength and duration of binding has been reported [39]. These findings suggest that while high doses of potent AhR agonists can induce acute gene expression changes in AhR competent adult animals, smaller doses during early life may be capable of eliciting effects not seen in models using adult animals using the same regimen.

We found small differences in lung function between early-life ETS exposed animals and age-matched controls. Human epidemiological studies have shown CCSP levels to be associated with reductions in FEV_1, FEF_{25-75}, and FEV_1/FVC in adolescents and young adults, and mechanistic work in a $CCSP^{-/-}$ mouse model provides evidence for CCSP deficiency being causative of lung function deficits [36]. The increased tissue damping in neonatally ETS exposed animals was consistent with the trend reported due to CCSP deficiency in knockout mice while other measures were not. Since we found reduced but not ablated CCSP in neonatally exposed mice in adulthood, this may represent an intermediate phenotype. It is also common for children that live with smokers to continue to be exposed for tobacco smoke throughout their lives even if

that exposure is believed to be more limited during adolescence. Instead of comparing chronological ages across species it is important to look at relevant developmental milestones. Mice are near completion of bulk alveolarization at postnatal day 7 when our exposure ends [52] which approximates the lung developmental stage of a 3-year-old human [53]; however, it is impossible to duplicate the same total exposure within this timeframe using an animal model. These limitations may indicate an underestimate the size of the effect seen in this study.

We found transiently increased numbers of IL-22$^+$ NCR- ILC3s in the lungs of neonatally exposed mice compared to adult controls. To the best of our knowledge, we are the first to report the increase in IL-22$^+$ pulmonary immune cells in neonatal lungs of an animal model of ETS exposure and the first to report that this effect is transient. Gray et al showed gut microbial colonization was essential to recruitment of IL-22$^+$ NCR+ and LTi ILC3s to the lung [31]. We found similar numbers of IL-22$^+$ ILC3s in the lungs of healthy animals with marked increases following neonatal ETS exposure or AhR agonist treatment. In the gut, IL-22$^+$ ILCs are essential for tertiary lymphoid tissues that are generated postnatally but not for prenatally determined Peyer's patches [54], but whether such a role for IL-22$^+$ ILCs in the lung exists is unknown. AhR agonist TCDD also induced IL-22$^+$ NCR- ILC3s in neonates our model; however, it did so to a lesser degree and for a longer duration than ETS exposure. AhR antagonist CH223191 reduced ETS induced IL-22$^+$ NCR- ILC3s in neonates to baseline levels. Together these data suggest that induction of IL-22$^+$ NCR- ILC3s in neonates following ETS exposure is initiated by AhR signaling. The discrepancy between ETS and TCDD may be the result of ligand strength, dose, or route of exposure. The affinity between AhR and stong ligands as well as duration has been shown to direct immune cell differentiation [39]. Neonates treated with TCDD received intraperitoneal injections that should circulate throughout the body, but breastfeeding and maternal grooming likely introduced some level of TCDD though the oral route. TCDD was delivered in corn oil and is strongly lipophilic which may result in the storage and delayed release of AhR agonists [55]. By

contrast ETS exposure would be through the lungs as well as the oral route due to thirdhand smoke exposures during feeding and grooming.

We found increased IL-22Ra1 protein in the airways of neonatally ETS exposed mice in adulthood. There are conflicting reports on the impact of tobacco smoke and it constituents on expression of IL-22Ra1. One study examined the effect of 1-10 μM nicotine or vehicle on *in vitro* wound healing of A549 lung epithelial cells or normal airway epithelial cells with varying concentrations of IL-22 and found nicotine reduced IL-22Ra1 expression and IL-22 production by t cells [56]. Our study differs in that we employed *in vivo* ETS exposure which contains nicotine as part of a complex milieu. While nicotine from ETS may suppress IL-22 and IL-22Ra1, factors including nutrient balance [42], prostaglandin E2 levels [57], and concentration and strength of AhR ligands [39] drive increased IL-22 production. A study that examined IL-22Ra1 gene expression and protein cleavage products from neutrophil elastase and cathepsin in a mouse model, smokers, and COPD patients found no significant difference in IL-22Ra1 gene expression in the lungs of nonsmokers, smokers, and COPD patients [58]. These findings suggest that increased pulmonary neutrophils that are often seen in smokers and COPD patients may decrease IL-22Ra1 available to convey signals by cleaving the receptor particularly during bouts of inflammation such as acute exacerbations of COPD. Our study differs in that we used both male and female C57BL/6J mice as opposed to female BALB/c mice, which are hyper-responsive to pulmonary insults, and exposed them during the beginning of alveologenesis before allowing them to rest as opposed to exposure in adulthood for 8-16 weeks. The short duration of exposure in our protocol resulted in no detectable changes in IL-22 or IL-22Ra1 in adult mice. IL-22Ra1 has been shown to be induced by STAT1 signaling due to TLR3 stimulation [23] which is consistent with previous findings of induction during influenza [22, 58]. Starkey et al found increased IL-22Ra1 in human COPD patients but non-statistically significant increases in IL-22Ra1 mRNA in 15-16 week-old C57BL/6 mice after 8 weeks of tobacco smoke exposure [18] similarly to findings

of no increase in IL-22Ra1 *in vitro* in human lung epithelial BEAS-2C cells and *in vivo* in adult female BALB/C mice [58]. These findings are consistent with our findings in adult controls.

There have been indications that IL-22 is involved in tobacco smoke induced pathology. An early report indicated that interleukin 6 (IL-6) was essential for responses to both ozone and ETS in an experimental rat model [44]. IL-6 in the presence of transforming growth factor beta (TGFβ) is important for initiating type 3 immune responses that include the induction of helper T cells that secrete interleukin 17 (IL-17) and IL-22 [59, 60]. IL-22 has been reported as being elevated in the serum and sputum from smokers and chronic obstructive pulmonary disease (COPD) patients compared to healthy nonsmokers [43], and IL-22$^+$ helper T cells have been reported elevated in current smokers with COPD [61]. An earlier report showed that STAT3, which is phosphorylated by IL-22 signaling, is important for tobacco smoke mediated inflammation in a murine model [62]. Another report indicated IL-22 and IL-22Ra1 are implicated in human and a murine model of COPD [18]. Further, IL-22 levels are elevated in smokers suffering from chronic pancreatitis, and IL-22 or AhR agonists TCDD and benzo-a-pyrene enhanced fibrosis in a murine caerulein-induced chronic pancreatitis model while anti-IL-22 antibodies abrogated the effects [17]. However, none of these studies examine the role of IL-22 in infants and children who are experiencing rapid lung development. Gray et al found that ILCs were the primary IL-22$^+$ cells in bronchoalveolar lavage from human newborns and that IL-22$^+$ NKp46$^+$ (NCR+) and LTi-like ILC3s were rapidly increased in the lungs of postnatal day 4 mice that was driven by commensal colonization and suppressed by antibiotic treatment [31]. AhR ligands in health are generally endogenous fermentation products from commensal microbiota in the gut, presumably these effects are part of the gut-lung axis. The role of exogenous AhR ligands from ETS on recruitment and activity of IL-22$^+$ cells in developing lungs has not been described.

Anti-IL-22 neutralizing antibody was unable to abrogate the changes in lung physiology seen in neonatally ETS exposed mice, namely increased tissue damping was still present. The treatment regimen was a single dose of antibody prior to exposure, and tobacco smoke

constituents may have persistent third-hand effects to the neonates after the exposure stopped. Numerous studies have shown that tobacco smoke constituents can linger well after smoking has stopped—third hand smoke—and particularly impact small children and pets that interact more closely with surfaces than adults [63-65]. Settled dust in houses of smokers has been found to have more than twice as much polycyclic aromatic hydrocarbons per square meter as that of non-smokers [63]. The composition of tobacco combustion products also changes during the aging process from second hand to third hand smoke. Following tobacco combustion, the composition of airborne particulate matter shifts from volatile and semivolatile amines to increasing levels of acetonitrile, alkanes, and alkenes at 2 hours and to carbonyls and nitriles by 18 hours post smoke exposure [65]. As such it is possible another mechanism may be responsible for altered pulmonary function or the effects of third hand smoke may be outlasting the lifespan of the administered antibody.

Neonatal ETS exposure resulted in reduced IL-1β and CCL17 in the lungs of adult mice. IL-1β induces IL-22 production and maintenance in ILC3s, helper T cells, and invariant natural killer T cells [47, 66-68]. The recruitment of lymphocytes to the lung is dependent on chemokine ligand C-C motif chemokine receptor 4 (CCR4) interactions [48]. CCR4 is induced on ILCs by cluster of differentiation 103 (CD103)+ CD11b+ dendritic cells from the intestines during development [31]. We did not measure CCR4 in this experiment, but deficiencies in CCR4 or its ligands have been shown to alter ILC migration [31, 48]. The CCR4 ligand CCL17 is produced in the lung and induced by gamma interferon, tumor necrosis factor alpha, and interleukin 4 as well as by a variety of toll-like receptor ligands [69, 70]. The reduction of CCL17 in the lung following neonatal ETS exposure requires further examination. CCL17 has been implicated in several diseases of the epithelial barriers but the strongest association is with atopic dermatitis [71]. IL-22^{+} ILC3s were induced during the neonatal period; however, IL-22 was not induced following LPS challenge in adulthood when CCL17 was suppressed. This indicates an inability to maintain

IL-22 production in adulthood in our model. Importantly, most infants that are exposed to ETS continue to be exposed throughout their lives as most exposures happen in the home, car, or other frequently visited space. Our model did not replicate this prolonged duration of exposure.

IL-22 contributes to enhanced secretion of mucins and antimicrobial peptides [19, 72], enhanced expression of tight junction proteins [73], and increased cellular proliferation and survival [22, 74]. IL-22 has also been described as having immunomodulatory or inflammatory roles depending on the disease state. In psoriasis [14], ulcerative colitis [15, 16], pancreatic fibrosis [17], and COPD [18] IL-22 has been described as an inflammatory mediator of disease. Other reports suggest that IL-22 is protective in an animal model of ulcerative colitis [75]. In a bleomycin model of acute lung injury in mice, Sonnenberg et al found that IL-22 was pathogenic in the presence of interleukin 17A (IL-17A) as shown by reduced inflammation in IL-$22^{-/-}$ mice and that IL-22 was protective in IL-$17A^{-/-}$ mice with more inflammation following treatment with anti-IL-22 antibodies [76]. IL-22 has also been shown to have a protective role in the progression of pulmonary fibrosis in a *Bacillus subtilis* induced mouse model with increased collagen deposition in AhR deficient mice or following anti-IL-22 antibody treatment despite significant numbers of IL-$17A^{+}$ $\gamma\delta$ t cells [77]. The role of IL-22 was recently confirmed using an IL-$22Ra1^{-/-}$ mouse model, recombinant IL-22 supplementation of bleomycin treated mice, and clinical specimens from pulmonary fibrosis patients that showed correlation between FEV_1 and serum IL-22 [78]. While we show excess IL-22 during early life is associated with reduced CCSP, the role and appropriate balance of IL-22 in health and disease during early life remains an opportunity for further investigation.

In addition, IL-22 signaling has been reported to modify stem and progenitor cell behavior. Boniface et al reported that IL-22 reduced expression of seven keratinocyte differentiation genes *in vitro* [14]. Human mesenchymal stromal cells treated with IL-22 *in vitro* alone resulted in the upregulation of osteogenic transcription factors Runx2 and Alpl with increases calcium deposition and apidogenic transcription factor Pparγ [79]. In the gut, IL-22 signaling has been reported to

increase the number of transit amplifying cells while reducing the number of crypt Lrg5^{+} stem cells within *in vitro* intestinal organoids and in a mouse model by inhibiting Notch and Wnt signaling [80]. A previous report also showed increased intestinal organoid growth with IL-22 treatment but found increased numbers of crypt Lrg5^{+} stem cells [81]; however, subsequent work suggests that transit amplifying cells are capable of dedifferentiating to reconstitute the intestinal crypt stem cell niche [82]. This may indicate the consistency with lost stem cells being subsequently replaced by transit amplifying cells. IL-22 signaling results in the phosphorylation of STAT3 [20]. Pulmonary IL-6 was shown to induce differentiation in favor of ciliated cells using a mouse model *in vivo* and tracheal organoids from basal stem cells *in vitro* in a STAT3 dependent fashion [83]. Given the role of IL-6 in inducing type 3 immune responses that include IL-22, it is possible that IL-22 modulates pulmonary stem cell behavior similarly to intestinal stem cell behavior. This possibility may be important for fully understanding the role of IL-22 in inhalation exposure during early development.

Consistent with the role of IL-22 in mediating host-microbe interactions, IL-22 production has been shown to be inducible by TLR ligands LPS and flagellin [45]. Tobacco smoke is a major source of LPS in the lung for smokers with each cigarette containing as much as 26.8 ± 7.3 μg/cigarette [84], so it is unsurprising that the finding that IL-22 is increased in sputum of smokers has been reported [43]. Our study did not assess the microbiome of the mice studied, and it is possible that ETS exposure during early life causes dysfunction due to the immature state of the pre-weening microbiome. Studies in humans and animal models have shown that the gut and skin microbiome change from very early in life as the organism matures [85, 86]. Disruptions in the developing microbiome have been associated with development of Crohn's disease in the gut among a pediatric cohort [87]. The dogma that the lung was a sterile environment persisted for many years, so knowledge of the lung microbiome is still developing. Recently the healthy adult human lung microbiome [88], developmental trajectory of upper respiratory tract microbiota in healthy children [89], and the differences between oral and lung microbiomes between smokers

and nonsmokers have been described [90]. What effect if any ETS has on the development of the lung or gut microbiome is unknown. Animal models that demonstrate altered microbiota influence behavior, metabolic disorder, and asthma that are also associated with ETS exposure make this an important area for future research [91, 92].

Despite the risks of ETS to human health being known for decades, millions of children around the world are exposed to ETS and millions more are exposed to other combustion products with as yet unknown health effects [2]. Recent shifts in preferences among young tobacco users toward electronic nicotine delivery systems or vaping, present new challenges for determining the impact on lifelong health. In addition, increasing exposure to wildfire smoke from combustion of homes in wildland-urban interface areas presents risks for future health problems in children and adults. Understanding cellular and molecular mechanisms for how existing inhaled toxicants cause harm will be helpful in guiding assessment as novel hazards arise.

3.6. Figures and Tables

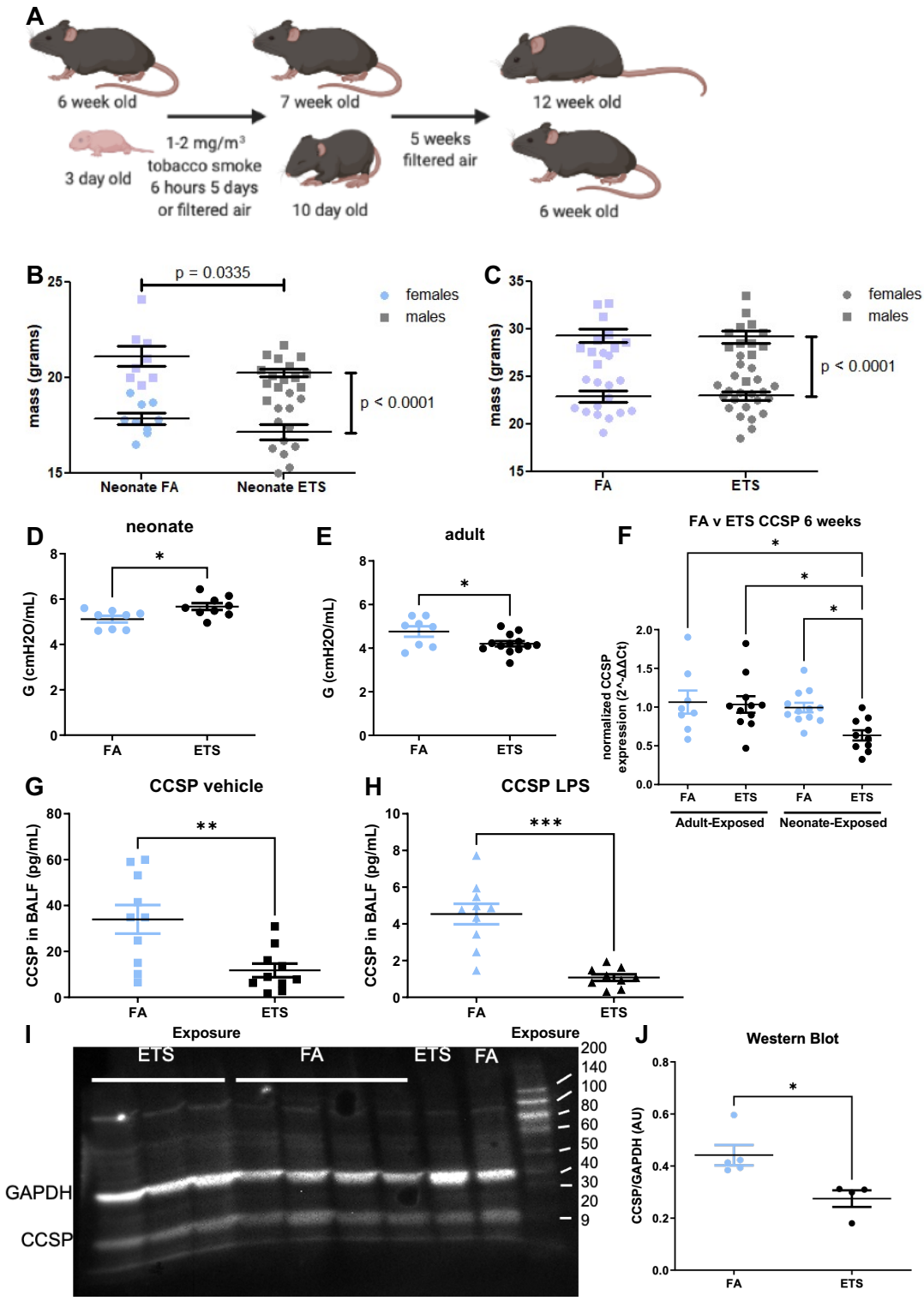

Figure 1: Neonatal ETS exposure results in reduced growth into adulthood and increased tissue damping. Experimental design for murine early-life ETS exposure **(A)**. Mass of neonatally exposed **(B)** and adult controls **(C)** were assessed 5 weeks post exposure prior to necropsy. Pulmonary function testing was performed on a subset of mice 5 weeks post exposure under anesthesia using a FlexiVent system running Deep Inflation, SnapShot, QuickPrime, and PV Loop protocols. Tissue damping in adult controls **(D)** and neonatally exposed mice **(E)**. Expression of club cell secretory protein (CCSP) in lungs from neonatally ETS exposed, age-matched controls, and adult controls was determined using Taqman qPCR and normalized to GAPDH by the ΔΔCt method **(F)**. Bronchoalveolar lavage fluid (BALF) from six-week-old mice neonatally-exposed to ETS or filtered air was used to detect CCSP protein by ELISA **(G)**. Some mice were challenged with LPS by oropharyngeal aspiration and BALF was collected to determine CCSP protein by ELISA **(H)**. Total lung protein was extracted from resting mice neonatally challenged with ETS or control and allowed to recover in filtered air. CCSP was assayed by Western blot **(I)** and band intensity was compared to GAPDH by ImageJ **(J)**. * $p<0.05$, ** $p<0.01$, *** $p<0.001$, **** $p<0.0001$ by ANOVA with Tukey post-hoc correction for multiple comparisons or student's t test.

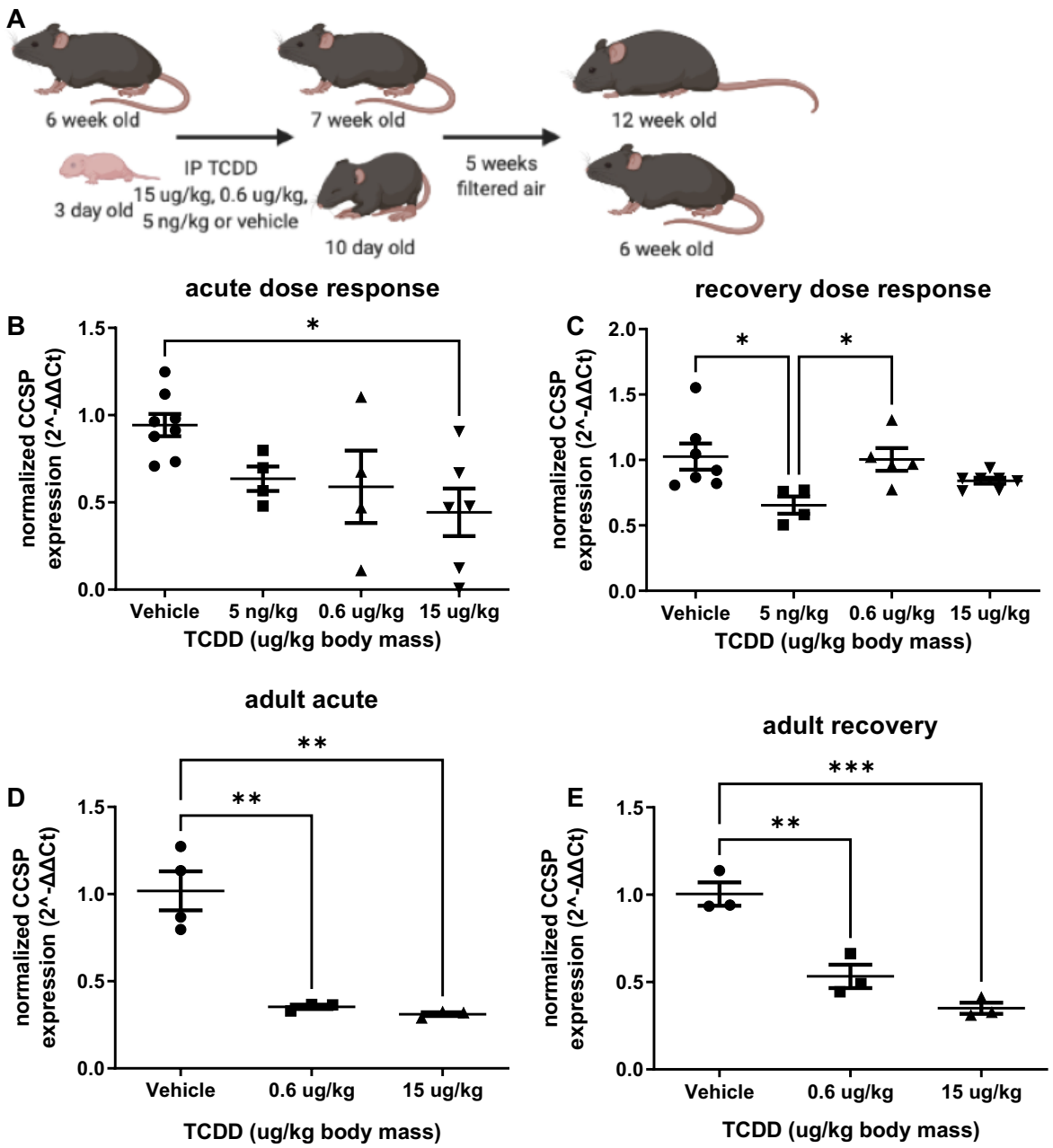

Figure 2: Aryl hydrocarbon receptor agonist TCDD induces a dose-dependent decrease in club cell secretory protein message in neonates and adults. Experimental design for intraperitoneal administration of AhR agonist TCDD or vehicle to postnatal day 3 pups and adult controls **(A)**. Expression of CCSP was assessed in mice treated at postnatal day 3 with TCDD at varying doses or vehicle one week **(B)** or six weeks post administration **(C)**. Expression of CCSP was also assessed in six-week-old mice treated with TCDD or vehicle one **(D)** and six weeks post

administration **(E)**. * $p<0.05$, ** $p<0.01$, *** $p<0.001$, **** $p<0.0001$ by ANOVA with Tukey post-hoc correction for multiple comparisons.

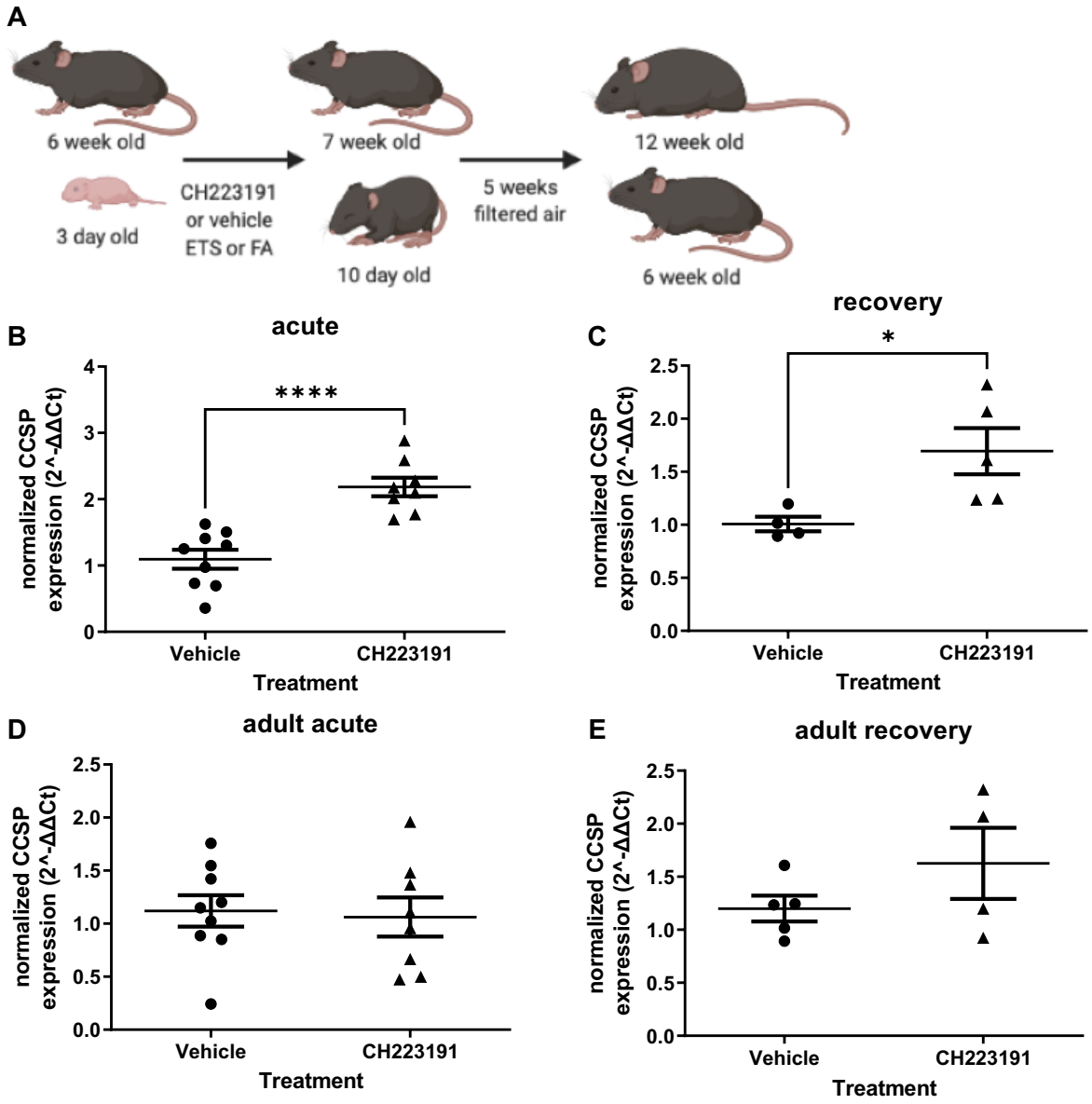

Figure 3: Aryl hydrocarbon receptor antagonist CH223191 abrogates neonatal ETS-induced reductions in club cell secretory protein. Experimental design for intraperitoneal administration of AhR antagonist CH223191 or vehicle to postnatal day 3 pups and adult controls **(A)**. Expression of CCSP was assessed in mice treated immediately prior to ETS exposure on postnatal day 3 with CH223191 or vehicle one week **(B)** or six weeks post administration **(C)**. Expression of CCSP was also assessed in ETS exposed six-week-old mice treated with

CH223191 or vehicle one **(D)** and six weeks post administration **(E)**. * $p<0.05$, ** $p<0.01$, *** $p<0.001$, **** $p<0.0001$ by student's t test.

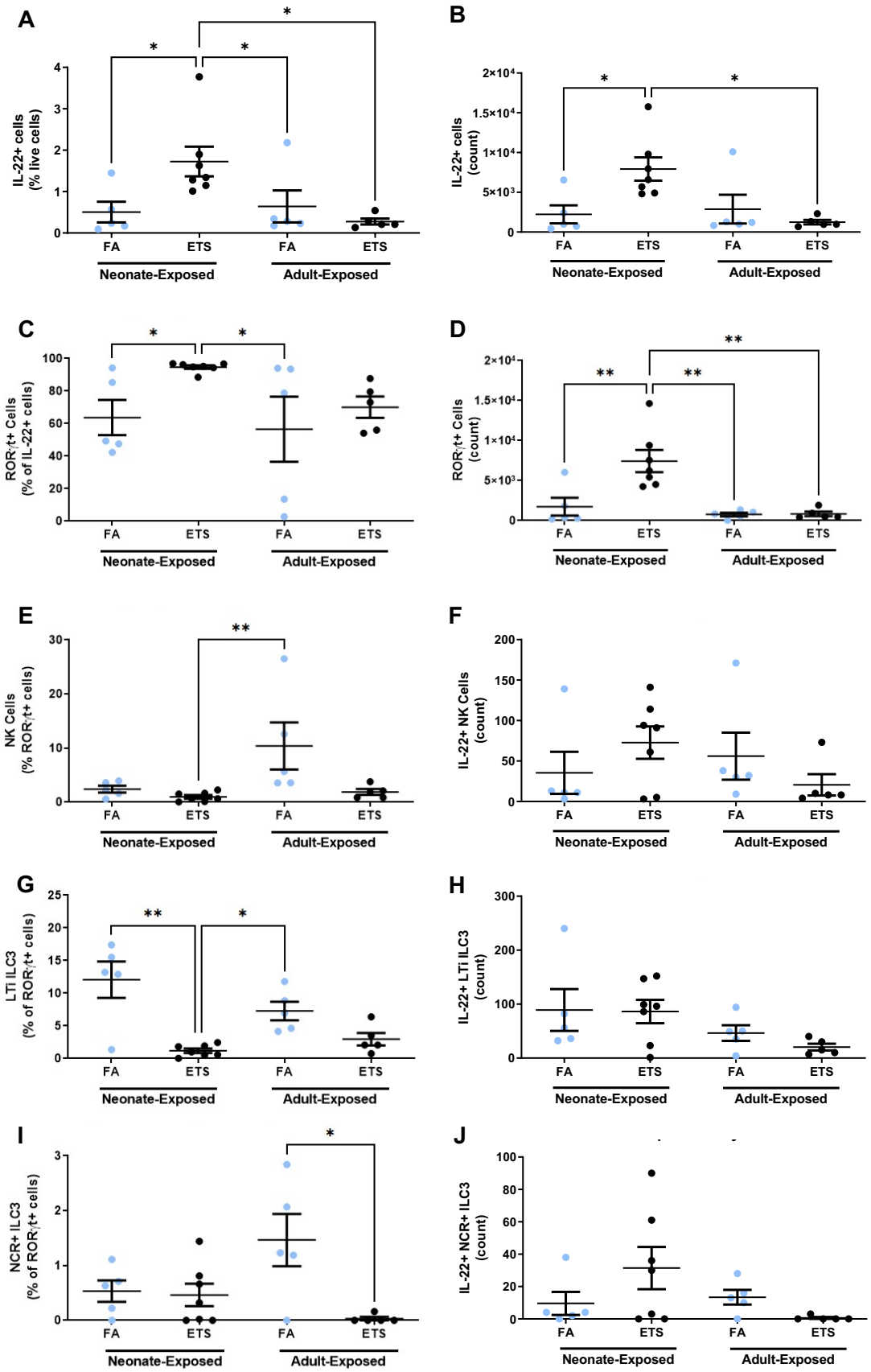
A
IL-22+ cells (% live cells)
B
IL-22+ cells (count)
C
RORγt+ Cells (% of IL-22+ cells)
D
RORγt+ Cells (count)
E
NK Cells (% RORγt+ cells)
F
IL-22+ NK Cells (count)
G
LTi ILC3 (% of RORγt+ cells)
H
IL-22+ LTi ILC3 (count)
I
NCR+ ILC3 (% of RORγt+ cells)
J
IL-22+ NCR+ ILC3 (count)
FA
ETS
Neonate-Exposed
Adult-Exposed

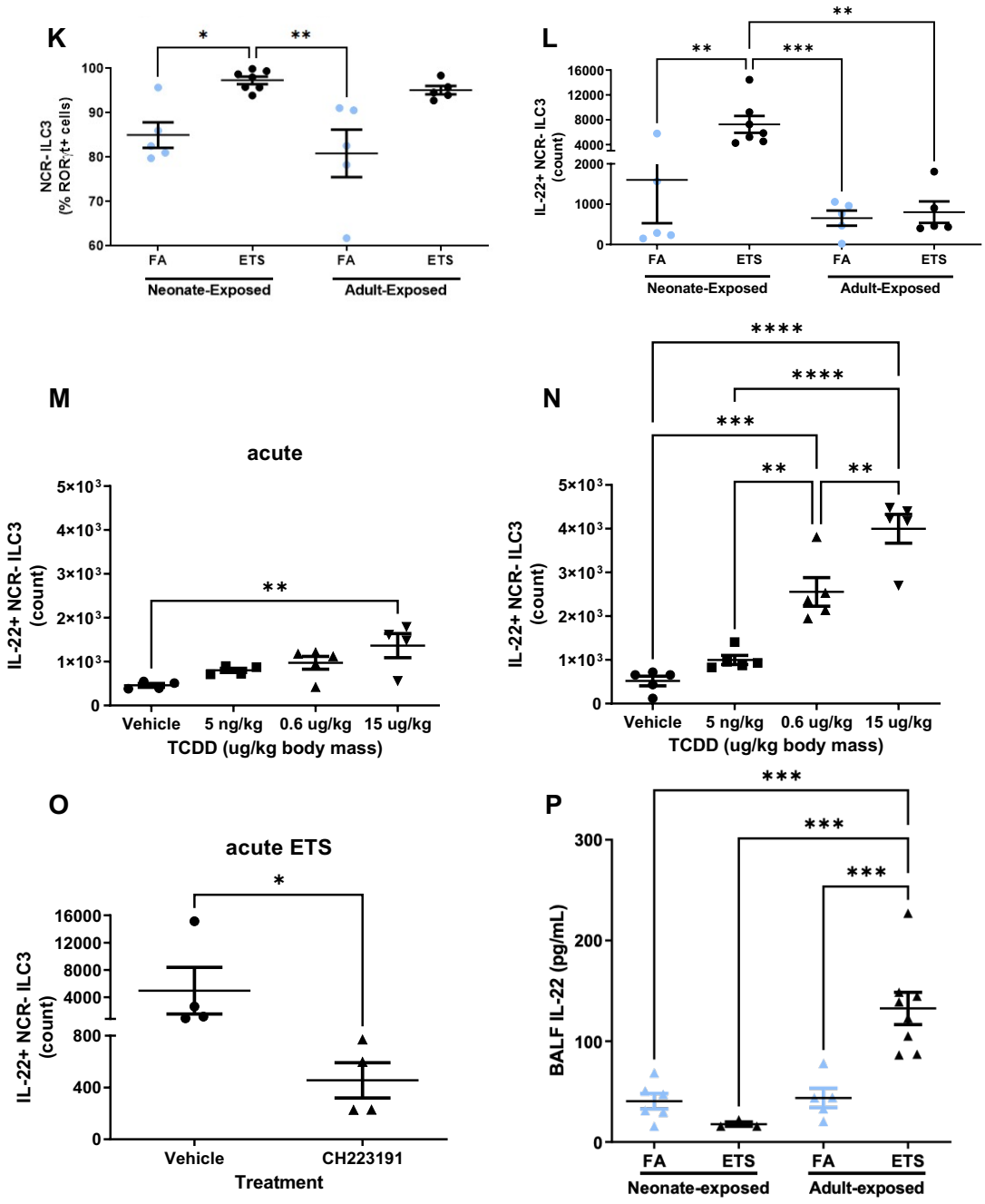

Figure 4: Neonatal ETS exposure transiently induces IL-22$^+$ innate lymphoid cells in the lung in an aryl hydrocarbon receptor-dependent manner. Mice were exposed to ETS or filtered air beginning postnatal day 3 or at six-weeks-old for adult controls. Mice were euthanized either following exposure or following recovery. Lungs were harvested after perfusion, and single cells were isolated, stimulated, and stained for flow cytometry to determine immunophenotype of

IL-22$^+$ cells. Neonatally ETS exposed mice had significantly increased percentage **(A)** and number **(B)** of IL-22$^+$ cells in their lungs at postnatal day 9 compared to filtered air and adult controls. Expression of RORγt was highly expressed in IL-22$^+$ cells as a percentage **(C)** and was significantly increased in ETS exposed neonates by count **(D)** compared to age-matched and adult controls. Further subdividing the RORγt$^+$ cells showed small percentages **(E)** and counts **(F)** of NK cells. Looking in the innate lymphoid cell type 3 (ILC3) compartment, Lymphoid tissue inducer-like ILC3s were a small percentage **(G)** and number **(H)** of RORγt$^+$ IL-22$^+$ cells as were natural kill cell receptor positive (NCR+) by percent **(I)** and count **(J)**. Natural killer cell receptor negative (NCR-) ILC3s represented the majority of RORγt$^+$ IL-22$^+$ cells in ETS-exposed neonates at postnatal day 9 by percent **(K)** and were significantly higher by count **(L)** than age-matched and adult controls. AhR agonist TCDD administered to neonates resulted in a trend toward increased IL-22$^+$ NCR- ILC3 counts in the lungs of neonates at postnatal day 9 **(M)** and counts increased at 6 weeks **(N)**. Mice treated with AhR antagonist prior to neonatal ETS exposure had significantly reduced pulmonary IL-22$^+$ NCR- ILC3 counts compared to vehicle treated mice at postnatal day 9 **(O)**. BALF assayed by ELISA for IL-22 following LPS challenge at 5 weeks post ETS exposure **(P)**. * $p<0.05$, ** $p<0.01$, *** $p<0.001$, **** $p<0.0001$ by ANOVA with Tukey post-hoc correction for multiple comparisons of student's t test.


A
6 week old
7 week old
12 week old
anti-IL-22 antibody
or control IgG
5 weeks
filtered air
3 day old
10 day old
6 week old

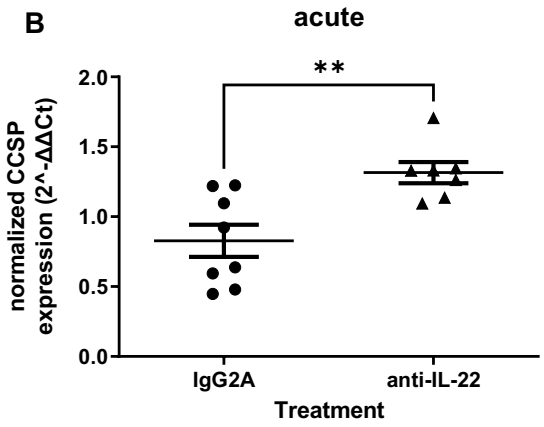
B
acute
**
normalized CCSP
expression (2^-ΔΔCt)
2.0
1.5
1.0
0.5
0.0
IgG2A
anti-IL-22
Treatment

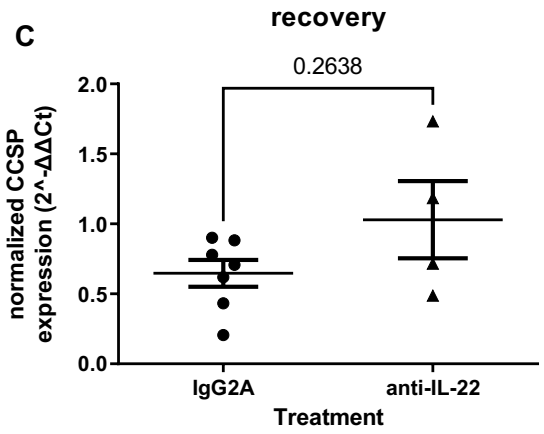
C
recovery
0.2638
normalized CCSP
expression (2^-ΔΔCt)
2.0
1.5
1.0
0.5
0.0
IgG2A
anti-IL-22
Treatment

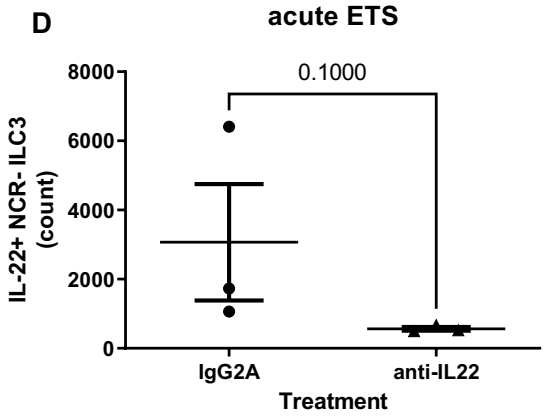
D
acute ETS
0.1000
IL-22+ NCR- ILC3
(count)
8000
6000
4000
2000
0
IgG2A
anti-IL22
Treatment

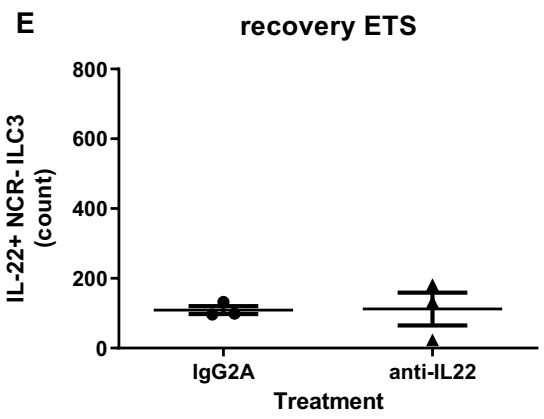
E
recovery ETS
IL-22+ NCR- ILC3
(count)
800
600
400
200
0
IgG2A
anti-IL22
Treatment

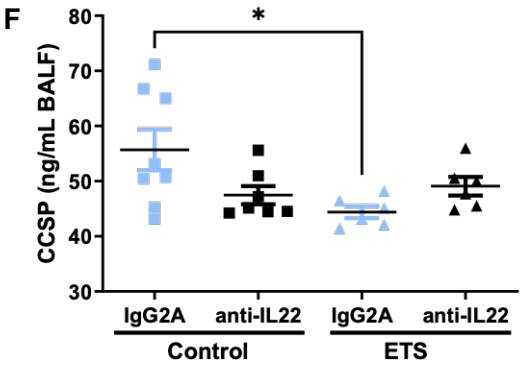
F
*
CCSP (ng/mL BALF)
80
70
60
50
40
30
IgG2A
anti-IL22
IgG2A
anti-IL22
Control
ETS

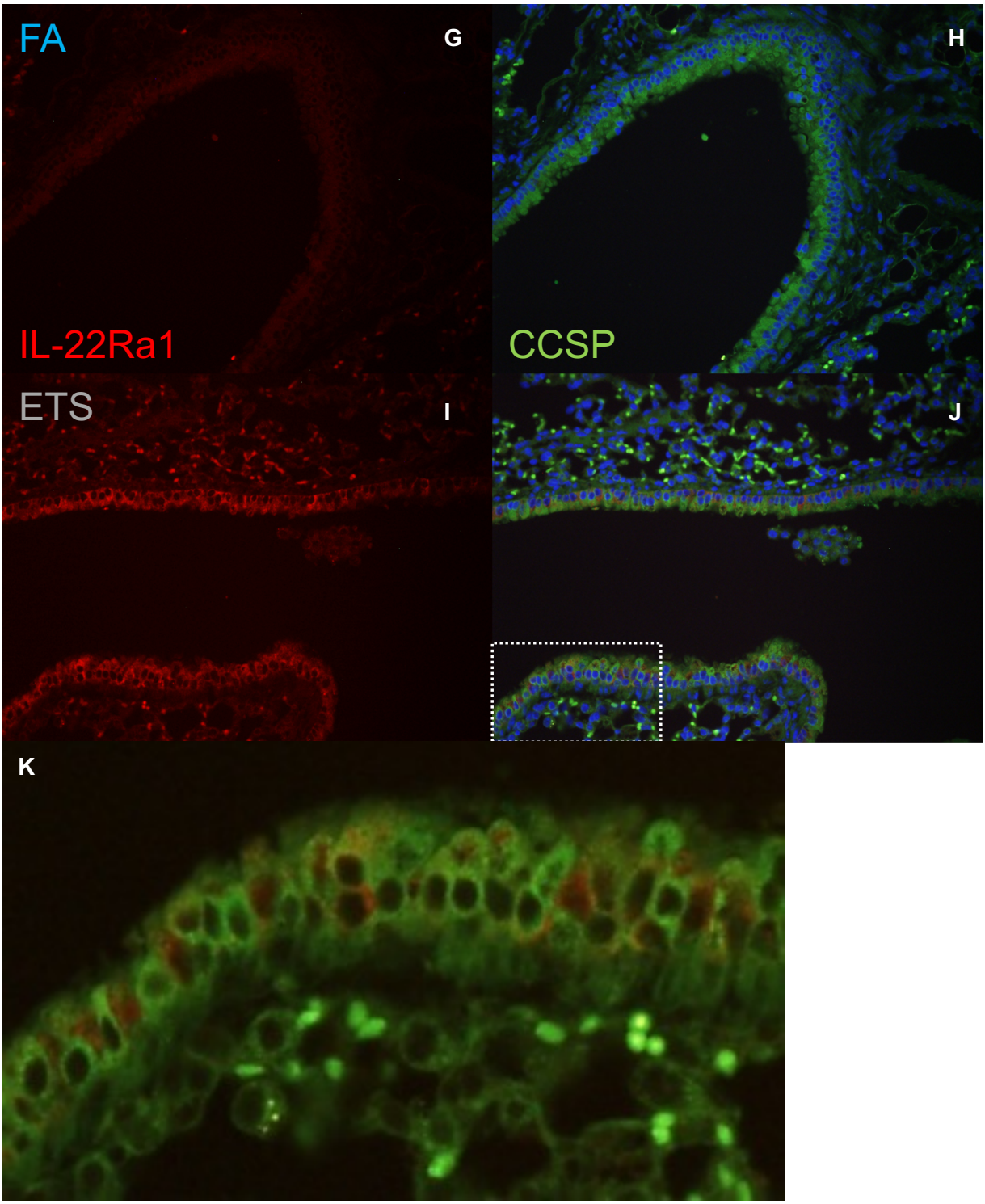

Figure 5: The IL-22/IL-22Ra1 axis in the lung modifies CCSP in neonatal ETS exposures. Experimental design for blocking IL-22 by intraperitoneal injection of 5 mg/kg anti-IL-22 neutralizing antibodies or IgG2A isotype control immediately prior to exposure to ETS beginning

at postnatal day 3 or six-weeks of age **(A)**. Pulmonary CCSP gene expression was measured in mice treated neonatally then exposed to ETS at acute **(B)** and persistent **(C)** timepoints with GAPDH as a housekeeping gene. Mice treated neonatally then exposed to ETS were assessed for acute **(D)** and persistent **(E)** induction of IL-22^{+} NCR- ILC3 counts by flow cytometry. BALF was examined for IL-22 protein by ELISA **(F)**. Lungs from neonatally ETS exposed mice and age-matched controls were inflation fixed with paraformaldehyde, and sections were strained for IL-22Ra1 and CCSP with DAPI counterstain for nuclei. IL-22Ra1 staining in the airways of control mice **(G)** and combined images **(H)**. IL-22Ra1 in the airways of neonatally ETS exposed mice **(I)** and combined images **(J)**. The presence of both IL-22Ra1 and CCSP including co-staining is visible zoomed in **(K)**. Images were captured at 40X. * $p<0.05$, ** $p<0.01$, *** $p<0.001$, **** $p<0.0001$ by student's t test or one-way ANOVA with Tukey's post-hoc test for multiple comparisons.

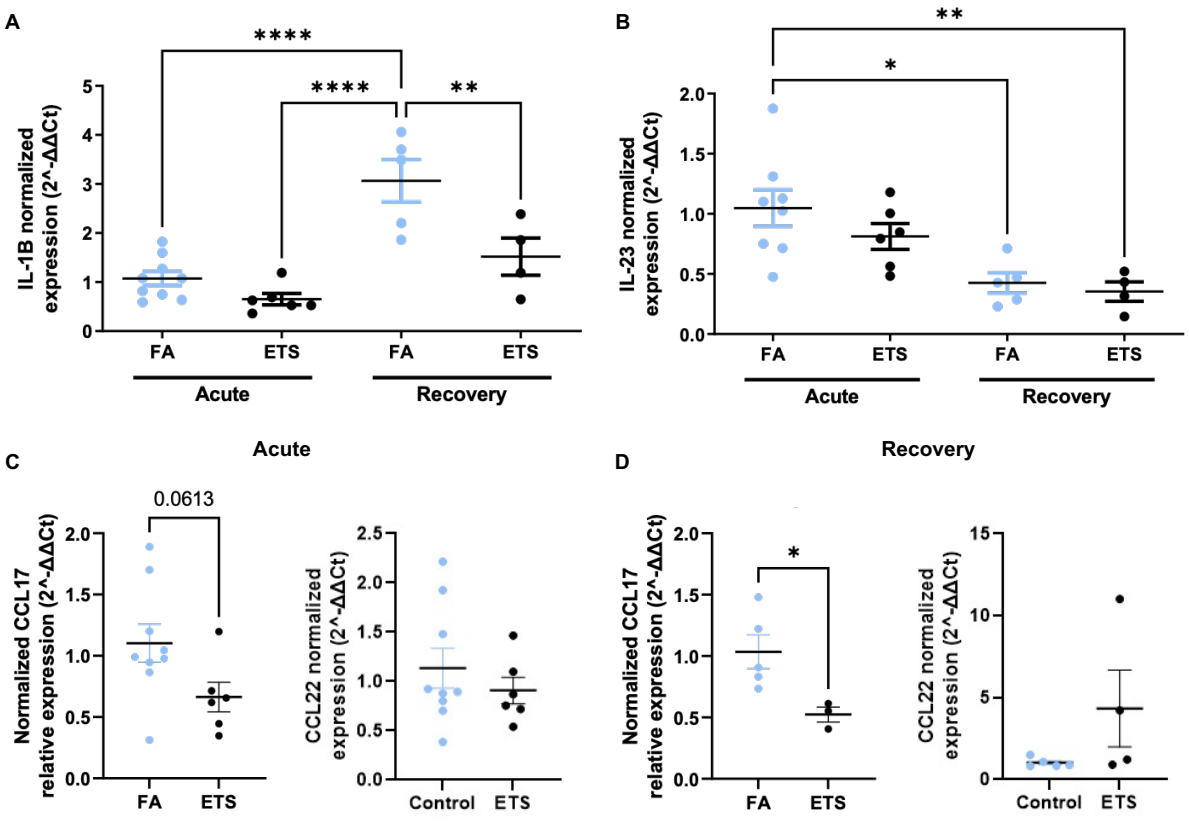

Figure 6: Neonatal ETS exposure reduces IL-22-inducing cytokines and ILC3 homing chemokines in the lungs. Gene expression of mRNA from whole lung homogenate at postnatal day 9 (acute) or six weeks of age (recovery) for IL-22-inducing cytokines **(A)** IL-1β **(B)** IL-23. ILC3 homing chemokines CCL17 and CCL22 at **(C)** acute and **(D)** recovery timepoints. All gene expression used GAPDH as a reference gene. * $p<0.05$, ** $p<0.01$, *** $p<0.001$, **** $p<0.0001$ by student's t test or one-way ANOVA with Tukey's post-hoc test for multiple comparisons.

Table 1: Taqman probes used for gene expression experiments

Gene	Assay ID
CCSP	Mm00442046_m1
GAPDH	Mm99999915_g1
IL-22	Mm01226722_g1
IL-22	Mm00444241_m1
IL-1β	Mm00434228_m1
IL-23A	Mm00518984_m1
CCL17	Mm00516136_m1
CCL22	Mm00436439_m1

Table 2: Antibodies used for flow cytometry, immunofluorescence, and Western blot experiments

Target	Conjugate	Clone	Manufacturer
IL-22	APC	poly	Biolegend
CD45	APC/Fire750	QA17A26	Biolegend
CD127	BV421	A7R34	Biolegend
CD8a	BV510	53-6.7	Biolegend
NKp46	BV711	29A1.4	Biolegend
ST2	BV785	DIH9	Biolegend
CCR6	PE/Cy7	29-2L17	Biolegend
$\gamma\delta$TCR	PerCP/Cy5.5	GL3	Biolegend
CD3e	BUV395	17A2	BD Biosciences
IL-12Rb2	AF488	305719	R&D Systems
RORγt	PE	B2D	eBioscience
CD45R/B220	BV605	RA3-6B2	Biolegend
CD127	PE/Cy5	A7R34	Biolegend
CCR6	BV785	29-2L17	Biolegend
NK1.1	AF700	PK136	Biolegend
AhR	PE/CF594	T49-550	BD Biosciences
$\gamma\delta$TCR	AF488	GL3	Biolegend
NKp46	APC/Fire750	29A1.4	Biolegend
CD45.2	BV421	104	Biolegend
CD3e	BV605	17A2	Biolegend
CD117	Pacific Blue	2B8	Biolegend
ST2	PE/Cy7	DIH4	Biolegend
CD8a	PE/dazzle594	53-6.7	Biolegend
CGRP	none	poly	Millipore Sigma
Krt5	none	poly	Biolegend
SCGB3A2	none	poly	Biorbyt
IL-22Ra1	none	poly	Bios
CCSP	none	E-11	SantaCruz
CCSP	none	EPR19846	Abcam
IL-22Ra1	none	496514	R&D Systems

Table 3:

Parameter		Neonate Exposed		Adult Exposed		p-value	
		FA	ETS	FA	ETS	Neonate FA-ETS	Adult FA-ETS
Quasistatic Resistance cmH2O*s/mL	Total	0.791±0.042	0.795±0.021	0.625±0.022	0.604±0.019	0.9193	0.4795
	Female	0.847±0.075	0.856±0.029	0.649±0.029	0.621±0.021	0.9275	0.4547
	Male	0.734±0.022	0.765±0.018	0.585±0.014	0.546±0.020	0.3154	0.1826
Quasistatic Elastance cmH2O/mL	Total	34.049±1.717	35.258±1.361	29.317±1.510	25.964+0.856	0.5854	0.0502
	Female	37.773±1.609	39.975±2.024	30.569±2.059	26.490±1.056	0.427	0.0701
	Male	30.326±1.386	32.899±0.539	27.230±1.916	24.212±0.567	0.0804	0.2053
Quasistatic Compliance mL/cmH2O	Total	0.030±0.002	0.029±0.001	0.035±0.002	0.039±0.001	0.5098	0.0613
	Female	0.027±0.001	0.025±0.001	0.033±0.002	0.038±0.002	0.4423	0.0989
	Male	0.033±0.002	0.030±0.0005	0.037±.003	0.041±0.001	0.0795	0.1979
Newtonian Resistance cmH2O*s/mL	Total	0.367±0.048	0.321±0.017	0.241±0.019	0.260±0.016	0.3654	0.4716
	Female	0.387±0.102	0.356±0.030	0.244±0.026	0.273±0.019	0.8078	0.3952
	Male	0.346±0.016	0.304±0.018	0.236±0.034	0.217±0.018	0.1387	0.6496
Tissue Damping cmH2O/mL	Total	5.118±0.146	5.670±0.150	4.764±0.237	4.203±0.121	**0.0191**	**0.0311**
	Female	5.435±0.068	5.658±0.181	4.982±0.316	4.245±0.157	0.2506	**0.0342**
	Male	4.800±0.167	5.677±0.217	4.398±0.292	4.063±0.040	**0.0199**	0.3191
Tissue Elastance cmH2O/mL	Total	30.884±1.658	31.912±1.307	26.697±1.625	23.491±0.823	0.6296	0.0658
	Female	34.347±1.619	36.163±1.945	27.739±2.393	23.803±1.051	0.5024	0.1
	Male	27.421±1.487	29.786±0.795	24.960±1.778	22.452±0.581	0.163	0.251
Static Compliance mL/cmH2O	Total	0.049±0.003	0.047±0.002	0.062±0.003	0.070±0.002	0.4463	**0.0273**
	Female	0.044±0.002	0.043±0.002	0.060±0.004	0.069±0.002	0.7424	0.0549
	Male	0.055±0.002	0.049±0.002	0.065±0.006	0.075±0.004	0.1133	0.2138
PV Loop Area mL*cmH2O	Total	1.279±0.086	1.387±0.049	1.822±0.073	1.735±0.047	0.2783	0.3049
	Female	1.101±0.109	1.321±0.027	1.840±0.098	1.709±0.054	0.1539	0.2246
	Male	1.457±0.038	1.420±0.070	1.793±0.131	1.820±0.097	0.7035	0.8754
PV Loop K /cmH2O	Total	0.125±0.004	0.124±0.002	0.121±0.003	0.128±0.002	0.8636	**0.0438**
	Female	0.117±0.003	0.125±0.002	0.120±0.004	0.128±0.003	0.1212	0.1308
	Male	0.132±0.005	0.123±0.003	0.121±0.004	0.128±0.002	0.1503	0.1738
Inspiratory Capacity mL	Total	0.567±0.024	0.555±0.018	0.720±0.025	0.782±0.020	0.5512	0.069
	Female	0.511±0.019	0.496±0.023	0.698±0.032	0.765±0.022	0.6399	0.1027
	Male	0.623±0.017	0.584±0.013	0.756±0.037	0.842±0.037	0.1016	0.18
n		4 Female, 4 Male	3 Female, 6 Male	5 Female, 3 Male	10 Female, 3 Male		

3.7. Supplementary Figures

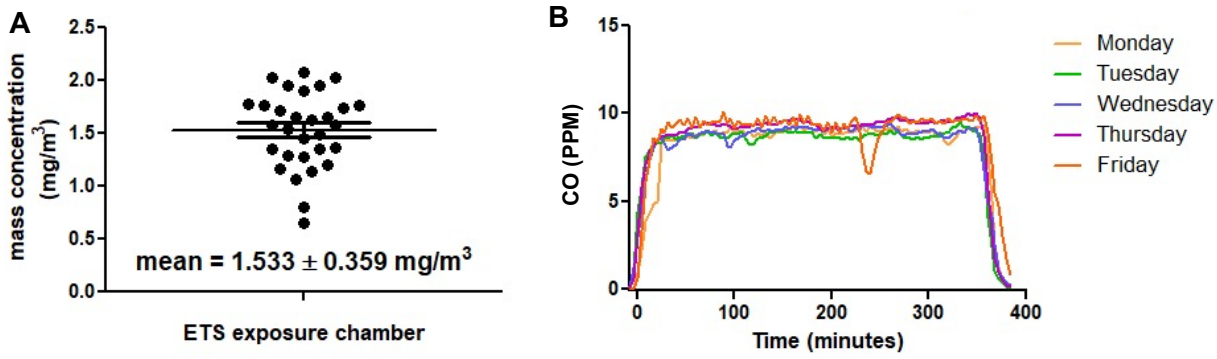

Supplemental Figure 1: Concentration of particulate matter and carbon monoxide in ETS exposure chamber. Concentration of particulate matter was measured twice daily by collecting particulate on pre-weighed filters for 1 hour at a known flow rate. Filters were weighed following collection and ambient particulate matter was calculated for each collection period **(A)**. Carbon monoxide was measured every four minutes as a surrogate for combustion products throughout the entire exposure period and mean CO concentration during exposure is reported **(B)**. Non-ETS chambers are sealed to the room and receive filtered air. CO levels were below 0.1 PPM within 30 minutes of the end of daily exposure.

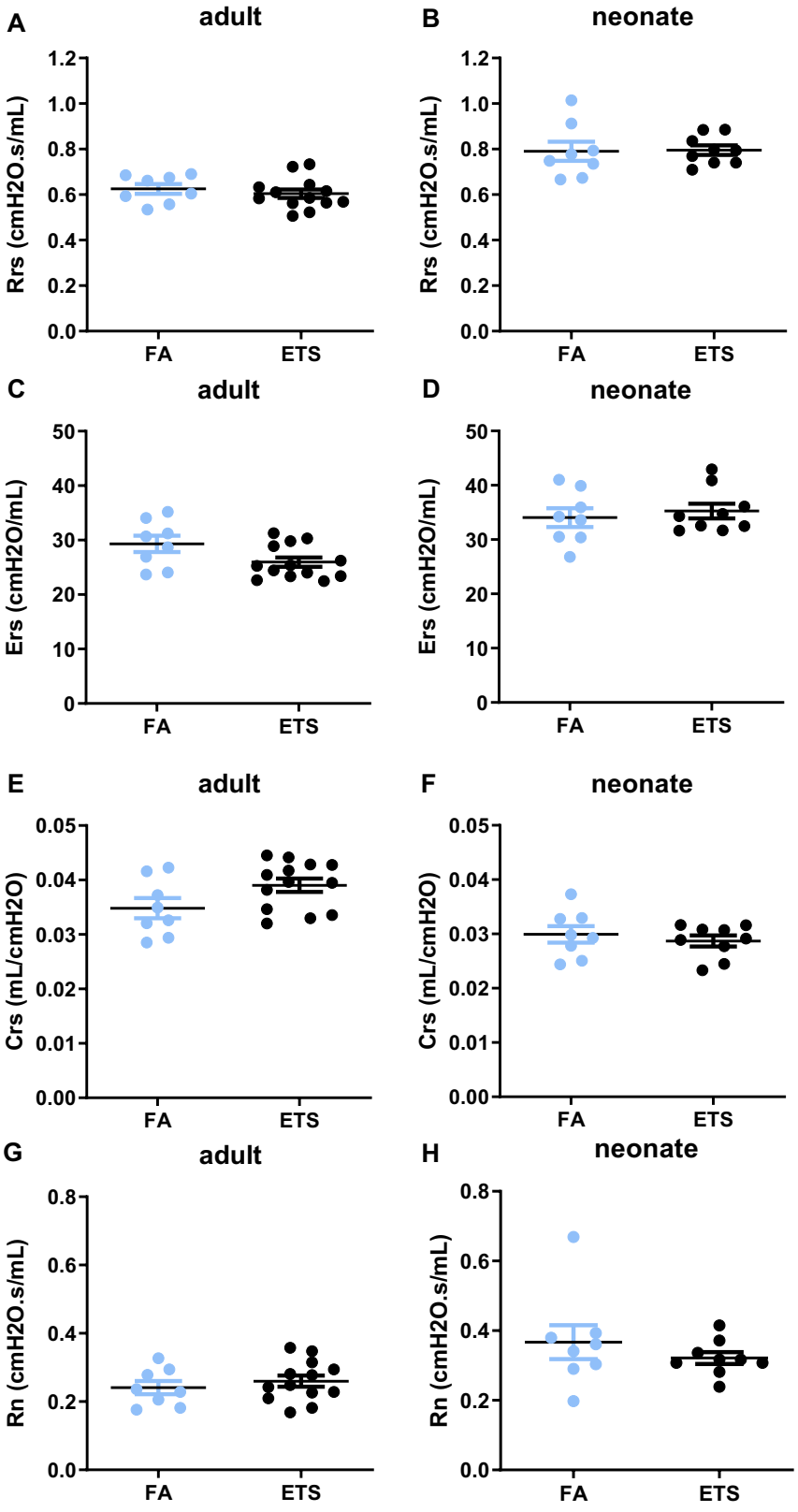
A
adult
Rrs (cmH2O.s/mL)
1.2
1.0
0.8
0.6
0.4
0.2
0.0
FA
ETS
B
neonate
Rrs (cmH2O.s/mL)
1.2
1.0
0.8
0.6
0.4
0.2
0.0
FA
ETS
C
adult
Ers (cmH2O/mL)
50
40
30
20
10
0
FA
ETS
D
neonate
Ers (cmH2O/mL)
50
40
30
20
10
0
FA
ETS
E
adult
Crs (mL/cmH2O)
0.05
0.04
0.03
0.02
0.01
0.00
FA
ETS
F
neonate
Crs (mL/cmH2O)
0.05
0.04
0.03
0.02
0.01
0.00
FA
ETS
G
adult
Rn (cmH2O.s/mL)
0.8
0.6
0.4
0.2
0.0
FA
ETS
H
neonate
Rn (cmH2O.s/mL)
0.8
0.6
0.4
0.2
0.0
FA
ETS

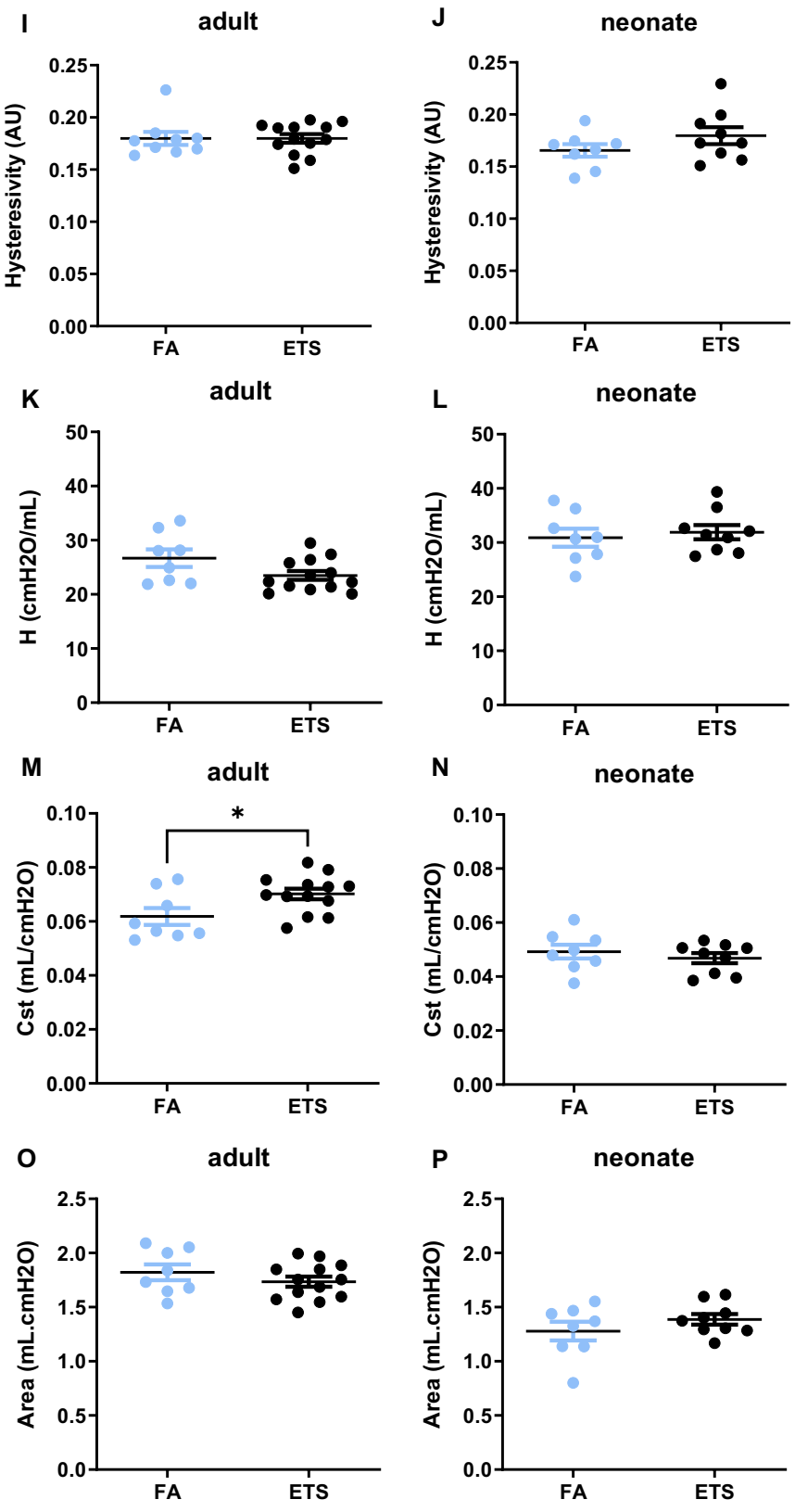
I
adult
Hysteresivity (AU)
0.25
0.20
0.15
0.10
0.05
0.00
FA
ETS
J
neonate
Hysteresivity (AU)
0.25
0.20
0.15
0.10
0.05
0.00
FA
ETS
K
adult
H (cmH2O/mL)
50
40
30
20
10
0
FA
ETS
L
neonate
H (cmH2O/mL)
50
40
30
20
10
0
FA
ETS
M
adult
*
Cst (mL/cmH2O)
0.10
0.08
0.06
0.04
0.02
0.00
FA
ETS
N
neonate
Cst (mL/cmH2O)
0.10
0.08
0.06
0.04
0.02
0.00
FA
ETS
O
adult
Area (mL.cmH2O)
2.5
2.0
1.5
1.0
0.5
0.0
FA
ETS
P
neonate
Area (mL.cmH2O)
2.5
2.0
1.5
1.0
0.5
0.0
FA
ETS

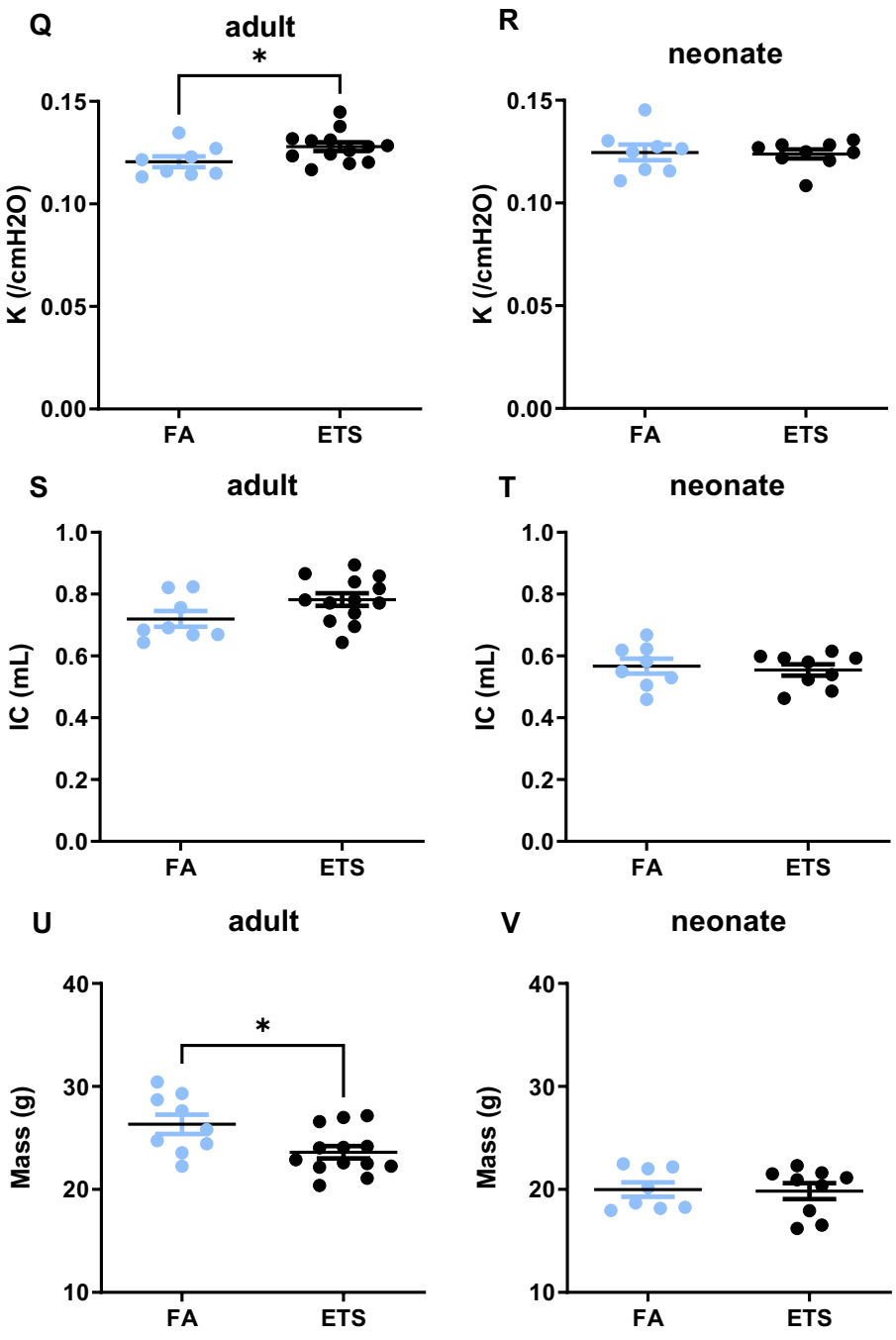

Supplemental Figure 2: Pulmonary function testing by flexiVent forced oscillation maneuvers following ETS exposure. Mice were exposed neonatally or at six-weeks-old to ETS or filtered air and allowed to recover for 5 weeks in filtered air before pulmonary function testing was performed on the flexiVent forced oscillation system. Quasistatic resistance of adults **(A)** and neonatally exposed mice **(B)**. Quasistatic elastance of adults **(C)** and neonatally exposed mice

(D). Quasistatic compliance of adults **(E)** and neonatally exposed mice **(F)**. Newtonian resistance of adults **(G)** and neonatally exposed mice **(H)**. Hysteresivity of adults **(I)** and neonatally exposed mice **(J)**. Tissue elastance of adults **(K)** and neonatally exposed mice **(L)**. Static compliance of adults **(M)** and neonatally exposed mice **(N)**. Pressure-volume loop area of adults **(O)** and neonatally exposed mice **(P)**. Pressure-volume loop K of adults **(Q)** and neonatally exposed mice **(R)**. Inspiratory capacity of adults **(S)** and neonatally exposed mice **(T)**. Mass for adult **(U)** and neonatally exposed mice that were tested **(V)**. $p<0.05$, ** $p<0.01$, *** $p<0.001$, **** $p<0.0001$ by student's t test.

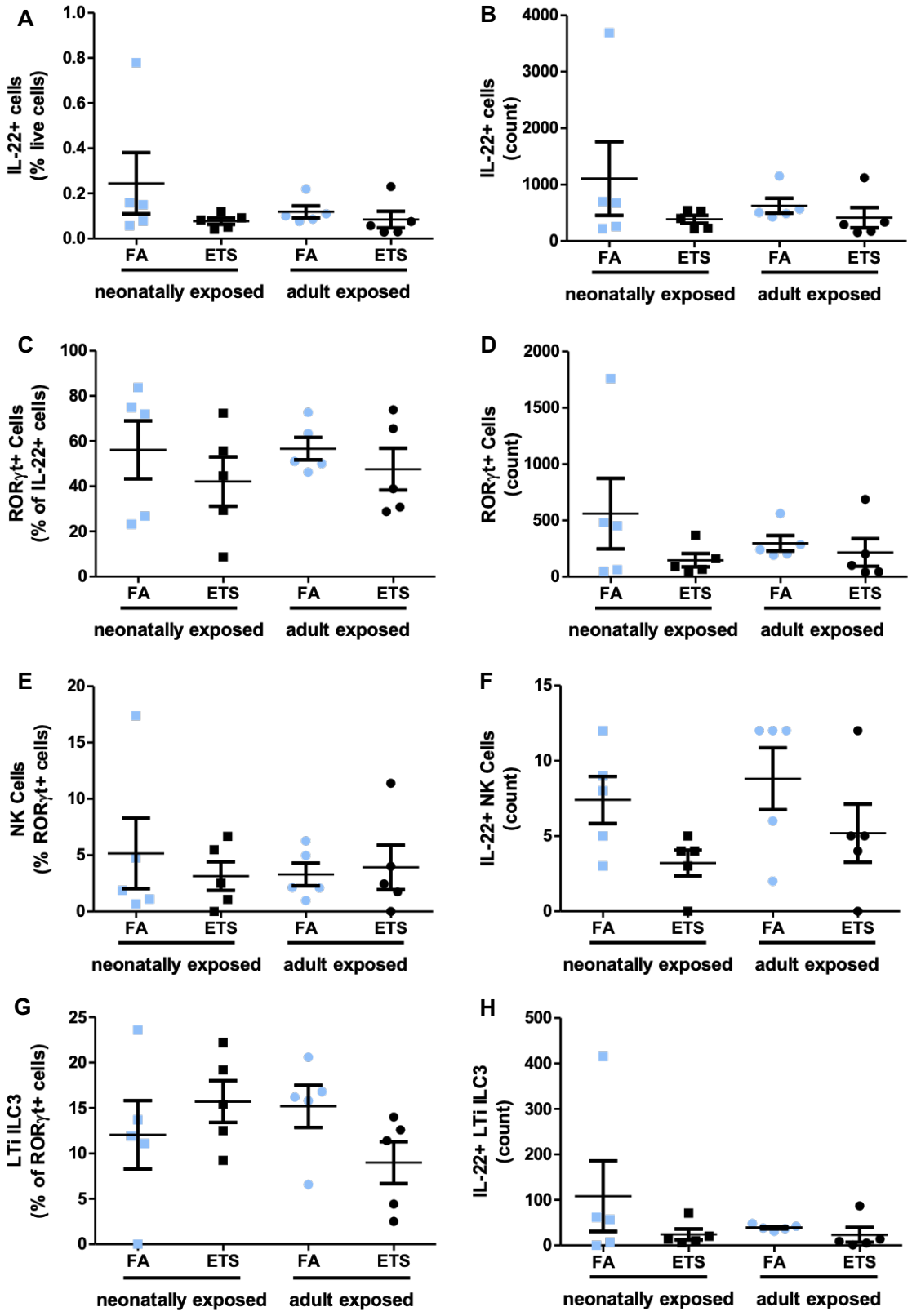
A
IL-22+ cells
(% live cells)
1.0
0.8
0.6
0.4
0.2
0.0
FA
ETS
FA
ETS
neonatally exposed
adult exposed
B
IL-22+ cells
(count)
4000
3000
2000
1000
0
FA
ETS
FA
ETS
neonatally exposed
adult exposed
C
RORγt+ Cells
(% of IL-22+ cells)
100
80
60
40
20
0
FA
ETS
FA
ETS
neonatally exposed
adult exposed
D
RORγt+ Cells
(count)
2000
1500
1000
500
0
FA
ETS
FA
ETS
neonatally exposed
adult exposed
E
NK Cells
(% RORγt+ cells)
20
15
10
5
0
FA
ETS
FA
ETS
neonatally exposed
adult exposed
F
IL-22+ NK Cells
(count)
15
10
5
0
FA
ETS
FA
ETS
neonatally exposed
adult exposed
G
LTi ILC3
(% of RORγt+ cells)
25
20
15
10
5
0
FA
ETS
FA
ETS
neonatally exposed
adult exposed
H
IL-22+ LTi ILC3
(count)
500
400
300
200
100
0
FA
ETS
FA
ETS
neonatally exposed
adult exposed

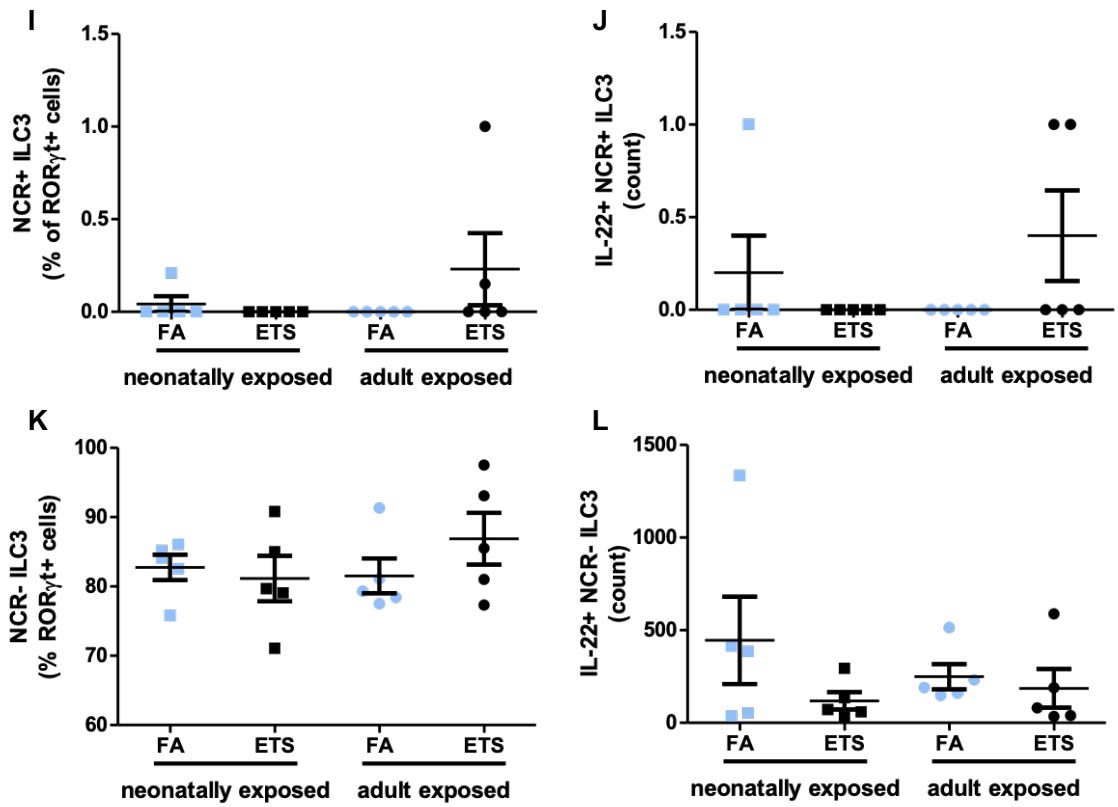

Supplemental Figure 3: IL-22$^+$ immune cells populations in the lung at 5 weeks post exposure are not detectably different between treatment groups. Postnatal day 3 and six-week-old adult control mice were exposed to ETS for 5 days and allowed to recover in filtered air for 5 weeks prior to necropsy. No difference was observed between any group in the percentage **(A)** or count **(B)** of IL-22$^+$ cells in the lung. No difference was seen in the percentage **(C)** or count **(D)** of RORγt$^+$ cells within the IL-22$^+$ gate. No difference was detected between groups in the percent **(E)** or count **(F)** of NK cells, percent **(G)** or count **(H)** of lymphoid tissue inducer-like ILC3s, percent **(I)** or count **(J)** of natural killer receptor positive ILC3s, or percent **(K)** or count **(L)** of natural killer cell receptor negative ILC3s between groups. $p<0.05$, ** $p<0.01$, *** $p<0.001$, **** $p<0.0001$ by ANOVA with Tukey's post-hoc test for multiple comparisons.

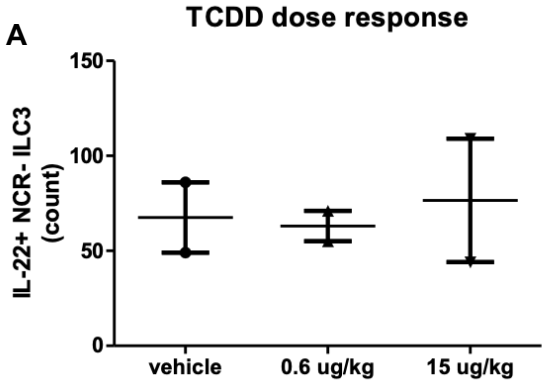
A
TCDD dose response
IL-22+ NCR- ILC3 (count)
150
100
50
0
vehicle
0.6 ug/kg
15 ug/kg

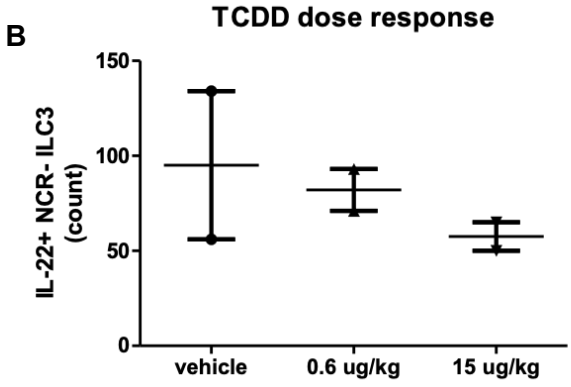
B
TCDD dose response
IL-22+ NCR- ILC3 (count)
150
100
50
0
vehicle
0.6 ug/kg
15 ug/kg

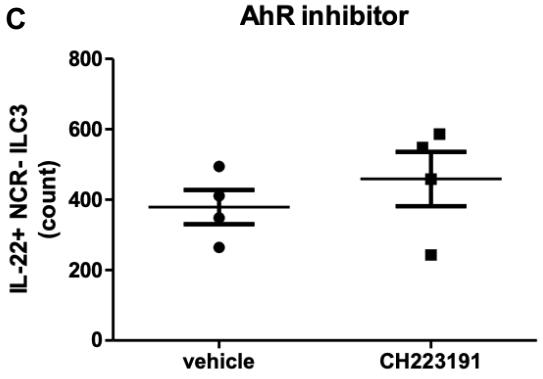
C
AhR inhibitor
IL-22+ NCR- ILC3 (count)
800
600
400
200
0
vehicle
CH223191

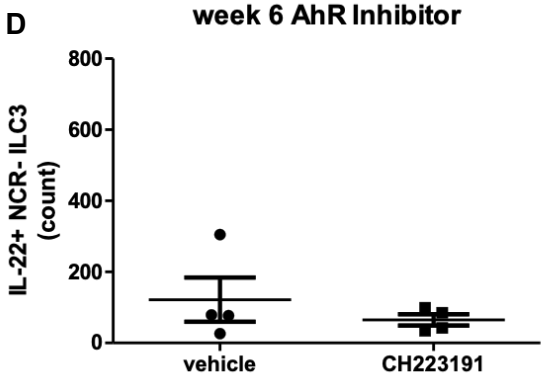
D
week 6 AhR Inhibitor
IL-22+ NCR- ILC3 (count)
800
600
400
200
0
vehicle
CH223191

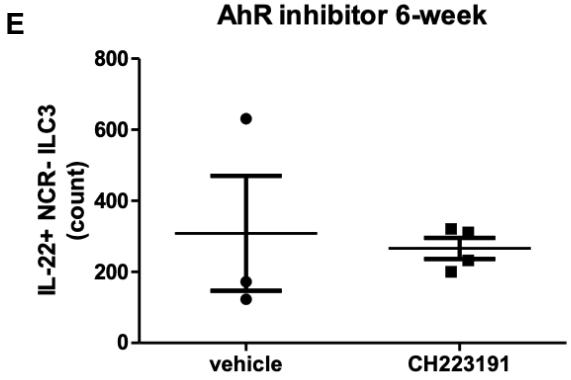
E
AhR inhibitor 6-week
IL-22+ NCR- ILC3 (count)
800
600
400
200
0
vehicle
CH223191

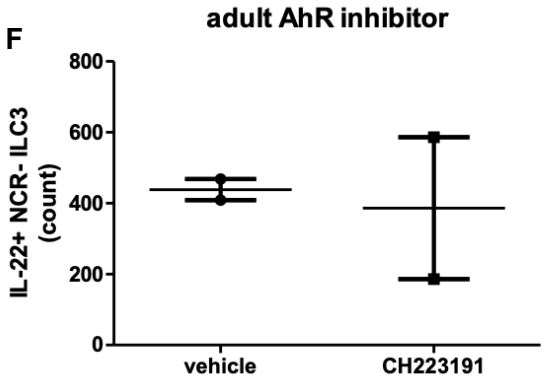
F
adult AhR inhibitor
IL-22+ NCR- ILC3 (count)
800
600
400
200
0
vehicle
CH223191

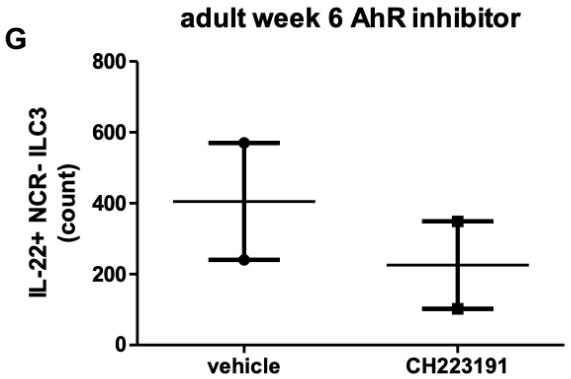
G
adult week 6 AhR inhibitor
IL-22+ NCR- ILC3 (count)
800
600
400
200
0
vehicle
CH223191

Supplemental Figure 4: IL-22^{+} NCR- ILC3s in murine lungs of mice treated with aryl hydrocarbon receptor modulating compounds. Six-week-old mice were administered AhR agonist TCDD or vehicle via intraperitoneal injection, and pulmonary IL-22+ NCR- ILC3 counts were assessed by flow cytometry at 1 week **(A)** and six weeks after treatment **(B)**. Postnatal day 3 mice were administered AhR antagonist CH223191 or vehicle and exposed to ETS followed by 5 weeks of recovery in filtered air, and pulmonary IL-22+ NCR- ILC3 counts were assessed by flow cytometry **(C)**. Postnatal day 3 mice were administered AhR antagonist CH223191 or vehicle and maintained in filtered air, and pulmonary IL-22+ NCR- ILC3 counts were assessed by flow cytometry at one week **(D)** and 6 weeks after treatment **(E)**. Six-week-old mice were administered AhR antagonist CH223191 or vehicle via intraperitoneal injection and exposed to ETS, and pulmonary IL-22+ NCR- ILC3 counts were assessed by flow cytometry after exposure **(F)** and after 5 weeks of recovery in filtered air **(G)**. $p<0.05$, ** $p<0.01$, *** $p<0.001$, **** $p<0.0001$ by student's t test.

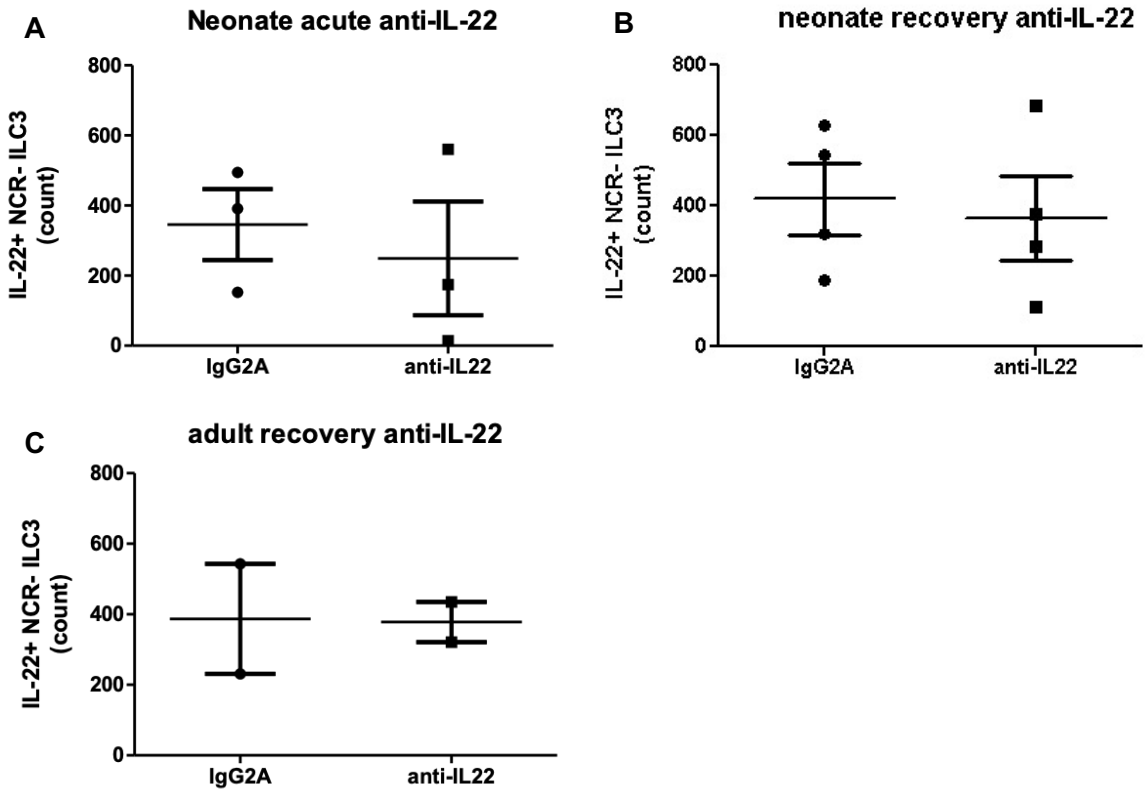

Supplemental Figure 5: IL-22 modulation in early life ETS exposure. Postnatal day 3 mice were treated with anti-IL-22 neutralizing or isotype control antibodies and exposed filtered air. Lungs were collected and IL-22^{+} cells were detected by flow cytometry at **(A)** acute and **(B)** recovery timepoints. Lungs of adult mice treated with anti-IL-22 and exposed ETS were assessed acutely following ETS exposure **(C)**.

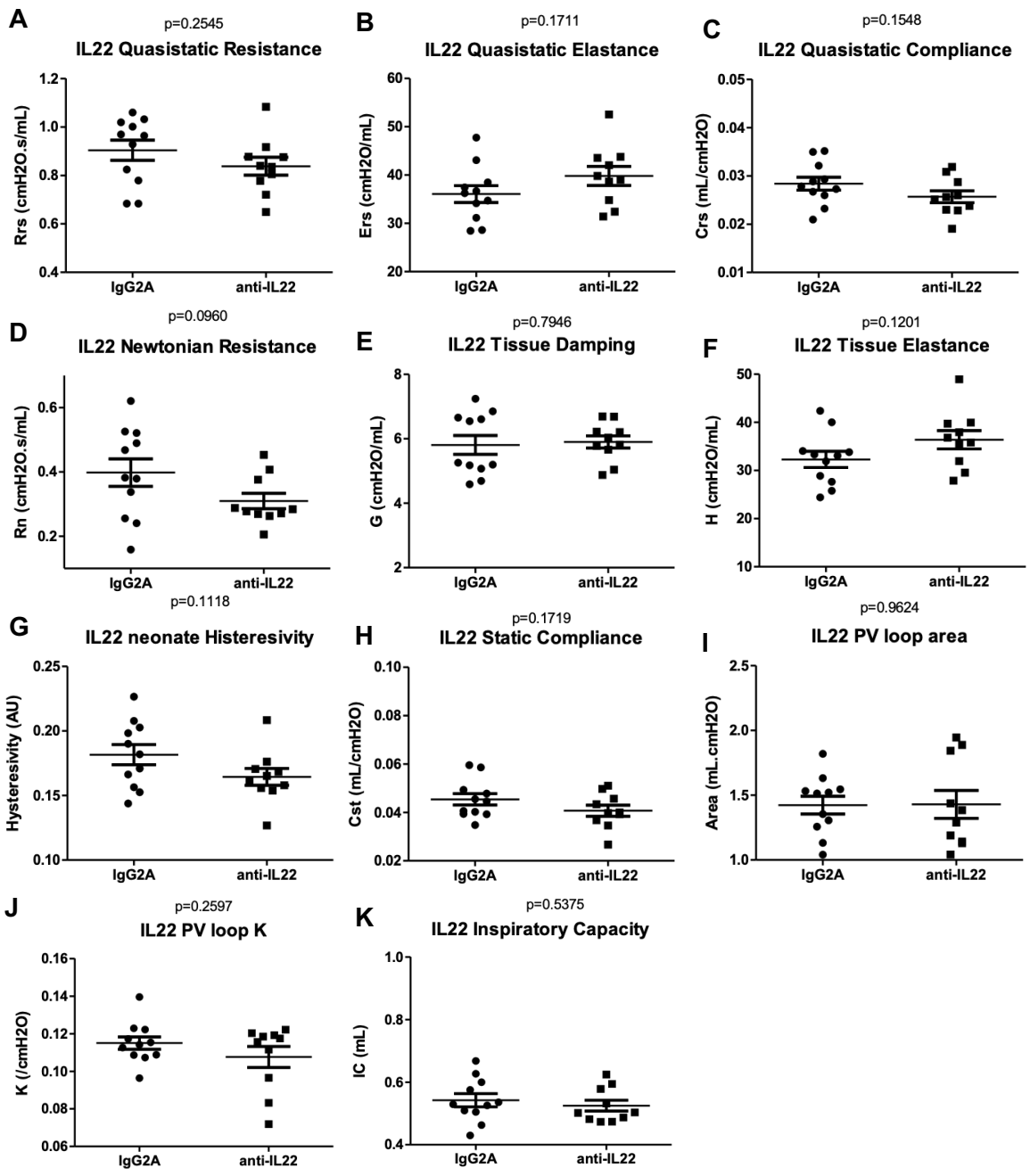

Supplemental Figure 6: Pulmonary function testing of neonatally anti-IL-22 antibody treated mice exposed to ETS. Postnatal day 3 mice were treated with 5 mg/kg anti-IL-22 neutralizing antibody or isotype control prior to ETS exposure and allowed to recover for 5 weeks in filtered air. At six-weeks-old, mice were subject to pulmonary function testing using felxiVent forced oscillations maneuvers. Quasistatic resistance **(A)**, quasistatic elastance **(B)**, quasistatic

compliance **(C)**, Newtonian resistance **(D)**, tissue damping **(E)**, tissue elastance **(F)**, hysteresivity **(G)** static compliance **(H)**, pressure-volume loop area **(I)**, pressure-volume loop K **(J)**, and inspiratory capacity **(K)** were measured. $p<0.05$, ** $p<0.01$, *** $p<0.001$, **** $p<0.0001$ by student's t test.

3.8. References

1. Do, E.K., et al., *Social determinants of smoke exposure during pregnancy: Findings from waves 1 & 2 of the Population Assessment of Tobacco and Health (PATH) Study.* Preventive medicine reports, 2018. **12**: p. 312-320.
2. Centers for Disease Control Prevention, *Current cigarette smoking among adults in the United States.* 2019.
3. Martinez, F.D., *Early-life origins of chronic obstructive pulmonary disease.* New England Journal of Medicine, 2016. **375**(9): p. 871-878.
4. Weiss, S.T., et al., *The health effects of involuntary smoking.* American Review of Respiratory Disease, 1983. **128**(5): p. 933-942.
5. US Department of Health and Human Services, *Public Health Services, National Toxicology Program 14th Report on Carcinogens*. 2016.
6. Stedman, R.L., *Chemical composition of tobacco and tobacco smoke.* Chemical reviews, 1968. **68**(2): p. 153-207.
7. Rubin, H., *Synergistic mechanisms in carcinogenesis by polycyclic aromatic hydrocarbons and by tobacco smoke: a bio-historical perspective with updates.* Carcinogenesis, 2001. **22**(12): p. 1903-1930.
8. Office on Smoking Centers for Disease Control Prevention, *How tobacco smoke causes disease: The biology and behavioral basis for smoking-attributable disease: A report of the surgeon general.* 2010.
9. Vogel, C.F., et al., *The aryl hydrocarbon receptor as a target of environmental stressors–Implications for pollution mediated stress and inflammatory responses.* Redox biology, 2020. **34**: p. 101530.

10. Rothhammer, V. and F.J. Quintana, *The aryl hydrocarbon receptor: an environmental sensor integrating immune responses in health and disease.* Nature Reviews Immunology, 2019. **19**(3): p. 184-197.

11. Wong, P.S., et al., *Arylhydrocarbon receptor activation in NCI-H441 cells and C57BL/6 mice: possible mechanisms for lung dysfunction.* American journal of respiratory cell and molecular biology, 2010. **42**(2): p. 210-217.

12. Veldhoen, M., et al., *The aryl hydrocarbon receptor links TH 17-cell-mediated autoimmunity to environmental toxins.* Nature, 2008. **453**(7191): p. 106-109.

13. Qiu, J., et al., *The aryl hydrocarbon receptor regulates gut immunity through modulation of innate lymphoid cells.* Immunity, 2012. **36**(1): p. 92-104.

14. Boniface, K., et al., *IL-22 inhibits epidermal differentiation and induces proinflammatory gene expression and migration of human keratinocytes.* The Journal of Immunology, 2005. **174**(6): p. 3695-3702.

15. Kamanaka, M., et al., *Memory/effector (CD45RBlo) CD4 T cells are controlled directly by IL-10 and cause IL-22–dependent intestinal pathology.* Journal of Experimental Medicine, 2011. **208**(5): p. 1027-1040.

16. Eken, A., et al., *IL-23R+ innate lymphoid cells induce colitis via interleukin-22-dependent mechanism.* Mucosal immunology, 2014. **7**(1): p. 143-154.

17. Xue, J., et al., *Aryl hydrocarbon receptor ligands in cigarette smoke induce production of interleukin-22 to promote pancreatic fibrosis in models of chronic pancreatitis.* Gastroenterology, 2016. **151**(6): p. 1206-1217.

18. Starkey, M.R., et al., *IL-22 and its receptors are increased in human and experimental COPD and contribute to pathogenesis.* European Respiratory Journal, 2019: p. 1800174.

19. Wolk, K., et al., *IL-22 increases the innate immunity of tissues.* Immunity, 2004. **21**(2): p. 241-254.

20. Dumoutier, L., et al., *Human interleukin-10-related T cell-derived inducible factor: molecular cloning and functional characterization as an hepatocyte-stimulating factor.* Proceedings of the National Academy of Sciences, 2000. **97**(18): p. 10144-10149.

21. Xie, M.-H., et al., *Interleukin (IL)-22, a novel human cytokine that signals through the interferon receptor-related proteins CRF2–4 and IL-22R.* Journal of Biological Chemistry, 2000. **275**(40): p. 31335-31339.

22. Pociask, D.A., et al., *IL-22 is essential for lung epithelial repair following influenza infection.* The American journal of pathology, 2013. **182**(4): p. 1286-1296.

23. Hebert, K., et al., *IL-22Ra1 is induced during influenza infection by direct and indirect TLR3 induction of STAT1.* Respiratory research, 2019. **20**(1): p. 1-10.

24. Dugger, D.T., J.E. Gerriets, and L.A. Miller, *Attenuated airway epithelial cell interleukin-22R1 expression in the infant nonhuman primate lung.* American journal of respiratory cell and molecular biology, 2015. **53**(6): p. 761-768.

25. Schittny, J.C., *Development of the lung.* Cell and tissue research, 2017. **367**(3): p. 427-444.

26. Teague, S.V., et al., *Sidestream cigarette smoke generation and exposure system for environmental tobacco smoke studies.* Inhalation toxicology, 1994. **6**(1): p. 79-93.

27. Kerkvliet, N., et al., *Influence of the Ah locus on the humoral immunotoxicity of 2, 3, 7, 8-tetrachlorodibenzo-p-dioxin: evidence for Ah-receptor-dependent and Ah-receptor-independent mechanisms of immunosuppression.* Toxicology and applied pharmacology, 1990. **105**(1): p. 26-36.

28. Schwetz, B., et al., *Toxicology of chlorinated dibenzo-p-dioxins.* Environmental health perspectives, 1973. **5**: p. 87-99.

29. Burleson, G.R., et al., *Effect of 2, 3, 7, 8-tetrachlorodibenzo-p-dioxin (TCDD) on influenza virus host resistance in mice.* Fundamental and Applied Toxicology, 1996. **29**(1): p. 40-47.

30. Kim, S.-H., et al., *Novel compound 2-methyl-2H-pyrazole-3-carboxylic acid (2-methyl-4-o-tolylazo-phenyl)-amide (CH-223191) prevents 2, 3, 7, 8-TCDD-induced toxicity by antagonizing the aryl hydrocarbon receptor.* Molecular pharmacology, 2006. **69**(6): p. 1871-1878.

31. Gray, J., et al., *Intestinal commensal bacteria mediate lung mucosal immunity and promote resistance of newborn mice to infection.* Science translational medicine, 2017. **9**(376): p. eaaf9412.

32. Lakatos, H.F., et al., *Oropharyngeal aspiration of a silica suspension produces a superior model of silicosis in the mouse when compared to intratracheal instillation.* Exp Lung Res, 2006. **32**(5): p. 181-99.

33. Lowe, C., *Effect of mothers' smoking habits on birth weight of their children*, in *Problems of Birth Defects*. 1959, Springer. p. 255-261.

34. Simpson, W.J., *A preliminary report on cigarette smoking and the incidence of prematurity.* American journal of obstetrics and gynecology, 1957. **73**(4): p. 808-815.

35. Shiono, P.H., M.A. Klebanoff, and G.G. Rhoads, *Smoking and drinking during pregnancy: their effects on preterm birth.* Jama, 1986. **255**(1): p. 82-84.

36. Zhai, J., et al., *Club cell secretory protein deficiency leads to altered lung function.* American journal of respiratory and critical care medicine, 2019. **199**(3): p. 302-312.

37. Arsalane, K., et al., *Clara cell specific protein (CC16) expression after acute lung inflammation induced by intratracheal lipopolysaccharide administration.* American journal of respiratory and critical care medicine, 2000. **161**(5): p. 1624-1630.

38. Andersson, O., et al., *Clara cell secretory protein: levels in BAL fluid after smoking cessation.* Chest, 2000. **118**(1): p. 180-182.

39. Ehrlich, A.K., et al., *TCDD, FICZ, and other high affinity AhR ligands dose-dependently determine the fate of CD4+ T cell differentiation.* Toxicological Sciences, 2018. **161**(2): p. 310-320.

40. Hines, R.N. and D.G. McCarver, *The ontogeny of human drug-metabolizing enzymes: phase I oxidative enzymes.* Journal of Pharmacology and Experimental Therapeutics, 2002. **300**(2): p. 355-360.

41. McCarver, D.G. and R.N. Hines, *The ontogeny of human drug-metabolizing enzymes: phase II conjugation enzymes and regulatory mechanisms.* Journal of Pharmacology and Experimental Therapeutics, 2002. **300**(2): p. 361-366.

42. Kastirr, I., et al., *Signal strength and metabolic requirements control cytokine-induced Th17 differentiation of uncommitted human T cells.* The Journal of Immunology, 2015. **195**(8): p. 3617-3627.

43. Zhang, L., et al., *Expression of interleukin (IL)-10, IL-17A and IL-22 in serum and sputum of stable chronic obstructive pulmonary disease patients.* COPD: Journal of Chronic Obstructive Pulmonary Disease, 2013. **10**(4): p. 459-465.

44. Yu, M., et al., *The role of interleukin-6 in pulmonary inflammation and injury induced by exposure to environmental air pollutants.* Toxicological Sciences, 2002. **68**(2): p. 488-497.

45. Van Maele, L., et al., *TLR5 signaling stimulates the innate production of IL-17 and IL-22 by CD3negCD127+ immune cells in spleen and mucosa.* The Journal of Immunology, 2010. **185**(2): p. 1177-1185.

46. Kotenko, S.V., et al., *Identification of the functional interleukin-22 (IL-22) receptor complex: the IL-10R2 chain (IL-10Rβ) is a common chain of both the IL-10 and IL-22 (IL-10-related T cell-derived inducible factor, IL-TIF) receptor complexes.* Journal of Biological Chemistry, 2001. **276**(4): p. 2725-2732.

47. Sutton, C.E., et al., *Interleukin-1 and IL-23 induce innate IL-17 production from γδ T cells, amplifying Th17 responses and autoimmunity.* Immunity, 2009. **31**(2): p. 331-341.

48. Sather, B.D., et al., *Altering the distribution of Foxp3+ regulatory T cells results in tissue-specific inflammatory disease.* The Journal of experimental medicine, 2007. **204**(6): p. 1335-1347.

49. Yogo, Y., et al., *Macrophage derived chemokine (CCL22), thymus and activation-regulated chemokine (CCL17), and CCR4 in idiopathic pulmonary fibrosis.* Respiratory research, 2009. **10**(1): p. 1-11.

50. Gebremichael, A., et al., *Ah-receptor-dependent modulation of gene expression by agedand diluted sidestream cigarette smoke.* Toxicology and applied pharmacology, 1996. **141**(1): p. 76-83.

51. U.S. Department of Health and Human Services and NIOSH, *2,3,7,8-Tetrachlorodibenzo-p-dioxin.* Current Intelligence Bulletin, Jan., 1984. **40**.

52. Mund, S.I., M. Stampanoni, and J.C. Schittny, *Developmental alveolarization of the mouse lung.* Developmental dynamics: an official publication of the American Association of Anatomists, 2008. **237**(8): p. 2108-2116.

53. Herring, M.J., et al., *Growth of alveoli during postnatal development in humans based on stereological estimation.* American Journal of Physiology-Lung Cellular and Molecular Physiology, 2014. **307**(4): p. L338-L344.

54. Lee, J.S., et al., *AHR drives the development of gut ILC22 cells and postnatal lymphoid tissues via pathways dependent on and independent of Notch.* Nature immunology, 2012. **13**(2): p. 144-151.

55. Joffin, N., et al., *Release and toxicity of adipose tissue-stored TCDD: Direct evidence from a xenografted fat model.* Environment international, 2018. **121**: p. 1113-1120.

56. Nguyen, H.M.-H., et al., *Nicotine impairs the response of lung epithelial cells to IL-22.* Mediators of inflammation, 2020. **2020**.

57. Tsuge, K., et al., *Molecular mechanisms underlying prostaglandin E2-exacerbated inflammation and immune diseases.* International immunology, 2019. **31**(9): p. 597-606.

58. Guillon, A., et al., *Neutrophil proteases alter the interleukin-22-receptor-dependent lung antimicrobial defence.* European Respiratory Journal, 2015. **46**(3): p. 771-782.

59. Mangan, P.R., et al., *Transforming growth factor-β induces development of the TH 17 lineage.* Nature, 2006. **441**(7090): p. 231-234.

60. Kimura, A., T. Naka, and T. Kishimoto, *IL-6-dependent and-independent pathways in the development of interleukin 17-producing T helper cells.* Proceedings of the National Academy of Sciences, 2007. **104**(29): p. 12099-12104.

61. Paats, M.S., et al., *Systemic CD4+ and CD8+ T-cell cytokine profiles correlate with GOLD stage in stable COPD.* European Respiratory Journal, 2012. **40**(2): p. 330-337.

62. Geraghty, P., et al., *STAT3 modulates cigarette smoke-induced inflammation and protease expression.* Frontiers in physiology, 2013. **4**: p. 267.

63. Hoh, E., et al., *Environmental tobacco smoke as a source of polycyclic aromatic hydrocarbons in settled household dust.* Environmental science & technology, 2012. **46**(7): p. 4174-4183.

64. Ferrante, G., et al., *Third-hand smoke exposure and health hazards in children.* Monaldi archives for chest disease, 2013. **79**(1).

65. Sleiman, M., et al., *Inhalable constituents of thirdhand tobacco smoke: chemical characterization and health impact considerations.* Environmental science & technology, 2014. **48**(22): p. 13093-13101.

66. Lee, Y., et al., *Intestinal Lin− c-Kit+ NKp46− CD4− Population Strongly Produces IL-22 upon IL-1β Stimulation.* The Journal of Immunology, 2013. **190**(10): p. 5296-5305.

67. Sutton, C., et al., *A crucial role for interleukin (IL)-1 in the induction of IL-17–producing T cells that mediate autoimmune encephalomyelitis.* Journal of Experimental Medicine, 2006. **203**(7): p. 1685-1691.

68. Paget, C., et al., *Interleukin-22 is produced by invariant natural killer T lymphocytes during influenza A virus infection: potential role in protection against lung epithelial damages.* Journal of Biological Chemistry, 2012. **287**(12): p. 8816-8829.

69. Sekiya, T., et al., *Inducible expression of a Th2-type CC chemokine thymus-and activation-regulated chemokine by human bronchial epithelial cells.* The Journal of Immunology, 2000. **165**(4): p. 2205-2213.

70. Alferink, J., et al., *Compartmentalized production of CCL17 in vivo: strong inducibility in peripheral dendritic cells contrasts selective absence from the spleen.* The Journal of experimental medicine, 2003. **197**(5): p. 585-599.

71. Renert-Yuval, Y., et al., *Biomarkers in atopic dermatitis-a review on behalf of the international eczema council.* Journal of Allergy and Clinical Immunology, 2021.

72. Li, A., et al., *IL-22 up-regulates β-defensin-2 expression in human alveolar epithelium via STAT3 but not NF-κB signaling pathway.* Inflammation, 2015. **38**(3): p. 1191-1200.

73. Hebert, K., et al., *Targeting the IL-22/IL-22BP axis enhances tight junctions and reduces inflammation during influenza infection.* Mucosal immunology, 2019: p. 1-11.

74. Mizoguchi, A., et al., *Clinical importance of IL-22 cascade in IBD.* Journal of gastroenterology, 2018. **53**(4): p. 465-474.

75. Sugimoto, K., et al., *IL-22 ameliorates intestinal inflammation in a mouse model of ulcerative colitis.* The Journal of clinical investigation, 2008. **118**(2): p. 534-544.

76. Sonnenberg, G.F., et al., *Pathological versus protective functions of IL-22 in airway inflammation are regulated by IL-17A.* Journal of Experimental Medicine, 2010. **207**(6): p. 1293-1305.

77. Simonian, P.L., et al., *γδ T cells protect against lung fibrosis via IL-22.* Journal of Experimental Medicine, 2010. **207**(10): p. 2239-2253.

78. Gu, P., et al., *Protective function of interleukin-22 in pulmonary fibrosis.* Clinical and translational medicine, 2021. **11**(8): p. e509.

79. El-Zayadi, A.A., et al., *Interleukin-22 drives the proliferation, migration and osteogenic differentiation of mesenchymal stem cells: a novel cytokine that could contribute to new bone formation in spondyloarthropathies.* Rheumatology, 2017. **56**(3): p. 488-493.

80. Zha, J.-M., et al., *Interleukin 22 Expands Transit-Amplifying Cells While Depleting Lgr5+ Stem Cells via Inhibition of Wnt and Notch Signaling.* Cellular and molecular gastroenterology and hepatology, 2019. **7**(2): p. 255-274.

81. Lindemans, C.A., et al., *Interleukin-22 promotes intestinal-stem-cell-mediated epithelial regeneration.* Nature, 2015. **528**(7583): p. 560.

82. Tetteh, P.W., et al., *Replacement of lost Lgr5-positive stem cells through plasticity of their enterocyte-lineage daughters.* Cell stem cell, 2016. **18**(2): p. 203-213.

83. Tadokoro, T., et al., *IL-6/STAT3 promotes regeneration of airway ciliated cells from basal stem cells.* Proceedings of the National Academy of Sciences, 2014. **111**(35): p. E3641-E3649.

84. Hasday, J.D., et al., *Bacterial endotoxin is an active component of cigarette smoke.* Chest, 1999. **115**(3): p. 829-835.

85. Mackie, R.I., A. Sghir, and H.R. Gaskins, *Developmental microbial ecology of the neonatal gastrointestinal tract.* The American journal of clinical nutrition, 1999. **69**(5): p. 1035s-1045s.

86. de Muinck, E.J. and P. Trosvik, *Individuality and convergence of the infant gut microbiota during the first year of life.* Nature communications, 2018. **9**(1): p. 1-8.

87. Gevers, D., et al., *The treatment-naive microbiome in new-onset Crohn's disease.* Cell host & microbe, 2014. **15**(3): p. 382-392.

88. Charlson, E.S., et al., *Topographical continuity of bacterial populations in the healthy human respiratory tract.* American journal of respiratory and critical care medicine, 2011. **184**(8): p. 957-963.

89. Biesbroek, G., et al., *Early respiratory microbiota composition determines bacterial succession patterns and respiratory health in children.* American journal of respiratory and critical care medicine, 2014. **190**(11): p. 1283-1292.

90. Morris, A., et al., *Comparison of the respiratory microbiome in healthy nonsmokers and smokers.* American journal of respiratory and critical care medicine, 2013. **187**(10): p. 1067-1075.

91. Carding, S., et al., *Dysbiosis of the gut microbiota in disease.* Microbial ecology in health and disease, 2015. **26**(1): p. 26191.

92. Martinez, F.D. and S. Guerra, *Early origins of asthma. Role of microbial dysbiosis and metabolic dysfunction.* American journal of respiratory and critical care medicine, 2018. **197**(5): p. 573-579.

Chapter 4

Persistent Effects of Early Life Exposure

4.1. Abstract

There is a growing awareness that several chronic diseases including COPD have origins in early life. Exposure to inhaled toxicants such as those in environmental tobacco smoke (ETS) have been shown to cause phenotypic changes through the modification of immune responses that are consistent with disease progression. We hypothesized that neonatal ETS exposure would result in altered lung pathophysiology and lung transcriptome in adulthood. We used a murine model of neonatal ETS expression with postnatal day 3 C57BL/6J mice being exposed to 1-2 mg/m^3 total particulate matter for 6 hours per day for 5 days. Mice were allowed to recover in filtered air until they reached 11-weeks. Bronchoalveolar lavage was collected for cell count and differential as well as total protein. Lavage cells and whole lung were homogenized and examined for gene expression by qPCR. We found that neonatally ETS exposed females had elevated lung macrophages and neutrophils at rest but not following LPS challenge. We found altered regulation of Cyp1A1 in the lungs of neonatally ETS exposed females and reduced B2M and GPR34 expression in the lavage cells of neonatally ETS exposed female mice. We also observed altered IL-6 and SP-B levels following neonatal ETS exposure. These findings demonstrate a lasting effect of ETS exposure during a key developmental window that may have relevance for progression to future disease states.

4.2. Introduction

Tobacco smoke exposure is among the leading preventable causes of morbidity today [1]. Tobacco use contributes to the development of cardiovascular disease, cancers, and lower respiratory disease, three of the leading causes of death in the United States and around the world. However, our understanding of the impact of tobacco smoke on human health is still evolving. A prospective longitudinal study recently demonstrated that pediatric lung function in infancy was related to maximal lung function in early adulthood [2]. It has also been suggested that reduced pulmonary function in the young is correlated to risk of development of chronic obstructive pulmonary disorder (COPD) [3].

COPD is defined as emphysema with or without chronic bronchitis [3]. While emphysema is the destruction of the alveolar septa, chronic bronchitis is the irreversible obstruction of the airways through thickening of the airway wall and mucus hypersecretion [4]. Whether significantly reduced lung function during early life is indicative of COPD development remains a topic of debate; however, the contribution of tobacco smoke to altered lung pathophysiology is well understood. Tobacco smoke induces inflammation while impairing immune responses to infection and reducing lung function through a variety of mechanisms [5]. Exposure to environmental tobacco smoke (ETS) during childhood is also associated with changes in immune function including increased rates and severity of respiratory infection [6] and increased asthma exacerbations [7] with earlier exposure typically being more detrimental. The lasting effects of neonatal ETS exposure on health in adulthood is an opportunity for further inquiry.

Studies have examined changes in the microbiome [8] and DNA methylation in children exposed to ETS [9]; however, there are few studies that examine adults neonatally exposed to ETS. Practically, a study of adults exposed to ETS during childhood may be difficult as adults may be unaware of their own exposure history, parents if still alive may be reluctant to share exposure history with their adult children, details of exposures decades in the past may be inaccurate, and tobacco use is often adopted by teenage children and young adults of smokers, which confounds

potential findings [10]. One study attempted a retrospective assessment of lung cancer risk based on self-reported exposures to tobacco smoke by activity and age [11], but the adjusted odds ratios are relatively modest at 1.08-1.57 for those exposed before age 25 and only 0.82-2.02 for those exposed to ETS before age 25. A murine model of cardiovascular disease in an apolipoprotein E knockout mouse following intrauterine or neonatal ETS exposure with assessment at 12-week-old or older found both intrauterine and neonatal ETS exposure contributed to development of atherogenesis [12]. A murine model of intrauterine ETS exposure followed by chronic exposure to ETS in adulthood starting at 11-weeks-old demonstrated that BALB/c mice have altered breathing and airways hyperresponsiveness as well as enlarged airspaces and increased collogen deposition [13].

We previously showed that neonatal ETS exposure was sufficient to induce altered lung pathophysiology and transcriptomic shifts in six-week-old adult mice (Chapter 2). We hypothesize that neonatal ETS exposure will alter the lung immune compartment and modify epithelial cell phenotype in a sex-dependent manner. To investigate the role of neonatal ETS exposure on adult lungs, we used a murine model of neonatal exposure to 1-2 mg/m^3 ETS for 6 hours/day for 5 days. Cell count and differential as well as protein concentration of bronchoalveolar lavage was evaluated along with gene expression based on top differentially regulated genes from our 6-week transcriptomics study as well as immunomodulatory markers and surfactants.

4.3. Methods

4.3.1. Animals

All experiments were performed under the auspices of the Animal Care and Use Committee of the University of California at Davis (protocols 19980 and 21794). Gestational day 8 C57BL/6J dams were purchased from the Jackson Laboratory (Sacramento, CA) and allowed to acclimate at the California National Primate Research Center for 14 days until pups were 3 days old prior to treatments. Pups were maintained with their dams until weening at postnatal day 21. As controls, five-week-old male and female C57BL/6J (000664) mice were purchased and allowed to acclimate 1 week prior to treatment.

4.3.2. Environmental Tobacco Smoke Exposures

Starting at postnatal day 3, C57BL/6J mouse pups housed with dams or six-week-old adult controls co-housed up to 4 per cage were exposed to filtered air or whole-body tobacco smoke. Exposure was performed for 6 hours/day for 5 days at a concentration of 1-2 mg/m^3 total particulate matter. Tobacco smoke was generated using a TE10 cigarette smoking machine (Teague Enterprises, Woodland, CA) with a 35-mL puff volume, a 2-second puff duration, once per minute (Federal Trade Commission smoking standard) on two 3R4F reference cigarettes (Center for Tobacco Reference Products, University of Kentucky) at a time for 10 puffs per cigarette [14]. Total suspended particles were measured twice daily during the exposure by drawing air from the exposure chamber at a known rate and collecting particulate matter on a submicron filter for 1-hour. Chamber carbon monoxide concentration was measured and recorded continuously during the week of exposure to assess consistency of exposure conditions. Following exposure, some mice were allowed to recover for 5 or 10 weeks in filtered air.

4.3.3. Oropharyngeal Aspiration of Lipopolysaccharide

Mice that were exposed to ETS or FA and allowed to recover were challenged by oropharyngeal aspiration of 0.25 μg LPS or sterile PBS and necropsied 24 hours later [15]. Briefly, mice were anesthetized by whole body exposure to 2% isoflurane in oxygen and then suspended by the cranial incisors by a silk suture tied to a slanted board. Anesthesia was maintained by continued administration of isoflurane through a nosecone. The tongue was pulled out and to the side to control the swallow reflex before 50 μL of LPS or PBS was injected into the pharynx with a micropipettor. The nose was held closed to force inhalation through the mouth. The fluid level and respiration were observed to ensure aspiration into the lungs which was accompanied with an audible crackling sound.

4.3.4. Bronchoalveolar Lavage Collection and Protein Concentration

Following exposure, mice were euthanized with an overdose of >100 mg/kg sodium pentobarbital diluted to 39 mg/mL in sterile PBS by intraperitoneal injection. The renal artery was severed, and lungs were perfused with 3 mL saline injected into the right ventricle. The trachea was cannulated, and 1 mL PBS was injected into the lungs and lavage was recovered immediately. Lavage was repeated with another 1 mL of PBS and both portions were pooled as bronchoalveolar lavage fluid (BALF).

Collected bronchoalveolar lavage was centrifuged at 300 rcf for 5 minutes at 4° C to pellet lavage cells. BALF was removed to separate tubes and stored at -80° C. Protein concentration was determined using Pierce BCA protein assay (ThernoFisher) using manufacturer's protocol. Briefly, standards and samples were added to duplicate wells with working reagent and incubated for 30 minutes at 37° C before optical density was measured at 562 nm on a microplate reader. Protein concentration of samples was calculated by subtracting the optical density of the blank and multiplying the optical density by the slope of the standard curve.

4.3.5. Bronchoalveolar Lavage Cell Count and Differential

Following exposure, mice were euthanized with an overdose of >100 mg/kg sodium pentobarbital diluted to 39 mg/mL in sterile PBS by intraperitoneal injection. The renal artery was severed, and lungs were perfused with 3 mL saline injected into the right ventricle. The trachea was cannulated, and 1 mL PBS was injected into the lungs and lavage was recovered immediately. Lavage was repeated with another 1 mL of PBS and both portions were pooled as bronchoalveolar lavage fluid (BALF).

BALF volume was measured with a serological pipet. BALF cellularity was determined by addition of 10 μL BALF to 10 μL trypan blue, and cells were counted on a Countess automated cell counter. Total BALF cells was calculated as the product of recovered volume and cell count. Cytospins were prepared by adding 100 μL BALF to a cytospin funnel and centrifuged onto slides for 5 minutes at 800 RPM in a Cytospin 4 (ThermoFisher, Waltham, MA). Slides were stained with Shandon Kwik-Diff (Thermo Shandon, Kalamazoo, MI) using manufacturer's protocol and differentials were counted by counting 300 cells per slide on an Olympus BH-2 polarizing trinocular microscope (Olympus Scientific Solutions Americas, Waltham, MA). Percent differential is the quotient of number of each type of leukocyte and total leukocytes counted. Total leukocyte differential is the product of the percent and the total BALF cells.

4.3.5 mRNA Isolation, cDNA Synthesis, and Gene Expression qPCR

Following perfusion, lungs were collected and homogenized in Trizol reagent (Invitrogen, Carlsbad, CA) using a tissue homogenizer. Extraction of mRNA was carried out according to the manufacturer's protocol. Concentration and purity of mRNA was measured on a Nanodrop ND-1000 (ThermoFisher). Reverse transcription and synthesis of 500 ng cDNA was performed using High-Capacity cDNA Reverse Transcription Kit (Applied Biosystems, Waltham, MA) in a Mastercycler Gradient thermocycler (Eppendorf, Enfield, CT). Gene expression was carried out

using TaqMan Gene Expression Master Mix (Applied Biosystems) and FAM TaqMan Gene Expression Assays in Table 1 (Applied Biosystems) on a QuantStudio 12 (Applied Biosystems) in the Primate Assay Laboratory at the California National Primate Research Center.

4.3.6. Statistical Analysis

Statistical analysis was performed using Prism 7.0 software (Graphpad, San Diego, CA). Significance was determined with one-way or two-way ANOVA or student's t-test.

4.4. Results

4.4.1. Neonatal ETS exposure results in increased immune cell abundance in the resting lungs of female mice

Exposure to environmental tobacco smoke (ETS) has been reported to acutely increase the number of circulating immune cells, particularly neutrophils, in adults acutely following exposure [16]. While data on pediatric populations is limited, a study on infant rhesus monkeys showed a decrease in cytokines related to type 1 immune responses commonly mounted against viral infections following intrauterine and neonatal ETS exposure [17]. We investigated the impact of neonatal ETS exposure in adulthood using a murine model. Postnatal day 3 mice were exposed to ETS at 1-2 mg/m^3 for 6 hours/day for 5 days or filtered air and then allowed to recover in filtered air for 10 weeks. At 11-weeks, mice were given 0.25 μg LPS or saline vehicle by oropharyngeal aspiration and lavage taken 24 hours later. The concentration of cells in neonatally ETS exposed female mice with vehicle was significantly higher than that of male mice (Figure 1A); however, this increased frequency was not maintained in LPS challenged mice (Figure 1B). The total number of lavage cells was calculated as the product of the concentration of cells in and the volume of lavage fluid. The total number of immune cells recovered by lavage in neonatally ETS exposed female mice was significantly higher than that of filtered air control females and all male mice following vehicle challenge (Figure 1C). This increase was despite a small but significant lower recover volume in the lavage fluid among neonatally ETS exposed mice (Supplemental Figure 1A). LPS challenge resulted in no differences by sex or exposure (Figure 1D). One potential explanation for differences in immune cell frequency in the lungs of female mice could be reduced tight junction integrity leading to increase extravasation. Tobacco smoke has been shown to reduce tight junction proteins and increase permeability of the epithelial layer by reducing transforming growth factor beta [18]. We measured lavage protein concentration to assess if there may be lasting differences in epithelial function. Female mice exposed to filtered air and challenged with LPS had an increase in lavage protein concentration compared to vehicle

challenged females that did not achieve statistical significance (Figure 1E). Neonatally ETS challenged females had significantly higher lavage protein following LPS challenge than vehicle challenged males and an increase over vehicle challenged females that did not reach statistical significance (Figure 1F); however, there was no difference between exposure groups. This shows a persistent imbalance in lung immune cells in neonatally ETS exposed females in adulthood.

4.4.2 Neonatally ETS exposed female mice have elevated lavage macrophages and neutrophils in the absence of LPS challenge.

Sex differences in the number and type of immune cells in the lungs have been shown [19]. To better understand the effect of neonatal ETS exposure on adult lung immune constitution, we performed a cell differential on cytospin slides prepared from lavage fluid recovered from vehicle or LPS challenged adult mice. There were no differences in percentages of lymphocytes, macrophages, or neutrophils between exposure groups (Supplemental Figure 2), but the percentage of macrophages was significantly lower and the percentage of neutrophils significantly higher in all groups following LPS challenge compared to vehicle challenge with no sex-dependent differences (Supplemental Figure 2C-F). Total cell differential was calculated as the product of the percent differential and the number of recovered cells. Neonatally ETS exposed female mice had significantly elevated macrophages following vehicle challenge compared to filtered air controls and male mice (Figure 2A), but there was no difference between groups following LPS challenge (Figure 2B). Interestingly, the total number of lavage macrophages in neonatally ETS exposed females was lower following LPS challenge than vehicle challenge. Neonatally ETS exposed female mice also had elevated numbers of neutrophils following vehicle challenge compared to filtered air control females (Figure 2C) while there was no difference between exposure groups following LPS challenge (Figure 2D). There were no differences in lymphocytes between exposure groups following either vehicle (Supplemental Figure 2G) or LPS challenge (Supplemental Figure 2H). This data shows an increase in the basal number of

macrophages and neutrophils in the lungs of female mice in adulthood following neonatal ETS exposure.

4.4.3. Neonatally ETS exposed female mice have elevated cyp1a1 in the lung tissue compared to their male littermates

We have previously shown altered gene transcription in the lungs of adult mice at 6-weeks-old following neonatal ETS exposure (Chapter 2). These included several Hallmark and KEGG pathways that were related to immune function with sex-dependent differences. Since neonatal ETS exposure has resulted in increased immune cells in the lungs of female mice, we examined several of the top differentially expressed genes in lung tissue by qPCR. In whole lung tissue, we examined expression of cytochrome P450 family 1 subfamily A member 1 (Cyp1A1), beta-2 microglobulin (B2M), cluster of differentiation 63 (CD63), G-protein-coupled receptor 34 gene (GPR34), and histocompatibility 2 class II antigen A beta 1 (H2-Ab1). Control exposed mice showed no difference in Cyp1A1 expression by sex or challenge (Figure 3A). Neonatally ETS exposed female mice had significantly elevated Cyp1A1 expression in lung tissue compared to males following vehicle challenge, and LPS challenge resulted in a significant reduction in Cyp1A1 gene expression in neonatally ETS exposed females (Figure 3B). LPS challenge resulted in lower Cyp1A1 expression in ETS exposed mice compared to vehicle challenge (Supplemental Figure 4B) and compared to control mice challenged with LPS (Supplemental Figure 4D). B2M expression in control males increased following LPS challenge (Supplemental Figure 3A). In vehicle challenged mice, neonatal ETS exposure resulted in reduced CD63 compared to control mice (Supplemental Figure 4S). No other differences in CD63, H2-Ab1, or GPR34 were seen in the lung tissue between groups (Supplemental Figure 3-4). These findings indicated that some differences in gene expression following neonatal ETS challenge occur in the airway resident cells and not the lung parenchyma.

4.4.4. Neonatal ETS exposure alters beta-2 microglobulin and G-protein-coupled receptor 34 expression in the airways of females

Neonatal ETS exposure has been shown to alter immune responses in the lungs during early life including increasing some immune cell frequencies [20]. To investigate if the changes in transcriptomics we had previously noted were due to changes in the immune compartment in airways, bronchoalveolar lavage cells were homogenized in Trizol and total RNA was extracted for qPCR. Beta-2 microglobulin expression was increased following LPS challenge in neonatally ETS exposed mice (Figure 4A) but not control mice (Supplemental Figure 5A). B2M expression was also lower in neonatally ETS exposed mice compared to controls following vehicle challenge (Figure 4B). In female mice, LPS challenge resulted in increased B2M gene expression in both control (Figure 4C) and neonatally ETS exposed mice compared to vehicle challenge (Figure 4D), but neonatally ETS exposed females had lower B2M gene expression than control females following both vehicle (Figure 4E) and LPS challenge (Figure 4F). There were no differences in B2M expression between control and neonatally ETS exposed males (Supplemental 5C-F). This demonstrates a sex-dependent response of B2M following neonatal ETS exposure.

Expression of CD63 was significantly upregulated following LPS challenge in neonatally ETS exposed (Supplemental Figure 5H) but not control mice (Supplemental Figure 5G). However, female control mice had significantly increased CD63 following LPS challenge (Supplemental Figure 5K), and neonatally ETS exposed female mice had a trend toward increased CD63 following LPS challenge (Supplemental Figure 5L). There were not significant differences in CD63 between exposure groups following vehicle (Supplemental Figure 5I) or LPS challenge (Supplemental Figure 5J) or in females following vehicle (Supplemental Figure 5M) or LPS challenge (Supplemental Figure 5N). There were no significant differences in H2-Ab1 expression between exposure groups or by sex (Supplemental Figure 5Q-Z). Unfortunately, recovery and processing of mRNA from lavage cells resulted in insufficient samples to perform qPCR for a number of male samples,

Expression of GPR34 was lower in LPS challenged control (Figure 4G) and neonatally ETS exposed mice (Figure 4H), and neonatally ETS exposed mice had lower GPR34 expression

following both vehicle (Figure 4I) and LPS challenge (Figure 4J). Female mice also showed reduced expression of GPR34 following LPS challenge in both control (Figure 4K) and neonatal ETS exposure groups (Figure 4L). There were trends toward reduced GPR34 expression in lavage cells of neonatally ETS exposed female adult mice following both vehicle (Figure 4M) and LPS challenge (Figure 4N). These findings show sex-dependent regulation of immune-related genes in the airway cells of adult mice exposed to ETS during the neonatal period.

4.4.5 Neonatal ETS exposure alters expression of inflammatory signals and surfactants

Finally, we wanted to investigate inflammatory signals expressed following neonatal exposure to ETS. IL-6 has been reported to be important in induction of epithelial damage in a rat model of ETS exposure [21]. We found IL-6 to be significantly elevated in airways of neonatally ETS exposed mice in adulthood compared to filtered air controls following vehicle challenge (Figure 5A). C-X-C motif chemokine ligand 1 (CXCL1) and C-X-C motif chemokine ligand 2 (CXCL2) were upregulated following LPS challenge in all exposure groups (Chapter 2). Expression of both CXCL1 (Figure 5B) and CXCL2 (Figure 5C) was significantly higher in control mice following LPS compared to vehicle challenge with trend toward being higher in control mice compared to neonatally ETS exposed mice following LPS challenge.

Surfactant proteins are important for pulmonary function, and some have immunomodulatory roles [22]. To understand if changes persist from neonatal exposure to ETS, qPCR was performed on samples from whole lungs. There were no sex-dependent changes to surfactant protein A, C, or D (SP-A, SP-C, and SP-D, respectively) due to LPS challenge (Supplemental Figure 6). Neonatally ETS exposed female mice had reduced surfactant protein B (SP-B) following LPS challenge compared to vehicle challenge (Supplemental Figure 6D). SP-A was significantly reduced following LPS challenge (Supplemental Figure 6R) but not vehicle challenge (Supplemental Figure 6Q) in neonatally ETS challenged compared to control mice. SP-B was significantly lower following LPS challenge in neonatally ETS exposed mice compared to vehicle challenge (Supplemental Figure 6L). SP-B was also lower in neonatally ETS challenged

mice compared to control mice following vehicle (Supplemental Figure 6S) and LPS challenge (Supplemental Figure 6T). SP-C was significantly lower following LPS challenge in neonatally ETS exposed mice compared to vehicle challenge (Supplemental Figure 6N), but no significant differences between neonatally ETS exposed, and control mice were detected (Supplemental Figure 6U-V). SP-D was significantly increased following LPS challenge compared to vehicle challenge in control mice (Supplemental Figure 6O), but no other differences were observed between exposure groups (Supplemental Figure 6P, W-X). These findings show a sex-dependent alteration in SP-B in neonatally ETS exposed female mice that persists into adulthood.

4.5. Discussion

We show that neonatal exposure to environmental tobacco smoke (ETS) results in persistent increases in lung macrophages and neutrophils without immune challenge in female mice during adulthood 10 weeks post-exposure. We demonstrate reduction of Cyp1A1 in the lung parenchyma following LPS challenge in female mice following neonatal ETS exposure. Further we present sex-dependent alterations in B2M and GRP34 expression in airway immune cells in female mice following neonatal ETS exposure. Changes in cytokines IL-6, CXCL1, and CXCL2 exist in neonatally ETS exposed mice into adulthood without sex dependence. Finally, we find that SP-B expression is altered in adult female mice exposed to ETS during the neonatal period compared to control female mice.

Altered immune cell populations in the lungs following tobacco smoke exposure has been previously observed. Exposure to ETS in human adults increases the number of circulating leukocytes in the blood and increases the chemotactic potential of neutrophils to N-formylmethionyl-leucyl-phenylalanine [16]. Another study of ETS exposure showed that females exposed to ETS had an acute reduction of sex hormones 17b-estradiol and progesterone after just one hour of exposure [23]. Changes in lavage cells in pediatric patients exposed to tobacco smoke are difficult to determine due to the invasive nature of lavage and ethical concerns with pediatric exposure to inhaled toxicants. A study in rhesus monkeys showed that intrauterine and early neonatal exposure to ETS induces increased monocytes, eosinophils, and lymphocytes in the lungs at 2.5 months of age [20]. Importantly they also noted that the phagocytic capacity of alveolar macrophages was reduced following ETS exposure. A murine study of prenatal mainstream tobacco smoke exposure demonstrated a reduction in cytotoxic lymphocyte activity in male mice that resulted in increased susceptibility to tumor formation when injected with a murine cutaneous t cell lymphoma in males at 5 weeks of age [24]. While spleenocyte populations were found to not differ by sex or treatment groups, there was no assessment of pulmonary immune populations. This study ultimately introduces a different exposure model from ours in that

all the exposures occurred in utero which precluded the inhalation of ETS toxicants directly by the pups. However, exposure to thirdhand tobacco smoke from the fur of the dam cannot be excluded as a postnatal exposure in their study and is one that likely occurs in our experiments as well. Increased macrophages with altered morphology in the lungs of smokers has long observed [25]. And subsequent studies have shown numerous changes in cytokine production, cell-surface markers, replication, and activity in macrophages from smokers compared to non-smokers [26]. Our study did not delve into the many differences between macrophages of smokers and non-smokers. One drawback is that most studies of macrophage alterations are following chronic tobacco smoke exposure or assess changes in current smokers or immediately following exposure. It would be interesting if these changes persist for many weeks post exposure; however, the short duration of our exposure and the long recovery period make this protocol unlikely to generate the robust changes to macrophage populations we see in active smokers.

We noted that Cyp1A1 is significantly reduced in female mice challenged with LPS following neonatal ETS exposure. Cyp1A1 is a phase 1 detoxification enzyme that is important for removal of toxicants including polycyclic aromatic hydrocarbons and has also been implicated in generation of oxidation products [27]. Previous work has shown that placental Cyp1A1 is elevated by maternal smoking in humans [28]; however, a rat model has shown that pulmonary Cyp1A1 is not changed in utero but inducible during the neonatal period by exposure to tobacco smoke [29]. A report that examined Cyp1A1 expression in normal human bronchial epithelial cells in vitro found that estrogen receptor alpha signaling modulated Cyp1A1 expression in conjunction with cigarette smoke extract but not alone [30]. A murine model of combined aryl hydrocarbon receptor agonist benzo-[*a*]-pyrene and LPS exposure showed a repression of Cyp1A1 in the combined exposure that correlated with increased DNA adducts due to persistence of the toxicant [31]. What the effect of reduced Cyp1A1 in our model needs further examination. One possible mechanism for reduction of Cyp1A1 is induction of transforming growth factor beta related SMAD family member 3 or hypoxia inducible factor 1 alpha, both of which have been shown to lead to

dissociation of the aryl hydrocarbon receptor-aryl hydrocarbon receptor nuclear translocator complex that is important for Cyp1A1 expression [32]. In addition to the major role as a phase 1 detoxification enzyme, Cyp1A1 has also been shown to be protective against oxidative damage from hyperoxia such as due to oxygen therapy [33]. Whether Cyp1A1 is protective or inflammatory can be viewed as context dependent and is worth further consideration following toxicant exposures due to concerns about the half-life of toxicants and storage of lipophilic compounds such as aryl hydrocarbon receptor agonist in adipose tissues.

We found B2M were reduced in neonatally ETS exposed female but not mice in adulthood. B2M is an integral part of the major histocompatibility complex I family that is expressed on all nucleated cells and has prognostic value in several cancers including multiple myeloma and some other blood cancers as well as renal failure [34]. Given that B2M is part of every nucleated cell, expression of B2M is generally stable. Investigation into the B2M is often related to its role in end stage renal disease [35] or immune evasion by viral-infected or cancer cells [36]. B2M is essential for major histocompatibility class I recognition by cytotoxic lymphocytes and as a negative regulator of natural killer cells [37]. However, cytomegalovirus has been shown to bind B2M and use envelope bound B2M to assist in infection of cells *in vitro* [36]. Importantly, nuclear factor kappa B (NFκB) and interferon regulatory factors 1, 2, 4, and 8 play a role in transcriptional activation of B2M expression in leukocytes [38]. As our mice are specific pathogen free, it is unlikely that cancer or viral infection are sex-dependent drivers of altered B2M expression following neonatal ETS exposure. It would be interesting to see if there are changes in expression of B2M regulatory factors at such a later timepoint following ETS exposure. A rat model of exposure to 80 mg/m^3 but not 30 mg/m^3 or filtered air resulted in significant reduction in NFκB subunits and increased apoptosis [39]. The same group showed perinatal exposure to levels of ETS used in our study also suppressed NFκB in infant rhesus monkeys [40]. A separate group investigated the role of tobacco smoke on NFκB in human peripheral blood and found induction of NFκB in low-pressure but not high-pressure exposure to cigarette smoke [41].

We also observed decreased expression of GPR34 in female mice following neonatal ETS exposure. GPR34 was discovered in 1999 based on sequence similarity to platelet-activating factor [42]. GPR34 is highly expressed in immune cells, and assessment of GPR34-knockout mice show increased migratory potential, altered osmotic regulation in glial cells, increased delayed type hypersensitivity following methyl-bovine serum albumin injection, and increased tumor necrosis factor alpha, interferon gamma, interleukin 2, interleukin 5, and interleukin 10 but not interleukin 1 beta at baseline and following challenge with methyl-bovine serum albumin [43]. Importantly GPR34 deficient mice were also shown to be more susceptible to inhaled pathogen *C. neoformans* in the lung and peripheral organs and had altered migration of monocytes and macrophages in the spleen following methyl-bovine serum albumin challenge. The ligand for GPR34 has been proposed to be lysophosphatidylserine, but there has been significant disagreement in the literature regarding the validity of this finding. One study found that the serine residue was essential for GRP34 recognition of the ligand and that phospholipase A1 activity is important for conversion of lysophosphatidylserine to 2-acyl-lysophosphatidylserine [44]. Interestingly a study on the regulation of GPR34 in murine dendritic cells found that NFκB, mitogen activated protein kinase (MAPK), and apoptosis signaling pathways are important and that NFκB and MAPK pathways downregulate GPR34 [45]. Further, GPR34 deficient cells had higher apoptosis rates. In our experiments, neonatally ETS exposed females had reduced GPR34 compared to filtered air controls and the number of macrophages paradoxically decreased following LPS challenge in the neonatally ETS exposed females. A partial deficiency in GPR34 induced by their exposure in a sex-dependent manner may be able to explain this phenomenon. There remains little information regarding GPR34 with only one paper referring to even the monitoring of GPR34 in tobacco smoke exposure [42]. The cited paper does not mention regulation of GPR34 as we understand it today in their data [46].

Interleukin 6 is serves as an inflammatory cytokine with various roles in the immune response and homeostasis [47]. While chronically elevated IL-6 can be pathogenic in

autoimmunity, IL-6 deficiency is a negative indicator in acute respiratory distress syndrome in an IL-6 knockout murine model with increased cellular infiltration and more rapid deterioration of elastance during mechanical ventilation and LPS challenge [48]. In a murine model of ETS exposure, IL-6 knockout mice had reduced cellular proliferation in the terminal bronchioles and alveoli following a combined ETS and ozone exposure but also did not have reduced club cell secretory protein following ETS or ozone exposures in contrast to wild-type mice [21]. An observational study of influenza infection in smokers, subjects exposed to secondhand smoke, and unexposed control subjects found that nasal IL-6 protein was inversely correlated to serum cotinine and influenza RNA in nasal cells [49]. These data suggest positive roles for IL-6 in respiratory immunity that is negatively regulated by tobacco smoke exposure. Our data shows increased IL-6 levels in vehicle challenged neonatally ETS exposed mice during adulthood. Whether this alters responses to viral or bacterial infections is unknown. It is well understood that children exposed to ETS have increased severity and frequency of respiratory infections [50]. However, there is an opportunity for further research on adults that were exposed to ETS as children and how they continue to respond to respiratory infections. Emerging research has shown that childhood pulmonary function is predictive of maximal lung function in early adulthood with increased risk for pulmonary diseases of aging related to alterations in pediatric lung function [2, 3].

We also observed persistent differences in expression of SP-B in neonatally ETS exposed female mice compared to adult controls. SP-B is an essential component of the lung lining fluid and important for organizing lamellar bodies in alveolar type II cells and tubular myelin in lung lining fluid [51]. Expression of SP-B is regulated by hepatocyte nuclear family member transcription factors in a cell type specific manner and in conjunction with thyroid transcription factor 1 [52, 53]. More recently it was reported that cell-cell contacts are important for mediating SP-B expression through improving mRNA stability [54]. This finding could be relevant for some disease models in which tight junction proteins downregulated. We did not assess tight junction

proteins in our study, but ETS exposure has been implicated in the regulation of cellular attachment in previous studies [55]. A murine model of partial SP-B deficiency indicates that altering expression in non-uniform patterns results in increased SP-C and morphologically abnormal lamellar bodies in SP-B deficient cells along with increased airspaces and increased residual volumes indicating chronic SP-B deficiency may result in changes to lung structure and function [56]. Congenital deficiency of SP-B is lethal in the neonatal period, and reduction in SP-B production in an inducible mouse model resulted in reversible severe respiratory failure accompanied by inflammation with increased IL-6, IL-1β, and MIP-2 [57]. We do not see a significant change in behavior or well-being that might be indicated by respiratory distress, so despite the observation of reduced SP-B in our animals it seems to remain a manageable level. SP-B is reduced in LPS-induced acute lung injury in mice [58], which is relevant to this study. We exposed mice to ETS during the neonatal period which includes inhalation of LPS in tobacco smoke [59]. Exposure to LPS has been shown to alter subsequent responses to LPS [60], and SP-B expression was significantly reduced in the lungs of neonatally ETS exposed mice following LPS challenge.

Neonatal ETS exposure remains a significant burden with millions of children exposed every year in the United States and nearly 80% of children being routinely exposed in some countries [61, 62]. Understanding the long-term impact of childhood exposure to ETS beyond will be important for allocating healthcare resources and guiding policies for future control efforts. The overwhelmingly negative impacts of tobacco usage are well understood, yet tobacco usage remains stubbornly high [63]. Emerging inhalation exposures also pose the risk of undoing the good done through tobacco mitigation as rates of vaping climb in young never-smokers and wildland-urban interface fires expose people to combinations of combustion products previously only common among firefighters [64]. While the sources and composition of these exposures may be novel, there is reason to believe many classes of chemicals are similar between some exposures.

4.6. Figures and Tables

Figure 1:

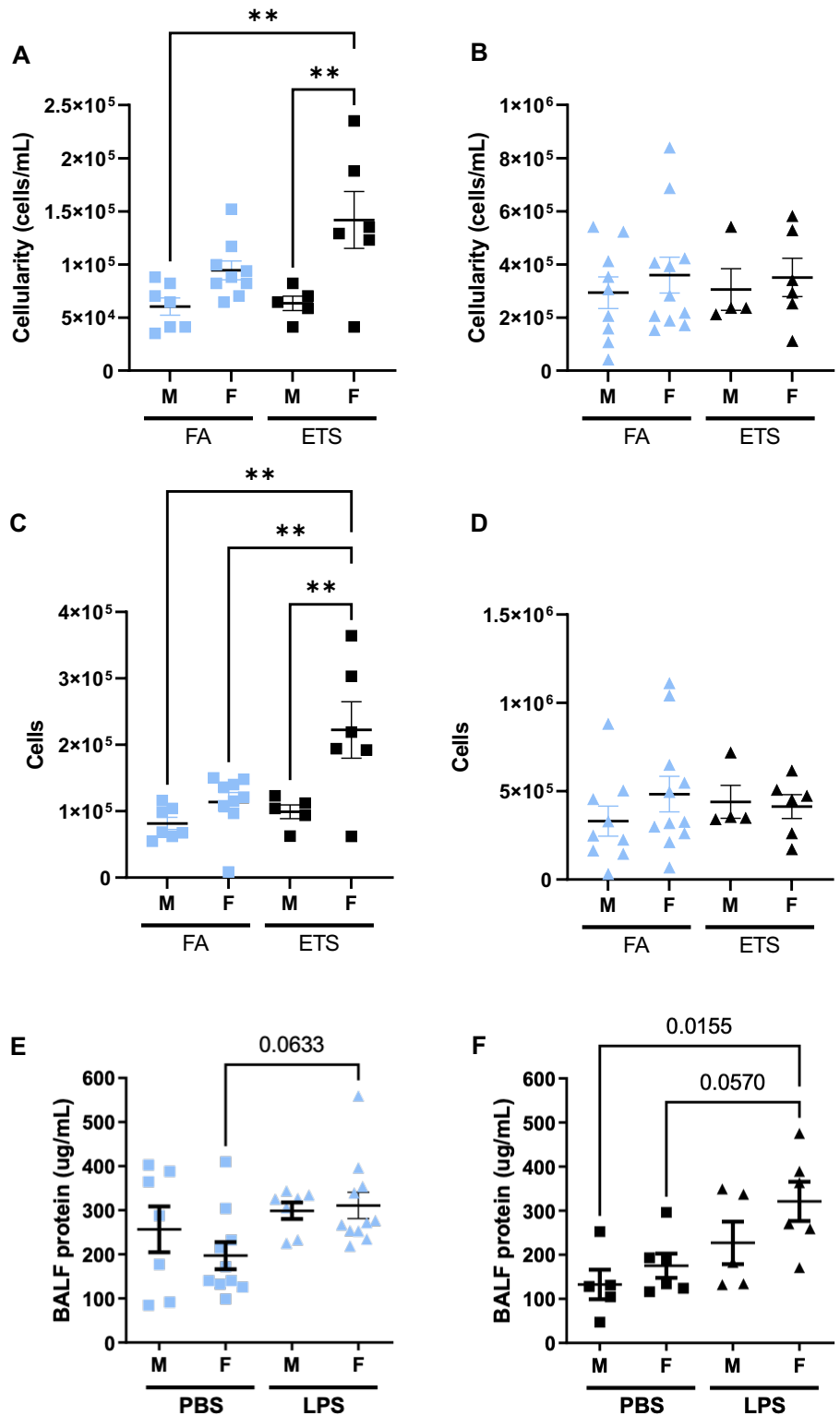

Figure 1: Neonatal ETS exposure alters the density and number of immune cells in the bronchoalveolar lavage fluid during adulthood in a sex-dependent manner. Postnatal day 3 C57BL/6J mice were exposed to ETS or filtered air for 6 hours per day until postnatal day 7 and allowed to recover in filtered air for 10 weeks. Mice were challenged with 0.25 μg LPS in 50 μL PBS or vehicle 24 hours prior to euthanasia. The frequency of cells per volume of BALF was determined in **A)** mice challenged with vehicle only and **B)** mice challenged with LPS. The total number of cells was calculated as the product of frequency per volume and volume of BALF. Total BALF cells were calculated for **C)** vehicle challenged and **D)** LPS challenged mice. Total protein in the bronchoalveolar lavage fluid was determined by BCA assay in **E)** vehicle challenged and **F)** LPS challenged mice. * $p<0.05$, ** $p<0.01$, *** $p<0.001$, **** $p<0.0001$ by ANOVA with Tukey post-hoc correction for multiple comparisons.

Figure 2:

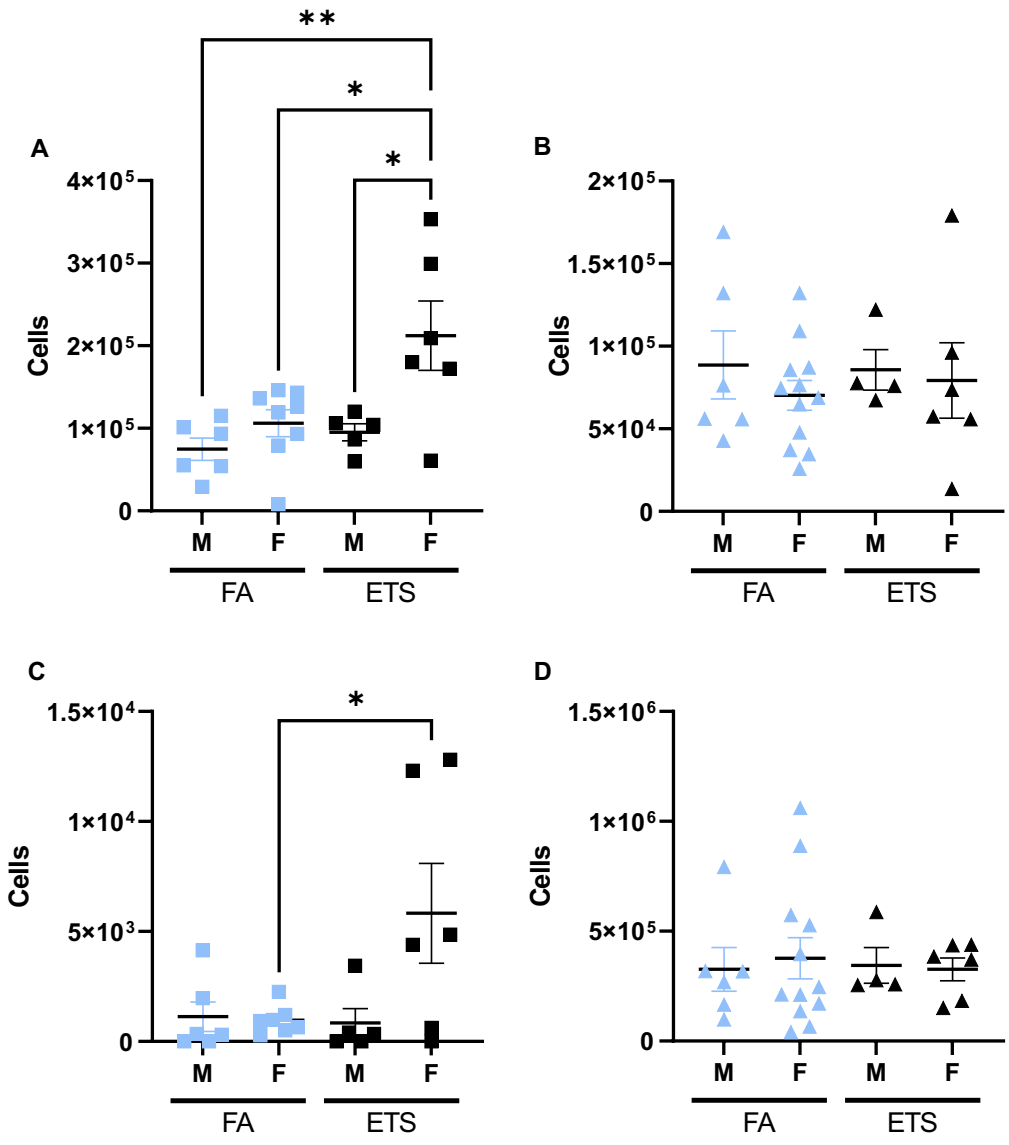

Figure 2: Neonatal ETS exposure induces increased abundance of neutrophils and macrophages in a sex-dependent manner. Cell differentials were counted from stained cytospin slides and total cell differentials were calculated as the product of percent cell frequency and total lavage cells. Macrophages in BALF from **A)** vehicle and **B)** LPS challenged and neutrophils in BALF from **C)** vehicle and **D)** LPS challenged mice were determined. * $p<0.05$, ** $p<0.01$, *** $p<0.001$, **** $p<0.0001$ by ANOVA with Tukey post-hoc correction for multiple comparisons.

Figure 3:

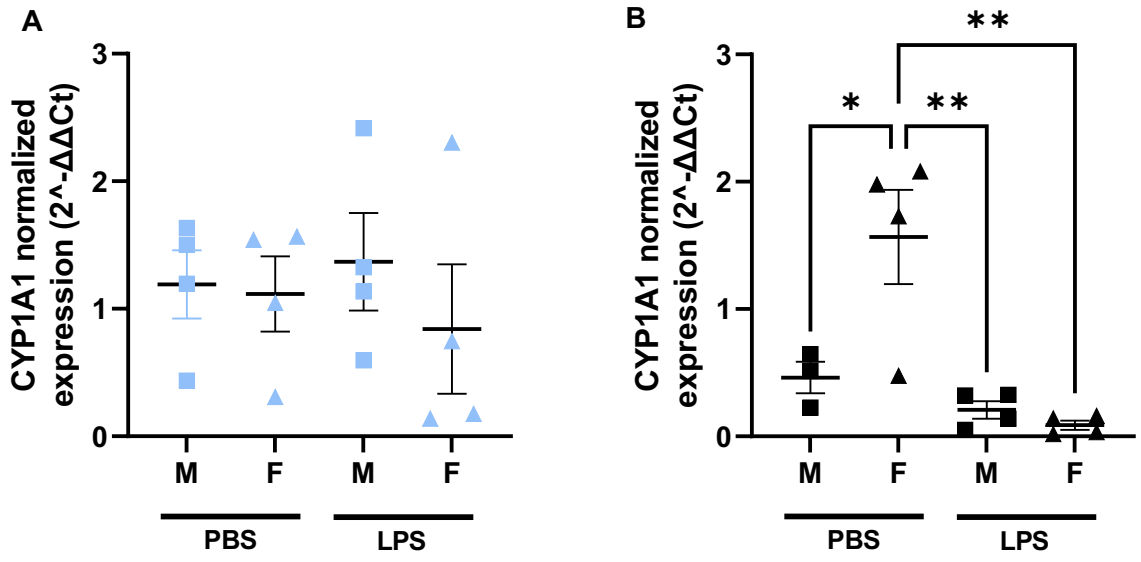

Figure 3: Neonatal ETS exposure induces differential gene expression in lung tissue in adulthood. Postnatal day 3 mice were exposed to 1-2 mg/m^3 ETS of filtered air for 6 hours/day for 5 days and then allowed to recover in filtered air for 10 weeks. Mice were challenged with oropharyngeal aspiration of saline or 0.25 μg LPS 24 hours prior to euthanasia. Lungs were perfused and lavaged, and whole lungs were homogenized in Trizol for RNA extraction. Expression of genes selected from transcriptomic sequencing of 6-week-old animals were assessed in **A)** vehicle and **B)** LPS challenged mice. * $p<0.05$, ** $p<0.01$, *** $p<0.001$, **** $p<0.0001$ by ANOVA with Tukey post-hoc correction for multiple comparisons.

Figure 4:

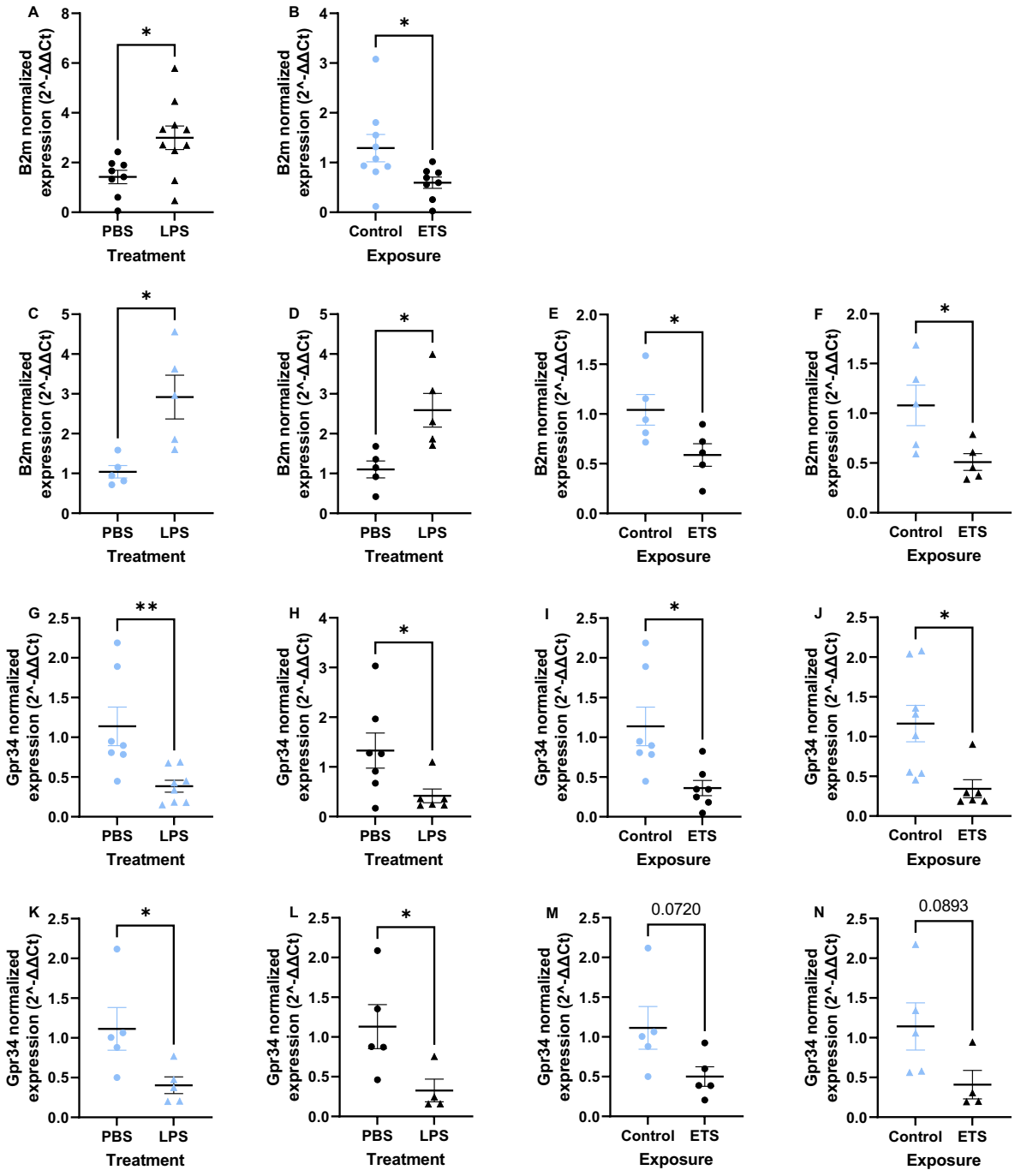

Figure 4: Neonatal ETS exposure induces differential gene expression in lavage cells in adulthood. Postnatal day 3 mice were exposed to 1-2 mg/m^3 ETS of filtered air for 6 hours/day for 5 days and then allowed to recover in filtered air for 10 weeks. Mice were challenged with oropharyngeal aspiration of saline or 0.25 μg LPS 24 hours prior to euthanasia. Lungs were

perfused and lavaged, and lavage cells were homogenized in Trizol for RNA extraction. Expression of genes selected from transcriptomic sequencing of 6-week-old animals were assessed. Beta-2 microglobulin gene expression in neonatally ETS exposed mice challenged with vehicle or LPS **A)** and in vehicle challenged mice neonatally exposed to filtered air or ETS **B)**. Female mice had differenced in B2M expression between vehicle and LPS challenge in neonatal control **C)** and ETS exposed mice **D)** as well as in vehicle **E)** and LPS challenged mice between control and neonatal ETS exposed groups **F)**. G-protein-coupled receptor 34 gene expression in control **G)** and neonatally ETS exposed mice challenged with vehicle or LPS **H)** as well as in vehicle challenged **I)** and LPS challenge mice neonatally exposed to filtered air or ETS **J)**. Female mice had differenced in GPR34 expression between vehicle and LPS challenge in neonatal control **K)** and ETS exposed mice **L)** as well as in vehicle **M)** and LPS challenged mice between control and neonatal ETS exposed groups **N)**. * $p<0.05$, ** $p<0.01$, *** $p<0.001$, **** $p<0.0001$ by student's t-test.

Figure 5:

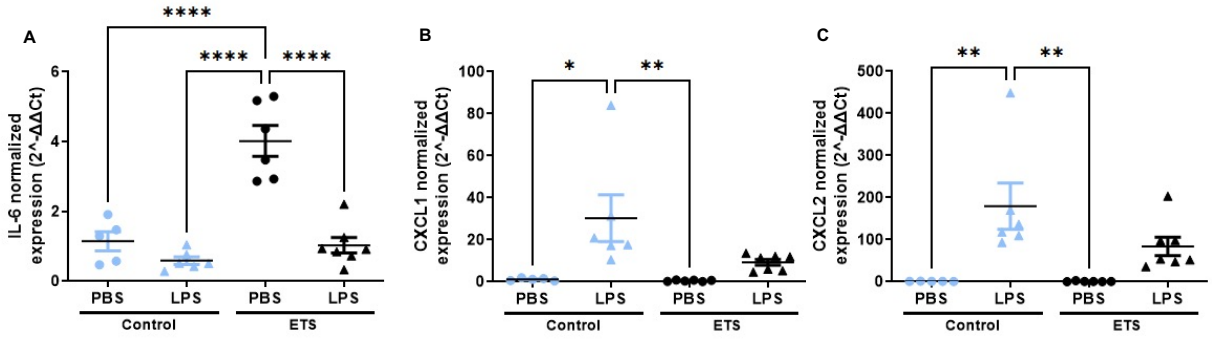

Figure 5: Expression of inflammatory mediators in the airways is altered in adulthood following neonatal ETS exposure. Expression of top inflammatory mediators were assessed by qPCR in the lavage cells of mice neonatally exposed to ETS or filtered air 10 weeks post exposure. IL-6 **A)**, CXCL1 **B)**, and CXCL2 **C)** were assessed. * $p<0.05$, ** $p<0.01$, *** $p<0.001$, **** $p<0.0001$ by ANOVA with Tukey post-hoc correction for multiple comparisons.

Table 1: Taqman probes used for gene expression experiments

Gene	Assay ID
GAPDH	Mm99999915_g1
Cyp1A1	Mm00487218_m1
B2M	Mm00437762_m1
GPR34	Mm02620221_s1
H2-Ab1	Mm00439216_m1
CD63	Mm01966817_g1
IL-6	Mm00446190_m1
CXCL1	Mm04207460_m1
CXCL2	Mm00436450_m1
SP-A1	Mm00499170_m1
SP-B	Mm00455678_m1
SP-C	Mm00488144_m1
SP-D	Mm00486060_m1

4.7. Supplementary Figures

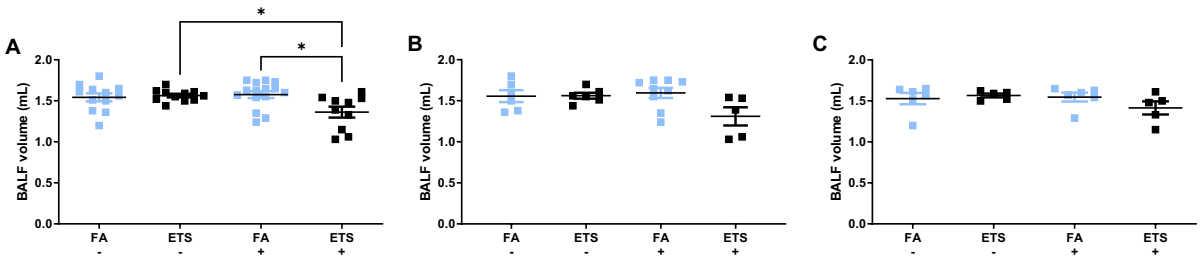

Supplemental Figure 1: Characterization of bronchoalveolar lavage volume and protein concentration. A) Bronchoalveolar lavage volumes from all mice within each treatment group. BALF volumes divided by **B)** female and **C)** male. * $p<0.05$, ** $p<0.01$, *** $p<0.001$, **** $p<0.0001$ by ANOVA with Tukey post-hoc correction for multiple comparisons.

Supplemental Figure 2:

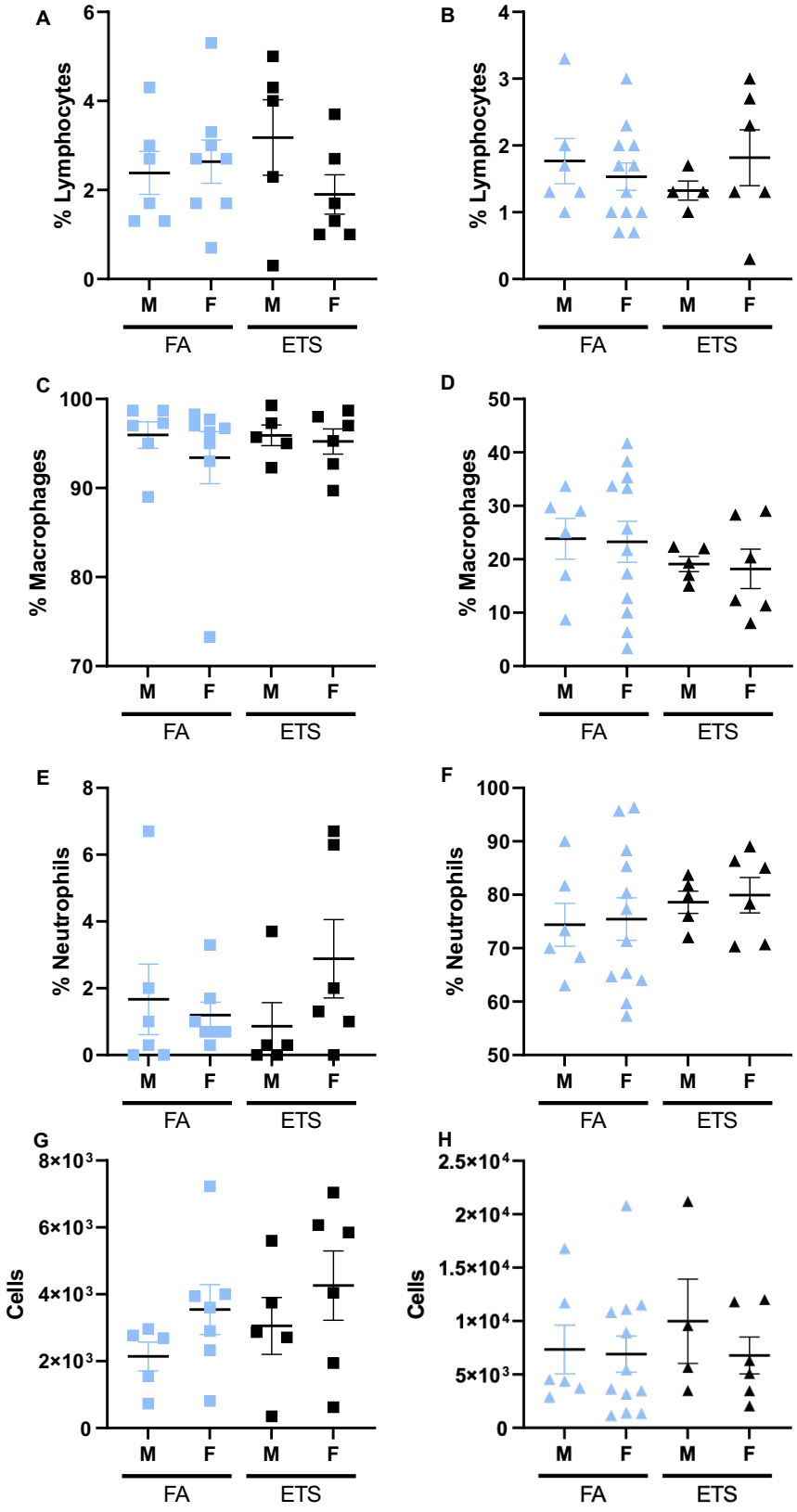

Supplemental Figure 2: Postnatal day 3 mice were exposed to 1-2 mg/m^3 ETS of filtered air for 6 hours/day for 5 days and then allowed to recover in filtered air for 10 weeks. Mice were challenged with oropharyngeal aspiration of saline or 0.25 μg LPS 24 hours prior to euthanasia. Bronchoalveolar lavage was collected, and cell differential performed by counting cell types on cytospin slides. Percent lymphocytes in vehicle **A)** and LPS challenged mice **B)**. Percent macrophages in vehicle **C)** and LPS challenged mice **D)**. Percent neutrophils in vehicle **E)** and LPS challenged mice **F)**. The total number of lymphocytes was calculated as the product of the total number of lavage cells and the percent lymphocytes in vehicle **G)** and LPS challenged mice **H)**. * $p<0.05$, ** $p<0.01$, *** $p<0.001$, **** $p<0.0001$ by ANOVA with Tukey post-hoc correction for multiple comparisons.

Supplemental Figure 3:

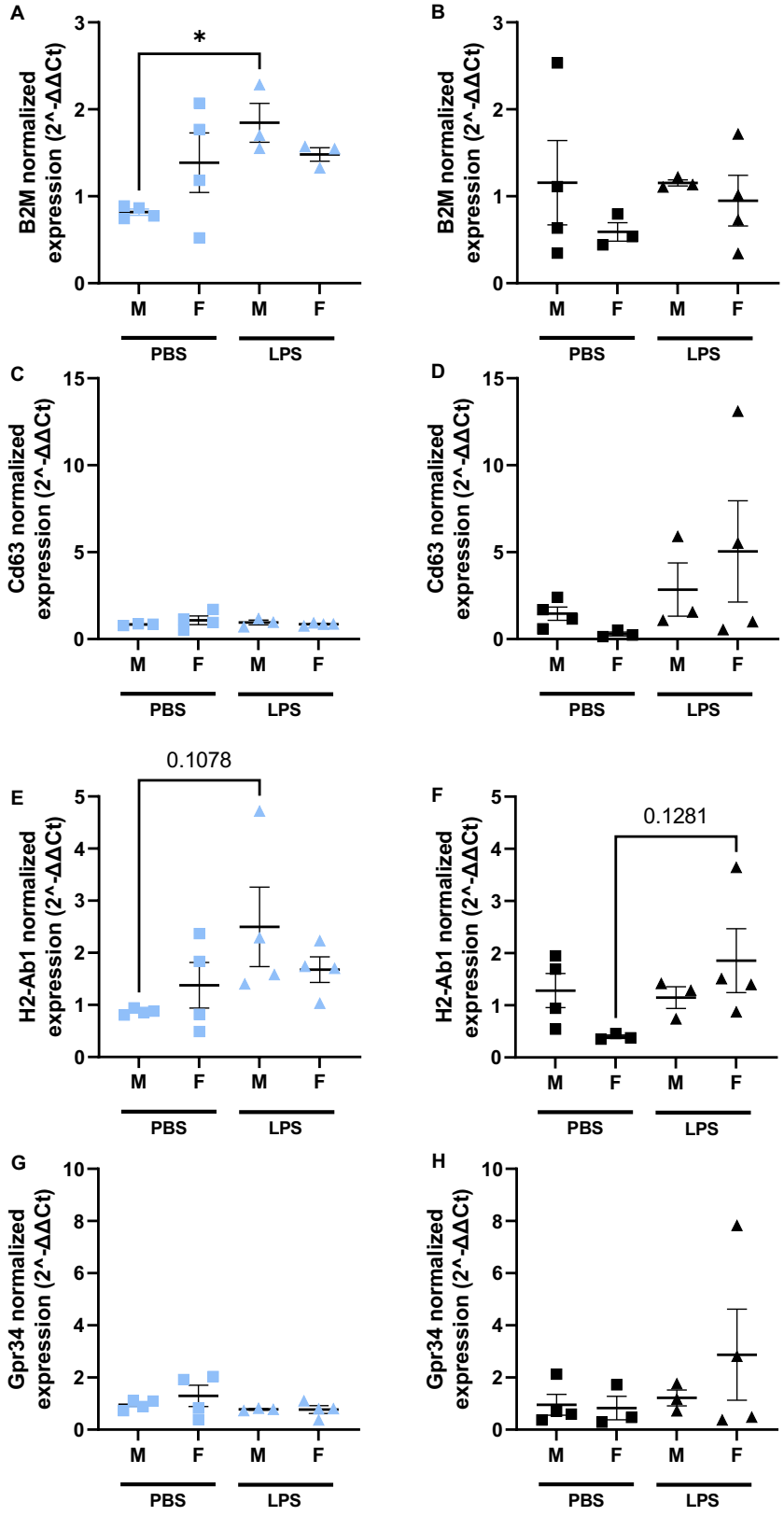

Supplemental Figure 3: The effect of neonatal ETS exposure on gene expression in lung tissue in adulthood. Postnatal day 3 mice were exposed to 1-2 mg/m^3 ETS of filtered air for 6 hours/day for 5 days and then allowed to recover in filtered air for 10 weeks. Mice were challenged with oropharyngeal aspiration of saline or 0.25 μg LPS 24 hours prior to euthanasia. Lungs were perfused and lavaged, and whole lungs were homogenized in Trizol for RNA extraction. Expression of genes selected from transcriptomic sequencing of 6-week-old animals were assessed: Beta-2-microglobulin in **A)** vehicle and **B)** LPS challenged mice, cluster of differentiation 63 in **C)** vehicle and **D)** LPS challenged mice, histocompatibility 2, class II antigen A, beta 1 in **E)** vehicle and **F)** LPS challenged mice, and G-protein coupled receptor 34 in **G)** vehicle and **H)** LPS challenged mice. * $p<0.05$, ** $p<0.01$, *** $p<0.001$, **** $p<0.0001$ by ANOVA with Tukey post-hoc correction for multiple comparisons.

Supplemental Figure 4:

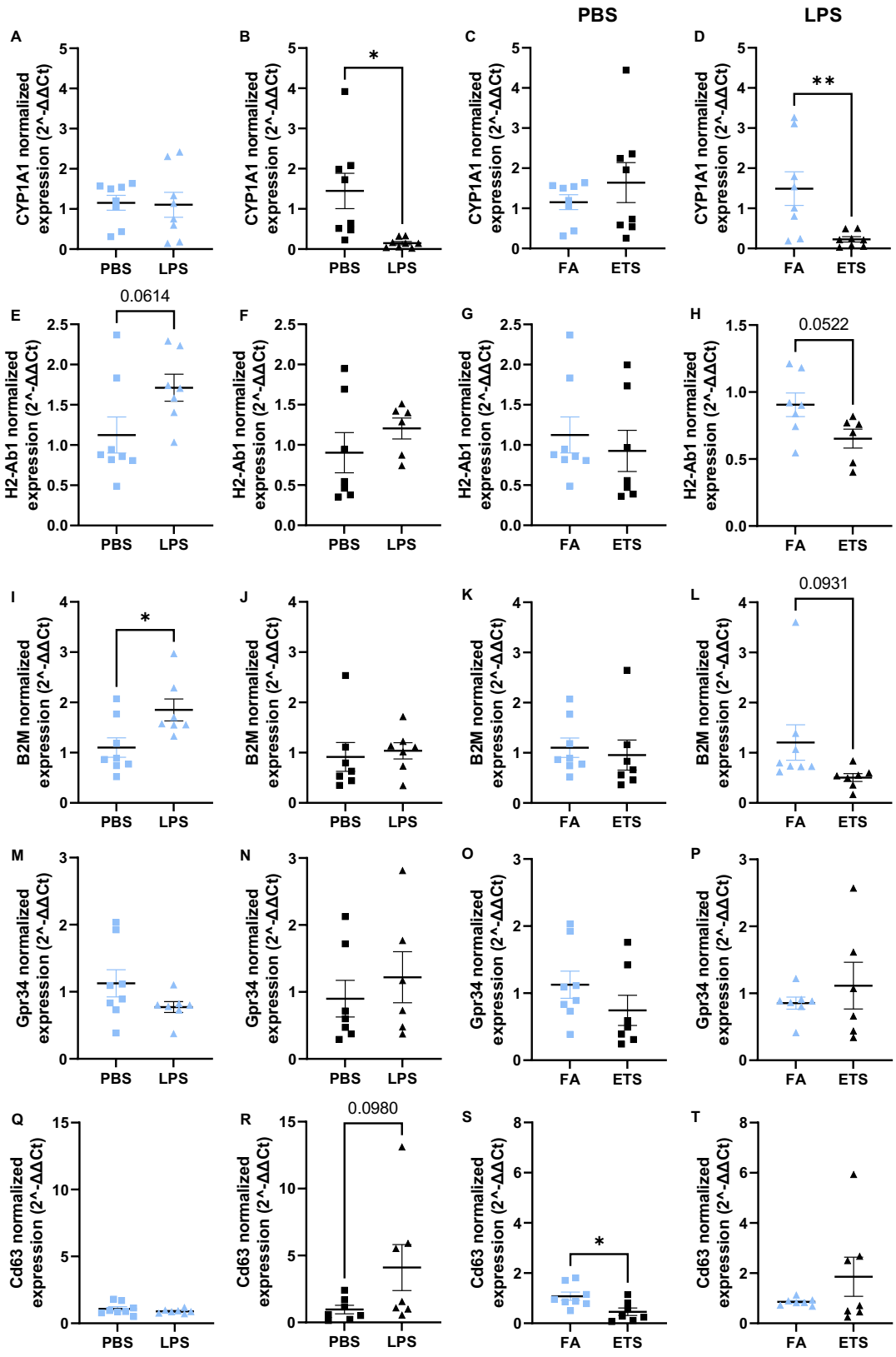

Supplemental Figure 4: Neonatal ETS exposure alters gene expression in lung tissue in adulthood. Postnatal day 3 mice were exposed to 1-2 mg/m^3 ETS of filtered air for 6 hours/day for 5 days and then allowed to recover in filtered air for 10 weeks. Mice were challenged with oropharyngeal aspiration of saline or 0.25 μg LPS 24 hours prior to euthanasia. Lungs were perfused and lavaged, and whole lungs were homogenized in Trizol for RNA extraction. Expression of genes selected from transcriptomic sequencing of 6-week-old animals were assessed. Cyp1a1 expression was determined in control **A)** and ETS exposed mice **B)** due to LPS challenge. Cyp1a1 expression was compared between control and ETS mice with vehicle **C)** and LPS challenge **D)**. Histocompatibility 2, class II antigen A, beta 1 expression was determined in control **E)** and ETS exposed mice **F)** due to LPS challenge. H2-Ab1 expression was compared between control and ETS mice with vehicle **G)** and LPS challenge **H)**. Beta-2-microglobulin expression was determined in control **I)** and ETS exposed mice **J)** due to LPS challenge. Beta-2-microglobulin expression was compared between control and ETS mice with vehicle **K)** and LPS challenge **L)**. G-protein coupled receptor 34expression was determined in control **M)** and ETS exposed mice **N)** due to LPS challenge. G-protein coupled receptor 34expression was compared between control and ETS mice with vehicle **O)** and LPS challenge **P)**. Cluster of differentiation 63 expression was determined in control **Q)** and ETS exposed mice **R)** due to LPS challenge. CD63 expression was compared between control and ETS mice with vehicle **S)** and LPS challenge **T)**. * $p<0.05$, ** $p<0.01$, *** $p<0.001$, **** $p<0.0001$ by student's t-test.

Supplemental Figure 5:

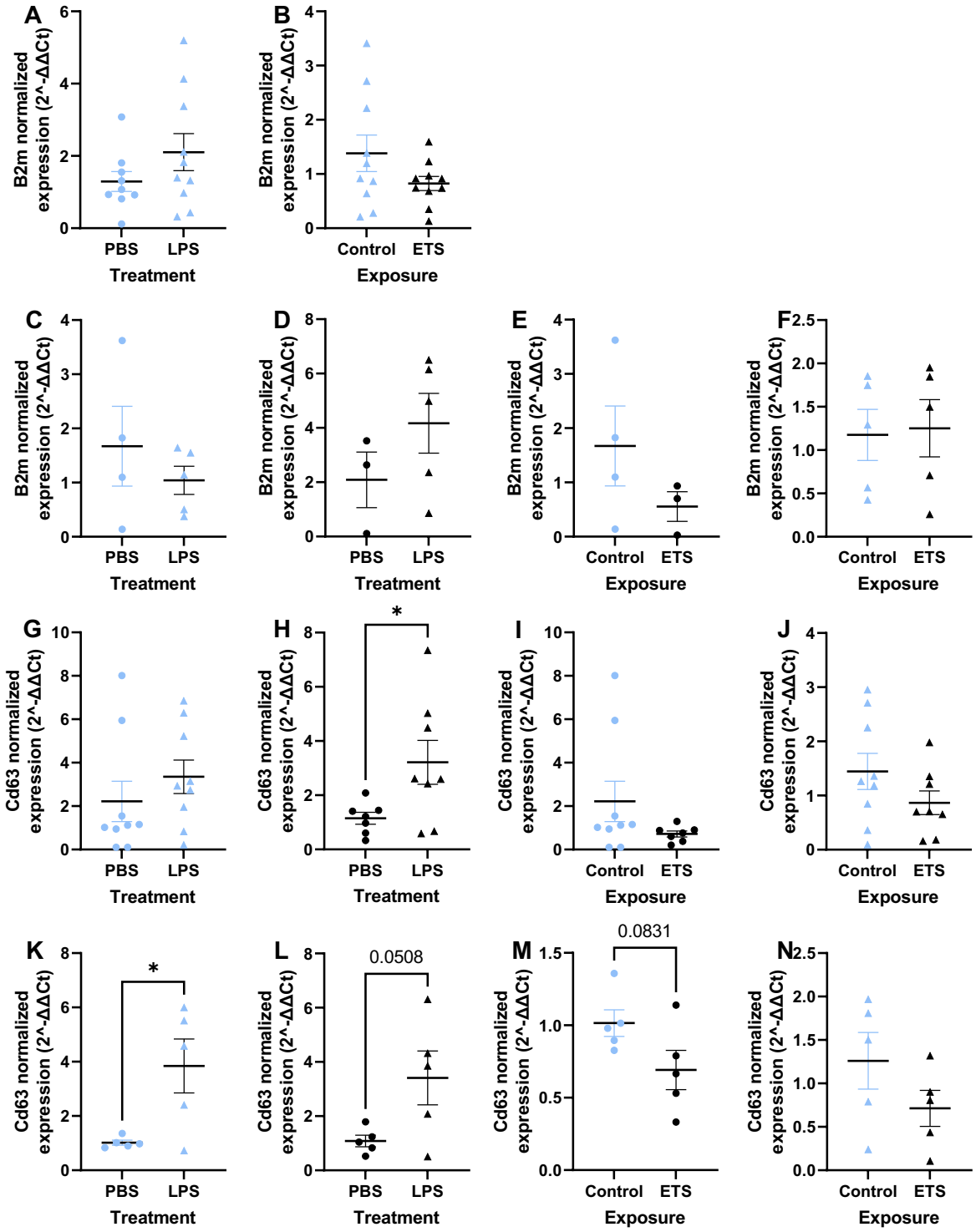

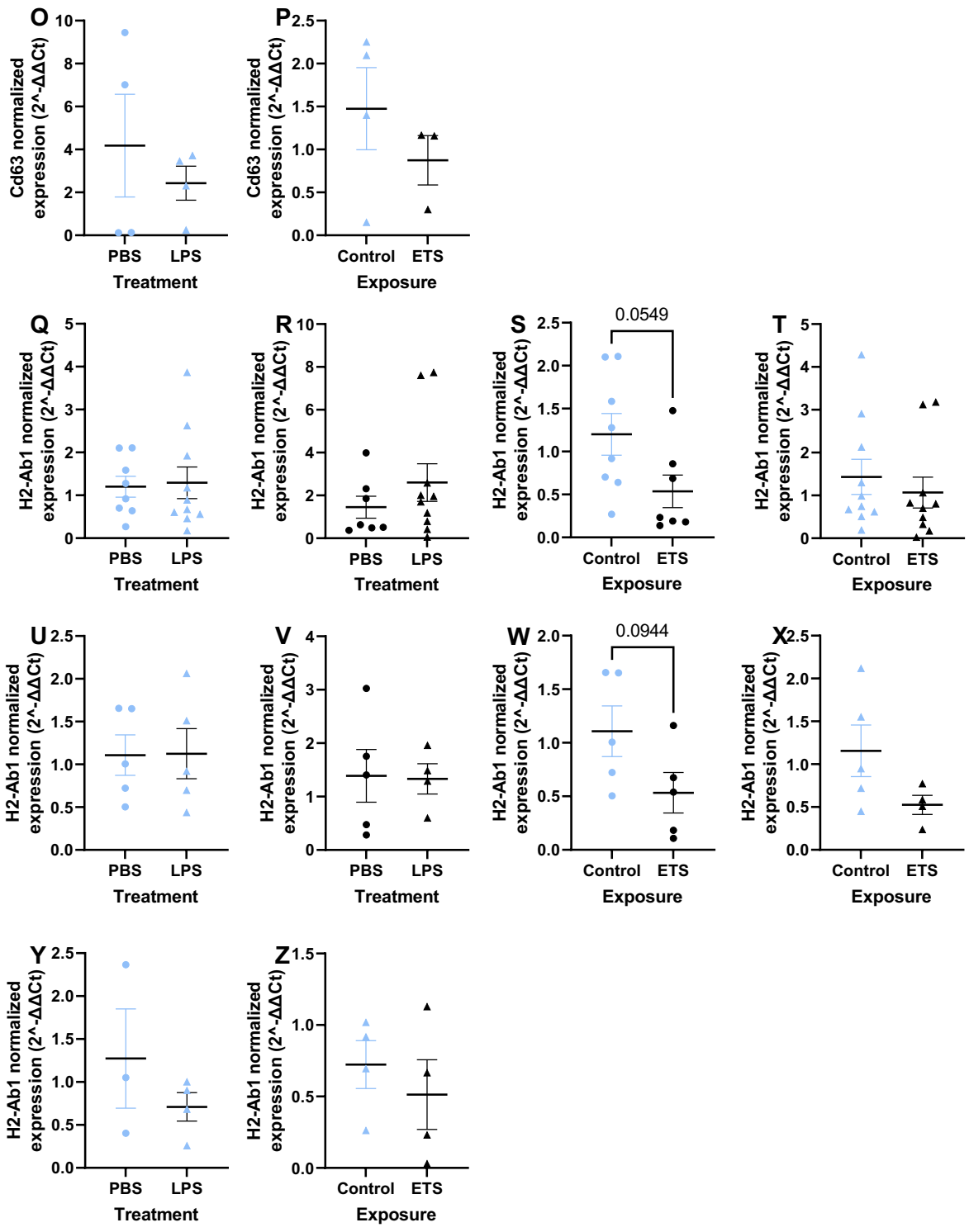

Supplemental Figure 5: Neonatal ETS exposure alters gene expression in airway cells in adulthood. Postnatal day 3 mice were exposed to 1-2 mg/m^3 ETS of filtered air for 6 hours/day for 5 days and then allowed to recover in filtered air for 10 weeks. Mice were challenged with

oropharyngeal aspiration of saline or 0.25 μg LPS 24 hours prior to euthanasia. Lungs were perfused and lavaged, and lavage cells were homogenized in Trizol for RNA extraction. Expression of genes selected from transcriptomic sequencing of 6-week-old animals were assessed. Expression of B2M in control mice by challenge group **A)** and LPS challenged mice by exposure group **B)**. B2M expression in male control **C)** neonatally ETS exposed mice **D)** by challenge as well as vehicle **E)** and LPS challenged mice by exposure **F)**. Expression of cluster of differentiation 63 in control **G)** and neonatally ETS exposed mice **H)** as well as between control and ETS exposed mice following vehicle **I)** and LPS challenge **J)**. Expression of CD63 in female control **K)** and neonatally ETS exposed mice **L)** as well as between control and ETS exposed female mice following vehicle **M)** and LPS challenge **N)**. Expression of CD63 in male control mice **O)** and LPS challenged control and neonatally ETS exposed males **P)**. Histocompatibility 2, class II antigen A, beta 1 gene expression in control **Q)** and neonatally ETS exposed mice **R)** as well as between control and ETS exposed mice following vehicle **S)** and LPS challenge **T)**. H2-Ab1 in female control **U)** and neonatally ETS exposed mice **V)** as well as between control and ETS exposed mice following vehicle **W)** and LPS challenge **X)**. Expression of H2-Ab1 in male control mice **Y)** and LPS challenged control and neonatally ETS exposed males **Z)**. * $p<0.05$, ** $p<0.01$, *** $p<0.001$, **** $p<0.0001$ by student's t-test.

Supplemental Figure 6:

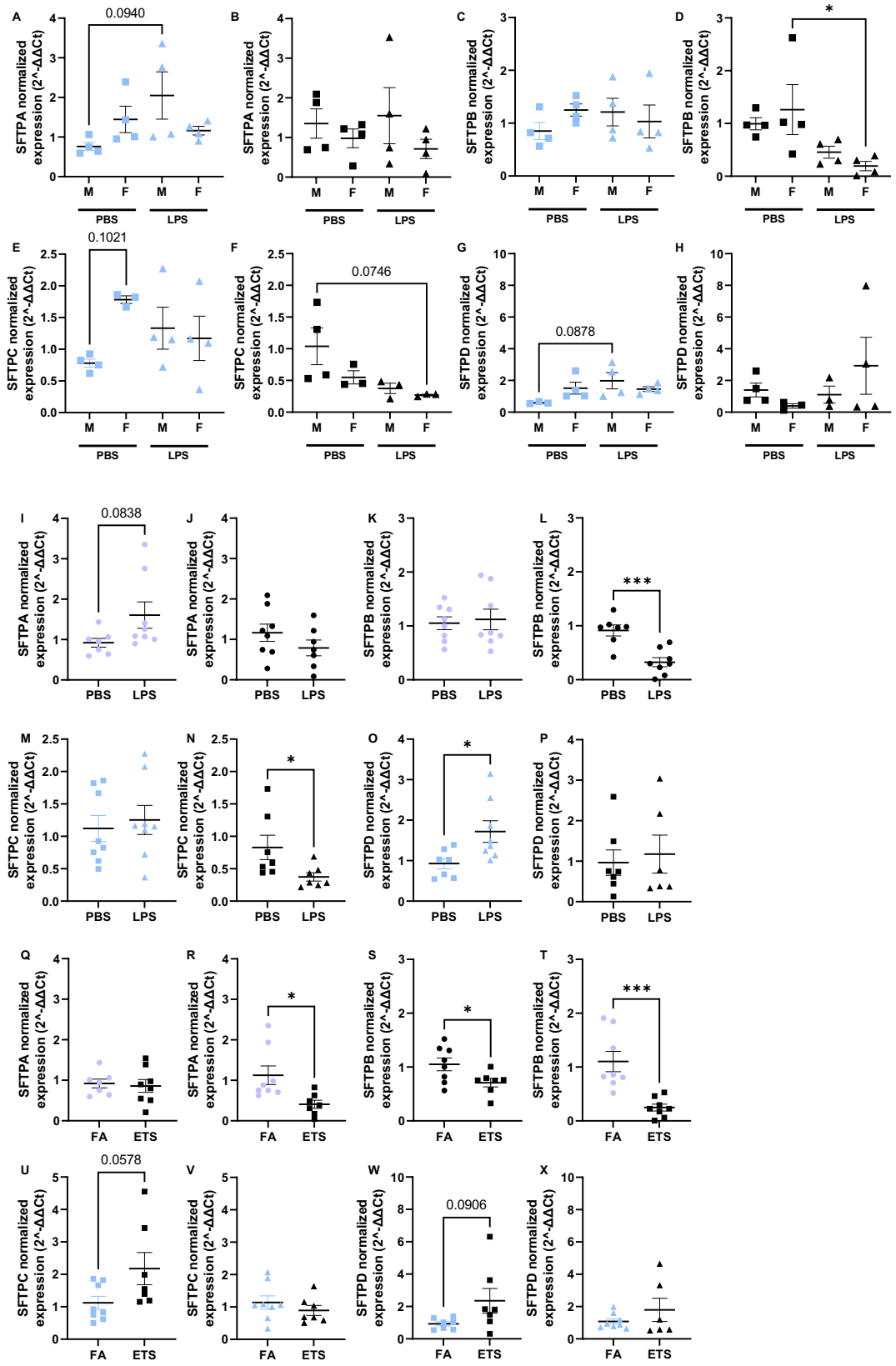

Supplemental Figure 6: Effect of neonatal ETS exposure on expression of pulmonary surfactants in adulthood by sex. Gene expression was carried out on RNA extracted from whole lung homogenate of 11-week-old mice. Expression of surfactant protein A in control **A)** and neonatally ETS exposed mice **B)**. Expression of surfactant protein B in control **C)** and neonatally ETS exposed mice **D)**. Expression of surfactant protein C in control **E)** and neonatally ETS exposed mice **F)**. Expression of surfactant protein D in control **G)** and neonatally ETS exposed mice **H)**. Expression of SP-A in combined male and female control **I)** and neonatally ETS exposed mice **J)**. Expression of SP-B in combined male and female control **K)** and neonatally ETS exposed mice **L)**. Expression of SP-C in combined male and female control **M)** and neonatally ETS exposed mice **N)**. Expression of SP-D in combined male and female control **O)** and neonatally ETS exposed mice **P)**. Expression of SP-A in combined male and female vehicle **Q)** and LPS challenged mice **R)**. Expression of SP-B in combined male and female vehicle **S)** and LPS challenged mice **T)**. Expression of SP-C in combined male and female vehicle **U)** and LPS challenged mice **V)**. Expression of SP-D in combined male and female vehicle **W)** and LPS challenged mice **X)**. * $p<0.05$, ** $p<0.01$, *** $p<0.001$, **** $p<0.0001$ by ANOVA with Tukey post-hoc correction for multiple comparisons or student's t-test.

4.8. References

1. McRobbie, H. and B. Kwan, *Tobacco use disorder and the lungs.* Addiction, 2021. **116**(9): p. 2559-2571.
2. Stern, D.A., et al., *Poor airway function in early infancy and lung function by age 22 years: a non-selective longitudinal cohort study.* The Lancet, 2007. **370**(9589): p. 758-764.
3. Soriano, J.B., F. Polverino, and B.G. Cosio, *What is early COPD and why is it important?* European Respiratory Journal, 2018. **52**(6).
4. Janson, C., et al., *Bronchodilator reversibility in asthma and COPD: findings from three large population studies.* European Respiratory Journal, 2019. **54**(3).
5. West, R., *Tobacco smoking: Health impact, prevalence, correlates and interventions.* Psychology & health, 2017. **32**(8): p. 1018-1036.
6. DiFranza, J.R., et al., *Systematic literature review assessing tobacco smoke exposure as a risk factor for serious respiratory syncytial virus disease among infants and young children.* BMC pediatrics, 2012. **12**(1): p. 1-16.
7. Gilliland, F.D., Y.-F. Li, and J.M. Peters, *Effects of maternal smoking during pregnancy and environmental tobacco smoke on asthma and wheezing in children.* American journal of respiratory and critical care medicine, 2001. **163**(2): p. 429-436.
8. Elwany, S., M.A. Gamea, and I. Talaat, *Passive smoking induces nasal biofilms in children.* International Journal of Pediatric Otorhinolaryngology, 2021. **146**: p. 110755.
9. Breton, C.V., et al., *Prenatal tobacco smoke exposure affects global and gene-specific DNA methylation.* American journal of respiratory and critical care medicine, 2009. **180**(5): p. 462-467.
10. DiFranza, J.R., et al., *Tobacco Use Disorder: A Family Disease.* Journal of addiction medicine, 2016. **10**(3): p. 143-147.
11. Asomaning, K., et al., *Second hand smoke, age of exposure and lung cancer risk.* Lung cancer, 2008. **61**(1): p. 13-20.

12. Fetterman, J.L., et al., *Developmental exposure to second-hand smoke increases adult atherogenesis and alters mitochondrial DNA copy number and deletions in apoE−/− mice.* PloS one, 2013. **8**(6): p. e66835.

13. Xiao, R., et al., *In utero exposure to second-hand smoke aggravates adult responses to irritants: adult second-hand smoke.* American journal of respiratory cell and molecular biology, 2012. **47**(6): p. 843-851.

14. Teague, S.V., et al., *Sidestream cigarette smoke generation and exposure system for environmental tobacco smoke studies.* Inhalation toxicology, 1994. **6**(1): p. 79-93.

15. Lakatos, H.F., et al., *Oropharyngeal aspiration of a silica suspension produces a superior model of silicosis in the mouse when compared to intratracheal instillation.* Exp Lung Res, 2006. **32**(5): p. 181-99.

16. Anderson, R., et al., *Passive Smoking by Humans Sensitizes Circulating Neutrophils1-3.* Am Rev Respir Dis, 1991. **144**: p. 570-574.

17. Wang, L., et al., *Effects of environmental tobacco smoke exposure on pulmonary immune response in infant monkeys.* Journal of allergy and clinical immunology, 2008. **122**(2): p. 400-406. e5.

18. Schamberger, A.C., et al., *Cigarette smoke-induced disruption of bronchial epithelial tight junctions is prevented by transforming growth factor-β.* Am J Respir Cell Mol Biol, 2014. **50**(6): p. 1040-52.

19. Melgert, B.N., et al., *Macrophages: regulators of sex differences in asthma?* American journal of respiratory cell and molecular biology, 2010. **42**(5): p. 595-603.

20. Yu, M., et al., *Perinatal environmental tobacco smoke exposure alters the immune response and airway innervation in infant primates.* Journal of Allergy and Clinical Immunology, 2008. **122**(3): p. 640-647. e1.

21. Yu, M., et al., *The role of interleukin-6 in pulmonary inflammation and injury induced by exposure to environmental air pollutants.* Toxicological Sciences, 2002. **68**(2): p. 488-497.

22. Akella, A. and S.B. Deshpande, *Pulmonary surfactants and their role in pathophysiology of lung disorders.* Indian J Exp Biol, 2013. **51**(1): p. 5-22.

23. Flouris, A.D., et al., *Sexual dimorphism in the acute effects of secondhand smoke on thyroid hormone secretion, inflammatory markers and vascular function.* American Journal of Physiology-Endocrinology and Metabolism, 2008. **294**(2): p. E456-E462.

24. Ng, S.P., et al., *Effects of prenatal exposure to cigarette smoke on offspring tumor susceptibility and associated immune mechanisms.* Toxicological sciences, 2006. **89**(1): p. 135-144.

25. Pratt, S.A., et al., *A comparison of alveolar macrophages and pulmonary surfactant (?) obtained from the lungs of human smokers and nonsmokers by endobronchial lavage.* The Anatomical Record, 1969. **163**(4): p. 497-507.

26. Strzelak, A., et al., *Tobacco smoke induces and alters immune responses in the lung triggering inflammation, allergy, asthma and other lung diseases: a mechanistic review.* International journal of environmental research and public health, 2018. **15**(5): p. 1033.

27. Costa, C., et al., *Exposure of human skin to benzo [a] pyrene: role of CYP1A1 and aryl hydrocarbon receptor in oxidative stress generation.* Toxicology, 2010. **271**(3): p. 83-86.

28. Boden, A., et al., *Human placental cytochrome P450 and quinone reductase enzyme induction in relation to maternal smoking.* Reproduction, fertility and development, 1995. **7**(6): p. 1521-1524.

29. Lee, C.Z., et al., *Effect of in utero and postnatal exposure to environmental tobacco smoke on the developmental expression of pulmonary cytochrome P450 monooxygenases.* Journal of biochemical and molecular toxicology, 2000. **14**(3): p. 121-130.

30. Han, W., et al., *Estrogen receptor α increases basal and cigarette smoke extract-induced expression of CYP1A1 and CYP1B1, but not GSTP1, in normal human bronchial epithelial cells.* Molecular Carcinogenesis: Published in cooperation with the University of Texas MD Anderson Cancer Center, 2005. **44**(3): p. 202-211.

31. Arlt, V.M., et al., *Pulmonary inflammation impacts on CYP1A1-mediated respiratory tract DNA damage induced by the carcinogenic air pollutant benzo [a] pyrene.* Toxicological Sciences, 2015. **146**(2): p. 213-225.

32. Nakano, N., et al., *Dissociation of the AhR/ARNT complex by TGF-β/Smad signaling represses CYP1A1 gene expression and inhibits benze [a] pyrene-mediated cytotoxicity: Negative regulation of CYP1A1 gene by TGF-β/Smad signaling.* Journal of Biological Chemistry, 2020. **295**(27): p. 9033-9051.

33. Lingappan, K., et al., *Mice deficient in the gene for cytochrome P450 (CYP) 1A1 are more susceptible than wild-type to hyperoxic lung injury: evidence for protective role of CYP1A1 against oxidative stress.* Toxicological Sciences, 2014. **141**(1): p. 68-77.

34. Bethea, M. and D. Forman, *Beta 2-microglobulin: its significance and clinical usefulness.* Annals of Clinical & Laboratory Science, 1990. **20**(3): p. 163-168.

35. Kazama, J.J., H. Maruyama, and F. Gejyo, *Reduction of circulating beta2-microglobulin level for the treatment of dialysis-related amyloidosis.* Nephrol Dial Transplant, 2001. **16 Suppl 4**: p. 31-5.

36. Grundy, J., *Role of β2-Microglobulin in Cytomegalovirus Infection.* Scandinavian Journal of Rheumatology, 1990. **19**(sup87): p. 98-101.

37. Zhang, Y., K.H. Rogers, and D.B. Lewis, *Beta 2-microglobulin-dependent T cells are dispensable for allergen-induced T helper 2 responses.* The Journal of experimental medicine, 1996. **184**(4): p. 1507-1512.

38. Gobin, S.J., P. Biesta, and P.J. Van den Elsen, *Regulation of human beta 2-microglobulin transactivation in hematopoietic cells.* Blood, 2003. **101**(8): p. 3058-64.

39. Zhong, C.-Y., Y.M. Zhou, and K.E. Pinkerton, *NF-κB inhibition is involved in tobacco smoke-induced apoptosis in the lungs of rats.* Toxicology and applied pharmacology, 2008. **230**(2): p. 150-158.

40. Zhong, C.-Y., et al., *Environmental tobacco smoke suppresses nuclear factor-κB signaling to increase apoptosis in infant monkey lungs.* American journal of respiratory and critical care medicine, 2006. **174**(4): p. 428-436.

41. Hasnis, E., et al., *Cigarette smoke-induced NF-kappa B activation in human lymphocytes: the effect of low and high exposure to gas phase of cigarette smoke.* Journal of Physiology and Pharmacology, 2007. **58**(5): p. 263-274.

42. Schöneberg, T., et al., *The G protein-coupled receptor GPR34–The past 20 years of a grownup.* Pharmacology & therapeutics, 2018. **189**: p. 71-88.

43. Liebscher, I., et al., *Altered immune response in mice deficient for the G protein-coupled receptor GPR34.* Journal of Biological Chemistry, 2011. **286**(3): p. 2101-2110.

44. Kitamura, H., et al., *GPR34 is a receptor for lysophosphatidylserine with a fatty acid at the sn-2 position.* The Journal of Biochemistry, 2012. **151**(5): p. 511-518.

45. Jäger, E., et al., *Dendritic cells regulate GPR34 through Mitogenic signals and undergo apoptosis in its absence.* The Journal of Immunology, 2016. **196**(6): p. 2504-2513.

46. Kazeros, A., et al., *Overexpression of apoptotic cell removal receptor MERTK in alveolar macrophages of cigarette smokers.* American journal of respiratory cell and molecular biology, 2008. **39**(6): p. 747-757.

47. Tanaka, T., M. Narazaki, and T. Kishimoto, *IL-6 in inflammation, immunity, and disease.* Cold Spring Harbor perspectives in biology, 2014. **6**(10): p. a016295-a016295.

48. Voiriot, G., et al., *Interleukin-6 displays lung anti-inflammatory properties and exerts protective hemodynamic effects in a double-hit murine acute lung injury.* Respiratory research, 2017. **18**(1): p. 1-14.

49. Noah, T.L., et al., *Tobacco smoke exposure and altered nasal responses to live attenuated influenza virus.* Environmental health perspectives, 2011. **119**(1): p. 78-83.

50. Cook, D.G. and D.P. Strachan, *Summary of effects of parental smoking on the respiratory health of children and implications for research.* Thorax, 1999. **54**(4): p. 357-366.

51. Hawgood, S., M. Derrick, and F. Poulain, *Structure and properties of surfactant protein B.* Biochimica et Biophysica Acta (BBA)-Molecular Basis of Disease, 1998. **1408**(2-3): p. 150-160.

52. Clevidence, D.E., et al., *Members of the HNF-3/forkhead family of transcription factors exhibit distinct cellular expression patterns in lung and regulate the surfactant protein B promoter.* Dev Biol, 1994. **166**(1): p. 195-209.

53. Warburton, D., et al., *The molecular basis of lung morphogenesis.* Mechanisms of development, 2000. **92**(1): p. 55-81.

54. Fehrholz, M., S. Seidenspinner, and S. Kunzmann, *Expression of surfactant protein B is dependent on cell density in H441 lung epithelial cells.* PloS one, 2017. **12**(9): p. e0184556-e0184556.

55. Olivera, D.S., et al., *Cellular mechanisms of mainstream cigarette smoke-induced lung epithelial tight junction permeability changes in vitro.* Inhalation toxicology, 2007. **19**(1): p. 13-22.

56. Nesslein, L.L., et al., *Partial SP-B deficiency perturbs lung function and causes air space abnormalities.* American Journal of Physiology-Lung Cellular and Molecular Physiology, 2005. **288**(6): p. L1154-L1161.

57. Ikegami, M., et al., *Reversibility of lung inflammation caused by SP-B deficiency.* American Journal of Physiology-Lung Cellular and Molecular Physiology, 2005. **289**(6): p. L962-L970.

58. Ingenito, E.P., et al., *Decreased surfactant protein-B expression and surfactant dysfunction in a murine model of acute lung injury.* American journal of respiratory cell and molecular biology, 2001. **25**(1): p. 35-44.

59. Larsson, L., et al., *Identification of bacterial and fungal components in tobacco and tobacco smoke.* Tobacco Induced Diseases, 2008. **4**(1): p. 1-8.

60. Hodyl, N.A., et al., *Prenatal endotoxin exposure alters behavioural pain responses to lipopolysaccharide in adult offspring.* Physiology & behavior, 2010. **100**(2): p. 143-147.

61. Centers for Disease Control Prevention, *Current cigarette smoking among adults in the United States.* 2019.

62. Cheraghi, M. and S. Salvi, *Environmental tobacco smoke (ETS) and respiratory health in children.* European journal of pediatrics, 2009. **168**(8): p. 897-905.

63. Azagba, S., et al., *Trends in smoking during pregnancy by socioeconomic characteristics in the United States, 2010–2017.* BMC pregnancy and childbirth, 2020. **20**(1): p. 1-7.

64. Stefanidou, M., S. Athanaselis, and C. Spiliopoulou, *Health impacts of fire smoke inhalation.* Inhalation toxicology, 2008. **20**(8): p. 761-766.

Conclusion

In this dissertation, we reviewed the impact of tobacco smoke and particularly environmental tobacco smoke (ETS) on health in children and adults. ETS exposure has been shown to reduce pulmonary function, increase the rate and severity of respiratory infections, increase asthma exacerbations, contribute to obesity, and is associated with cognitive and behavioral problems in children. ETS alters immune responses that may contribute to many of the conditions linked to ETS exposure. Of particular concern are the lasting impacts of ETS exposure in young populations that can result in chronic pulmonary diseases. Discrepancies between onset of chronic respiratory diseases associated with tobacco use and the increasing rate of some diseases, such as chronic obstructive pulmonary disease, in never smokers has led some researchers to speculate that early-life exposures may create a preventable predisposition that is not fully understood. We also reviewed the composition of tobacco smoke and note several chemical classes that are relevant to emerging inhalation exposures. This makes tobacco smoke exposure an important area for translational research that can inform researchers in other inhalation fields, policy makers, and the public.

We used a murine model of neonatal tobacco smoke to examine the persistent impact of ETS exposure into adulthood. Using assessment of lavage fluid for total protein and cell count and differential we showed sex-dependent differences in persistent lung injury and elevated immune cell populations at rest. Since ETS exposure has been implicated in altered immune responses, we used transcriptomic analysis to assess differential responses to bacterial products in the lung. We found that neonatally ETS exposed females had significant differences in Hallmark Pathways compared to control females at rest and following immune challenge. While males had no differences in Hallmark Pathways, neonatal ETS exposure resulted in reduced resolution of immune responses based on KEGG pathway analysis compared to control males. These

differences show a persistent and meaningful change in the response to bacterial pathogens following neonatal ETS exposure.

We also examined the mechanism by which neonatal ETS exposure alters lung function in the young. We found that neonatal ETS exposure resulted in increased tissue damping at six-weeks-old. This altered pulmonary function was associated with a reduction in club cell secretory protein (CCSP) and was due to aryl hydrocarbon receptor (AhR) ligands in tobacco smoke as indicated by ablation of reduction in gene expression by pretreatment with an AhR antagonist. AhR ligands also modulated pulmonary IL-22 expression by transiently inducing an ILC3 population. We show for the first time that IL-22 modulates CCSP and is persistently reduced following neonatal ETS exposure.

We also looked at mice of a more advanced age to determine long term impacts of neonatal ETS exposure on lung pathophysiology. At ten weeks post exposure, we found that neonatally ETS exposed female mice had elevated macrophages and neutrophils in their lungs at rest. Using a model of immune challenge with bacterial products, we found that the macrophage population in neonatally ETS exposed female mice decreased. We assessed these mice for expression of several relevant markers indicated by our transcriptomic analysis with an emphasis on immune related genes that may be important for macrophages. We noted a sex-dependent change in gene expression for GPR34 due to neonatal ETS exposure, which has previously been shown to be important in myeloid cell maintenance.

We believe these studies will improve our understanding of the age and sex-dependent effects of tobacco smoke exposure. Further, these results should improve our understanding of gene expression patterns induced by constituents of tobacco smoke that may be relevant to understanding how novel inhaled toxicants may impact pulmonary health. We hope these findings could be used to identify diagnostic markers of lung damage from early life exposures and potential could lead to advances in prevention and treatment of potentially chronic conditions resulting from such exposures.